
FACTORS FOR STABILITY, ASSEMBLY AND FUNCTION OF PHOTOSYNTHETIC COMPLEXES

Serena Schwenkert

Dissertation
an der Fakultät für Biologie
der Ludwig-Maximilians-Universität
München

vorgelegt von
Serena Schwenkert
aus München

Juli 2008

Erstgutachter:

PD Dr. Jörg Meurer

Zweitgutachter:

Prof. Dr. Jürgen Soll

Tag der mündlichen Prüfung:

19.09.2008

Table of Contents

ZUSAMMENFASSUNG	4
SUMMARY	5
1. INTRODUCTION	6
1.1 Origin of plastids	6
1.2 Thylakoid membrane complexes – patchwork families	6
1.3 Photosynthesis in higher plants	7
1.4 Biosynthesis of iron-sulfur clusters	12
2. PROJECT AIMS	14
2.1 Function of low molecular weight components of Photosystem II and the Cytochrome <i>b₆f</i> complex	14
2.2 Maturation of [Fe-S] clusters as essential cofactors of plastid protein complexes	15
3. DISCUSSION	16
3.1 Involvement of low molecular weight subunits in assembly, structure and function of Photosystem II	16
3.2 PsbI, PsbTc and PsbM are involved in reoxidation of the plastoquinone pool in darkness	17
3.3 PetL is essential for dimerisation of the Cytochrome <i>b₆f</i> complex	19
3.4 Nuclear encoded HCF101 is a [4Fe-4S] scaffold protein in the chloroplast	20
4. LITERATURE CITED	23
5. ORIGINAL PUBLICATIONS AND MANUSCRIPTS AS PART OF THE CUMULATIVE THESIS	28
EHRENWÖRTLICHE VERSICHERUNG	
ACKNOWLEDGEMENTS	
<i>Curriculum vitae</i>	

ZUSAMMENFASSUNG

Photosynthetische Organismen verfügen über die einzigartige Fähigkeit, Lichtenergie in chemische Energie umzuwandeln. In höheren Pflanzen findet dieser Prozess in den Chloroplasten statt, die sich aus einem einst freilebenden, den heutigen Cyanobakterien ähnlichen Organismus entwickelt haben. Das photoautotrophe Bakterium wurde im Laufe der Endosymbiose durch horizontalen Gentransfer vom Endosymbionten zum Genom der Wirtszelle in ein eukaryotisches System integriert. Aus diesem Grund besteht das plastidäre Proteom sowohl aus plastidär, als auch aus nukleär kodierten Untereinheiten.

Zu den wenigen noch in den Chloroplasten kodierten Strukturkomponenten der Thylakoidmembrankomplexe gehören einige niedermolekulare Untereinheiten mit meist unbekannter Funktion. Um die Aufgaben dieser Proteine genauer zu untersuchen, wurden *knock-out* Mutanten in Tabak hergestellt. Biochemische und spektroskopische Untersuchungen zeigten, dass die Untereinheiten PsbI und PsbT an der Photosystem II Assemblierung sowie der strukturellen Stabilität der hochmolekularen Photosystem II und Antennenkomplexe beteiligt sind, obwohl sie für autotrophes Wachstum nicht essentiell sind. PsbI, PsbT und PsbM sind weiterhin für eine PSII vermittelte sauerstoffabhängige Reoxidation des Plastoquinons im Dunklen unentbehrlich, ein Prozess, der unter Umständen über die Q_B -Bindestelle vermittelt wird. Diese Analysen liefern neue Einblicke in chlororespiratorische Vorgänge.

Untersuchungen der niedermolekularen Untereinheiten des Cytochrom *b₆f* Komplexes haben gezeigt, dass PetL, obwohl es nicht für photoautotrophes Wachstum benötigt wird, an der Stabilisierung der Konformation des Rieske Proteins beteiligt ist. Dies ist für die Dimerisierung des Komplexes wichtig.

In der Biogenese photosynthetischer Komplexe und deren Kofaktoren spielen nicht nur deren konstitutive Untereinheiten eine Rolle, sondern es werden auch viele nukleär kodierte Proteine benötigt. Ein solcher Faktor ist HCF101, der für die Assemblierung von Photosystem I, welches drei [4Fe-4S] Cluster enthält, benötigt wird. HCF101 ist eine ubiquitär konservierte P-loop ATPase, die *in vitro* ein transientes [4Fe-4S] Cluster bindet, welches auf andere Zielproteine, möglicherweise Photosystem I und die Ferredoxin-Thioredoxin-Reduktase übertragen werden kann. Weiterhin konnte gezeigt werden, dass drei von den acht in höheren Pflanzen konservierten Cysteinen an der Cluster-Bindung beteiligt sind.

SUMMARY

Photosynthetic organisms possess the unique ability to convert light energy into chemical energy. In higher plants this process takes place in chloroplasts, which derived from a once free-living cyanobacterial-like cell. In the course of endosymbiotic events, the phototrophic bacterium was integrated into a eukaryotic system by transfer of many chloroplast genes to the host genome. Therefore, the chloroplast proteome represents a chimeric system of plastid and nuclear encoded proteins.

Among the few remaining plastid encoded structural components of all thylakoid membrane complexes are many low molecular weight (LMW) subunits with mostly unknown functions. To analyse their specific roles, knock-out mutants of all LMW subunits were generated in tobacco. Biochemical and spectroscopic experiments revealed that the photosystem (PS)II subunits PsbI and PsbTc are involved in the assembly, phosphorylation and structure maintenance of PSII and its associated light harvesting complex (LHCII), although they are not required for photoautotrophic growth. PsbI, PsbT and PsbM are further important for oxygen dependent PSII mediated reoxidation of the PQ pool in darkness, likely involving the Q_B binding site of PSII. These findings shed new light on chlororespiratory processes.

Analysis of plastid encoded LMW subunits of the Cytochrome *b₆f* (Cyt *b₆f*) complex revealed that, unlike PetN and PetG, PetL is not required for photoautotrophic growth, but involved in the stabilisation of the conformation of the Rieske protein necessary for dimerisation of the complex.

Not only the constituent subunits play a role in the biogenesis and stability of photosynthetic complexes and their cofactors, but many nuclear encoded proteins which are not part of the functional complexes are required. HCF101 represents such a factor and is essential for accumulation of PSI, which contains three [4Fe-4S] clusters. HCF101 is a ubiquitously conserved P-loop ATPase and was shown to bind a transient [4Fe-4S] cluster *in vitro* that can be transferred to target proteins, presumably PSI and ferredoxin-thioredoxin-reductase (FTR). Additionally, three of eight cysteines in HCF101 conserved among higher plants were identified to be important for cluster binding.

1. INTRODUCTION

1.1 Origin and function of plastids

The engulfment of a cyanobacterial-like cell by a eukaryotic ancestor, a process known as primary endosymbiosis, was the first crucial step of introducing photosynthesis into eukaryotic organisms (Mereschkowsky, 1905; Sommer *et al.*, 2006). The once free living bacterium had the ability to transform sunlight into chemical energy and was converted into different plastid organelles in the diverting lineages during the course of evolution. The loss and gain of genetic material or its transfer to other genetic compartments played a crucial role in the development of the regulatory network between chloroplast and nucleus (Martin and Herrmann, 1998; Martin 1998; Richly and Leister, 2004). Plastids are not only responsible for energy supply via photosynthesis, but are also involved in the synthesis of vitamins, amino acids, essential cofactors and lipids as well as in nitrogen and sulphur metabolism.

1.2 Thylakoid membrane complexes – patchwork families

Thylakoid membranes are highly specialised biomembranes and harbour the five major protein and antennae complexes involved in photosynthesis which span the lipid bilayer and are associated with both peripheral and soluble polypeptides in stroma and lumen (Figure 1). Ontogenetic biogenesis of chloroplasts from undifferentiated types of plastids, proplastids, is triggered by light (Goldschmidt-Clermont, 1998). In developed chloroplasts the thylakoid membrane system of higher plants consists of grana stacks interconnected by unstacked stroma lamellae. The photosynthetic protein complexes are unevenly distributed along these membranes. Both photosystems are located separately, as PSI is mainly found in stroma lamellae, whereas PSII accumulates in grana stacks. The ATP synthase complex accumulates preferentially in stroma lamellae, whereas the Cyt b_6f complex is found in the marginal areas of both membrane types (Dekker and Boekema, 2005). As a result of endosymbiosis all thylakoid membrane complexes are composed of both chloroplast and nuclear encoded proteins requiring a complicated regulation of gene expression and protein targeting during the assembly of thylakoid membrane complexes (Soll and Schleiff, 2004). For efficient biogenesis of these oligomeric protein complexes, the individual subunits and

their cofactors have to be formed in stoichiometrical amounts, translocated, inserted into the membrane and assembled to functional protein complexes (Rochaix, 2004). This complicated process is subject to various regulatory control mechanisms and requires an additional set of proteins, which are often of nuclear origin.

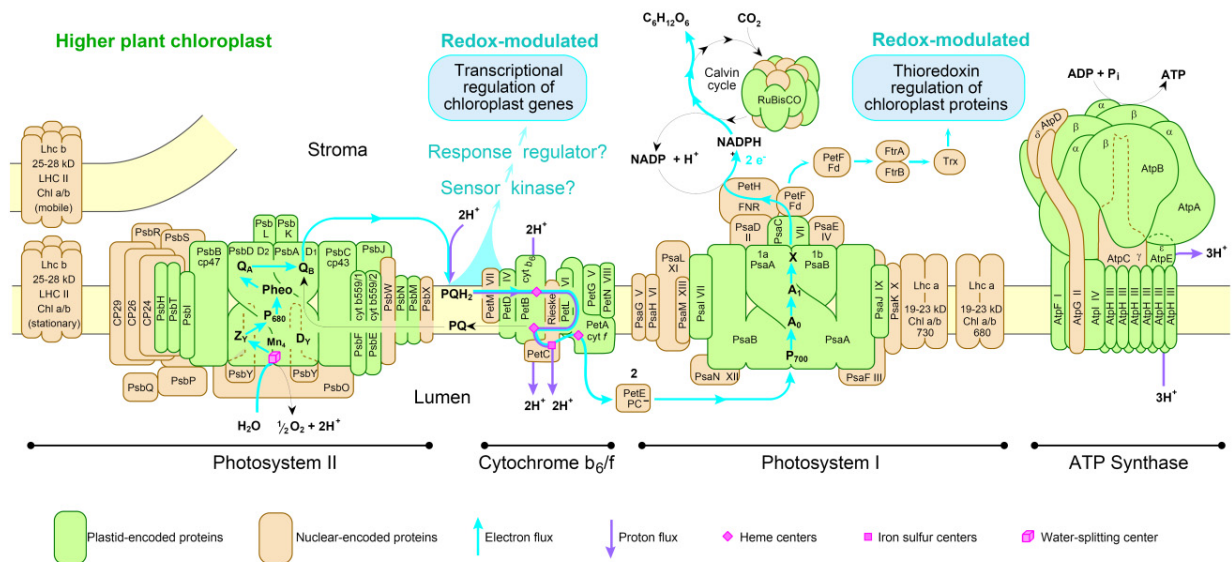


Figure 1: Scheme of the thylakoid membrane system. Each complex consists of nuclear (yellow) and plastid encoded (green) components (Race *et al.*, 1999, modified).

1.3 Photosynthesis in higher plants

All five complexes of the thylakoid membrane are indispensable for efficient photosynthetic activity (reviewed in Nelson and Yocum, 2006). Both photosystems harvest sunlight with the help of light harvesting complexes which are only present in prochlorophyta, algae and higher plants. The energy is transferred to the reaction centre of the photosystems, where a specialised chlorophyll initiates the translocation of an electron through the membrane, finally reducing ferredoxin, which in turn serves as a donor of electrons for several other components such as NADP^+ and thioredoxin. The induced charge separation in the reaction centre results in the reduction of a quinone, which is bound to the Q_B binding pocket, as a first step of the photosynthetic electron transport chain. Water, which is oxidised by PSII on the luminal side of the membrane, serves as an electron donor. Upon reduction with two electrons and protonation PQH_2 is released from the Q_B pocket and replaced by PQ. Each

excitation with one photon leads to extraction of one electron from the manganese cluster, which passes through five oxidation states during the reduction of one PQ.

PSII is composed of more than 20 polypeptides, which have been localised by means of high resolution X-ray crystal structures in *Thermosynechococcus elongatus* (Ferreira *et al.*, 2004; Loll *et al.*, 2005; Figure 2A). The reaction centre of the complex consists of the D1/D2 heterodimer, adjacent to which are the two light harvesting chlorophyll-containing proteins CP47 and CP43 forming. In close proximity are three of the low molecular weight subunits (LMW), the α and β chain of Cytochrome b_{559} (Cyt b_{559}) and PsbI, forming the core complex. Cyt b_{559} consists of a heterodimer, both containing histidines providing ligands for binding a heme as cofactor. It is essential for PSII activity, as its deletion results in the loss of PSII function and stability (Swiatek *et al.*, 2003). Besides these, about 13 other LMW subunits are found associated to PSII. They all consist of a hydrophobic domain and span the thylakoid membrane once. Apart from the b_{559} none of them bind cofactors and most of them are encoded by the plastid genome (Shi and Schroeder, 2004; Thornton *et al.*, 2005; Müh *et al.*, 2007). Three extrinsic proteins (PsbO, PsbP and PsbQ) at the luminal side of the membrane form the oxygen-evolving complex (OEC), which is closely connected to the manganese-cluster of PSII and is possibly involved in the optimisation of the oxygen evolving process (Roose *et al.*, 2007). Most of the chlorophyll pigments are found in the peripheral light-harvesting antenna complexes existing as a trimer of LHCb1-3 involved in transferring excitation energy to the core complex. The minor antenna CP29, CP26 and CP24 interconnect this energy transfer. These antenna proteins assemble with the dimeric core proteins to PSII-LHCII supercomplexes (Minagawa and Takahashi, 2004; Dekker and Boekema, 2005; Figure 2B).

The second photosystem, PSI, is involved in linear and cyclic electron transport (Munekage *et al.*, 2004, Jensen *et al.*, 2007). At least 13 highly conserved subunits are present in PSI and have been resolved by crystal structure analysis in plants at 4.4 Å (Ben-Shem *et al.*, 2003). Two major plastid encoded subunits, PsaA and PsaB, form the central heterodimer and bind cofactors essential for light absorbance and photochemical reactions. They bind the chlorophyll dimer (P700), where charge separation occurs, as well as the primary electron acceptors chlorophyll A_0 and the phylloquinone A_1 . The heterodimer also includes an [4Fe-4S] cluster F_x as cofactor. Another two [4Fe-4S] clusters (F_A and F_B) are bound to plastid-

encoded PsaC transferring electrons from F_x to ferredoxin. Additionally, the LHCI proteins comprise as many as 167 chlorophylls (Ben-Shem *et al.*, 2003). The remaining subunits play a role in the docking of plastocyanin and ferredoxin and the formation of supercomplexes with LHCI (Amunts *et al.*, 2007).

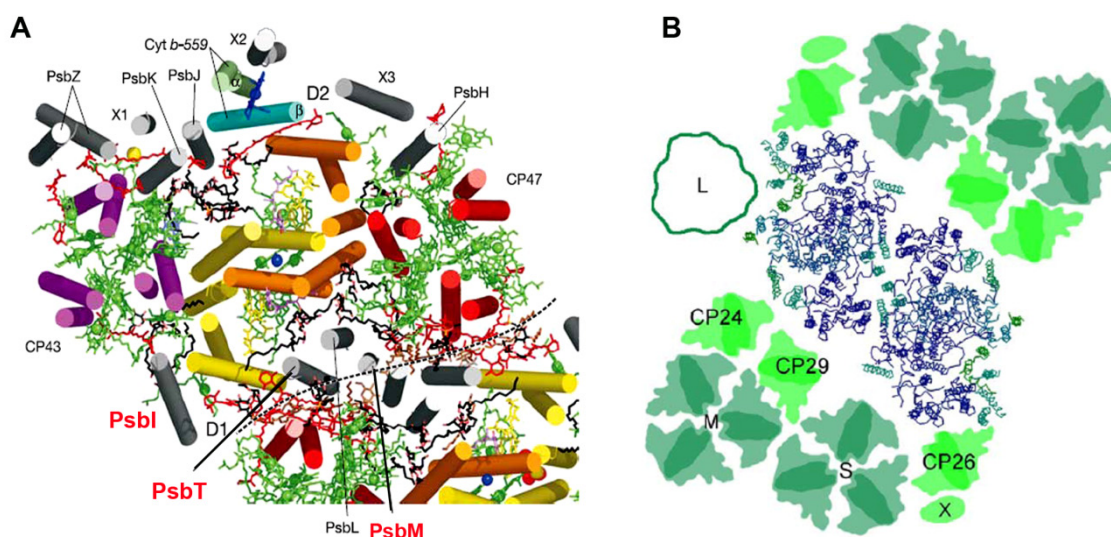


Figure 2: **A**, X-ray crystal structures of PSII in *Thermosynechococcus elongatus* at 3.0 Å. View of the PSII monomer along the membrane from the cytoplasmic side. The subunits analysed in this thesis, PsbI, PsbTc and PsbM, are indicated in red (Loll *et al.*, 2005). **B**, Top view of the spinach PSII-LHCII supercomplex consisting of the PSII core proteins and the LHCII trimers (strongly (S), moderately (M) and loosely (L) bound), as well as the minor antennas CP24, CP26 and CP29 in spinach (Dekker and Boekema, 2005).

For photosynthetic organisms it is vital to modify their light harvesting capacity in relation to environmental circumstances, as high light conditions cause photoinhibition and damage to the proteins. These must be continuously replaced by degradation of the inactivated proteins, *de novo* synthesis and integration of the newly synthesised proteins into the complex. Therefore, plants have developed regulative mechanisms for the prevention of extensive damage such as down-regulation of antenna size, redistribution of LHC complexes (state transition) and nonphotochemical quenching to decrease the photosynthetic efficiency (reviewed in Rochaix, 2007; Kargul and Barber, 2008). The redistribution of peripheral antenna proteins involves phosphorylation as well as dephosphorylation and migration of LHCII proteins between the two photosystems, thus changing the level of excitation energy. This phosphorylation is mediated by a phosphoprotein kinase (STN7),

which is controlled by the redox state of the PQ pool (Vaionen *et al.*, 2005; Bonardi, 2005). Under light conditions preferentially exciting PSII, the PQ pool is mostly reduced, leading to phosphorylation and migration of LHCII from PSII to PSI. Under oxidising conditions the LHCII is dephosphorylated and detached from PSI. The mechanism is summarised in Figure 3. The Cyt b_6f complex acts as a sensor for the redox state of the PQ pool and is involved in signal transduction leading to kinase activation (Zito *et al.*, 1999). Not only the LHCII proteins undergo reversible phosphorylation, the PSII core proteins D1, D2 and CP43 are also phosphorylated, a process mediated by a different kinase (STN8) (Vaionen *et al.*, 2005; Bonardi *et al.*, 2005), although the function of these modifications is still enigmatic (reviewed in Allen, 2005).

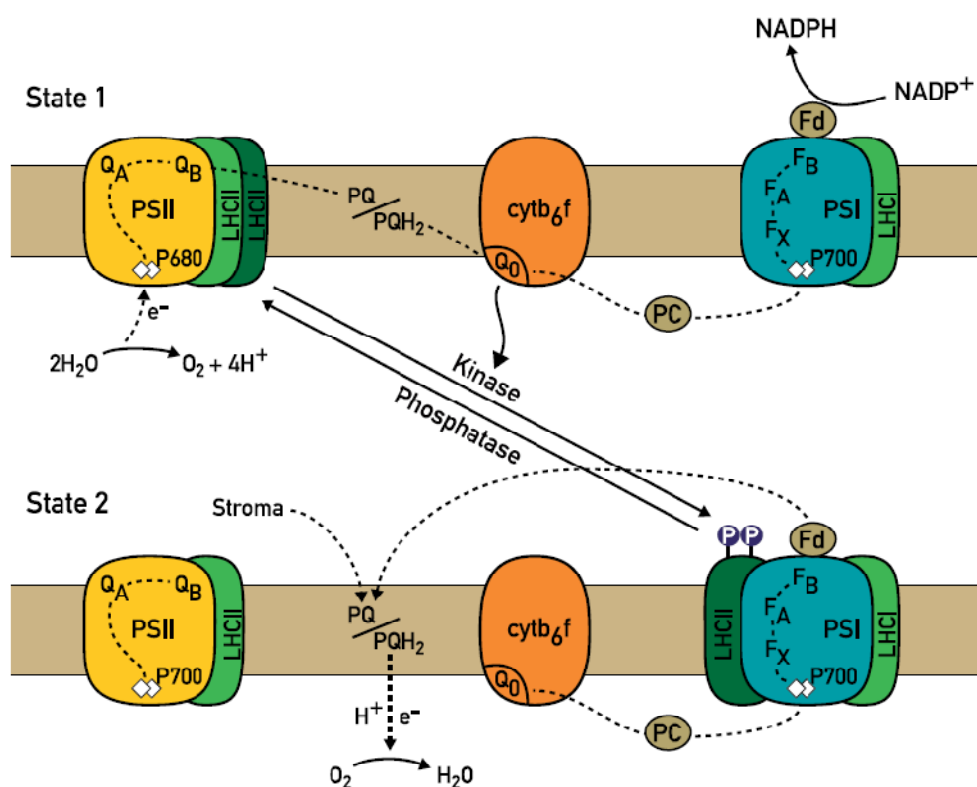


Figure 3: State transition: Light preferentially exciting PSII leads to reduction of the PQ pool. Via the Cyt b_6f complex a kinase (STN7) is activated, leading to phosphorylation of the LHCII. Phosphorylated mobile LHCII is detached from PSII and migrates to PSI, thus allowing optimised distribution of the excitation energy (state II). State II can also be induced in darkness under anaerobic conditions through the chlororespiratory electron transport chain, preventing oxidation of the plastoquinone pool. Upon preferential excitation of PSI the LHCII is dephosphorylated (state I) (Rochaix, 2007).

The Cytochrome complex, which mediates electron transport from PSII to PSI functions as a plastoquinone-plastocyanin oxidoreductase. It transports one electron from PQH₂ through the Rieske iron-sulfur protein and cytochrome *f* reducing plastocyanin. The second electron is transferred through two *b* hemes of cytochrome *b*₆ reducing another quinone from the PQ pool at the stromal side. In a second reduction event at the stromal face two protons are absorbed and subsequently released in the lumen generating an electrochemical gradient across the membrane. This recycling of one of the electrons from the PQ pool is referred to as Q-cycle. Like PSII, the complex forms a dimer and consists of at least eight subunits, two of which (*petM* and *petC*) are encoded by nuclear genes, *petC* codes for the Rieske iron-sulfur protein, which contributes to the stability of the dimer by domain swapping (Kurisu *et al.*, 2003) and has a highly mobile extrinsic domain. The remaining subunits (*petA*, *petB*, *petD*, *petG*, *petL* and *petN*) are encoded by the plastid genome. The presentations of the crystal structures (Kurisu *et al.*, 2003; Stroebel *et al.*, 2003) have clarified the architectural composition of the complex (Figure 4). Apart from the described eight subunits, the complex contains one chlorophyll *a* and one β -carotene. An unexpected heme was discovered, which might be involved in the cyclic electron transport around PSI (reviewed in Cramer *et al.*, 2006).

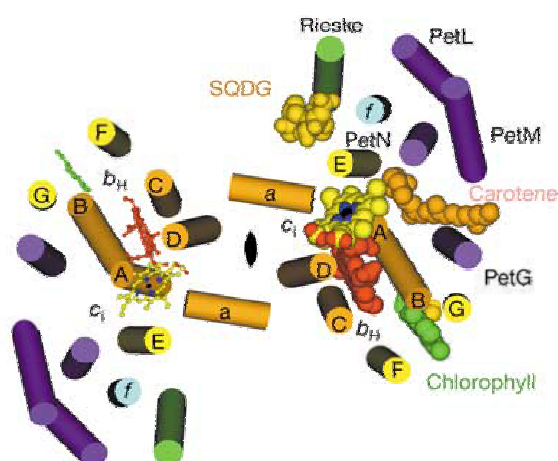


Figure 4: Crystal structure of the Cyt *b*₆*f* complex: The dimeric complex is composed of four major subunits *cytf*, *cytb*₆, the Rieske protein, SUIV and four LMW subunits (PetL, PetG, PetN and PetM) (Stroebel *et al.*, 2003).

1.4 Biosynthesis of iron-sulfur clusters

Iron-sulfur [Fe-S] clusters are thought to be one of the most ancient cofactors of proteins. They are ubiquitously conserved in all living organisms and required for essential processes, such as electron transfer, regulation of gene expression, enzyme activity and iron storage (Beinert, 2000; Johnson *et al.*, 2005). The most common formations are [4Fe-4S] and [2Fe-2S] clusters, which are usually ligated by cysteines. Their capability to take up and transfer electrons makes them indispensable components of the photosynthetic electron transport chain and respiration processes. In plants, both plastids and mitochondria are capable of [Fe-S] cluster biosynthesis. In recent years many highly conserved genes of eubacterial origin have been identified, which are involved in various assembly steps of [Fe-S] clusters. This process can be divided into three steps: 1) the enzymatic mobilisation of sulfur from cysteine catalysed by a desulfurase 2) the assembly of the cluster itself, usually mediated by scaffold proteins, 3) insertion of the cluster into apoproteins (Figure 5; Balk and Lobreaux, 2005).

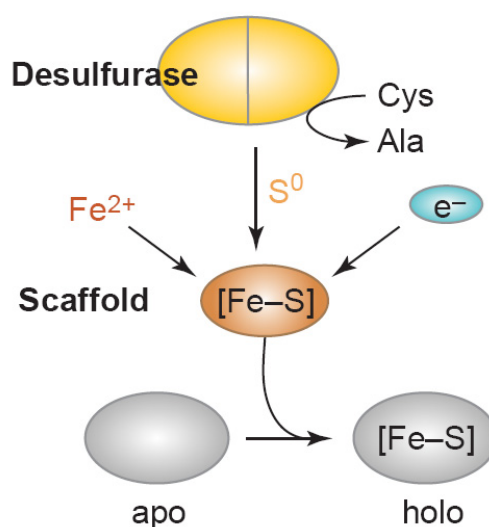


Figure 5: Essential steps in iron-sulfur cluster biogenesis: Cysteine desulfurases catalyse the mobilisation of sulfur from cysteine and transfer it to the scaffold proteins. The cluster is then transferred and inserted into target proteins (Balk and Lobreaux, 2005).

Three phylogenetically related pathways for [Fe-S] cluster assembly have been described in bacteria and eukaryotes, the ISC system, the NIF system and the SUF system (Takahashi and Tokumoto, 2002; Frazzon and Dean, 2003). The ISC homologues are responsible in [Fe-S] cluster biogenesis in bacteria, mitochondria (Lill and Mühlenhoff, 2008) and in hydrogenosomes (Tachezy *et al.*, 2001), whereas the NIF system is found in nitrogen fixing bacteria. Apart from these two systems the SUF pathway is also found in *E.coli*, where it is mostly used under oxidative stress conditions (Takahashi and Tokumoto, 2002; Lee *et al.*, 2004). Homologues of all six SUF proteins are found in the chloroplasts (Pilon *et al.*, 2006; Kessler and Papenbrock, 2005), but it remains a challenge to investigate the exact roles of the individual players.

2. PROJECT AIMS

In order to elucidate the assembly of the photosynthetic machinery, the function of both plastid encoded constituent subunits of the thylakoid membrane complexes as well as a nuclear encoded protein, HCF101, which is essential for PSI assembly, were analysed in this work.

2.1 Function of low molecular weight components of Photosystem II and the Cytochrome *b₆f* complex

Besides the rather well characterised larger subunits of the photosynthetic complexes, about 16 LMW subunits, i. e. proteins with molecular masses below 10 kDa, can be found associated with PSII. Although most of them are conserved among cyanobacteria and higher plants, the function of many of these proteins remained unclear. Some of them are important for the assembly and structural maintenance of PSII, whereas others are even involved in electron transport (Shi and Schroeder, 2004; Thornton *et al.*, 2005; Müh *et al.*, 2007). One major aim of this work was to elucidate the roles of these proteins. This was achieved by detailed spectroscopic analysis of PSII function and a biochemical approach to study the assembly and phosphorylation patterns of PSII proteins of the *PsbI*, *PsbTc* and *PsbM* knockout mutants.

Concerning the Cyt *b₆f* complex little is known as yet about its biogenesis and the participation of the LMW subunits. Three of the four LMW subunits are encoded in the plastid genome and were likewise inactivated in tobacco. These mutants were analysed in respect to assembly and stability of the complex as well as effects upon electron flow and state transition processes.

2.2 Maturation of [Fe-S] clusters as essential cofactors of plastid protein complexes

The biogenesis of thylakoid membrane complexes is not only dependant on their constituent subunits, but also on the assembly of their cofactors. PSI harbours three [Fe-S] clusters, which have important functions in electron transport. As very little is known about the [Fe-S] cluster assembly machinery in plastids, a closer characterisation of the recently identified nuclear encoded protein HCF101 was performed in this study on a biochemical level to elucidate its function in iron-sulfur cluster biosynthesis. HCF101 is especially interesting as it does not share any of the conserved cysteines, which serve as ligands for the iron sulfur cluster, with homologues proteins in animals, yeast or bacteria. To gain better insight into the [Fe-S] cluster assembly in chloroplasts the protein was overexpressed in *E.coli* and purified to analyse its function *in vitro*. The obtained results were complemented by *in vivo* analysis in *Arabidopsis*.

3. DISCUSSION

3.1 Involvement of low molecular weight subunits in assembly, structure and function of Photosystem II

Although many of the LMW subunits are highly conserved among cyanobacteria and higher plants, the PSII organisation and environmental living conditions differ significantly. Therefore, an attempt has been made to study the function of these subunits in the same organism. *Nicotiana tabacum* as a model plant was chosen to perform a series of knock-out mutants by chloroplast transformation. Table 1 summarises the information that has been obtained studying these mutants. It was shown that each individual subunit seems to serve a special function, despite the close location of some of them. Some of them are essential for photoautotrophic growth, whereas others play important roles in the biogenesis, structure and maintenance of the PSII complex, PSII phosphorylation, electron flow from and within PSII as well as light trapping.

Table 1: Plastid encoded LMW subunits of PSII in higher plants. The major function and the assembly status of PSII as well as the ability of photoautotrophic growth of the mutants are described. Indicated in red are the subunits analysed in this thesis.

<i>Protein</i>	<i>Function</i>	<i>Assembly</i>	<i>Lethal</i>	<i>References</i>
PsbE/F	Early PSII assembly, Photoprotection	no core assembly	+	Swiatek <i>et al.</i> , 2003
PsbH	Affects non photochemical quenching	supercomplexes	-	Meurer, unpublished data
PsbI	Dimerisation of PSII, Reoxidation of PSII	monomer	-	Schwenkert <i>et al.</i> , 2006
PsbJ	Forward electron flow from Q _A to Q _B	monomer	+	Ohad <i>et al.</i> , 2004 Suorsa <i>et al.</i> , 2004 Regel <i>et al.</i> , 2001
PsbK	Connection of inner and outer antennae	dimer	-	Eichacker, Meurer, unpublished data
PsbL	Prevents back electron flow to PSII	monomer	+	Ohad <i>et al.</i> , 2004 Suorsa <i>et al.</i> , 2004
PsbM	Reoxidation of PQ	supercomplexes	-	Umate <i>et al.</i> , 2007
PsbTc	Connection of LHCII, Reoxidation of PQ	monomer	-	Umate <i>et al.</i> , 2008
PsbZ	Connection of LHCI	dimer	-	Swiatek <i>et al.</i> , 2001

3.2 PsbI, PsbTc and PsbM are involved in reoxidation of the PQ pool in darkness

In this study especially the functions of the LMW subunits PsbI, PsbTc and PsbM were analysed. Of the three, PsbI is part of the PSII core complex and all of them are located close to the dimerisation axis of PSII. Yet it is noteworthy that several crystal structures of cyanobacterial PSII have been released in recent years and especially the exact assignment of the LMW subunits remains a controversial issue (Loll *et al.*, 2005; Müh *et al.*, 2008; Ferreira *et al.*, 2004; Kamiya *et al.*, 2003). Structural differences observed in the $\Delta psbI$ and $\Delta psbTc$ mutant are in good agreement with their localization within PSII. Both mutants are affected in dimerisation or stability of the PSII dimer, respectively and cannot form stable PSII-LHCII supercomplexes. PsbM in contrast does not show any structural effects in complex assembly. A common feature we observed in all mutants was their effect on state transition processes. In all mutants the PQ pool was already phosphorylated in darkness and found attached to PSI, whereas in WT this is only the case under light conditions preferentially exciting PSII. As the phosphorylation could be abolished under far red light illumination, thus oxidising the PQ pool, we concluded that phosphorylation resulted from a reduced PQ pool in darkness. Moreover, all mutants were affected in Q_B site properties of PSII. Measurements of charge recombination between Q_B^- and the S-states (oxidation states) of the manganese cluster indicated that the ratio of reduced and oxidised quinone bound to the Q_B binding sites in darkness, which is 1:1 in WT, was higher in the mutants due to structural changes of the Q_B binding pocket, as revealed by studies with inhibitors of the Q_B binding site.

It is well established that nonphotochemical reduction of the PQ pool takes place in darkness, partially mediated by the plastid encoded NDH, which is homologue to the mitochondrial NADH dehydrogenase (complex I), and a complex consisting of PGR5 and PGRL1 (Dal Corso *et al.*, 2008; reviewed in Peltier and Cournac, 2002 and Rumeau *et al.*, 2007). In order to keep the PSII acceptor site oxidised the plant has to be able to reoxidise the PQ pool. A plastid terminal oxidase (PTOX) has been identified, which uses electrons from the PQ pool for carotenoid biosynthesis and might thus be partially responsible for the reoxidation of the PQ pool, although it is mainly present in stoma lamellae (Aluru *et al.*, 2004). It is further evident that oxygen is the final electron acceptor from PQ, as we could show indirectly via LHCII phosphorylation that the PQ pool is reduced under anaerobic conditions in strict darkness. Most interestingly, the addition of herbicides blocking the Q_B

binding site and thus inhibiting binding of PQ to the Q_B pocket, such as 3-(3,4-Dichlorophenyl)-1,1-dimethylurea (DCMU) and loxynil, to WT leaves in darkness likewise leads to LHCII phosphorylation, indicating an accumulation of reduced PQ or failure to reoxidise the PQ pool. We therefore conclude that PSII must be involved in reoxidation of the PQ pool in darkness, as the constant reduction of the PQ pool through chlororespiration and other processes leads to phosphorylation of LHCII in WT inhibited with DCMU and loxynil and in $\Delta psbTc$, $\Delta psbI$ and $\Delta psbM$, which seem to be impaired in this function. The electrons are most likely transported via the Q_B site, possibly Cyt b_{559} plays an additional role in this pathway, as has been proposed (Kruk and Strzalka, 2001; Bondarava *et al.*, 2003). The novel hypothetical pathway and its integration into chlororespiration and cyclic electron flow processes are summarised in Figure 6.

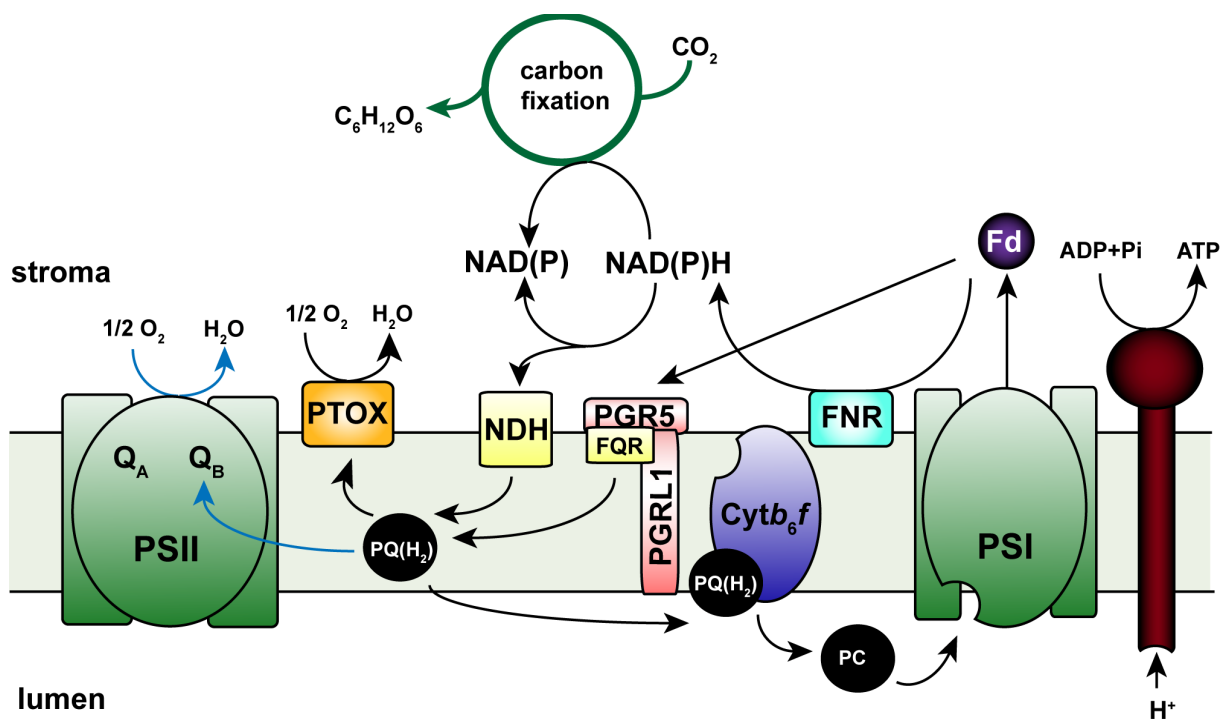


Figure 6: Model of chlororespiration and cyclic electron flow in dark adapted plants. It is suggested that PSII has a function in reoxidation of the PQ pool. The novel hypothetical pathway is indicated in blue. Cyclic electron flow around PSI I is accomplished by two different pathways, either involving the NDH complex or a complex of PGR5 and PGRL1 and a hypothetical ferredoxin-plastoquinone reductase (FQR).

3.3 PetL is essential for dimerisation of the Cyt *b₆f* complex

Not only PSII contains a number of LMW subunits, in the homodimeric Cyt *b₆f* complex four of the eight subunits of each monomer are of low molecular weight. Three of those components are plastid encoded, PetG, PetN and PetL. In order to investigate their function we have knocked out these genes in tobacco. In our biochemical and spectroscopic analysis we demonstrate that all three subunits play a role in the biogenesis and structural arrangement of the complex. PetN and PetG proved to be vital for photoautotrophic growth and seem to be early components of the complex assembly process, as no complex is formed in these mutants. In contrast, the $\Delta petL$ mutant assembles 50% of the Cyt *b₆f* complex, although photoautotrophic growth is not impaired. Disruption of the gene in *Chlamydomonas* likewise caused reduction of the Cyt *b₆f* complex and retarded growth rates (Takahashi *et al.*, 1996). However, $\Delta petL$ is not able to form dimeric complexes, 90% of the complex is found in its monomeric form. Moreover, in contrast to WT upon treatment with detergents the Rieske protein, which is composed of a transmembrane and an extrinsic domain, dissociates from the complex in the $\Delta petL$ mutant. These circumstances might lead to the assumption that due to an instable bound Rieske protein in the mutant the dimeric complex is instable and dissociates. However, we were able to show that a mutant which lacks the Rieske protein completely is still able to efficiently form dimeric Cyt *b₆f* complexes. Consequently, monomerisation of the complex in the absence of PetL cannot be accounted for by loss of the Rieske protein from the complex. It seems far more likely that PetL is necessary to stabilise the proper conformation of the Rieske protein. Upon its deletion the correct conformational position is disturbed, which prevents dimerisation of the Cyt *b₆f* complex and leads to its dissociation upon detergent treatment (Figure 7).

The Cytochrome complex plays a key role in signal transduction from the reduced PQ pool to an activation of a kinase resulting in reversible phosphorylation of the LHCII (state transition) (Aro and Ohad, 2003). Therefore, it was interesting to investigate the impact of a monomerised, reduced complex on this process. Surprisingly, state transition itself was not affected in the mutant. Studies of the phosphorylated LHCII and its attachment to PSI revealed that equal amounts of LHCII are associated to PSI under state II conditions. However, the total level of phosphorylation was reduced in the mutant, revealing that not

the total pool of phosphorylated LHCII moves to PSI, but part of it either remains attached to PSII or is present as a free LHCII trimer.

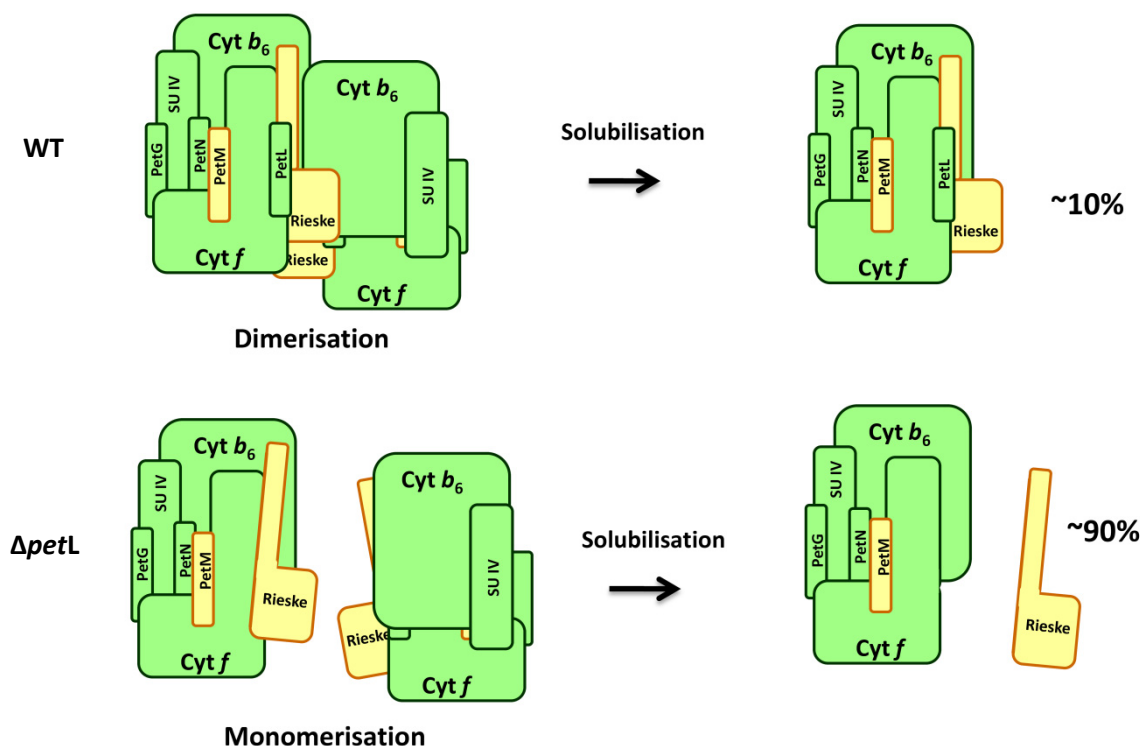


Figure 7: PetL results in conformational change of the Rieske protein. WT Cyt *b*₆/*f* complex is mainly present as a dimer and dissociates into a monomer to approx. 10% upon solubilisation. Without PetL dimerisation is impaired and during solubilisation the Rieske protein is released from the monomer.

3.4 Nuclear encoded HCF101 is a [4Fe-4S] scaffold protein in the chloroplast

Cofactors such as chlorophylls, cytochromes or iron-sulfur clusters are essential components of all photosynthetic complexes. So far only a few factors have been identified which are parts of the chloroplast [Fe-S] assembly machinery. Most of these components originate from the bacterial SUF system, which has been found to play a role in *E.coli* as an alternative pathway for [Fe-S] cluster maturation, especially under oxidative stress. Among these factors are the cysteine desufurylases CpNifS and SuFE1-3 (van Hoewyk *et al.*, 2007; Ye *et al.*, 2005; Ye *et al.*, 2006) as well as two scaffold proteins for [2Fe-2S] clusters, IscA and NFU2 which have been shown to transfer their clusters onto target proteins such as ferredoxin (Yabe *et al.*, 2004; Touraine *et al.*, 2004; Abdel-Gahny *et al.*, 2005), similar as in bacteria. HCF101 was previously identified in a mutant screen as an essential assembly factor for PSI. Besides the deficiency of PSI, levels of the plastid FTR were likewise reduced, which also contains an

[4Fe-4S] cluster (Lezhneva *et al.*, 2004). Therefore, HCF101 proved to be a candidate for [Fe-S] cluster biosynthesis in plastids. Moreover, HCF101 belongs to an ancient family of P-loop ATPases and homologues of HCF101 in yeast, humans and bacteria have been described to be essential for the maturation of [Fe-S] clusters in the cytosol and in mitochondria (Roy *et al.*, 2003; Hausmann *et al.*, 2005; Netz *et al.*, 2007; Stehling *et al.*, 2008, Bych *et al.*, 2008 Boyd *et al.*, 2008). These related proteins all share a number of conserved cysteines which form the ligands for [Fe-S] cluster binding. Surprisingly, these cysteine residues are not conserved in HCF101. It was therefore a challenge to discover, whether HCF101 also has the ability to bind an [Fe-S] cluster. By overexpression in *E.coli* and spectroscopic analyses of the purified protein, we could prove that HCF101 does bind an [4Fe-4S] cluster. By *in vitro* analysis and *in vivo* analysis in *E. coli* with recombinant proteins containing cysteine to serine exchanges we could further identify three cysteine residues which are important for cluster binding.

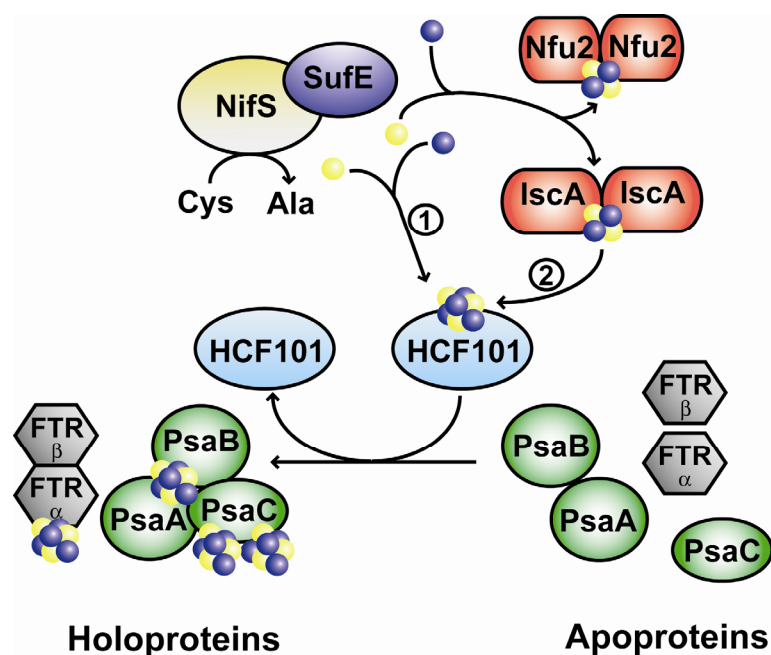


Figure 8: HCF101 acts as a scaffold protein for [4Fe-4S] clusters in the chloroplast – a working model. Two possible pathways for the assembly of [4Fe-4S] on HCF101 are presented. In either case the cysteine desulfurylases CpNifS and SufE activate sulfur from cysteine. Either the ions are directly assembled to an [4Fe-4S] cluster on HCF101 ①, or previously assembled [2Fe-2S] clusters are transferred from scaffold proteins such as Nfu2 or IscA to HCF101 ②. Finally, the apo-target protein complexes, such as PSI or FTR, are provided with [4Fe-4S] clusters from HCF101.

HCF101 was found to be part of a larger protein complex of about 145 kDa in *Arabidopsis* chloroplasts and is therefore likely to interact with other components of the iron-sulfur cluster assembly machinery. In an *in vitro* assay we could transfer the [4Fe-4S] from HCF101 onto an unspecific [4Fe-4S] target protein, Leu1, as such assays are difficult to perform with hydrophobic proteins like PSI. This information indicate that HCF101 might act as a scaffold protein for [4Fe-4S] cluster biosynthesis in plastids and even transfers its cluster to PSI and other complexes *in vivo* (Figure 8).

4. LITERATURE CITED

1. Abdel-Ghany SE, Ye H, Garifullina GF, Zhang L, Pilon-Smits EA, Pilon M. (2005) Iron-sulfur cluster biogenesis in chloroplasts. Involvement of the scaffold protein CplscA. *Plant Physiol.* 138, 161-172.
2. Allen JF. (2005) Photosynthesis: the processing of redox signals in chloroplasts. *Curr Biol.* 15, 929-932.
3. Aluru MR, Rodermeil SR. (2004) Control of chloroplast redox by the IMMUTANS terminal oxidase. *Physiol Plant.* 120, 4-11.
4. Amunts A, Drory O, Nelson N. (2007) The structure of a plant photosystem I supercomplex at 3.4 Å resolution. *Nature*, 44758-44763.
5. Aro EM, Ohad I. (2003) Redox regulation of thylakoid protein phosphorylation. *Antioxid Redox Signal.* 1, 55-67.
6. Balk J, Lobréaux S. (2005) Biogenesis of iron-sulfur proteins in plants. *Trends Plant Sci.* 7, 324-31.
7. Beinert H. (2000) Iron-sulfur proteins: ancient structures, still full of surprises. *J Biol Inorg Chem.* 5, 2-15.
8. Ben-Shem A, Frolov F, Nelson N. (2003) Crystal structure of plant photosystem I. *Nature.* 426, 630-635.
9. Bonardi V, Pesaresi P, Becker T, Schleiff E, Wagner R, Pfannschmidt T, Jahns P, Leister D. (2005) Photosystem II core phosphorylation and photosynthetic acclimation require two different protein kinases. *Nature.* 437, 1179-1182.
10. Bondarava N, De Pascalis L, Al-Babili S, Goussias C, Golecki JR, Beyer P, Bock R, Krieger-Liszkay A. (2003) Evidence that cytochrome *b*₅₅₉ mediates the oxidation of reduced plastoquinone in the dark. *J Biol Chem.* 278, 13554-13560.
11. Boyd JM, Pierik AJ, Netz DJ, Lill R, Downs DM. (2008) Bacterial ApcC Can Bind and Effectively Transfer Iron-Sulfur Clusters. *Biochemistry.* *In press*
12. Bych K, Kerscher S, Netz DJ, Pierik AJ, Zwicker K, Huynen MA, Lill R, Brandt U, Balk J (2008) The iron-sulphur protein Ind1 is required for effective complex I assembly. *EMBO J.* 27, 1736-1746.
13. Cramer WA, Zhang H, Yan J, Kurisu G, Smith JL. (2006) Transmembrane traffic in the cytochrome *b*_{6f} complex. *Annu Rev Biochem.* 75, 769-790.
14. DalCorso G, Pesaresi P, Masiero S, Aseeva E, Schünemann D, Finazzi G, Joliot P, Barbato R, Leister D. (2008) A complex containing PGRL1 and PGR5 is involved in the switch between linear and cyclic electron flow in *Arabidopsis*. *Cell.* 132, 273-285.

15. Dekker JP, Boekema EJ. (2005) Supramolecular organization of thylakoid membrane proteins in green plants. *Biochim Biophys Acta*. 1706, 12-39.
16. Ferreira K, Iverson T, Maghlaoui K, Barber J, Iwata S. (2004) Architecture of the photosynthetic oxygen-evolving center, *Science*. 303, 1831-1838.
17. Frazzon J, Dean DR. (2003) Formation of iron-sulfur clusters in bacteria: an emerging field in bioinorganic chemistry. *Curr Opin Chem Biol*. 2, 166-173.
18. Goldschmidt-Clermont M. (1998) Coordination of nuclear and chloroplast gene expression in plant cells. *Int. Rev. Cytol*. 177, 115-80.
19. Hausmann A, Aguilar Netz DJ, Balk J, Pierik AJ, Mühlenhoff U, Lill R. (2005) The eukaryotic P-loop NTPase Nbp35: an essential component of the cytosolic and nuclear iron-sulfur protein assembly machinery. *Proc Natl Acad Sci U S A*. 102, 3266-3271.
20. Jensen PE, Bassi R, Boekema EJ, Dekker JP, Jansson S, Leister D, Robinson C, Scheller HV. (2007) Structure, function and regulation of plant photosystem I. *Biochim Biophys Acta*. 1767, 335-52.
21. Johnson DC, Dean DR, Smith AD, Johnson MK. (2005) Structure, function, and formation of biological iron-sulfur clusters. *Annu Rev Biochem*. 74, 247-281.
22. Kamiya N, Shen JR. (2003) Crystal structure of oxygen-evolving photosystem II from *Thermosynechococcus vulcanus* at 3.7-Å resolution. *Proc Natl Acad Sci U S A*. 100, 98-103.
23. Kargul J, Barber J. (2008) Photosynthetic acclimation: structural reorganisation of light harvesting antenna - role of redox-dependent phosphorylation of major and minor chlorophyll *a/b* binding proteins. *FEBS J*. 275, 1056-1068.
24. Kessler D, Papenbrock J. (2005) Iron-sulfur cluster biosynthesis in photosynthetic organisms. *Photosynth Res*. 86, 391-407.
25. Kruk J, Strzalka K. (2001) Redox changes of cytochrome *b(559)* in the presence of plastoquinones. *J Biol Chem*. 276, 86-91.
26. Kurisu G, Zhang H, Smith J, Cramer W. (2003) Structure of the *b₆f* complex of oxygenic photosynthesis: tuning the cavity. *Science*. 302, 1009-1014.
27. Lezhneva L, Amann K, Meurer J. (2004) The universally conserved HCF101 protein is involved in assembly of [4Fe-4S]-cluster-containing complexes in *Arabidopsis thaliana* chloroplasts. *Plant J*. 37, 174-185.
28. Lill R, Mühlenhoff U. (2008) Maturation of Iron-Sulfur Proteins in Eukaryotes Mechanisms, Connected Processes, and Diseases. *Annu Rev Biochem*. 77, 669-700.
29. Loll B, Kern J, Saenger W, Zouni A, Biesiadka J. (2005) Towards complete cofactor arrangement in the 3.0 Å resolution structure of photosystem II. *Nature*. 438, 1040-1044.

30. Martin W, Herrmann RG. (1998) Gene transfer from organelles to the nucleus: how much, what happens, and Why? *Plant Physiol.* 118, 9-17.
31. Martin W, Stoebe B, Goremykin V, Hapsmann S, Hasegawa M, Kowallik, KV. (1998) Gene transfer to the nucleus and the evolution of chloroplasts, *Nature.* 393, 162-165.
32. Mereschkowsky C. (1905) Über Natur und Ursprung der Chromatophoren im Pflanzenreiche, *Biol. Centralbl.* 25, 593-604.
33. Minagawa J, Takahashi Y. (2004) Structure, function and assembly of Photosystem II and its light-harvesting proteins. *Photosynth Res.* 82, 241-63.
34. Müh F, Renger T, Zouni A. (2008) Crystal structure of cyanobacterial photosystem II at 3.0 Å resolution: a closer look at the antenna system and the small membrane-intrinsic subunits. *Plant Physiol Biochem.* 46, 238-264.
35. Munekage Y, Hashimoto M, Miyake C, Tomizawa K, Endo T, Tasaka M, Shikanai T. (2004) Cyclic electron flow around photosystem I is essential for photosynthesis. *Nature.* 429, 579-582.
36. Nelson N, Yocum CF. Structure and function of photosystems I and II. (2006) *Annu Rev Plant Biol.* 57, 521-565.
37. Netz DJ, Pierik AJ, Stümpfig M, Mühlhoff U, Lill R. (2007) The Cfd1-Nbp35 complex acts as a scaffold for iron-sulfur protein assembly in the yeast cytosol. *Nat Chem Biol.* 3, 278-286.
38. Ohad I, Dal Bosco C, Herrmann RG, Meurer J. (2004) Photosystem II proteins PsbL and PsbJ regulate electron flow to the plastoquinone pool, *Biochemistry.* 43, 2297-2308.
39. Peltier G, Cournac L. (2002) Chlororespiration. *Annu Rev Plant Biol.* 53, 523-550.
40. Pilon M, Abdel-Ghany SE, Van Hoewyk D, Ye H, Pilon-Smits EA. (2006) Biogenesis of iron-sulfur cluster proteins in plastids. *Genet Eng (N Y).* 27, 101-117.
41. Race HL, Herrmann RG, Martin W. (1999) Why have organelles retained genomes? *Trends Genet.* 15, 364-370.
42. Regel RE, Ivleva NB, Zer H, Meurer J, Shestakov SV, Herrmann RG, Pakrasi HB, Ohad I. (2001) Deregulation of electron flow within photosystem II in the absence of the PsbJ protein. *J Biol Chem.* 276, 41473-41478.
43. Richly E and Leister D. (2004) An improved prediction of chloroplast proteins reveals diversities and commonalities in the chloroplast proteomes of *Arabidopsis* and rice. *Gene.* 329, 11-16.
44. Rochaix JD. (2004) Genetics of the biogenesis and dynamics of the photosynthetic machinery in eukaryotes. *Plant Cell.* 16, 1650-1660.
45. Rochaix JD. (2007) Role of thylakoid protein kinases in photosynthetic acclimation. *FEBS Lett.* 581, 2768-2775.

46. Roose JL, Wegener KM, Pakrasi HB. (2007) The extrinsic proteins of Photosystem II. *Photosynth Res.* 92, 369-887.
47. Roy A, Solodovnikova N, Nicholson T, Antholine W, Walden WE. (2003) A novel eukaryotic factor for cytosolic Fe-S cluster assembly. *EMBO J.* 22, 4826-4835.
48. Rumeau D, Peltier G, Cournac L. (2007) Chlororespiration and cyclic electron flow around PSI during photosynthesis and plant stress response. *Plant Cell Environ.* 30, 1041-1051. Peltier G, Cournac L. (2002) Chlororespiration. *Annu Rev Plant Biol.* 53, 523-550.
49. Schwenkert S, Legen J, Takami T, Shikanai T, Herrmann RG, Meurer J. (2007) Role of the low-molecular-weight subunits PetL, PetG, and PetN in assembly, stability, and dimerization of the cytochrome *b₆f* complex in tobacco. *Plant Physiol.* 144, 1924-1935.
50. Schwenkert S, Umate P, Dal Bosco C, Volz S, Mlčochová L, Zoryan M, Eichacker LA, Ohad I, Herrmann RG, Meurer J. (2006) PsbI affects the stability, function, and phosphorylation patterns of photosystem II assemblies in tobacco. *J Biol Chem.* 281, 34227-34238.
51. Shi L-X, Schröder W. (2004) The low molecular mass subunits of the photosynthetic supracomplex, photosystem II, *Biochimica et Biophysica Acta.* 1608, 75-96.
52. Soll J, Schleiff E. (2004) Protein import into chloroplasts. *Nat Rev Mol Cell Biol.* 3, 198-208.
53. Sommer MS, Gould SB, Kawach O, Klemme C, Voss C, Maier U-G, Zauner S. (2006) Photosynthetic organelles and endosymbiosis. In *Genome Evolution in Eukaryotic Microbes* (Katz LA, Bhattacharya D, eds) pp. 94-108, Oxford University Press, Oxford
54. Stehling O, Netz DJ, Niggemeyer B, Rösser R, Eisenstein RS, Puccio H, Pierik AJ, Lill R. (2008) The human CIA component huNbp35 is essential for both cytosolic iron-sulfur protein assembly and iron homeostasis. *Mol Cell Biol.* In press
55. Stroebel D, Choquet Y, Popot J-L, Picot D. (2003) An atypical haem in the cytochrome *b₆f* complex. *Nature.* 426, 413-418.
56. Suorsa M, Regel RE, Paakkari V, Battchikova N, Herrmann RG, Aro EM. (2004) Protein assembly of photosystem II and accumulation of subcomplexes in the absence of low molecular mass subunits PsbL and PsbJ. *Eur J Biochem.* 271, 96-107.
57. Swiatek M, Kuras R, Sokolenko A, Higgs D, Olive J, Cinque G, Müller B, Eichacker LA, Stern D B, Bassi R, Herrmann RG, Wollman F-A. (2001) The chloroplast gene *ycf9* encodes a photosystem II (PSII) subunit, PsbZ, that participates in PSII supramolecular architecture. *The Plant Cell.* 13, 1347-1367.
58. Swiatek M, Regel R, Meurer J, Wanner G, Pakrasi HB, Ohad I, Herrmann RG. (2003) Effects of selective inactivation of individual genes for low-molecular-mass subunits on the assembly of photosystem II, as revealed by chloroplast transformation: the *psbEFLJ* operon in *Nicotiana tabacum*. *Mol. Gen. Genomics.* 268, 699-710.

59. Takahashi Y, Rahire M, Breyton C, Popot JL, Joliot P, Rochaix JD (1996) The chloroplast *ycf7* (*petL*) open reading frame of *Chlamydomonas reinhardtii* encodes a small functionally important subunit of the cytochrome *b₆f* complex. *EMBO J.* 15, 3498–3506.
60. Takahashi Y, Tokumoto U. (2002) A third bacterial system for the assembly of iron-sulfur clusters with homologs in archaea and plastids. *J Biol Chem.* 277, 28380-28383.
61. Thornton LE, Roose JL, and Pakrasi H. (2005) in *Photosystem II: the Water/Plastoquinone Oxido-reductase in Photosynthesis* (Wydrzynski T and Satoh K, eds) pp. 121-138, Kluwer Academic Publishers, Dordrecht, The Netherlands
62. Touraine B, Boutin JP, Marion-Poll A, Briat JF, Peltier G, Lobréaux S. (2004) Nfu2: a scaffold protein required for [4Fe-4S] and ferredoxin iron-sulphur cluster assembly in *Arabidopsis* chloroplasts. *Plant J.* 40, 101-111.
63. Umate P, Schwenkert S, Karbat I, Dal Bosco C, Mlcòchová L, Volz S, Zer H, Herrmann RG, Ohad I, Meurer J. (2007) Deletion of PsbM in tobacco alters the Q_B site properties and the electron flow within photosystem II. *J Biol Chem.* 282, 9758-9767.
64. Vainonen JP, Hansson MA, Vener V. (2005) STN8 protein kinase in *Arabidopsis thaliana* is specific in phosphorylation of photosystem II core proteins. *J. Biol. Chem.* 280, 33679-33686.
65. Van Hoewyk D, Abdel-Ghany SE, Cohu CM, Herbert SK, Kugrens P, Pilon M, Pilon-Smits EA. (2007) Chloroplast iron-sulfur cluster protein maturation requires the essential cysteine desulfurase CpNifS. *Proc Natl Acad Sci U S A.* 104, 5686-5691.
66. Yabe T, Morimoto K, Kikuchi S, Nishio K, Terashima I, Nakai M. (2004) The *Arabidopsis* chloroplastic NifU-like protein CnfU, which can act as an iron-sulfur cluster scaffold protein, is required for biogenesis of ferredoxin and photosystem I. *Plant Cell.* 16, 993-1007.
67. Ye H, Abdel-Ghany SE, Anderson TD, Pilon-Smits EA, Pilon M. (2006) CpSufE activates the cysteine desulfurase CpNifS for chloroplastic Fe-S cluster formation. *J Biol Chem.* 281, 8958-8969.
68. Ye H, Garifullina GF, Abdel-Ghany SE, Zhang L, Pilon-Smits EA, Pilon M. (2005) The chloroplast NifS-like protein of *Arabidopsis thaliana* is required for iron-sulfur cluster formation in ferredoxin. *Planta.* 220, 602-608.
69. Zito F, Finazzi G, Delosme R, Nitschke P, Picot D, Wollman F-A. (1999) The Q_o site of cytochrome *b₆f* complexes controls the activation of the LHCII kinase. *EMBO J.* 18, 2961-2969.

5. ORIGINAL PUBLICATIONS AND MANUSCRIPTS AS PART OF THE CUMULATIVE THESIS

1. **Schwenkert S^{*}, Umate P^{*}, Dal Bosco C, Volz S, Mlčochová L, Zoryan M, Eichacker LA, Ohad I, Herrmann RG and Meurer J.** (2006) PsbI affects the stability, function, and phosphorylation patterns of photosystem II assemblies in tobacco. *J Biol Chem.* 281, 34227-34238.

S. S. performed the Western, Blue Native and phosphorylation analysis and was involved in writing the manuscript.

2. **Schwenkert S, Legen J, Takami T, Shikanai T and Herrmann RG, Meurer J.** (2007) Role of the low-molecular-weight subunits PetL, PetG, and PetN in assembly, stability, and dimerization of the Cyt *b₆f* complex in tobacco. *Plant Physiol.* 144, 1924-1935.

S. S. performed all experiments except the generation of the knock-out plants and the measurement of cyclic electron flow. The manuscript was written by S. S. and revised by J. M.

3. **Umate P^{*}, Schwenkert S^{*}, Karbat I, Dal Bosco C, Mlčochová L, Volz S, Zer H, Herrmann RG, Ohad I and Meurer J.** (2007) Deletion of PsbM in tobacco alters the Q_B site properties and the electron flow within photosystem II. *J Biol Chem.* 282, 9758-9767.

S. S. performed Northern, Western, Blue Native, phosphorylation and spectroscopic analysis and was involved in writing the manuscript.

4. Umate P^{*}, Fellerer C^{*}, Schwenkert S, Zoryan M, Eichacker LA, Sadanandam A, Ohad I, Herrmann RG and Meurer J. (2008) Impact of PsbTc on electron flow, assembly and phosphorylation patterns of photosystem II in tobacco. *(in revision)*

S. S. performed phosphorylation, Blue Native and photoinhibition analysis. S. S. was involved in planning experiments and in the writing of the manuscript.

5. Schwenkert S, Frazzon J, Gross J, Bill E, Netz D, Pierik A, Lill R and Meurer J. (2008) Chloroplast HCF101 is a scaffold protein for [4Fe4S] cluster assembly. *(in preparation)*

The experiments were mainly performed by S. S. Mössbauer and EPR analyses were performed in collaboration with Dr. Eckhard Bill and Prof. Roland Lill. The manuscript was written by S. S. and revised by J. M.

* Both authors contributed equally to this work.

I hereby confirm the above statements

Serena Schwenkert

PD Dr. Jörg Meurer

PsbI Affects the Stability, Function, and Phosphorylation Patterns of Photosystem II Assemblies in Tobacco*

Received for publication, May 22, 2006, and in revised form, August 18, 2006 Published, JBC Papers in Press, August 18, 2006, DOI 10.1074/jbc.M604888200

Serena Schwenkert^{†1}, Pavan Umate^{‡1,2}, Cristina Dal Bosco[‡], Stefanie Volz[‡], Lada Mlčochová[‡], Mikael Zoryan[‡], Lutz A. Eichacker[‡], Itzhak Ohad[§], Reinhold G. Herrmann[‡], and Jörg Meurer^{‡3}

From the [†]Department Biology I, Botany, Ludwig-Maximilians-University Munich, Menzingerstrasse 67, 80638 Munich, Germany and [§]Department of Biological Chemistry and the Minerva Center of Photosynthesis Research, The Hebrew University of Jerusalem, Jerusalem 91904, Israel

Photosystem II (PSII) core complexes consist of CP47, CP43, D1, D2 proteins and of several low molecular weight integral membrane polypeptides, such as the chloroplast-encoded PsbE, PsbF, and PsbI proteins. To elucidate the function of PsbI in the photosynthetic process as well as in the biogenesis of PSII in higher plants, we generated homoplastomic knock-out plants by replacing most of the tobacco *psbI* gene with a spectinomycin resistance cartridge. Mutant plants are photoautotrophically viable under green house conditions but sensitive to high light irradiation. Antenna proteins of PSII accumulate to normal amounts, but levels of the PSII core complex are reduced by 50%. Bioenergetic and fluorescence studies uncovered that PsbI is required for the stability but not for the assembly of dimeric PSII and supercomplexes consisting of PSII and the outer antenna (PSII-LHCII). Thermoluminescence emission bands indicate that the presence of PsbI is required for assembly of a fully functional Q_A binding site. We show that phosphorylation of the reaction center proteins D1 and D2 is light and redox-regulated in the wild type, but phosphorylation is abolished in the mutant, presumably due to structural alterations of PSII when PsbI is deficient. Unlike wild type, phosphorylation of LHCII is strongly increased in the dark due to accumulation of reduced plastoquinone, whereas even upon state II light phosphorylation is decreased in $\Delta psbI$. These data attest that phosphorylation of D1/D2, CP43, and LHCII is regulated differently.

Analyses of the polypeptide composition of the oxygen-evolving PSII,⁴ the most complex assembly of the thylakoid system, have uncovered the presence of the intriguing number of 16 low molecular weight proteins (LMWs) that are generally conserved from cyanobacteria to higher plants (for review, see Refs. 1–3). In photosynthetic eukaryotes, the majority, namely

PsbE, F, H, I, J, K, L, M, N, Tc, and Z, are plastome-encoded; the remaining five, PsbR, Tn, W, X, and Y1/Y2, are encoded by nuclear genes (4). The high homology between the plastome-encoded and cyanobacterial LMWs suggests conserved roles, as has been proposed for PsbE and PsbF, the α and β subunits of the two-chain cytochrome *b*₅₅₉. Cytochrome *b*₅₅₉ is a mandatory constituent of PSII that plays a major role in PSII function and biogenesis (5–7).

The LMW components of PSII are generally bitopic, *i.e.* harbor a single transmembrane helix, and in all members, except for PsbK and PsbTc, the N-terminal domain has been suggested to be exposed to the stromal face of the membrane complex (PsbE, PsbF, PsbH, PsbI, PsbJ, PsbL, and PsbM) (for review, see Ref. 2). PsbH is the only known LMW component, which is phosphorylated in the chloroplast, but its phosphorylation is missing in cyanobacteria (8). Apart from PsbH, the other major thylakoid phosphoproteins are those of the light-harvesting protein complex (LHCII) and of the PSII core (CP43 and the reaction center proteins D1 and D2) (9–11).

Biochemical approaches and x-ray crystallography have been instrumental in determining the localization of the LMW proteins within the PSII assembly. For the thermophile cyanobacterial PSII core complex, the location of these proteins has been specified with increasing precision (12–18). These components are either located at the periphery of the PSII core monomers or centrally, at the interface of the two PSII monomers forming a dimer (17). However, besides the *psbEFLJ* operon products (19, 7), relatively little is known about the function of the other LMWs, their interactions with PSII core components, or their relevance for lipid-protein interactions for the assembly and the energy transfer processes.

The majority of LMWs of PSII in cyanobacteria define the boundary between the dimeric complex and the surrounding lipids of the thylakoid membrane, whereas in the chloroplast many of these proteins form the border between the core complex and the minor light-harvesting antenna system, CP29, CP26, and CP24, and presumably also the trimeric LHCII, constituting the mobile antenna of the complex (3). Consequently, the LMWs in the chloroplast may be involved in processes different from those of their cyanobacterial counterparts and, for instance, affect regulation of state transition or antenna-related processes like light-trapping or non-photochemical quenching (20–21). Because of an evolutionary functional divergence, inactivation of homologous LMWs in cyanobacteria and green algae/higher plants can lead to quite different phenotypes, as

* This work was supported by German Science Foundation Grants SFB184 and SFB TR1. The costs of publication of this article were defrayed in part by the payment of page charges. This article must therefore be hereby marked "advertisement" in accordance with 18 U.S.C. Section 1734 solely to indicate this fact.

¹ These authors contributed equally to this work.

² Recipient of a fellowship from the Deutscher Akademischer Austauschdienst.

³ To whom correspondence should be addressed. Tel.: 49-89-17861288; Fax: 49-89-1782274; E-mail: joerg.meurer@lrz.uni-muenchen.de.

⁴ The abbreviations used are: PS, photosystem; BN, blue native; DCMU, 3-[3', 4'-dichlorophenyl]-1,1-dimethylurea; LHCII, light-harvesting protein complex (outer antenna of photosystem II); LMW, low molecular weight; RC, reaction center; TL, thermoluminescence; WT, wild type.

PsbI Affects Phosphorylation, Stability, and Function of PSII

has recently been shown for PsbJ and PsbL (22). Although the loss of these proteins has only a minor effect in *Synechocystis* sp. PCC6803, relatively dramatic changes of PSII function and stability have been noted in the corresponding tobacco mutants. Inactivation of PsbJ and PsbL in plants affects the Q_A re-oxidation kinetics and the back-electron flow from plastoquinol to Q_A , respectively (19, 22). Similarly, inactivation of PsbH, PsbI, and PsbK in cyanobacteria and chloroplasts of algae resulted in quite diverse phenotypes (for details and review, see Refs. 1 and 2). It is, therefore, conceivable to conduct comparative studies on different evolutionary lineages in a phylogenetic context. Moreover, the biogenesis of PSII components differs in cyanobacteria and higher plants. Because of the dual genetic origin of the thylakoid system in higher plants, the biogenesis depends largely on factors encoded by the nuclear genome. For instance, HCF136, one of these factors, is essential for the biogenesis of the PSII core complex in higher plants, but its homologous protein appears to be largely dispensable in cyanobacteria (23, 24).

The assignment of several LMW subunits including PsbI (4.8 kDa) to the x-ray structure of PSII still remains to be settled (25, 26). Earlier studies of the cyanobacterial PSII x-ray structure placed the transmembrane helix of PsbI opposite to the dimerization axis and close to Chlz D2 (13), whereas the crystallographic studies located the PsbI protein at the periphery of PSII core, in close proximity to Chlz D1, the helices A and B of the D1 protein, and the helix VI of CP43 (17, 18). PsbI was present in PSII reaction center (RC) preparations of both spinach and cyanobacteria (27). No knock-out strains for *psbI* are currently available from higher plants. Mutants lacking PsbI have been generated from *Chlamydomonas reinhardtii* (28) and *Synechocystis* (29). Inactivation of *psbI* in *Synechocystis* and *Thermosynechococcus elongatus* strain BP-1 caused some reduction of PSII activity, resulting in decreased oxygen evolution to 70–80% of WT levels, but the mutants grew photoautotrophically. The *Synechocystis* $\Delta psbI$ mutant was found to be slightly more sensitive to light than the corresponding WT (29). Deletion of *psbI* in *C. reinhardtii* caused a more severe effect compared with that in cyanobacteria (28). Although the *C. reinhardtii* $\Delta psbI$ mutant grows photoautotrophically under low light, its growth rate was quite sensitive to high light. Both the amounts of PSII and the oxygen evolution activity in the mutant were found to be only 10–20% of WT levels.

In an attempt to evaluate the roles as well as biogenetic and phylogenetic aspects of the enigmatic LMW PSII subunits, we have systematically inactivated individual genes using a transplastomic approach in tobacco. Here we demonstrate that PsbI exerts a crucial role in the stability of dimeric PSII and the intrinsic electron flow as well as in the phosphorylation of proteins of the core complex and the light-harvesting antenna of PSII in tobacco.

EXPERIMENTAL PROCEDURES

Knock-out Construct Strategy for $\Delta psbI$ —In the tobacco plastome the *psbI* gene is located downstream of *psbK*, which also encodes a LMW PSII polypeptide (30–32). In a transplastomic approach, the *psbI* gene of *Nicotiana tabacum* cv. Petit Havana, 110 bp in length (nucleotide position 8398–8508 on

the plastid chromosome; GenBankTM/EBI accession number Z00044), was inactivated by replacing most of the gene with the terminator-less, chimeric amino glycoside 3' adenylyl transferase (*aadA*) cassette conferring resistance to spectinomycin in reading frame orientation (7). For this, two PCR reactions were performed with primers *psbI-1* (5'-GGA TCC AAA ATG CAA TTA TCT CTC C-3') and *psbI-2* (5'-AAG CTT GCA GCT GAA TTC TAC ACA ATC TCC AAG ATG-3') and with primers *psbI-3* (5'-GAA TTC AGC TGC AAG CTT ATCCCG GAC GTA ATC CTG G-3') and *psbI-4* (5'-ATC TCG AGA TTA CAA CTA TAA CAG GC-3'). *PsbI-2* and *psbI-3* generated overlapping products and introduced a diagnostic EcoRI restriction site. The third reaction was performed with primers *psbI-1* and *psbI-4* using the first PCR product as a template. Primers *psbI-1* and *psbI-4* introduced two flanking restriction sites, BamHI and XhoI, used for cloning into the vector pBlue-script II KS- (Stratagene Inc., La Jolla, CA). The presence of a unique restriction site, BtrI, within the disrupted *psbI* gene allowed the insertion of the *aadA* cassette between the EcoRI and BtrI restriction sites. The details of the map construction, location of restriction sites, and primer annealing positions are shown in Fig. 1 A and B. The resulting construct (carrying the *aadA* cassette in the same polarity as *psbI*) was sequenced to verify correct copying of the gene and used for plastid transformation employed in a biolistic approach (33). Selection and culture conditions of the transformed material as well as the check for homoplastomy were carried out as described (7).

Independent transformants were obtained displaying an identical phenotype (data not shown). The transformed material was first grown (12-h photoperiod at 25 °C, 10–20 $\mu\text{mol m}^{-2} \text{s}^{-1}$ light intensity) for 4–5 weeks on Murashige and Skoog (34) medium supplemented with 3% sucrose, 0.8% agar, and 500 mg/liter spectinomycin. Before transferring the plants to the greenhouse, they were kept for 4–5 weeks on Murashige and Skoog medium without sucrose. If not otherwise indicated, all analyses were carried out with young leaves of ~2-month-old plants grown *in vitro* and under greenhouse conditions (day 27 °C, night 20 °C), respectively. Tobacco lines carrying the *aadA* cassette in a neutral insertion site and referred to as RV plants were used as WT control plants (22).

SDS-PAGE and Immunoblot Analysis—Thylakoid membrane proteins of 3–4-week-old plants were isolated and solubilized for SDS-PAGE as described (7). Proteins separated by SDS-Tris-glycine-PAGE (15% acrylamide) (35) were electroblotted to polyvinylidene difluoride membranes (Amersham Biosciences), incubated with monospecific polyclonal antisera (7), and visualized by the enhanced chemiluminescence technique (Amersham Biosciences). Equal loading of proteins was always checked by zinc-imidazole staining of the gels before blotting.

Separation of Thylakoid Membrane Complexes by Sucrose Density Gradient Centrifugation—Thylakoid membranes used for the separation of protein complexes by sucrose density gradient centrifugation were isolated as described earlier (7).

Resolution of Isolated Thylakoid Membrane Complexes by Blue Native (BN)-PAGE and *in Vivo* Labeling—Labeling of thylakoid membrane proteins was performed by incubation of cotyledons with [³⁵S]methionine for 40 min as described (36).

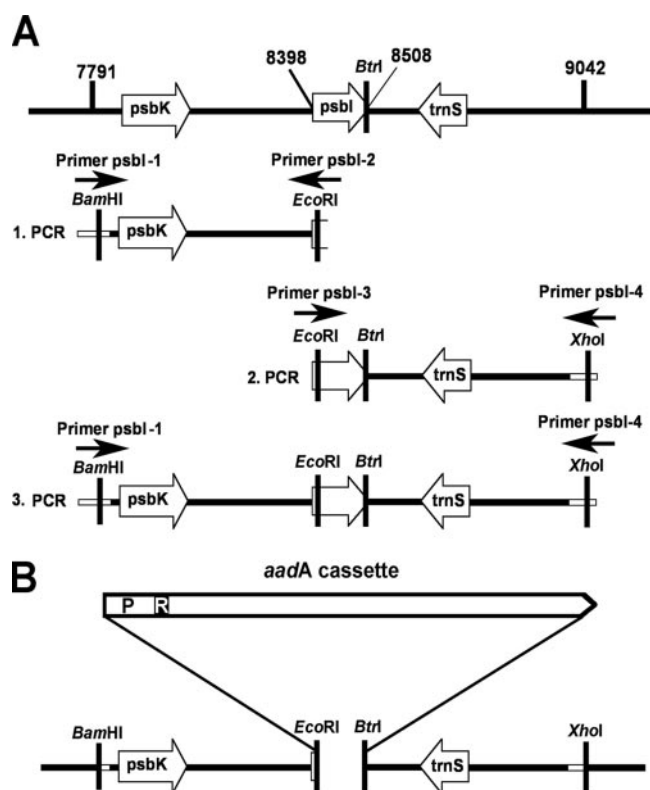


FIGURE 1. Construct map for replacing most of *psbI* with the *aadA* cassette. *A*, the PCR-based site-directed mutagenesis strategy for disruption of *psbI* and for introduction of the restriction sites *EcoRI*, *BamHI*, and *XhoI* using 4 primer combinations (primers *psbI* 1, 2, 3, and 4) is indicated. The base-pair positions of the gene *psbI* (8398–8508) and the PCR primers containing introduced restriction sites are indicated in brackets. Plasmid DNA was used as the template for the first two PCR reactions, and the resulting products were used for the third PCR. The arrows indicate the transcriptional direction of the genes *psbK*, *psbI*, and *trnS*. *BtrI*, restriction site downstream of *psbI*. The resulting PCR product was ligated into the *BamHI* and *XhoI* sites of the transformation vector pBluescript KS– (Stratagene). *B*, the map shows the introduction of the *EcoRI*- and *SmaI*-digested aminoglycoside 3' adenylyl transferase (*aadA*) selection cassette into the disrupted *psbI* gene at the *BtrI* and the introduced *EcoRI* restriction sites. *P*, 16 S rDNA promoter; *R*, ribosome binding site.

BN-PAGE analysis was performed as described earlier (37). All solutions were supplemented with 10 mM NaF. Thylakoid membranes equivalent to 30 μg of chlorophyll were solubilized with dodecyl- β -D-maltoside (1% final concentration) and separated on a 4–12% acrylamide gradient. After electrophoresis, lanes of the BN polyacrylamide gel were excised, denatured, and run in the second dimension in SDS-PAGE with 15% acrylamide and 4 M urea. Subsequently, the gels were silver-stained or used for immunoblotting. Individual spots were labeled according to their determination by mass spectrometry (38).

In Vitro Phosphorylation of PSII Proteins—Redox-dependent LHCII phosphorylation of WT and mutant thylakoids was carried out as described (39). Activation of the protein kinase in the dark was obtained by the addition of reduced duroquinol (1 mM) (40). Phosphorylation was terminated by the addition of denaturing sample buffer, and the sample proteins were resolved by SDS-PAGE. The extent of phosphorylation was detected with phosphothreonine antibodies (Zymed Laboratories Inc., Berlin, Germany; New England Biolabs, County Road, MA).

Chlorophyll *a* Fluorescence Induction Kinetics—Chlorophyll *a* fluorescence induction kinetics of tobacco WT and mutant leaves was measured using a pulse-modulated fluorimeter (PAM101, Waltz, Effeltrich, Germany) (22). Leaves were dark-adapted for 5 min before the fluorescence measurements. The minimal (F_0) and maximal (F_m) fluorescence yield and the variable fluorescence (F_v), calculated as $(F_m - F_0)$ as well as the ratio F_v/F_m , which reflects the potential yield of the photochemical reaction of PSII (41), were recorded at room temperature. Photochemical and non-photochemical quenching (qP and NPQ, respectively) were calculated as $(F_m - F_m')/F_m'$ and $(F_m' - F)/F_m' - F_0$, respectively (42).

Measurements of PSI Activity—Photosystem I activity was measured on leaves as absorption changes at 830 nm induced by far red light (ΔA_{max}) (730 nm; 12 watts m^{-2}) and in the absence or presence of actinic light (ΔA) (650 nm, 20 and 250 μmol of photons $\text{m}^{-2} \text{s}^{-1}$) using the PSI attachment of PAM101 (Walz, Effeltrich, Germany) (43). The oxidation status of PSI at the light intensities indicated was expressed as the fraction $\Delta A/\Delta A_{\text{max}}$.

Thermoluminescence (TL) Measurements—TL measurements were performed using a home built apparatus (22). Thylakoid fractions were prepared by grinding leaves in a buffer containing 20 mM Tris-HCl, pH 7.4, 5 mM MgCl_2 , 20 mM NaCl, and 100 mM sorbitol. Homogenized material was filtered through nylon micromesh and used immediately for measurements. Samples (200 μl ; 10–15 μg chlorophyll/sample) were dark-adapted on the TL stage at 20 $^{\circ}\text{C}$ for 3 min and then rapidly frozen to -20°C . The samples were then excited with saturating flashes delivered by a xenon arc discharge lamp (EG&G, 0.05-microfarad capacitor, charged at 1000 V, 3 μs at 70% light emission). TL was recorded upon heating the sample at a constant rate of 0.6 $^{\circ}\text{C} \text{s}^{-1}$. The herbicides DCMU (3-[3',4'-dichlorophenyl]-1,1-dimethylurea) or Ioxynil (4-hydroxy-3,5-di-iodobenzonitrile) were added at concentrations of 10 and 5 μM , respectively, to inhibit the electron transfer from Q_A to Q_B . For measuring the B band ($Q_B/S_2/S_3$ recombination) oscillations, the dark-adapted samples were slowly cooled, and consecutive flashes (1–6 flashes, time interval 300 ms) were applied between 1 and 0 $^{\circ}\text{C}$ followed by rapid cooling to -10°C .

Low Temperature Fluorescence Measurements—Low temperature (77 K) emission spectra were performed with thylakoids prepared from young dark-adapted leaves of WT and ΔpsbI plants (44). Thylakoid membranes (40 μg chlorophyll/ml) were transferred into a glass tube (0.7-mm internal diameter) for fluorescence measurements and immediately frozen in liquid nitrogen. Fluorescence was excited at 440 nm, and the emission was recorded between 650 and 800 nm. All spectra were recorded with a Jobin Yvon Spex Fluorolog spectrofluorometer (Horiba, France) equipped with a photomultiplier (R 374, Hamamatsu, Japan). Slits of 1 nm were used.

Photoinhibition—To determine the sensitivity of PSII to oxidative stress, leaves of WT and ΔpsbI plants grown under greenhouse conditions were exposed to 500 μmol of photons $\text{m}^{-2} \text{s}^{-1}$, and the photoinactivation of PSII was measured as $\Delta(F_v/F_m)/\text{time}$. To estimate the PSII recovery process during the exposure to the high light treatment, leaf discs were exposed to a similar light treatment after prefiltration with a

PsbI Affects Phosphorylation, Stability, and Function of PSII

TABLE 1
Spectroscopic and fluorimetric data of WT and $\Delta psbI$ mutant

	Non-photochemical quenching ^a		Photochemical quenching ^b		Redox state of PSI ($\Delta A/\Delta A_{max}$) ^c		F_{PSI}/F_{PSII} ^d	
	20 $\mu E/m^2 s^{-1}$	250 $\mu E/m^2 s^{-1}$	20 $\mu E/m^2 s^{-1}$	250 $\mu E/m^2 s^{-1}$	20 $\mu E/m^2 s^{-1}$	250 $\mu E/m^2 s^{-1}$	Dark	50 $\mu E/m^2 s^{-1}$ (650 nm)
WT	0.17 \pm 0.03	1.21 \pm 0.21	0.94 \pm 0.01	0.76 \pm 0.12	1	28	2.28 \pm 0.13	2.53 \pm 0.09
$\Delta psbI$	0.24 \pm 0.06	0.77 \pm 0.25	0.99 \pm 0.02	0.78 \pm 0.09	7	66	4.23 \pm 0.20	3.77 \pm 0.17

^a Quenching of excitation states of PSII reaction centers mostly by heat dissipation.

^b Quenching of excitation states of PSII reaction centers by photochemistry.

^c $\Delta A/\Delta A_{max}$, P700 oxidation ratio.

^d F_{PSI}/F_{PSII} , ratio of 77K fluorescence emitted by PSI and PSII.

solution of D-threo-chloramphenicol (200 $\mu g ml^{-1}$) for 30 min before the light exposure. For control purposes leaf discs were incubated in water.

To assess the photoinhibition and the capacity to recover from photoinhibition, leaves were also exposed to 1500 μmol of photons $m^{-2} s^{-1}$ until a similar loss of activity was reached in both WT and $\Delta psbI$ (measured as $F_v/F_m = 0.17$), and subsequently incubated at low light (3 μmol photons $m^{-2} s^{-1}$) for up to 6 h, measuring the F_v/F_m level every 1 h.

RESULTS

Disruption of *psbI* in the tobacco plastid chromosome caused an increased light sensitivity, but young leaves appeared normal green in independent transformants. Comparable with $\Delta psbZ$ but different from $\Delta psbE$, $-F$, $-L$, or $-J$ (19, 7), $\Delta psbI$ was capable of growing photoautotrophically on soil under greenhouse conditions. Initial fluorescence kinetic data of $\Delta psbI$ suggested a defect in PSII (see below).

$\Delta psbI$ Mutants Exhibit a Low Photosystem II Quantum Yield—Measurements of PSII quantum yield of $\Delta psbI$ plants grown autotrophically exhibited an increased minimal fluorescence, F_0 , causing a reduced ratio F_v/F_m between 0.25 and 0.74 depending on the leaf age as compared with a stable ratio of 0.81 ± 0.02 in the WT. The lower value was found exclusively in older leaves, indicating a gradual loss of quantum efficiency with aging of the leaf. The average F_v/F_m value in rapidly expanding young leaves detached from the upper part of the plants was in the range of 0.66–0.74. Fluorimetric measurements indicated a higher NPQ (0.24 ± 0.06 versus 0.17 ± 0.03 in WT) elicited at low actinic light intensity (20 μmol of photons $m^{-2} s^{-1}$) and a lower NPQ (0.77 ± 0.25 versus 1.21 ± 0.21 in WT) when the actinic light intensity was raised to 250 μmol of photons $m^{-2} s^{-1}$. The photochemical quenching (qP) part in $\Delta psbI$ remained almost unchanged at both light regimes (0.99 ± 0.02 versus 0.94 ± 0.01 in WT and 0.78 ± 0.09 versus 0.76 ± 0.12 in WT at 20 and 250 μmol of photons $m^{-2} s^{-1}$, respectively) (Table 1).

To compare the efficiency of the electron flow between PSII and PSI with that between PSI and its final electron acceptors in intact leaves, the extent of PSI oxidation expressed as $\Delta A/\Delta A_{max}$ was monitored using absorption changes at 830 nm in the background of different intensities of actinic light in the steady state (20 and 250 μmol of photons $m^{-2} s^{-1}$, 650 nm) (Table 1). The results showed significantly higher levels of oxidized PSI in the steady state excited by both actinic light intensities in the mutant as compared with the WT (Table 1). The results are indicative of a significantly lower rate of electron

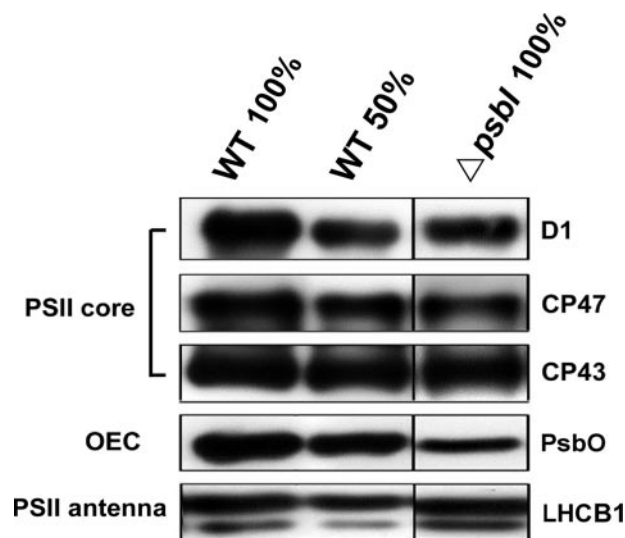


FIGURE 2. Immunoblot analysis of thylakoid membrane proteins of WT and $\Delta psbI$. Thylakoid proteins from 4-week-old plant material were isolated, separated by SDS-PAGE, electroblotted to polyvinylidene difluoride membranes, and probed with antisera as indicated. Eight (100%) and four (50%) μg of thylakoid membrane proteins were loaded per lane. OEC, oxygen evolving complex.

flow from PSII to the plastoquinone pool in the mutant relative to plastoquinol oxidation activity *via* PSI.

Levels of PSII Core Components Are Specifically Reduced in the $\Delta psbI$ Mutant—To corroborate that inactivation of *psbI* did not affect the expression of genes for PSII antenna and other photosynthetic membrane complexes, immunoblotting using specific antisera against distinct thylakoid proteins was performed. The data obtained confirmed that the stationary protein levels of PSII antenna (LHCb1, CP29, CP26, and CP24), PSI (PsaF and LHCI), ATP synthase (α and β subunits), and cytochrome b_6/f complex (cytochrome *f*) were comparable with those of the WT (Fig. 2 and data not shown). Levels of the PSII core proteins D1, CP43, and CP47 as well as of the oxygen evolving complex protein PsbO were reduced to about 50% compared with the WT, indicating that the relative content of the PSII RC is lower in $\Delta psbI$ (Fig. 2).

The Q_A Midpoint Potential Is Affected in $\Delta psbI$ as Measured by Charge Recombination—Charge recombination between the different oxidation states (S_1 – S_3) of the Mn_4Ca complex at the electron donor side and reduced primary and secondary semiquinone acceptors of PSII Q_A or Q_B , respectively, serves as an indicator of the forward and back electron flow activity within photosystem II (45, 46). During the recombination process P_{680+} is generated that is reduced by electron flow from Q_B or Q_A , a process accompanied by luminescence (46, 47). Back

electron flow uphill the redox potential requires energy input that can be supplied by heat and thus the glow generated by the charge recombination in darkness is termed thermoluminescence (TL) (48). The temperature at which the luminescence is maximal is related to the energy gap between the recombining pairs. The maximal TL signal generated by recombination of $Q_B^-/S_{2,3}$ pairs, the B band emission, occurs in tobacco thylakoids at about 35 °C (22, 49). To measure the recombination of the Q_A^-/S_2 pair, one has to block reduction of the Q_B quinone during the excitation of the sample by a single turnover flash. This can be achieved by addition of electron flow inhibitors binding specifically at the Q_B site such as the urea or phenol derived herbicides, DCMU or Ioxynil, respectively. Because back electron flow from Q_A^- to P_{680+} presents a lower energy gap, the resulting TL signal, termed Q band, occurs at a lower temperature. In WT tobacco, the Q band in presence of DCMU occurs at about 15 °C, whereas that obtained in presence of Ioxynil occurs at about 3 °C (Fig. 3) (22, 50, 51). This difference between the Q band temperature resulting from the recombination of the same charge separated pair (Q_A^- to P_{680+}) is ascribed to changes in the conformation of the Q_B site upon binding of DCMU that affects the midpoint potential of the Q_A site. Conversely, binding of Ioxynil to the Q_B site is supposed not to affect the midpoint potential of the Q_A (50). Thus, use of these herbicides may give information not only on their efficiencies to bind to the Q_B site but also on the effect of their binding on the conformation of this site and the resulting effect on its interaction with the Q_A site expressed as alterations in the midpoint potential $Q_B^-/Q_B:Q_A/Q_A^-$.

Measurements of the TL emission of $\Delta psbI$ thylakoids showed that the peak temperatures of the B band and that of the Q band induced by the addition of Ioxynil were the same, 35 and 3 °C, respectively, for both mutant and WT control (Figs. 3, A and B). However, the Q band was downshifted to 10 °C in DCMU-treated mutant samples (Fig. 3B).

In light-exposed thylakoids, the Q_B site quinone exhibits a binary oscillation between the quinone and semiquinone reduced states. The double-reduced quinone is protonated to quinol that leaves the site and is replaced by a quinone molecule from the plastoquinone pool. Upon transition from light to darkness, half of the PSII population is in the Q_B^- and half in the Q_B states. In illuminated thylakoids, the stable S-states of the Mn_4Ca complex exhibit a four steps oscillation, S_0 and three increasing oxidation steps, S_1 to S_3 . The states S_4 and S_4' are highly unstable, extract 4 electrons from water, releasing dioxygen and returning to the S_0 state (52).

Upon transition to darkness, the population of PSII consists of the S_0 to S_3 states. However, during dark adaptation at 25 °C for 3 min back electron flow from the Q_B^- population to that of the oxidized states of the Mn_4Ca complex and, thus, charge recombination, will occur driven by the thermal energy and potential difference between the oxidized S_2 and S_3 states and Q_B^- . The S_1 state practically does not recombine (47). Under the experimental condition used, this will result in a final ratio of 75% S_1 , 25% S_0 and practically equal amounts of Q_B and Q_B^- (47). Consecutive single turnover excitations of dark-adapted thylakoids leads to oscillations of the ratio of recombining $Q_B^-/S_3:Q_B^-/S_2$ pairs and respective light emission with a higher

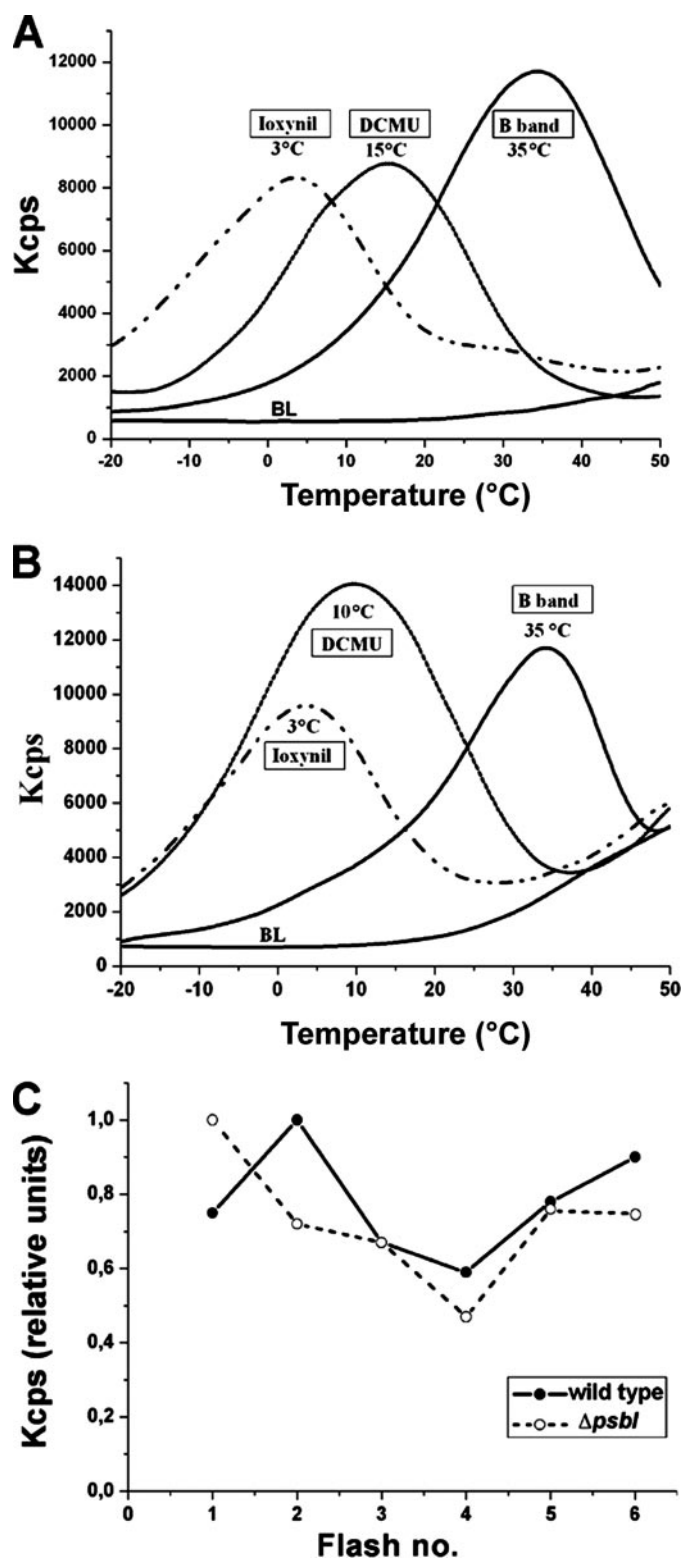


FIGURE 3. Thermoluminescence Q and B band emissions and oscillations of the B band in $\Delta psbI$ mutant and WT. Shown are thylakoids of WT (A) and mutants (B) were dark-adapted on the TL stage at 20 °C for 3 min. Before cooling to -20 °C, two saturating single turnover flashes were applied at 0 °C to induce the B band emission. Q band emission was induced by flashing at -20 °C in the presence of the inhibitors Ioxynil (5 μM) and DCMU (10 μM). Peak temperature positions for the TL glow Q and B band are indicated. C, the maxima of the oscillating B band emissions are expressed relative to consecutive flashes (1–6) at 0 °C as indicated. Emission is expressed as number of photons per second (cps).

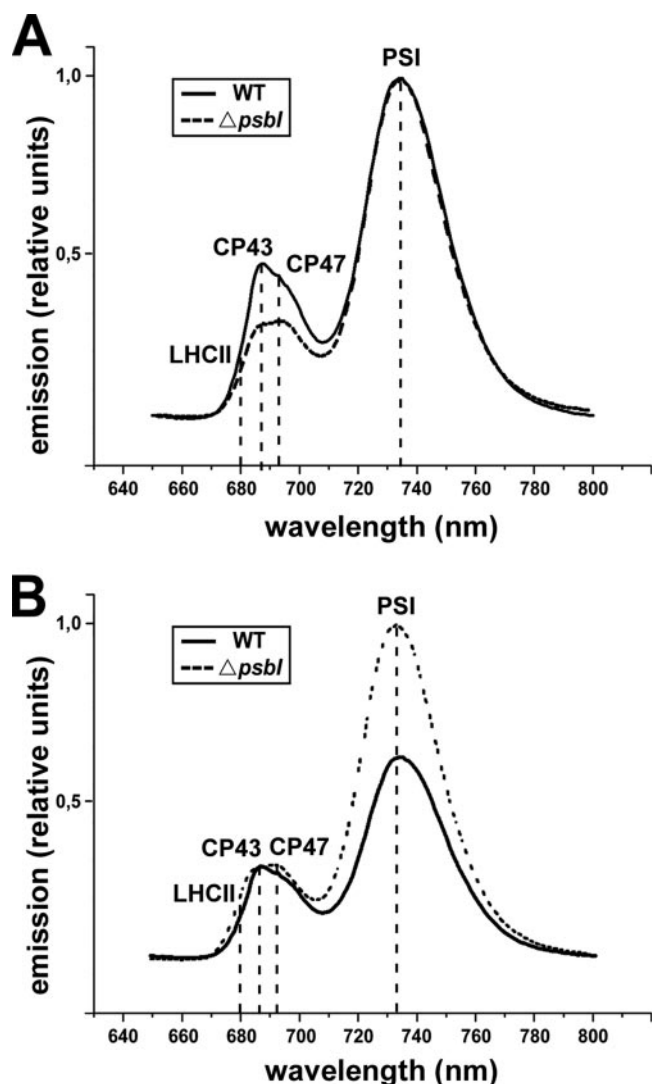


FIGURE 4. Low temperature (77 K) fluorescence spectra. The fluorescence emission of thylakoid samples was excited at 440 nm and recorded between 650 and 800 nm using a sensitive photomultiplier. Young leaves of wild type and the $\Delta psbI$ mutants showing Fv/Fm ratios of ~ 0.70 were compared. The figure shows representative data. The signals were normalized to the PSI (A) and the CP43 peak (B) at 735 and 688 nm, respectively.

emission for the recombination of the Q_B^-/S_3 pair. Thus, the TL signal intensity of the B band oscillates with the number of single turnover exciting flashes given to dark-adapted thylakoids, with a period of 4, the maxima being at the second and sixth flash (46, 47, 52).

The changes in the properties of the Q_B site of the $\Delta psbI$ mutant may be exhibited not only in the TL measurements elicited by a single turnover flash in presence of DCMU but also under conditions of multiple excitations sustaining forward electron flow. Therefore, we tested whether the mutation affects the oscillation pattern of the TL signal with the number of excitation flashes due to a limited forward electron flow. Indeed, the WT exhibits the normal 2/6 oscillation pattern, whereas the mutant shows an unusual 1/5 oscillation type, indicating an interference with the electron transfer on either the donor or the acceptor side of PSII (Fig. 3C). These results indicate possible changes in both back and forward electron flow in the mutant, suggesting that the mutation affects the interaction

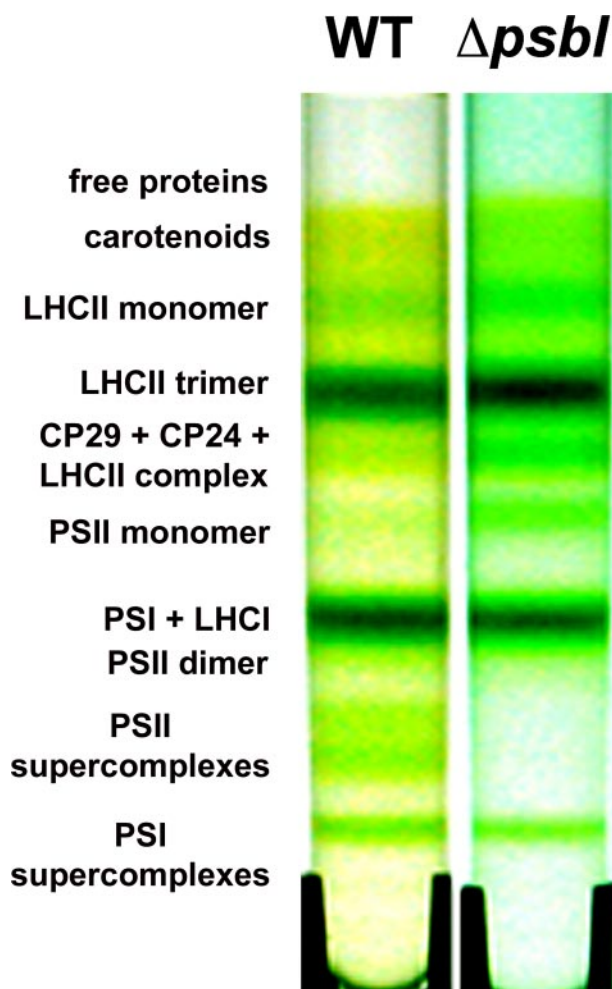


FIGURE 5. Sucrose gradients of partially solubilized thylakoid membranes. Thylakoids of WT and mutants plants were solubilized with 1% of *n*-dodecyl- β -D-maltoside, and multisubunit membrane assemblies were separated by centrifugation in 0.1–1.0 M sucrose gradients. The identities of the resolved green bands are indicated (7).

between the Q_A/Q_B sites and, thus, possibly resulting in alteration of the Q_A midpoint potential under continuous forward electron flow.

The Ratio PSII/PSI and Energy Transfer to the PSII RC Are Reduced in the $\Delta psbI$ Mutant—The ratio of PSI to PSII (F_{PSI}/F_{PSII}) and the functional connection of the LHCII antenna to the RC were monitored by 77 K fluorescence spectroscopy (Fig. 4, A and B). Thylakoid suspensions prepared from young mutant leaves, which displayed a relatively high ratio Fv/Fm of ~ 0.70 , were used. A significantly increased ratio F_{PSI}/F_{PSII} appeared in all mutant samples tested as compared with WT (Fig. 4A). The data indicate an excess of PSI relative to PSII. When the signal intensities of the low temperature emission spectra were normalized to the CP43-related peak at 688 nm, leaves of the $\Delta psbI$ mutant yielded a higher CP47-related fluorescence at 697 nm as compared with the WT (Fig. 4B). This is indicative of a decreased energy transfer to CP43 and a favored fluorescence emission from CP47 in the mutant. Mutant leaves exhibited an emission shoulder at 680 nm, which is missing in the wild type, indicating a partial dissociation of the outer LHCII antenna from the PSII RC (Fig. 4B). This may also reflect

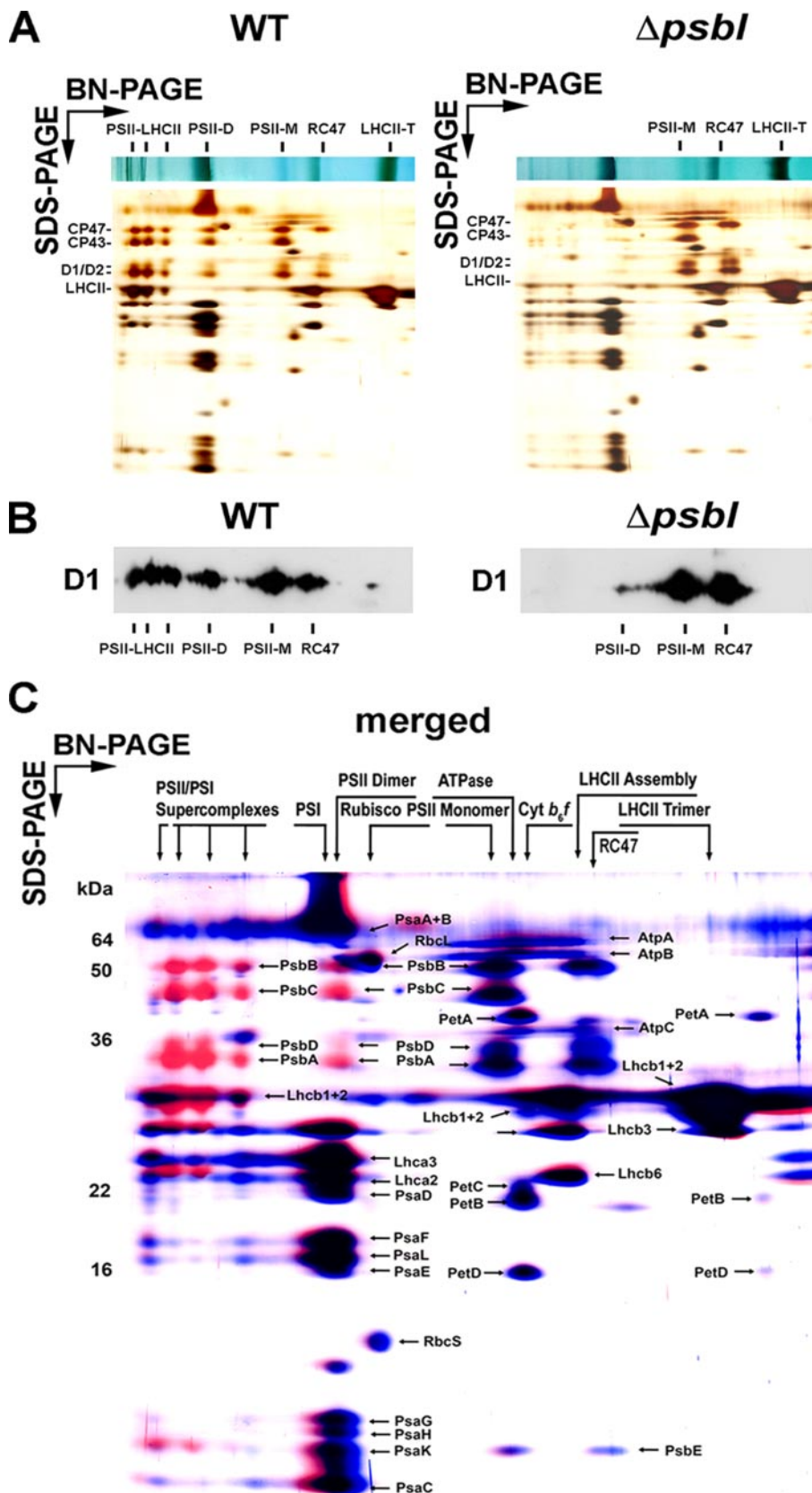


FIGURE 6. BN gel electrophoresis of thylakoid membrane complexes and analysis of the second dimension. *A*, thylakoids were solubilized with 1% *n*-dodecyl- β -D-maltoside, and electrophoresis was performed in the first (BN-PAGE) and second (SDS-PAGE) dimension. Individual protein spots were silver-stained. *B*, immunological analysis of the D1 protein was performed of the second dimension. An overexposure could not even detect traces of PSII-LHC supercomplexes but low amounts of the dimer in $\Delta psbI$ samples. *C*, the patterns of *A* were selectively stained *in silico* in red (WT) and in blue (mutant) (Photoshop Version 8.0.1), and the figures were subsequently merged. Note that the PSII dimer and the supercomplexes are missing in $\Delta psbI$. Individual spots, which appear in the second dimension of solubilized thylakoid membrane complexes, were sequenced by mass spectrometry and are labeled accordingly (38).

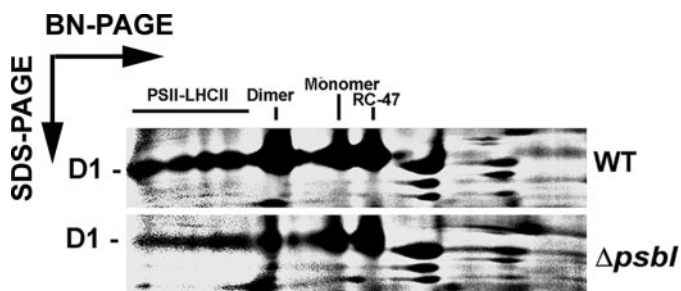


FIGURE 7. Two-dimensional gel electrophoresis of freshly labeled thylakoid membrane complexes. Pulse-labeled thylakoid membrane proteins were separated by two-dimensional gel electrophoreses. The proteins were transferred to a polyvinylidene difluoride membrane and analyzed by phosphorimaging (BAS2000 software package and the AIDA software package Version 3.25 beta; Raytest, Straubenhardt, Germany). Substantial amounts of PSII-LHCII supercomplexes and dimers were detectable.

the reduced amount of the core components relative to the antenna of PSII (Fig. 2).

Effect of the *ΔpsbI* Mutation on the Stability of Dimeric PSII and Higher Order PSII-LHCII Complexes—The presence and the relative content of chlorophyll-protein complexes have been investigated by separation of solubilized thylakoid membrane complexes in sucrose density gradients. The chlorophyll-protein banding patterns showed that the PSII-LHCII supercomplexes were below the limit of detection, whereas levels of the PSII monomer as well as of trimeric LHCII complexes associated with CP29 and CP24 antenna were predominant in mutant thylakoids (Fig. 5). A moderate increase was noted in the relative intensity of free LHCII monomers to that of the WT control sample. These results indicated the presence of unstable dimeric PSII-LHCII supercomplexes in the *psbI* mutant. To confirm these data native membrane complexes were separated by BN-PAGE followed by SDS-PAGE in the second dimension. In accordance with the data described, trimeric LHCII complexes, monomeric PSII and monomeric RC47 complexes lacking CP43, accumulated to higher levels at the expense of PSII dimers and PSII-LHCII supercomplexes in *ΔpsbI* (Fig. 6, A–C). The potential of *ΔpsbI* to assemble higher order PSII complexes was checked by immunological detection of the D1 protein; however, only minute amounts of dimeric PSII complexes could be detected in *ΔpsbI* upon prolonged exposure (Fig. 6B). Interestingly, when *de novo* synthesized native complexes were investigated by *in vivo* radiolabeling, substantial amounts of dimers and higher order PSII-LHCII supercomplexes were found to assemble in the mutant (Fig. 7). We, therefore, conclude that PsbI is not essential for an efficient assembly process but rather for the stability of dimeric PSII and PSII-LHCII supercomplexes. Other thylakoid protein complexes, such as PSL, ATP synthase, and cytochrome *b₆f* complex, were found to be unaltered in size and abundance (data not shown and Fig. 6, A and C).

Phosphorylation of PSII Core Proteins Is Remarkably Decreased and That of LHCII Is Reversely Regulated in *psbI* Mutants—Light-induced phosphorylation of the LHCII is mediated by the redox state of the plastoquinol pool, whereas that of the RC has not been studied extensively. Photoautotrophically grown tobacco WT plants showed an increased phosphorylation of D1, D2, and CP43 with increasing light

intensity from 30 to 200 $\mu\text{mol m}^{-2} \text{s}^{-1}$ and with increasing incubation time from 5 to 15 min.

DCMU treatment inhibits the light-induced phosphorylation of the RC proteins in the WT and, thus, resulted in a phosphorylation status similar to that of dark-adapted plants (Fig. 8A). Phosphorylation of PSII-RC proteins was almost equally distributed in WT supercomplexes, dimers, monomers, and RC47 complexes separated by BN-PAGE (Fig. 8B). However, in *ΔpsbI* plants phosphorylation of D1 and D2 was close to the limit of detection and that of CP43 was reduced to $\leq 5\%$ in the dark and under all chosen light treatments (Fig. 8, A–C). We conclude that the responsible kinase does not phosphorylate RC proteins efficiently in the *psbI* mutants.

Phosphorylation of the LHCII antenna is barely detectable in darkness (state I) but increases with increasing light intensity at 650 nm from 10 to 40 $\mu\text{mol photons m}^{-2} \text{s}^{-1}$ (state II) in the WT (Fig. 8, C and D). High light treatment (500 $\mu\text{mol photons m}^{-2} \text{s}^{-1}$) caused a decrease in LHCII phosphorylation in the WT (39). Strikingly, phosphorylation of LHCII was high in state I (dark) in the mutant and decreased already under low light (650-nm light at 10 $\mu\text{mol m}^{-2} \text{s}^{-1}$). Therefore, it is evident that the phosphorylation of LHCII is reversely regulated in *ΔpsbI* compared with the wild type upon dark/light changes. Phosphorylation of LHCII in the dark induced a re-distribution of light energy in favor of PSI in the mutant as revealed by calculation of the $F_{\text{PSI}}/F_{\text{PSII}}$ ratio (Table 1).

Remarkably, compared with dark-adapted plants, light treatment also reduces phosphorylation of CP43 in the mutant but had no effect on the phosphorylation of the RC proteins D1 and D2 (Fig. 8C). To test whether the responsible kinase is unable to access the RC proteins or whether a reduced PSII activity caused dephosphorylation of the RC proteins in *ΔpsbI*, the plastoquinone pool was reduced *in vitro* by adding reduced duroquinone. The duroquinol-dependent activation of LHCII phosphorylation in the mutant was comparable with that of the WT (Fig. 8E). Moreover, phosphorylation of the RC proteins of duroquinol-treated samples was increased in the WT. Surprisingly substantial amounts of CP43 could be phosphorylated upon duroquinol treatment. On the other hand, phosphorylation of D1 and D2 remained barely detectable in the mutant (Fig. 8E). This implies that the phosphorylation of CP43 and that of D1/D2 can be differently regulated in plants and that structural changes of PSII caused the failure to efficiently phosphorylate RC proteins in the *ΔpsbI* mutant.

To test whether structural alterations or a reduced plastoquinone pool in the dark are also responsible for phosphorylation of the LHCII in *ΔpsbI*, PSI-specific far-red light (730 nm; 6 watts m^{-2}) was applied to leaves for 15 min (Fig. 8F). It appears that LHCII proteins were dephosphorylated under these conditions, showing that indeed reduction of the plastoquinone pool causes phosphorylation of LHCII in the dark in *ΔpsbI*.

The *psbI* Mutant Shows an Increased Light Sensitivity—The lower rate of forward electron flow through PSII in *ΔpsbI* as well as the alteration of the Q_B binding site suggest an increased back electron transfer and charge recombination in PSII, thus increasing the probability of damage of the PSII-RC through chlorophyll triplet formation, free radical production, and photo-oxidation (53–56). To verify this assumption, leaves of WT

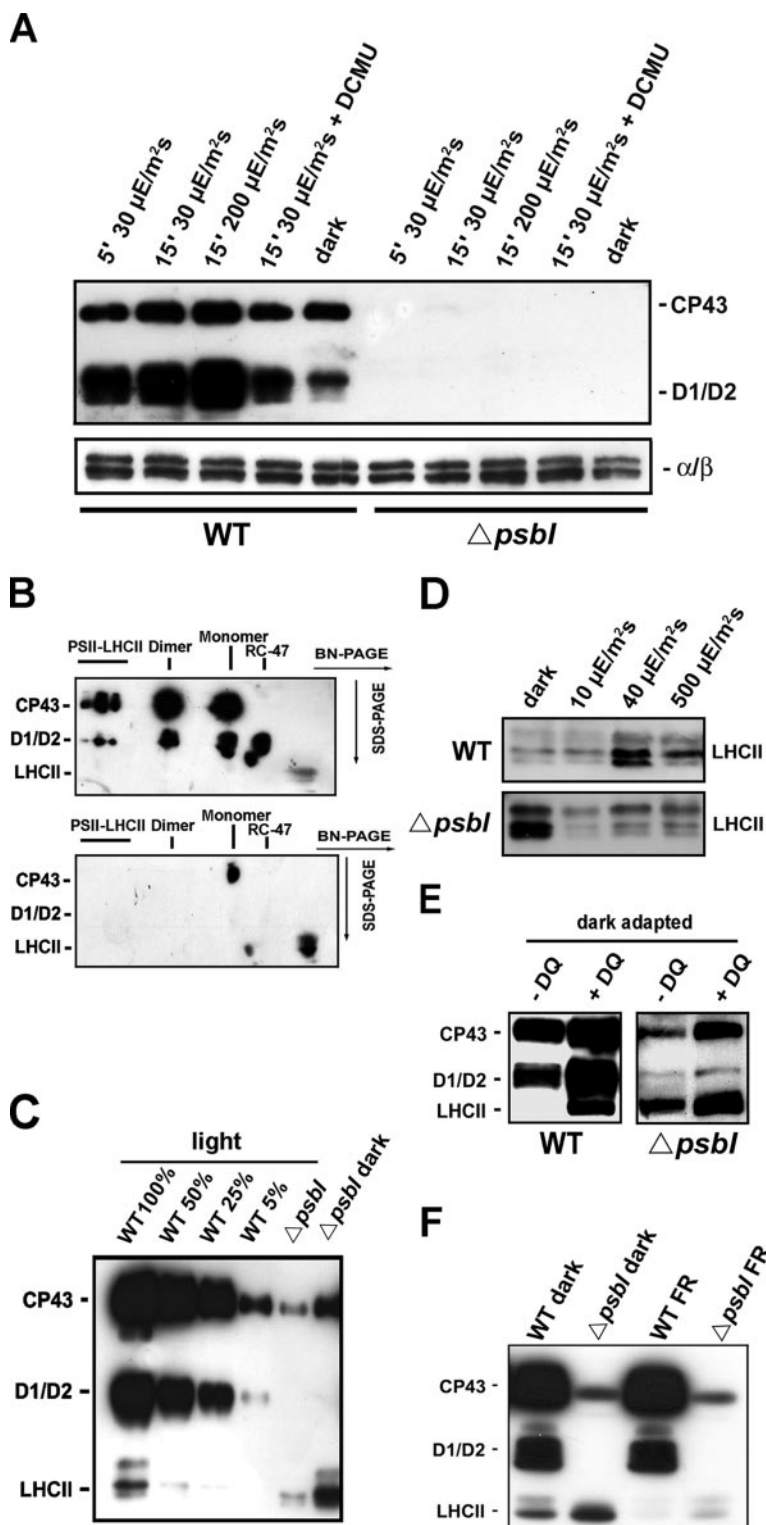


FIGURE 8. Redox- and light-dependent phosphorylation of PSII reaction center and antenna proteins. *A*, immunoblot analysis of thylakoid membrane proteins were performed using an anti-phosphothreonine antibody from Zymed Laboratories Inc. (*A*) or New England Biolabs (*B–E*). In agreement with previous reports, the antiserum from Zymed Laboratories Inc. hardly recognizes phosphorylated LHCII proteins (11). Phosphorylation of reaction center proteins CP43, D1, and D2 is induced by light (heterochromatic) in the WT but is almost absent in $\Delta psbI$. The immunoblot performed with antisera raised against the ATP synthase α and β subunits demonstrates equal loading. *B*, immunological analysis of the second dimension demonstrates that only traces of CP43 are detectable and that LHCII proteins are highly phosphorylated in dark-adapted mutants. *C*, a dilution series of the WT was chosen to estimate the lowered amount of phosphorylation of reaction center and antenna proteins in the mutant in the dark and in the light. *D*, the phosphorylation of LHCII in thylakoids of dark-adapted and red light-incubated plants showed a reverse regulation of the phosphorylation pattern in the mutant (state I = dark, state II = $40 \mu\text{mol}$ of photons $\text{m}^{-2} \text{s}^{-1}$ at 650 nm). *E*, phosphorylation of LHCII and reaction center proteins of dark-adapted thylakoids is significantly induced by reduced duroquinone in the WT. Duroquinol activates phosphorylation of the LHCII but only traces of CP43 in the mutant. *F*, oxidation of the plastoquinone pool was achieved by applying PSI-specific far-red (FR) light ($6 \text{ watts } \text{m}^{-2}$) for 15 min to leaves. This treatment induced dephosphorylation of LHCII in the mutant, indicating that the reduced plastoquinone pool caused phosphorylation of LHCII in the dark.

PsbI Affects Phosphorylation, Stability, and Function of PSII

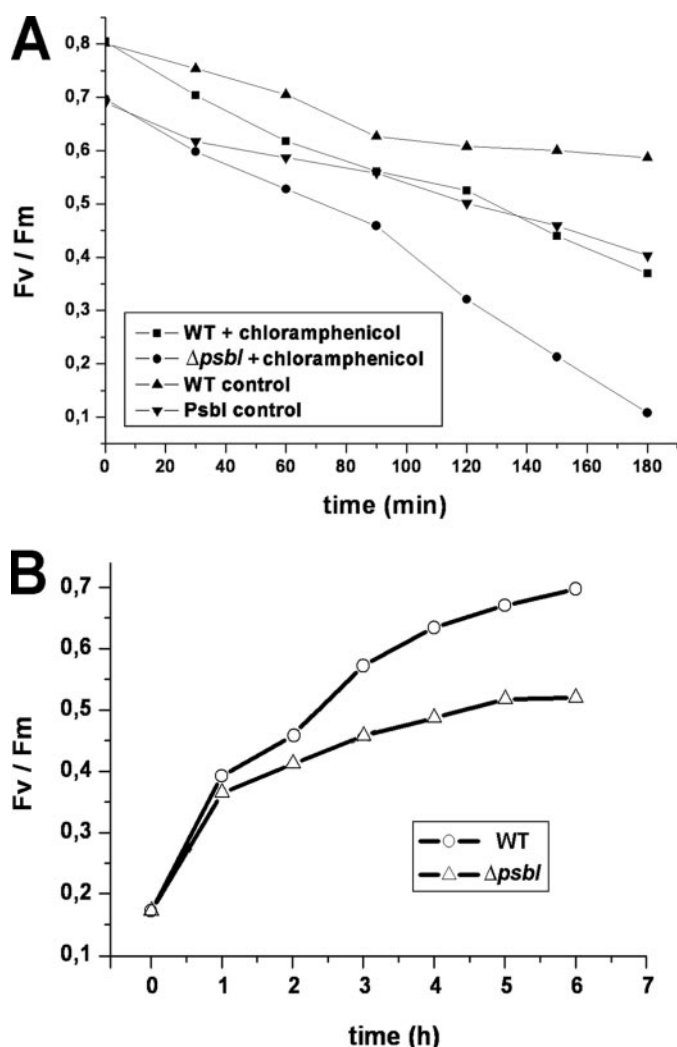


FIGURE 9. Photoinhibition of PSII and recovery kinetics in WT and mutant leaves. A, measurement of photoinhibition was based on the recording of the Fv/Fm ratio using $1,500 \mu\text{mol m}^{-2} \text{s}^{-1}$ of irradiance (▲ and ▼, WT and mutant without chloramphenicol, respectively; ■ and ●, WT and mutant with chloramphenicol, respectively). B, the restoration of Fv/Fm was recorded for 6 hours after photoinhibition (Fv/Fm = 0.17) at $3 \mu\text{mol}$ of photons $\text{m}^{-2} \text{s}^{-1}$ in WT (○) and ΔpsbI (△).

and mutant plants were exposed to high irradiance ($1,500 \mu\text{mol}$ of photons $\text{m}^{-2} \text{s}^{-1}$), and PSII photoinactivation was measured as a function of exposure time with and without the chloroplast translational inhibitor chloramphenicol. The results indicate that PSII photoinactivation is faster in the mutant as compared with the WT (Fig. 9A). To evaluate the cause of light sensitivity in ΔpsbI , the recovery rate of photo-damaged PSII was measured after photoinactivation. Within the first hour the recovery rate was almost identical in both cases. The mutant restored 75% of its original PSII quantum yield as compared with 88% for that of the WT after 6 h of recovery, indicating that ΔpsbI is primarily light-sensitive but is basically able to assemble photodamaged PSII complexes and, therefore, to recover from photoinhibitory injury (Fig. 9B).

DISCUSSION

Transplastomic psbI Knock-out Mutants in Tobacco Grow Photoautotrophically—Stability of the PSII core complex in higher plants depends not only on the presence and subsequent

assembly of D1, D2, CP43, and CP47 but also on several LMW proteins such as *psbE*, *psbF*, *psbL*, and *psbJ*, which are all encoded by the plastid chromosome (19, 7, 22). This is consistent with the succession of subunit integration during the assembly process that has been settled for the order given: cytochrome *b₅₅₉*, D2, D1, CP47, and CP43 (57–59). It is, therefore, not surprising that deletion of either of those early assembled as well as structurally and functionally crucial components is deleterious to the photosynthetic process, since no functional PSII complexes are formed.

Limited information is available on LMWs (4, 7), including PsbI, which is also present in the PSII core complex (60). Unlike other components, which are present in core preparations (1–2), PsbI is not essential for photoautotrophic growth in *Synechocystis* and *C. reinhardtii* (28–29). To understand the biogenetic and structural as well as functional aspects of PSII in higher plants more profoundly, we have generated tobacco knock-out plants lacking *psbI* and characterized the mutant using biochemical, spectroscopic, and fluorimetric approaches. The data obtained show that different from all other core components, PsbI is dispensable for the assembly of the RC core in higher plant thylakoids. Moreover, its loss even allows photoautotrophic growth, but its requirement is disclosed only under distinct light regimes. This differs from other LMWs, such as PsbE, F, L, and J (7), the latter two involved primarily in governing the redox potential of cofactors ligated by the D1/D2 heterodimer to ensure efficient charge separation and the following forward electron transfer through and out of PSII (19, 22).

PsbI Confers Stability to Dimeric PSII-LHCII Supercomplexes—Analysis of PSII assemblies illustrates that only traces of PSII dimer and supercomplexes could be found in the absence of PsbI (Figs. 6 and 7). However, *in vivo* labeling experiments revealed that ΔpsbI mutants possess the potential to form various PSII-LHCII supercomplexes (Fig. 7D). Therefore, it is evident that the PsbI protein is essential for the stability of dimeric PSII and, depending on it, of PSII-LHCII complexes. In addition, PsbI is crucial for an efficient forward electron transport within photosystem II. In summary, PsbI exerts a dual function. It is less important for the basic assembly of this photosystem; however, it is required for the stability of higher order complexes of PSII and the proper functioning of PSII.

Although the precise localization of PsbI in the PSII assembly is still a matter of debate based on the crystal structure of the cyanobacterial PSII dimer and the proposed location of the individual LMW subunits, PsbI was assigned toward the outer side of the monomeric core (17–18). At this position it may be involved in binding the antenna protein Lhcb4 (CP29), which in turn could interact with the LHCII trimers M and/or S (3). If this were true, dimer stability could be influenced by low mass subunits residing at two positions, centrally at the monomer interphase, such as PsbL (22), and peripherally, such as PsbI, with its interaction along the pseudo 2-fold axis of symmetry with the other monomeric core (17). Thus, PsbI could “bracket” two monomers forming a PSII dimer. Its absence would destabilize the dimer and, as a consequence, the interaction between PSII and the CP29-LHCII. This could explain the effects on the energy transfer to the core complex in the mutant. The low temperature fluorescence (77 K) analysis is consistent with a

reduced rate of energy transfer to the core, especially to CP43, in the $\Delta psbI$ mutant. Monomeric cores attached to LHCII proteins have never been observed in mixed populations of disrupted grana as recognized in cryoelectron micrographic images after quick and mild solubilization of the membranes (for review, see Ref. 3). Furthermore, antenna proteins tend to readily dissociate from monomerized PSII core complexes. Thus, it is conceivable that disruption of *psbI* affects primarily the stability of the dimer and only secondarily, the formation of supercomplexes.

Examination of the PSII₂LHCII₈₊₂ model (3) suggests that one of the functions of PsbI is to provide a flexible interface between the rather rigid structure of the PSII core, the fixed antennae, and the mobile LHCII. PsbI may serve as a structural buffer between the ever-changing positions and interaction strength of the peripheral antennae and the photochemical core. It may also play a direct role in stabilization of the dimeric form of PSII. Inactivation of PsbI not only alters energy transfer from the major antenna but also stability of structure/function of the PSII core dimer. The relatively pronounced effects in $\Delta psbI$ attest the flexibility of the connection of the photosynthetic machinery with the "outer world."

Increased Light Sensitivity of PSII in PsbI Mutants—Accumulation of monomeric PSII complexes in $\Delta psbI$ may generate β -like PSII centers impaired in plastoquinone reduction (61) and, thus, be responsible for the slow reduction of oxidized P700, an increased sensitivity to photoinactivation, and a somewhat slower re-assembly of photodamaged PSII.

Inhibition of electron flow from the primary (Q_A) to the secondary (Q_B) quinone acceptor and the resulting accumulation of reduced Q_A species are the principal events that initiate damage of PSII by photooxidative stress (62, 54). Under high light conditions, the primary cause for photoinactivation of PSII is thought to be due to damage of the D1 protein (for review, see Ref. 55). Therefore, the sensitivity of PSII to high light and its ability to restore photochemical efficiency under conditions of low light was analyzed in mutant and WT. It appears that PSII is more rapidly degraded than repaired in $\Delta psbI$ with increasing light intensity. Three hours of photoinhibitory light treatment were required to lose 75% of PSII quantum yield in the WT; however, a similar loss was noted already after 2 h in $\Delta psbI$, reinforcing an increased light sensitivity of its PSII (data not shown). Although the initial recovery rate is identical in mutant and WT, the overall capability to recover was lower in the mutant. The delayed repair of photoinactivated PSII in $\Delta psbI$ suggests that PsbI also influences the recovery process, although this may be a secondary effect of the mutation. Furthermore, an increased light sensitivity of the mutant when synthesis of D1 is inhibited corroborates that D1 protein degradation occurs at substantially higher rates in $\Delta psbI$ than in the WT.

The $\Delta psbI$ Mutation Destabilizes the Q_A Midpoint Potential—TL measurements, performed to check the effect of the mutation on the electron flow within PSII, indicated an alteration in the properties of the Q_B binding site that affects the binding of ligands, resulting in changes of the midpoint potential of the Q_B/Q_A site. The effect of the mutation is expressed not only in the presence of DCMU occupying the Q_B site but also in its

absence as indicated by the alteration from the normal 2/6 (63) to the unusual 1/5 oscillation pattern. The above changes may result from an aberration of the theoretical 3:1 ratio of $S_1:S_0$ states and/or the 1:1 occupancy of the state populations $Q_B^-:Q_B$ in dark-adapted samples (51, 64). This in turn may reflect alterations in the midpoint potential of the Q_A site.

The down-shift in the emission temperature of the DCMU-induced Q band indicates an accelerated charge recombination from Q_A^- to S_2 and, thus, a partial inhibition of back electron flow from Q_B^- and charge recombination via P_{680+} that will affect the synchronization of the Q_B^-/S_2 transition of the PSII population. In conclusion, in the absence of PsbI the structural dynamics of the Q_B binding site during light excitation may be destabilized, possibly affecting the Q_A/Q_B midpoint potential and, thus, back and forward electron flow of PSII. Therefore, the properties of electron transport appear modified by alterations in catalytic rather than changes in regulatory characteristics.

PsbI Is Required for Phosphorylation of PSII Core Proteins and a Reduced Plastoquinone Pool in the Dark Causes Phosphorylation of LHCII in the Dark in $\Delta psbI$ —Phosphoproteins of the RC, i.e. D1, D2, and CP43, have been reported to depend on the protein kinase STN8 in *Arabidopsis*, whereas those of the LHCII depend on STN7 and STT7 in *Arabidopsis* and *Chlamydomonas*, respectively (9–11). However, the direct targets of the kinases and whether the orthologous proteins in tobacco exert the same functions remain elusive.

Strikingly, phosphorylation of LHCII was regulated in response to light in the mutant, but regulation was reverse to the WT behavior when dark and light adapted probes were compared. Irrespective of chosen light conditions (10, 40 (state II), and 500 μmol of photons $\text{m}^{-2} \text{s}^{-1}$, 650 nm), LHCII phosphorylation was abolished by light, indicating an imbalance of electron transport causing excitation re-distribution between the two photosystems as also shown by 77 K measurements (Table 1).

It has been suggested that cytochrome b_{559} functions in the re-oxidation of the plastoquinone pool in dark-adapted leaves (65). Therefore, it is conceivable that PsbI also supports this function and that the plastoquinone pool remains predominantly reduced in the dark (Table 1). This may cause a redox-regulated activation of the corresponding kinase(s) in the dark in $\Delta psbI$. Our data unequivocally demonstrate that phosphorylation of the LHCII in the dark is not due to structural changes of PSII in the mutant but due to the reduced plastoquinone pool (Fig. 8F). Unlike WT, the increased re-oxidation rate of the plastoquinone induced by PSI as compared with the lower PSII-dependent reduction rate in $\Delta psbI$ leads to oxidation of the plastoquinone pool under any light conditions. This explains the light-induced inactivation of the kinase and the dephosphorylation of LHCII.

Remarkably, $\Delta psbI$ lost its capability to efficiently phosphorylate PSII-RC proteins. Phosphorylation of LHCII proteins is regulated and induced by duroquinol, but that of D1 and D2 cannot be induced under all chosen conditions. Therefore, we conclude that physiological responses cause the reverse regulation of LHCII phosphorylation but that structural alterations of PSII result in the loss of D1/D2 phosphorylation in the muta-

tion. It is reasonable to assume that the PsbI protein allows a close contact of the kinase to the RC presumably by a direct interaction. It is also likely that the lack of phosphorylation of the core complex subunits D1, D2, and CP43 in $\Delta psbI$ partially causes the increased light sensitivity since nuclear *Arabidopsis* mutants defective in phosphorylation of reaction center proteins show a slightly pale phenotype and a somewhat increased photosensitivity (10–11). The fact that phosphorylation of CP43 can be induced by duroquinol but that of D1 and D2 cannot either implies that an earlier unidentified protein kinase could be involved in the phosphorylation of the PSII-RC and/or that access of the kinase to CP43 is favored as compared with D1 and D2.

Acknowledgments—We are very grateful to Martina Reymers and Gisela Nagy for excellent technical assistance.

REFERENCES

1. Minagawa, J., and Takahashi, Y. (2004) *Photosynth. Res.* **82**, 241–263
2. Shi, L.-X., and Schröder, W. P. (2004) *Biochim. Biophys. Acta* **1608**, 75–96
3. Dekker, J. P., and Boekema, E. J. (2005) *Biochim. Biophys. Acta* **1706**, 12–39
4. Thornton, L. E., Roose, J. L., and Pakrasi, H. (2005) in *Photosystem II: the Water/Plastoquinone Oxido-reductase in Photosynthesis* (Wydrzynski, T. and Satoh, K., eds) pp. 121–138, Kluwer Academic Publishers, Dordrecht, The Netherlands
5. Pakrasi, H. B., Williams, J. G., and Arntzen, C. J. (1988) *EMBO J.* **2**, 325–332
6. Morais, F., Kuhn, K., Stewart, D. H., Barber, J., Brudvig, G. W., and Nixon, P. J. (2001) *J. Biol. Chem.* **276**, 31986–31993
7. Swiatek, M., Regel, R. E., Meurer, J., Wanner, G., Pakarasi, H. B., Ohad, I., and Herrmann, R. G. (2003) *Mol. Genet. Genomics* **268**, 699–710
8. Bennett, J. (1977) *Nature* **269**, 344–346
9. Bellafiore, S., Barneche, F., Peltier, G., and Rochaix, J. D. (2005) *Nature* **433**, 892–895
10. Bonardi, V., Pesaresi, P., Becker, T., Schleiff, E., Wagner, R., Pfannschmidt, T., Jahns, P., and Leister, D. (2005) *Nature* **437**, 1179–1182
11. Vainonen, J. P., Hansson, M., and Vener, A. V. (2005) *J. Biol. Chem.* **280**, 33679–33686
12. Vasil'ev, S., Orth, P., Zouni, A., Owens, T. G., and Bruce, D. (2001) *Proc. Natl. Acad. Sci. U. S. A.* **98**, 8602–8607
13. Zouni, A., Witt, H. T., Kern, J., Fromme, P., Krauss, N., Saenger, W., and Orth, P. (2001) *Nature* **409**, 739–743
14. Kamiya, N., and Shen, J. R. (2003) *Proc. Natl. Acad. Sci. U. S. A.* **100**, 98–103
15. Kashino, Y., Lauber, W. M., Carroll, J. A., Wang, Q., Whitmarsh, J., Satoh, K., and Pakarasi, H. B. (2002) *Biochemistry* **41**, 8004–8012
16. Biesiadka, J., Loll, B., Kern, J., Irrgang, K.-D., and Zouni, A. (2004) *Phys. Chem. Chem. Phys.* **6**, 4733–4736
17. Ferreira, K. N., Iverson, T. M., Maghlaoui, K., Barber, J., and Iwata, S. (2004) *Science* **303**, 1831–1838
18. Loll, B., Kern, J., Saenger, W., Zouni, A., and Biesiadka, J. (2005) *Nature* **15**, 1040–1044
19. Regel, R. E., Ivleva, N. B., Zer, H., Meurer, J., Shestakov, S. V., Herrmann, R. G., Pakarasi, H. B., and Ohad, I. (2001) *J. Biol. Chem.* **276**, 41473–41478
20. Bassi, R., Sandona, D., and Croce, R. (1997) *Physiol. Plant.* **100**, 769–779
21. Niyogi, K. K. (1999) *Annu. Rev. Plant Physiol. Plant Mol. Biol.* **50**, 333–359
22. Ohad, I., Dal Bosco, C., Herrmann, R. G., and Meurer, J. (2004) *Biochemistry* **43**, 2297–2308
23. Meurer, J., Plücker, H., Kowallik, K. V., and Westhoff, P. (1998) *EMBO J.* **17**, 5286–5297
24. Shen, G., Zhao, J., Reimer, S. K., Antonkine, M. L., Cai, Q., Weiland, S. M., Golbeck, J. H., and Bryant, D. A. (2002) *J. Biol. Chem.* **277**, 20343–20354
25. Kern, J., Loll, B., Zouni, A., Saenger, W., Irrgang, K. D., and Biesiadka, J.

- (2005) *Photosynth. Res.* **84**, 153–159
26. Zheleva, D., Sharma, J., Panico, M., Morris, H. R., and Barber, J. (1998) *J. Biol. Chem.* **273**, 16122–16127
27. Ikeuchi, M., Koike, H., and Inoue, Y. (1989) *FEBS Lett.* **251**, 155–160
28. Künstner, P., Guardiola, A., Takahashi, Y., and Rochaix, J. D. (1995) *J. Biol. Chem.* **270**, 9651–9654
29. Ikeuchi, M., Shukla, V. K., Pakarasi, H. B., and Inoue, Y. (1995) *Mol. Gen. Genet.* **249**, 622–628
30. Webber, A. N., Packman, L., Chapman, D. J., Barber, J., and Gray, J. C. (1989) *FEBS Lett.* **242**, 259–262
31. Murata, N., Miyao, M., Hayashida, N., Hidaka, T., and Sugiura, M. (1988) *FEBS Lett.* **235**, 283–288
32. Ikeuchi, M., and Inoue, Y. (1988) *FEBS Lett.* **241**, 99–104
33. Svab, Z., Hajdukiewicz, P., and Maliga, P. (1990) *Proc. Natl. Acad. Sci. U. S. A.* **87**, 8526–8530
34. Murashige, T., and Skoog, F. (1962) *Physiol. Plant.* **15**, 493–497
35. Laemmli, U. K. (1970) *Nature* **227**, 680–685
36. Amann, K., Lezhneva, L., Wanner, G., Herrmann, R. G., and Meurer, J. (2004) *Plant Cell* **16**, 3084–3097
37. Ossenbühl, F., Göhre, V., Meurer, J., Krieger-Liszkay, A., Rochaix, J. D., and Eichacker, L. A. (2004) *Plant Cell* **16**, 1790–1800
38. Granvogl, B., Reisinger, V., and Eichacker, L. A. (2006) *Proteomics* **6**, 3681–3695
39. Zer, H., Vink, M., Scochat, S., Herrmann, R. G., Andersson, B., and Ohad, I. (2003) *Biochemistry* **42**, 728–738
40. Allen, J., and Horton, P. (1981) *Biochim. Biophys. Acta* **638**, 290–295
41. Krause, G. H., and Weis, E. (1991) *Annu. Rev. Plant Physiol. Plant Mol. Biol.* **42**, 313–349
42. van Kooten, O., and Snel, J. F. H. (1990) *Photosynth. Res.* **25**, 147–150
43. Klughammer, C., and Schreiber, U. (1994) *Planta* **192**, 261–268
44. Weis, E. (1985) *Photosynth. Res.* **6**, 73–86
45. Rutherford, A. W., Govindjee, and Inoue, Y. (1984) *Proc. Natl. Acad. Sci. U. S. A.* **81**, 1107–1111
46. Vass, I., and Govindjee (1996) *Photos. Res.* **48**, 117–126
47. Ducruet, J. M. (2003) *J. Exp. Bot.* **54**, 2419–2430
48. Demeter, S., and Vass, I. (1984) *Biochim. Biophys. Acta* **764**, 24–32
49. Vass, I., and Inoue, Y. (1992) in *The Photosystems: Structure, Function, and Molecular Biology* (Barber, J., ed) pp. 259–294, Elsevier Science Publishers B. V., Amsterdam
50. Krieger, A., Rutherford, W., and Johnson, G. N. (1995) *Biochim. Biophys. Acta* **1229**, 193–201
51. Krieger-Liszkay, A., and Rutherford, A. W. (1998) *Biochemistry* **37**, 17339–17344
52. Haumann, M., Liebisch, P., Müller, C., Barra, M., Grabolle, M., and Dau, H. (2005) *Science* **310**, 1019–2101
53. Prasil, O., Adir, N., and Ohad, I. (1992) *Topics in Photosynthesis*, 1st Ed., Vol. II, pp. 293–348, Elsevier Science Publishers B. V., Amsterdam
54. Keren, N., Berg, A., van Kan, P. J. M., Levanon, H., and Ohad, I. (1997) *Proc. Natl. Acad. Sci. U. S. A.* **94**, 1579–1584
55. Adir, N., Zer, H., Shochat, S., and Ohad, I. (2003) *Photosynth. Res.* **76**, 343–370
56. Zilard, A., Sass, I., Hideg, E., and Vass, I. (2005) *Photosynth. Res.* **84**, 15–20
57. Müller, B., and Eichacker, L. A. (1999) *Plant Cell* **11**, 2365–2377
58. Aro, E.-M., Suorsa, M., Rokka, A., Allahverdiyeva, Y., Paakkari, V., Saleem, A., Battchikova, N., and Rintamaki, E. (2005) *J. Exp. Bot.* **56**, 347–356
59. Rokka, A., Surosa, M., Saleem, A., Battchikova, N., and Aro, E.-M. (2005) *Biochem. J.* **388**, 159–168
60. Tomo, T., Enami, I., and Satoh, K. (1993) *FEBS Lett.* **323**, 15–18
61. Govindjee (1990) *Photosynth. Res.* **25**, 151–160
62. Vass, I., Styring, S., Hundal, T., Koivuniemi, A., Aro, E.-M., and Andersson, B. (1992) *Proc. Natl. Acad. Sci. U. S. A.* **89**, 1408–1412
63. Bowes, J. M., and Crofts, A. R. (1980) *Biochim. Biophys. Acta* **590**, 373–384
64. Rutherford, A. W., Crofts, A. R., and Inoue, Y. (1982) *Biochim. Biophys. Acta* **682**, 457–465
65. Bondarava, N., De Pascalis, L., Al-Babili, S., Goussias, C., Golecki, J. R., Beyer, P., Bock, R., and Krieger-Liszkay, A. (2003) *J. Biol. Chem.* **278**, 13554–13560

Role of the Low-Molecular-Weight Subunits PetL, PetG, and PetN in Assembly, Stability, and Dimerization of the Cytochrome b_6f Complex in Tobacco^{1[C]}

Serena Schwenkert, Julia Legen², Tsuneaki Takami³, Toshiharu Shikanai³, Reinhold G. Herrmann, and Jörg Meurer*

Department of Biology I, Botany, Ludwig-Maximilians-University, 80638 Munich, Germany

The cytochrome b_6f (Cyt b_6f) complex in flowering plants contains nine conserved subunits, of which three, PetG, PetL, and PetN, are bitopic plastid-encoded low-molecular-weight proteins of largely unknown function. Homoplasmic knockout lines of the three genes have been generated in tobacco (*Nicotiana tabacum* 'Petit Havana') to analyze and compare their roles in assembly and stability of the complex. Deletion of *petG* or *petN* caused a bleached phenotype and loss of photosynthetic electron transport and photoautotrophy. Levels of all subunits that constitute the Cyt b_6f complex were faintly detectable, indicating that both proteins are essential for the stability of the membrane complex. In contrast, Δ *petL* plants accumulate about 50% of other Cyt b_6f subunits, appear green, and grow photoautotrophically. However, Δ *petL* plants show increased light sensitivity as compared to wild type. Assembly studies revealed that PetL is primarily required for proper conformation of the Rieske protein, leading to stability and formation of dimeric Cyt b_6f complexes. Unlike wild type, phosphorylation levels of the outer antenna of photosystem II (PSII) are significantly decreased under state II conditions, although the plastoquinone pool is largely reduced in Δ *petL*, as revealed by measurements of PSI and PSII redox states. This confirms the sensory role of the Cyt b_6f complex in activation of the corresponding kinase. The reduced light-harvesting complex II phosphorylation did not affect state transition and association of light-harvesting complex II to PSI under state II conditions. Ferredoxin-dependent plastoquinone reduction, which functions in cyclic electron transport around PSI in vivo, was not impaired in Δ *petL*.

The cytochrome b_6f (Cyt b_6f) complex in cyanobacteria and plants resides in thylakoid membranes and links the electron transport between PSII and PSI. It functions as plastoquinol-plastocyanin oxidoreductase and mediates both linear and PSI cyclic electron flow, proton translocation across the membrane, as well as photosynthetic redox control of energy distribution between the two photosystems and gene expression (Allen, 2004; Cramer and Zhang, 2006). In flowering plants, the complex is composed of at least nine subunit species, forms a dimer, and is of dual genetic origin. Two subunits, PetC (Rieske FeS subunit) and PetM, are encoded by nuclear genes. The other subunits are encoded in plastid chromosomes. Of these,

three genes encode large subunits PetA, PetB, and PetD, representing Cyt f , Cyt b_6 , and subunit IV, respectively. The remaining low-molecular-weight (LMW) subunits, PetG, PetL, and PetN, are hydrophobic and span the membrane once (de Vitry et al., 1996; Cramer et al., 2005). A further constituent subunit, PetO, which has only been described in *Chlamydomonas*, is reversibly phosphorylated upon state transition, but could not be detected in the crystal structure (Hamel et al., 2000). In contrast to other subunits analyzed, PetM is not essential for assembly or stability of the complex in cyanobacteria (Schneider et al., 2001, 2007). PetC possesses a highly mobile extrinsic domain and is assumed to contribute to the stability of the dimer by domain swapping (Kurisu et al., 2003). Mutants of PetC in *Arabidopsis* (*Arabidopsis thaliana*) and *Chlamydomonas* are able to assemble the complex (de Vitry et al., 1999; Maiwald et al., 2003); however, analyses of PetC mutants in maize (*Zea mays*; Miles, 1982), *Oenothera* (Stubbe and Herrmann, 1982), and *Lemna* (Bruce and Malkin, 1991) have shown that the FeS protein is essential for assembly of the complex in these organisms.

Crystallographic studies have uncovered structural details of the complex in cyanobacteria and *Chlamydomonas* (Kurisu et al., 2003; Stroebel et al., 2003). Apart from the constituent subunits and the two cytochromes, Cyt b_6 and Cyt f , the complex contains one chlorophyll a and one β -carotene molecule. An unexpected heme (c-type cytochrome) has recently been discovered, which may be involved in the cyclic electron

¹ This work was supported by the German Science Foundation (DFG; grant SFB TR1 to J.M. and R.G.H.).

² Present address: Institute of Biology, Department of Biology, Chemistry and Pharmacy, Freie Universität Berlin, Koenigin-Luise-Str. 12-16, 14195 Berlin, Germany.

³ Present address: Graduate School of Agriculture, Kyushu University, Fukuoka 812-8581, Japan.

* Corresponding author; e-mail joerg.meurer@lrz.uni-muenchen.de; fax 49-89-1782274.

The author responsible for distribution of materials integral to the findings presented in this article in accordance with the policy described in the Instructions for Authors (www.plantphysiol.org) is: Jörg Meurer (joerg.meurer@lrz.uni-muenchen.de).

[C] Some figures in this article are displayed in color online but in black and white in the print edition.

www.plantphysiol.org/cgi/doi/10.1104/pp.107.100131

transport around PSI (Kurisu et al., 2003; Stroebel et al., 2003; Cramer and Zhang, 2006). The LMWs are all located at the periphery of the complex, yet the two available crystal structures are not consistent in the exact assignments of PetG, PetL, and PetN. A knockout mutant of *petG* has been described in *Chlamydomonas reinhardtii*, demonstrating that the subunit is essential for either stability or assembly of the complex (Berthold et al., 1995). *PetN*, which represents the smallest open reading frame in the plastid genome, has a comparable stabilizing effect on the cytochrome complex, as judged from a tobacco (*Nicotiana tabacum*) knockout mutant (Hager et al., 1999). *PetN* and *PetG* are likewise essential in *Synechocystis* (Schneider et al., 2007). Disruption of *petL* has been reported to cause impaired photoautotrophic growth, reduced electron transfer, and reduced levels of the Cyt *b₆f* complex in *Chlamydomonas*, but almost no effect in *Synechocystis* (Takahashi et al., 1996; Schneider et al., 2007). A corresponding knockout in tobacco indicated reduced stability of the complex, especially in aging leaves, although photoautotrophy was not affected (Fiebig et al., 2004; Schöttler et al., 2007). Although all three subunits are present in cyanobacteria and higher plants, the similarity between them in these two lineages is quite different (approximately 73%, approximately 52%, and approximately 29% for *petG*, *petN*, and *petL*, respectively), indicating a relatively high divergence of *petL*.

Several deletion mutants of *petA*, *petB*, and *petD*, in *Chlamydomonas*, *Oenothera*, and tobacco, have been described, which exert different effects in the assembly of the Cyt *b₆f* complex (Herrmann et al., 1985; Kuras and Wollman, 1994; Monde et al., 2000). Two mechanisms have been suggested to explain the significantly reduced levels/stability of all subunits that constitute the complex in most of these mutants. Failure to assemble the complex could be due to faster degradation of improperly assembled proteins, which was verified for $\Delta petB$ and $\Delta petD$ by in vivo labeling experiments in *Chlamydomonas* (Kuras and Wollman, 1994). Alternatively, disruption of the hierarchical organization of expression of Cyt *b₆f* complex subunits, designated as a controlled epistasy of synthesis (CES) process, may cause loss of assembly, as is the case for *petA* in *Chlamydomonas*. In this alga, each of the thylakoid membrane complexes contains at least one CES subunit, whose translation depends on the availability of its assembly partners (Choquet et al., 2001). It remains to be shown whether CES-like processes also exist in higher plants.

Besides linear and PSI cyclic electron flow and proton translocation, the Cyt *b₆f* complex seems to be involved in redox signaling and state transition (Allen, 2004; Shikanai, 2007). For photosynthetic organisms, it is vital to modify and adjust their light-harvesting capacity depending on environment because high light causes photoinhibition, whereas low light limits photosynthesis. Therefore, regulatory mechanisms to prevent extensive damage include down-regulation of

antenna size, nonphotochemical quenching, and redistribution of light-harvesting complex II (LHCII; state transition) to adapt and optimize photosynthetic efficiency. Redistribution of peripheral antenna proteins involves reversible phosphorylation and migration of LHCII proteins between the two photosystems, thus redistributing excitation energy between the photosystems (Aro and Ohad, 2003). Phosphorylation of thylakoid membrane proteins is mediated by two protein kinases, of which at least one (STN7) is controlled by the redox state of the plastoquinone (PQ) pool (Allen, 1992; Wollman, 2001; Bellafiore et al., 2005; Bonardi et al., 2005; Vainonen et al., 2005). It has been shown that the cytochrome complex senses the redox state of the PQ pool and is involved in signal transduction that activates LHCII kinase (Vener et al., 1998; Zito et al., 1999; Wollman, 2001).

To further elucidate the function of the LMW subunits of the Cyt *b₆f* complex in higher plants, we have inactivated *petG*, *petN*, and *petL* in tobacco 'Petit Havana'. *PetG* and *PetN* are essential for the stability of the entire Cyt *b₆f* complex and for photoautotrophic growth. In contrast to this, *PetL* is dispensable for photoautotrophic growth, but crucial for accumulation of dimeric Cyt *b₆f* complexes and photosynthetic redox regulation in tobacco.

RESULTS

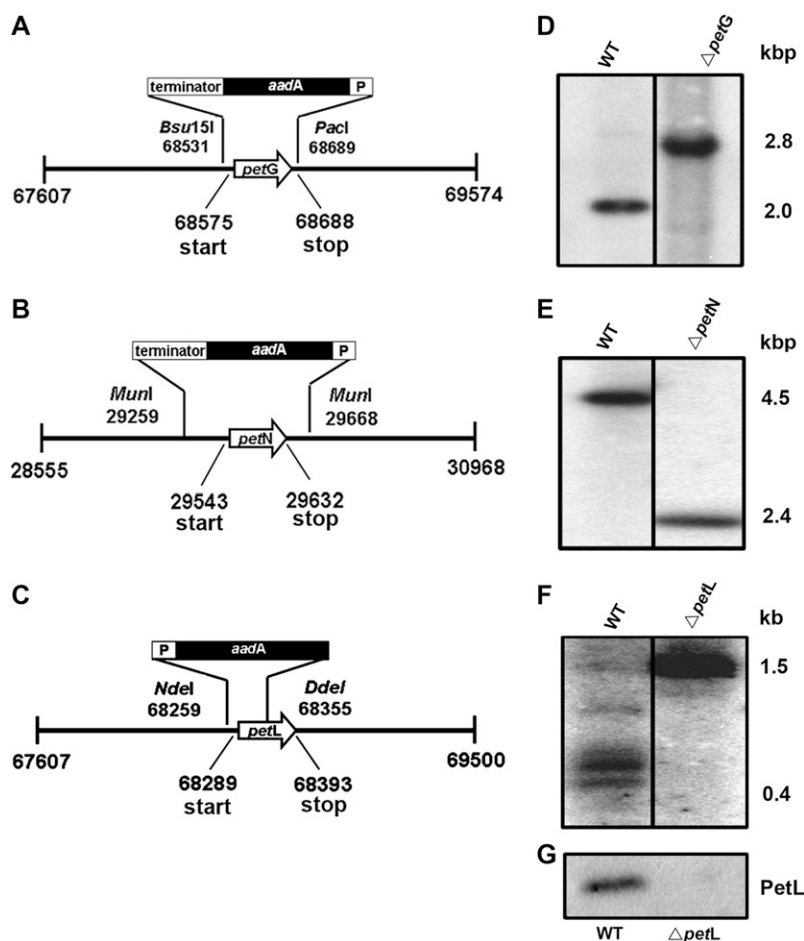
Inactivation of *petG*, *petN*, and *petL*

Independent transformants were selected from each knockout type ($\Delta petG$, $\Delta petL$, and $\Delta petN$), compared, and one line of each was finally used for detailed study (Fig. 1, A–C). Insertion of the *aadA* cassette into the respective genes and homoplastomy were verified by PCR analysis, sequence, Southern, northern, and western analysis (Swiatek et al., 2003; Fig. 1, D–F; data not shown). A transplastomic, spectinomycin resistance line containing the *aadA* insertion in a neutral site was used as wild-type control (Ohad et al., 2004). If not otherwise indicated, third to sixth leaves appearing from the meristem were used because transplastomic knockout lines in tobacco frequently exhibit secondary effects in older leaves (Ohad et al., 2004; Schwenkert et al., 2006; Schöttler et al. 2007; Umate et al., 2007).

Phenotypic Characterization of the Mutants

$\Delta petG$ and $\Delta petN$ deletion mutants lost their ability for photoautotrophic growth. They bleached when grown under normal tissue culture conditions ($100 \mu\text{mol photons m}^{-2} \text{s}^{-1}$) and even under very low light ($4 \mu\text{mol photons m}^{-2} \text{s}^{-1}$). Remarkably, their growth was severely retarded, $\Delta petN$ stronger than $\Delta petG$, as compared to wild type and homoplastomic *petA* and *petB* mutants, also deficient in assembly of the cytochrome complex (data not shown). In contrast to $\Delta petG$ and $\Delta petN$, $\Delta petL$ did not show any photobleaching and is viable even when grown on soil. *PetL* protein

Figure 1. Knockout constructs DNA and RNA gel-blot analysis of wild type and mutants. Each gene was replaced by the amino glycoside 3' adenyl transferase *aadA* cassette. The direction of transcription is symbolized by arrows. The 16S rDNA promoter of the cartridge is indicated (P). A, The entire *petG* gene was deleted by exchanging a *Bsu*151-*Pac*I fragment with the *aadA* cassette. B, Two *Mun*I restriction sites were used to delete the entire *petN* gene. C, The N-terminal part of *petL* was exchanged with the terminatorless *aadA* cassette. D and E, Southern analysis was performed to verify homoplastomy and the correct insertion of the *aadA* cassette. DNA obtained from Δ *petG* and Δ *petN* was restricted with *Eco*RI and *Eco*RV, respectively. F, Northern analysis of Δ *petL* confirmed homoplastomy because no *petL* transcript was detectable. G, Immunoblot analysis performed with PetL antisera did not even detect traces of PetL, again confirming homoplastomy of the knockout. Equal loading of wild-type and mutant material was verified in D to G (data not shown).



does not accumulate in Δ *petL* as judged from immunoblot analysis confirming homoplastomy of the knockout line (Fig. 1G).

Electron Transport Is Retarded in Δ *petL* and Abolished in Δ *petG* and Δ *petN*

Chlorophyll *a* fluorescence measurements showed that no photochemical quenching occurred in Δ *petG* and Δ *petN* at any light intensity, indicating that electron transport is completely blocked. The maximal PSII yield, F_v/F_m , is significantly decreased in Δ *petG* and Δ *petN*, but apparently unchanged in Δ *petL* (wild type 0.81 ± 0.01 ; Δ *petG* 0.54 ± 0.03 ; Δ *petN* 0.58 ± 0.02 ; and Δ *petL* 0.78 ± 0.02). This indicates increased light sensitivity as a secondary effect of the Δ *petG* and Δ *petN* mutations. At lower light intensities, photochemical quenching in Δ *petL* is comparable to wild type, but, at increased light intensities, above $500 \mu\text{mol photons m}^{-2} \text{s}^{-1}$, the photosynthetic yield is significantly reduced in Δ *petL* plants (Fig. 2A), whereas nonphotochemical quenching remains largely unchanged (data not shown). This indicates that, especially at higher light intensities, the PQ pool remains relatively reduced and the electrons are not transferred efficiently

from PSII to PSI, presumably due to reduced activity of the cytochrome complex.

PSI yield in terms of the light-induced redox state of P700^+ was measured as absorbance changes at 830 nm. Although PSI is functionally not affected in Δ *petL*, PSI yield is significantly impaired in the mutant, indicating that the electron flow from the Cyt *b₆f* complex to PSI is impaired in the mutant (Fig. 2B).

Accumulation of Cyt *b₆f* Complex Subunits in the Mutants

Immunoblot analysis demonstrated that subunits of the Cyt *b₆f* complex, Cyt *f*, Cyt *b₆*, and subunit IV, are faintly detectable in both Δ *petG* and Δ *petN*. This demonstrates that both LMW subunits are essential for proper assembly of the Cyt *b₆f* complex in higher plants, although they are located peripherally in the complex (Stroebel et al., 2003; Fig. 3). In Δ *petL*, subunits of the cytochrome complex accumulate to levels of approximately 50% of the wild type. PSII and PSI components are slightly affected in Δ *petG* and Δ *petN* as illustrated by immunoblot analysis with antibodies raised against subunits CP43 and PsaF of these photosystems. Remarkably, levels of ATP synthase subunit

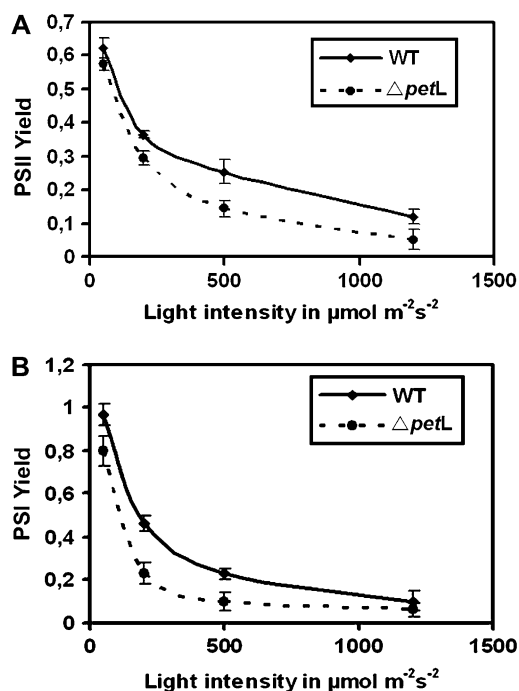


Figure 2. Maximal PSII quantum yield and PSI oxidation state of wild type and $\Delta petL$ at increasing light intensities. A, PSII quantum yield is reduced in $\Delta petL$ at higher light intensities. B, $\Delta petL$ shows a lower PSI yield at all light intensities. Mean values of five independent experiments are shown and error bars indicate SDs.

α are significantly up-regulated in $\Delta petN$ and $\Delta petG$, but unchanged in $\Delta petL$ as compared to wild type.

Assembly of the Cyt *b₆f* Complex in $\Delta petL$

To investigate the Cyt *b₆f* complex in $\Delta petL$, isolated mutant and wild-type thylakoids were solubilized with 1% β -dodecylmaltoside (β -DM). The membrane assemblies separated by nondenaturing blue-native (BN) gel electrophoresis in the first dimension were subjected to SDS-PAGE in the second dimension. The components of thylakoid membrane complexes are designated according to serological and mass spectrometric identification (Granvogl et al., 2006; Schwenkert et al., 2006). The analysis revealed that predominantly dimers of the Cyt *b₆f* complex accumulate in the wild type, but surprisingly only the monomeric form of the complex is detectable in silver-stained gels of $\Delta petL$ (Fig. 4). Immunoblot analysis uncovered that the Rieske FeS protein is detached from the monomeric form of the complex in mutant and wild type (Fig. 6B). Assembly and amounts of all other thylakoid membrane complexes are not affected by the mutation.

To clarify whether the dimer in $\Delta petL$ is absent due to instability during the solubilization process, milder lysis conditions for solubilization of thylakoid membranes were used. Thylakoid membranes were partially solubilized with 0.2% α -DM and the lysates were

separated by Suc density centrifugation. Under these conditions, preferentially the LHClI and PSII monomer, ATP synthase, as well as the dimeric and monomeric Cyt *b₆f* complex were released from the membrane, whereas other higher order assemblies tend to remain in the pelleted residual membrane fraction (Fig. 5A). Even under these mild conditions of solubilization and separation, dimeric cytochrome complexes could not be detected in $\Delta petL$. In contrast to BN-PAGE using 1% β -DM, the Rieske FeS protein is not released from the monomer in wild type, but is found detached in $\Delta petL$ and detected in the upper part of the gradient containing free proteins (Fig. 5B). This indicates that PetL is involved in stabilizing the Rieske FeS protein.

To investigate further whether loss of PetL prevents dimerization or causes instability of the complex, in vivo radiolabeling experiments were performed. For this, rapidly expanding young leaves of wild-type and mutant plants were incubated in ^{35}S -Met-containing medium. After 40 min of incubation, BN-SDS-PAGE showed predominantly the assembled dimeric form of the Cyt *b₆f* complex and only minor amounts of the monomer in wild type. Again, in $\Delta petL$ exclusively, the monomeric form of the Cyt *b₆f* complex could be detected, suggesting that dimer assembly is impaired in the mutant (Fig. 6A).

It has been reported that amount and thus stability of the cytochrome complex in $\Delta petL$ plants could depend on leaf age (Schöttler et al., 2007). Immunoblot analysis of the second dimension performed with leaves of different age probing with antisera elicited against subunits of the cytochrome complex detected monomer and dimer in the wild type, but the dimer was below the limit of detection in $\Delta petL$ leaves of

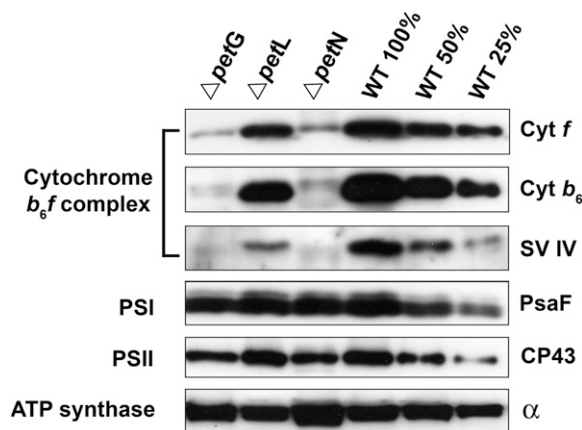


Figure 3. Immunoblot analysis of wild type, $\Delta petG$, $\Delta petL$, and $\Delta petN$ thylakoid membrane proteins. Proteins were separated by SDS-PAGE on a 15% polyacrylamide gel, electroblotted onto polyvinylidene difluoride membranes, and probed with antisera against Cyt *f*, Cyt *b₆*, and subunit IV of the cytochrome complex, and representative subunits of PSI (PsaF), PSII (CP43), of the ATP synthase α - and β -subunits. Five micrograms of chlorophyll (100% of wild type and mutant) were loaded per lane.

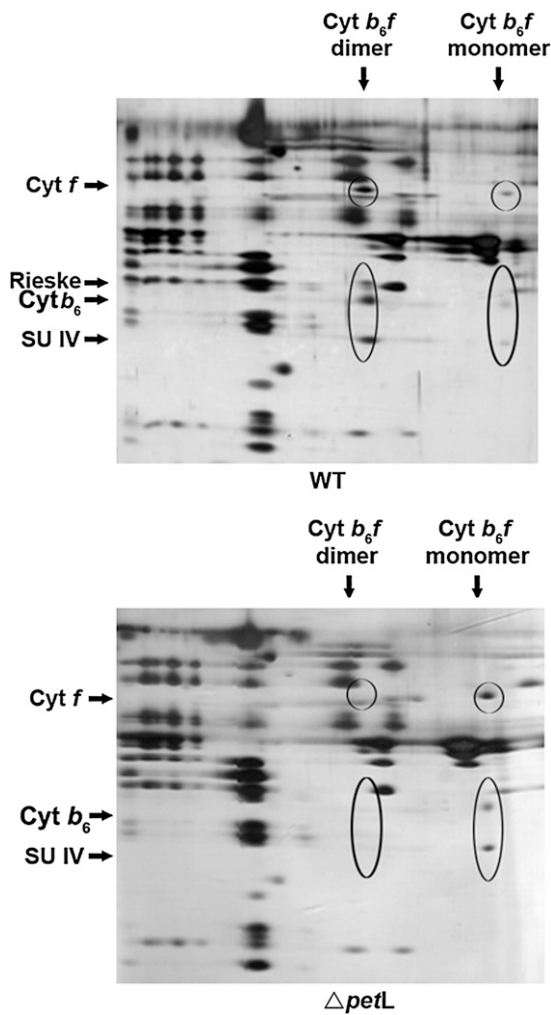


Figure 4. BN-PAGE with wild type and $\Delta petL$ thylakoid membrane proteins. Thylakoid membranes were lysed with 1% β -DM and separated on a 4% to 12% polyacrylamide gel. The second-dimension SDS-PAGE was silver stained and complexes were labeled according to their identification by mass spectrometry (Granvogel et al., 2006) or serology. In wild-type plants, both dimers and monomers of the Cyt b_6/f complex were detectable, whereas the $\Delta petL$ mutant accumulated only monomers. Under the chosen conditions, the Rieske protein is missing in the monomeric form of the complex in both wild type and $\Delta petL$ mutants.

middle age (Fig. 6B). However, in the first two leaves appearing from the meristem, traces of dimer were detectable in the mutant (Fig. 6C), indicating that PetL is not primarily required for dimerization, but rather for stability of the dimer. Taken together, both assembly and stability of the complex appear to be more strongly affected, particularly with increasing leaf age. The Rieske protein is not detectable in the monomer both in the wild type and $\Delta petL$, implying that it is lost during solubilization with 1% β -DM.

Because the data presented above indicate that an unstable association of the Rieske protein might lead to monomerization in $\Delta petL$, a stable *Arabidopsis petC*

transposon insertion line, which lacks the Rieske protein (Maiwald et al., 2003), was analyzed by BN- and SDS-PAGE. In contrast to other Rieske mutants, lack of the Rieske protein does not prevent accumulation of other Cyt b_6/f subunits in *Arabidopsis*. Interestingly, the second dimension, immunoblotted and probed with an antiserum against Cyt f , demonstrated that this mutant is well able to accumulate dimeric Cyt b_6/f complexes (Fig. 7).

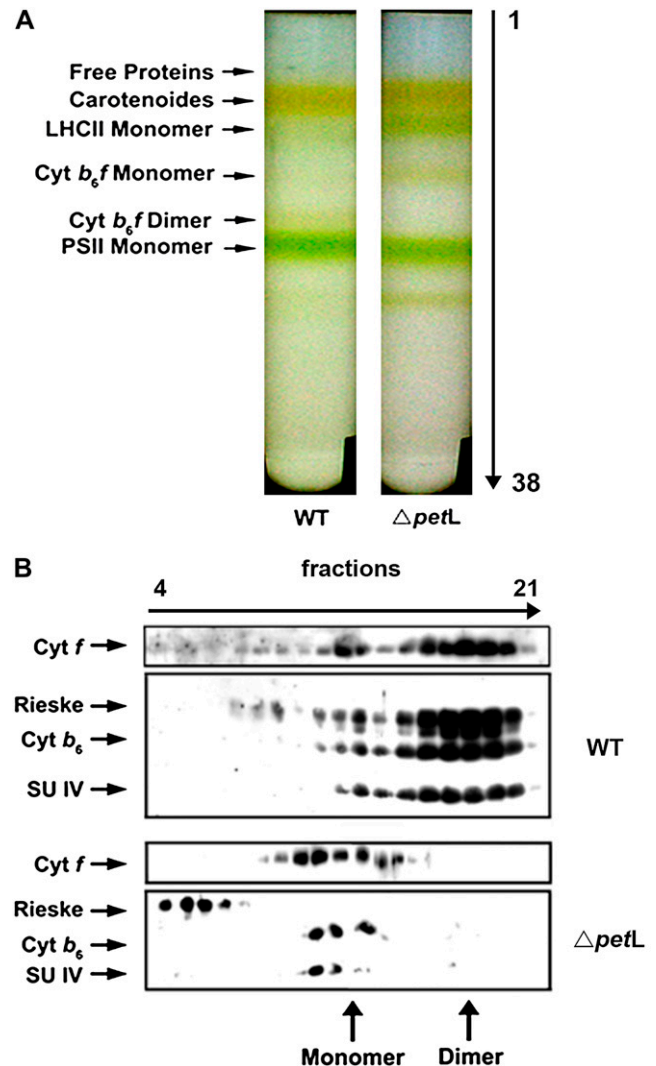


Figure 5. Suc density gradients and immunoblot analysis of the fractions. A, Supernatants of wild type and $\Delta petL$ thylakoid membranes lysed with 0.2% α -DM were loaded onto a 5% to 30% Suc gradient. Predominantly the monomer of PSII as well as monomeric and dimeric Cyt b_6/f complexes were released from the membranes. B, Immunoblot analysis performed with fractions from Suc gradients shown in A and probed with antisera against the major subunits of the Cyt b_6/f complex. Fractions numbered from top to the bottom of the gradients were loaded. In the mutant only monomeric Cyt b_6/f complex was detectable and the released Rieske protein accumulated at the top of the gradient along with free proteins. [See online article for color version of this figure.]

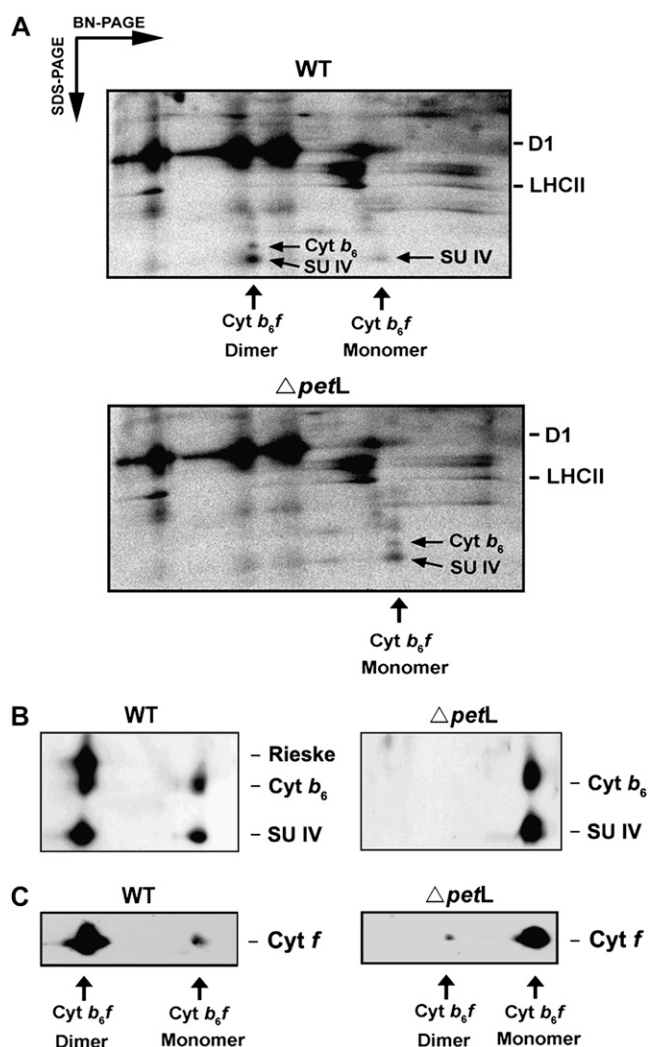


Figure 6. In vivo labeling of wild-type and $\Delta petL$ leaves, followed by BN-PAGE and immunoblot analysis. **A**, The first two appearing leaflets of wild-type and mutant plants were infiltrated with ^{35}S -Met. Subsequently, thylakoids were isolated, solubilized with 1% β -DM, separated by BN-SDS-PAGE, and detected by fluorography. **B**, Immunoblot analysis of the second dimension performed with mature leaves. No dimer of the Cyt *b₆f* complex was detectable in the mutant. **C**, Although no dimer could be detected by in vivo labeling in $\Delta petL$ (**A**), traces could be detected by immunology when using the same plant material as in **A**.

$\Delta petL$ Is Defective in Phosphorylation of the LHCII

The phosphorylation state of PSII reaction center proteins and LHCII was investigated by illumination with far-red light of 728 nm (state I) and with increasing light intensities of 650 nm (state II) for 30 min. Thylakoids were then rapidly isolated and immunoblot analysis was performed with anti-phospho-Thr antibodies. In both the wild type and the $\Delta petL$ mutant, the PSII reaction center proteins CP43, D1, and D2 were phosphorylated upon illumination. Furthermore, LHCII proteins were more phosphorylated with increasing light intensities. This process appears to be

impaired in $\Delta petL$ because phosphorylation is reduced to approximately 50% of wild-type levels (Fig. 8A).

To show that hindered LHCII phosphorylation is primarily due to reduced levels of the cytochrome complex and not because of the reduction state of the PQ pool or other secondary effects of the $\Delta petL$ mutation, the PQ pool was reduced in darkness by adding duroquinol to isolated wild-type and $\Delta petL$ thylakoids. Immunoblot analysis showed that phosphorylation of D1 and D2 proteins was equally activated in both wild type and mutant, but phosphorylation of LHCII remained significantly reduced in $\Delta petL$ (Fig. 8B).

Association of the PSI-LHCII supercomplex under state II conditions can be observed in BN gels after solubilization of thylakoids with digitonin (Fig. 8C). In the second dimension of the BN gel, the phosphorylated LHCII can be detected in the free LHCII trimer and PSII supercomplexes, as well as associated with PSI as confirmed by electrophoretic mobility and the use of a specific PsaF antiserum (Fig. 8E). Although there is less LHCII phosphorylation in $\Delta petL$, the PSI-LHCII supercomplex is formed (Fig. 8, C and D). Upon analysis of the BN-SDS-PAGE second dimension with phospho-Thr antibodies, it appeared that equal amounts of PSI-LHCII are present in wild type and mutant, whereas there is less phosphorylated trimeric LHCII in the mutant (Fig. 8D).

PetL Is Not Essential for Ferredoxin-Dependent PQ Reduction

In higher plants, the principal pathway of cyclic electron transport around PSI is sensitive to antimycin A and depends on the function of a small thylakoid protein, PGR5 (Munekage et al., 2002). Activity of PGR5-dependent PSI cyclic electron transport can be detected as ferredoxin (Fd)-dependent PQ reduction in ruptured chloroplasts. It has long been discussed whether this electron transport occurs through the Cyt *b₆f* complex (Kurisu et al., 2003; Stroebel et al., 2003; Okegawa et al., 2005; Cramer and Zhang, 2006). To test

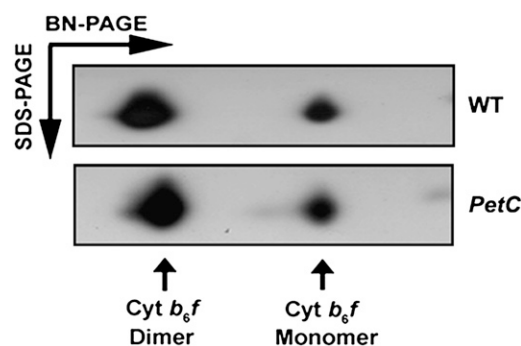
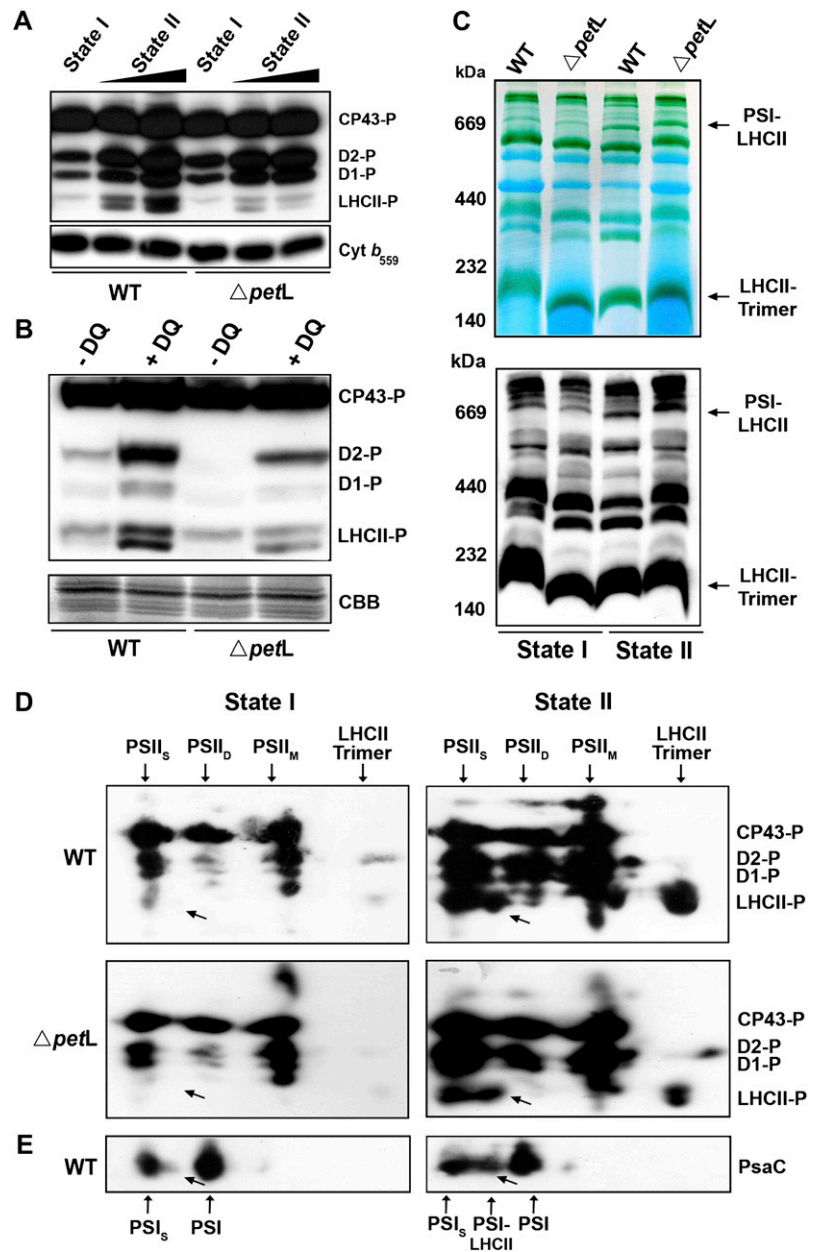


Figure 7. Arabidopsis wild-type and *petC* plants were analyzed by BN-SDS-PAGE. Immunoblot analysis of the second dimension with antisera against Cyt *f* demonstrates that dimeric and monomeric complexes accumulate at normal levels in the mutant.

Figure 8. Phosphorylation patterns and formation of PSI-LHCII supercomplexes. A, Wild-type and $\Delta petL$ plants were illuminated with far-red light of 728 nm (state I) or treated with increasing light intensities of 10, 20, and 40 $\mu\text{mol photons m}^{-2} \text{s}^{-1}$ at 650 nm (state II). Thylakoids were isolated and immunoblot analysis was performed using a phospho-Thr-specific antibody (New England Biolabs). Equal amounts of chlorophyll (5 μg) were loaded per lane. Immunoblot analysis with an antiserum specific for Cyt b_{559} was performed as a loading control. B, Kinase activation was induced in darkness by addition of reduced duroquinol to isolated thylakoids. Five micrograms of chlorophyll were loaded per lane and equal loading was checked by Coomassie Brilliant Blue (CBB). C, BN-PAGE was performed with thylakoids isolated from plants incubated under state I and state II conditions (40 $\mu\text{mol m}^{-2} \text{s}^{-1}$). Thylakoids were solubilized with 1.5% digitonin, allowing the detection of PSI-LHCII supercomplex under state II conditions in wild type as shown by immunoblot analysis of the BN-PAGE gel with antisera against LHCBI (bottom). Equal amounts of chlorophyll (100 μg) were loaded per lane. D, Second-dimension SDS-PAGE and immunoblot analysis with phospho-Thr antibodies were performed with the BN gel shown in C. Under state II conditions, an additional complex is detectable, representing an association of LHCII-P with PSI (indicated by arrows). E, Wild type under state I and state II conditions was probed with a PsaC antiserum showing the additional LHCII-P-PSI complex appearing only under state II conditions. [See online article for color version of this figure.]



this possibility and to evaluate the effect of monomerization of the cytochrome complex on electron transport, the activity of Fd-dependent PQ reduction was measured in $\Delta petL$ (Fig. 9). Although addition of NADPH to ruptured chloroplasts did not change the reduction level of PQ, subsequent addition of Fd reduced PQ in both wild type and $\Delta petL$, as monitored by increased chlorophyll fluorescence (Fig. 9). Both reduction rate and the final level of reduction were almost identical in wild type and $\Delta petL$, indicating that PetL is not essential for PGR5-dependent PSI cyclic electron transport. Addition of antimycin A drastically impaired PQ reduction in both mutant and wild type. The remaining PQ reduction activity depends on the

chloroplast NDH complex rather than PGR5 (Munekage et al., 2004). We conclude that PGR5-dependent PQ reduction via Fd does not require dimerization of the Cyt b_6f complex.

DISCUSSION

To clarify and compare the roles of the plastid-encoded LMW subunits PetG, PetL, and PetN in assembly and stability of the Cyt b_6f complex, transplastomic knockout lines were generated in tobacco. Whereas $\Delta petL$ grew photoautotrophically, growth of $\Delta petN$ and $\Delta petG$ was retarded even when cultivated

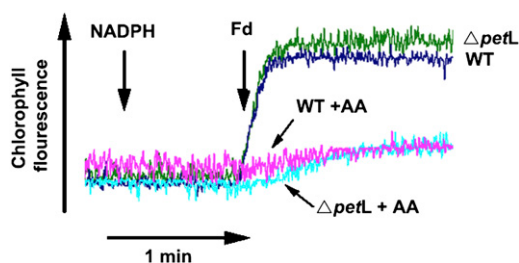


Figure 9. Fd-dependent PQ reduction activity in ruptured chloroplasts. Chloroplasts were isolated from wild-type and $\Delta petL$ leaves and osmotically shocked in hypotonic buffer (10 μg of chlorophyll/mL). Electron donation to PQ was monitored as increase in chlorophyll fluorescence by addition of 0.25 mM NADPH and 5 μM Fd under weak illumination (1 $\mu\text{mol photons m}^{-2} \text{s}^{-1}$). To inhibit the PGR5-dependent PQ reduction, 10 μM antimycin A (AA) was added prior to analysis. The fluorescence level was standardized by F_m . [See online article for color version of this figure.]

on Suc-supplemented medium in comparison to wild type. The latter mutants lack the cytochrome complex almost completely.

$\Delta petG$ and $\Delta petN$ Lack the Cyt *b₆f* Complex Almost Completely

$\Delta petG$ and $\Delta petN$ accumulate only traces of other subunits of the Cyt *b₆f* complex, suggesting that they represent constituent subunits that are required for early stages of complex assembly. Although they reside only peripherally in the complex, their absence causes assembly problems or leads to rapid degradation of the assembly. Deficiencies in $\Delta petN$ were less pronounced, indicating that PetG functions in the nucleation process of assembly, whereas PetN represents a later addition. It is surprising that these small subunits exert such a crucial role on the assembly and/or stability of the cytochrome complex, specifically because they are not located at a central position. Either this is due to rapid degradation of the translation products, to a CES-like process involved in the coordination of protein stoichiometry of the cytochrome complex, or to CES-independent assembly deficiencies. This pattern is reminiscent of the essential role of the LMW subunits PsbE, PsbF, PsbL, and PsbJ on the assembly/stability of PSII and photoautotrophic growth in tobacco (Swiatek et al., 2003; Ohad et al., 2004). Other LMW subunits of PSII, like PsbH, PsbI, PsbK, PsbM, and PsbZ, are dispensable for assembly of at least monomeric complexes, but exert crucial roles on light trapping and regulation of the redox components involved in primary photochemical reactions (Swiatek et al. 2001; Minagawa and Takahashi, 2004; Shi and Schröder, 2004; Schwenkert et al., 2006; Umate et al., 2007).

Severe light sensitivity of $\Delta petN$ and $\Delta petG$ could account for reduced levels of PSI and especially PSII proteins as has been reported earlier for mutants deficient in photosynthesis (Barkan et al., 1986). This could lead to rapid degradation and impaired synthe-

sis of photosynthetic proteins. Higher levels detected for ATP synthase subunits in $\Delta petN$ and $\Delta petG$ compared to the wild type could be explained as compensation either from a physiological or from a structural point of view (Fig. 3) to compensate for impaired ATP production, to maintain membrane structure, or, rather, to maintain a high protein-lipid ratio. Interestingly, the same effect has been observed for a Cyt *b₆f* complex mutant in *Oenothera* and *Arabidopsis* (data not shown), and a reverse effect has been noted in mutants lacking ATP synthase but accumulating higher levels of subunits of the cytochrome complex (Dal Bosco et al., 2004).

PetL Stabilizes Rieske Conformation, Leading to Dimerization of the Cyt *b₆f* Complex

Structural alterations of the cytochrome complex in $\Delta petL$ lead to impaired electron flow, as shown by fluorescence and spectroscopic analyses *in vivo*. PSII quantum yield is reduced at higher light intensities and PSI is far more oxidized in the mutant. The outlined data demonstrate that PetL is either involved in stability or dimerization of the cytochrome complex as has been discussed previously (Takahashi et al., 1996; Breyton et al., 1997). Formation of the dimer is severely impaired and only traces could be found in the two youngest leaves in $\Delta petL$ (Fig. 6C). The PetL-deficient dimer is highly unstable and below the limit of detection in mature leaves. Even under mild solubilization conditions and separation in Suc density gradients, the dimeric form of the complex could not be detected in the mutant. *In vivo* labeling experiments using comparable conditions of solubilization suggest, as well, that dimer formation is affected. In young $\Delta petL$ plants, only monomeric complexes are labeled (Fig. 6A). The lower amount of cytochrome complex in $\Delta petL$ could be due to faster degradation of the monomeric form of the complex, which accumulates in $\Delta petL$. Nevertheless, photoautotrophic growth was not impaired in tobacco, but considerably in *Chlamydomonas* (Takahashi et al., 1996).

The Rieske FeS protein is composed of a hydrophilic region and a single C-terminal membrane-spanning hydrophobic stretch. It acts as a link between two monomers, with the membrane domain spanning one monomer and the extrinsic domain stabilizing the other monomer of the complex (Kurisu et al., 2003). It is evident that loss of the Rieske protein from monomeric complexes in $\Delta petL$ must be a secondary effect of the mutation because the Rieske protein is essential for PQ oxidation; otherwise, plants would not be viable. The Rieske protein is lost from the monomeric complex in $\Delta petL$ even during mild solubilization conditions. This and the fact that it remains attached to the complex under the same conditions in the wild type indicate that PetL is directly involved in the attachment of the Rieske protein to the complex. Applying somewhat harsher solubilization conditions, as is the case in BN gels, the Rieske protein is also missing in

the monomeric wild-type cytochrome complex, which could be caused by simultaneous loss of both PetL and the Rieske protein (Breyton et al., 1997).

The recently released crystal structures (Kurisu et al., 2003; Stroebel et al., 2003) assign the PetL protein to the periphery of the complex opposite the dimerization axis. This positioning does not support the idea that the protein is directly involved in the dimerization process. Yet, it is likely that lack of PetL destabilizes the attachment of the Rieske protein, either via conformational changes or its association with the Cyt *b₆f* complex leading to destabilization of the dimer.

We have demonstrated that an Arabidopsis *petC* mutant has the ability to form a dimeric Cyt *b₆f* complex (Fig. 7) and another *petC* mutant has been described from *Chlamydomonas* with a similar phenotype (de Vitry et al., 1999). This suggests that loss of the Rieske protein from the complex is a consequence of monomerization rather than its cause. Therefore, it is evident that loss of PetL leads to a conformational change instead of loss of the Rieske protein, thus preventing dimerization or leading to decreased stability of the dimer.

The Cyt *b₆f* Complex Is Involved in State Transition

Binding of plastoquinol at the quinol oxidation site of the cytochrome complex is directly involved in the activation of LHCII phosphorylating kinases and thus in state transition (Vener et al., 1997; Zito et al., 1999). A transgenic line expressing fusion between *petL* and *petD*, which has been described from *C. reinhardtii*, is not impaired in reducing the PQ pool but is unable to perform state transition (Zito et al., 2002). This work reinforces the direct involvement of the cytochrome complex in the activation of the LHCII kinase in tobacco. LHCII phosphorylation is significantly reduced upon both state II conditions and reduction of the PQ pool in darkness. As phosphorylation in general is not affected, it appears that the reduced level of LHCII phosphorylation is caused by decreased amounts of the cytochrome complex and/or loss of dimerization.

The fact that formation of PSI-LHCII supercomplexes is not affected in Δ *petL* is consistent with the finding that state transition is not impaired (data not shown; Schöttler et al., 2007). Still, how can the PSI-LCHII supercomplex be formed if there is less phosphorylation? This is explained by the fact that association of the phosphorylated LHCII with the photosystems is a competitive and dynamic process (Wollman, 2001; Rochaix, 2007). Presumably, a limited amount of LHCII-P can be bound to PSI, leading to accumulation of a mobile LHCII-P trimer pool of different size depending on the LHCII phosphorylation status. Indeed, levels of LHCII-P trimer are significantly reduced in the mutant as compared to the wild type (Fig. 8D), although it is evident that accumulation of the trimer is identical (Fig. 8C). Similarly, a Rieske knock-down is not affected in state transition despite a greatly photochemically reduced PQ pool (Anderson et al., 1997).

Dimerization of the Cyt *b₆f* Complex Is Not Essential for PSI Cyclic Electron Transport

In Δ *petL*, Fd-dependent PQ reduction, which functions in PSI cyclic electron transport in vivo, was not impaired (Fig. 9). This is consistent with the fact that induction of nonphotochemical quenching was not affected in the mutant. We obtained similar results with the Arabidopsis mutant *pgr3-2* (Yamazaki et al., 2004), in which levels of PetL and probably also PetG are reduced (data not shown). Previously, we have characterized electron transport in the Arabidopsis mutant *pgr1*, which has a conditional defect in the activity of the cytochrome complex (Okegawa et al., 2005). Due to an amino acid alteration in the Rieske subunit, the Cyt *b₆f* complex is hypersensitive to lumenal acidification in *pgr1* (Munekage et al., 2001; Jahns et al., 2002). We did not find any evidence suggesting that Fd-dependent PQ reduction is affected by the *pgr1* defect (Okegawa et al., 2005). None of the results suggests that Fd-dependent PQ reduction in the PGR5-dependent PSI cyclic pathway involves the Cyt *b₆f* complex, although we still cannot rigorously rule out this possibility.

MATERIALS AND METHODS

Strategies for Generation of Knockout Constructs and Plastid Transformation

In a transplastomic approach, the *petG*, *petL*, and *petN* genes of tobacco (*Nicotiana tabacum* 'Petit Havana') have been inactivated by replacing all (*petG*, *petN*) or most (*petL*) of the genes with the chimeric amino glycoside 3' adenylyl transferase (*aadA*) cassette conferring resistance to spectinomycin (Koop et al., 1996). The individual constructs were inserted into the pBluescript KS II+ plasmid (Stratagene) and the constructs were introduced into tobacco leaf chloroplasts applying biolistic transformation (Boynton et al., 1988; Svab et al., 1990; Svab and Maliga, 1993). The transformed material was regenerated, selected, and cultured as described recently (Schwenkert et al., 2006).

The *Bsf*YI fragment of the tobacco chloroplast genome (position 67,607–69,574 bp) was obtained from clones described earlier (Shinozaki et al., 1986) and cloned into the *Bam*HI site of pBluescript. The *Bsu*151-*Pac*I fragment (position 68,531–68,689) spanning the *petG* region was replaced by the *aadA* cassette, thus removing the entire *petG* gene. The *Hind*III-*Bsp*HI fragment (position 28,555–30,968) containing *petN* was cloned into the pBluescript *Eco*R32I-*Ecl*136II sites. The gene was removed completely by replacing the *aadA* cassette with the internal *Mun*I fragment (position 29,259–29,668). The *Sal*I-*Sma*I fragment (position 67,607–69,500) was cloned into the corresponding sites of pBluescript. The N-terminal part of *petL* (position 68,259–68,355) was cut off with *Nde*I and *Dde*I, and exchanged with a terminatorless *aadA* cassette excised with *Sma*I and *Sph*I. Thus, 19 of the 31 amino acids coding for *petL* were removed (Fig. 1).

Growth Conditions

Tobacco plants were grown under standard light conditions ($100 \mu\text{mol m}^{-2} \text{s}^{-1}$) or under lower light regimes (approximately $4\text{--}10 \mu\text{mol photons m}^{-2} \text{s}^{-1}$) generally at 25°C and 16-h-light/8-h-dark cycles (Osram L85W/25 universal white fluorescent lamps). Plants from photoautotrophic mutant lines were grown on soil under greenhouse conditions. If not otherwise indicated, all analyses were carried out with young leaves of 6- to 8-week-old plants, grown in vitro and under greenhouse conditions (day 26°C, night 20°C), respectively. Tobacco lines carrying the *aadA* cassette in a neutral insertion site and referred to as RV plants served as wild-type control (Ohad et al., 2004).

Arabidopsis (*Arabidopsis thaliana*) wild-type (ecotype Landsberg *erecta*) and mutant plants were grown on Murashige and Skoog medium containing 1.4%

Suc in a growth chamber at 30 $\mu\text{mol m}^{-2} \text{s}^{-1}$, 16-h-light/8-h-dark cycles, and at 22°C.

DNA Gel-Blot Analysis

For Southern analysis, total wild-type and mutant DNA (5 $\mu\text{g}/\text{lane}$) was restricted with appropriate enzymes and the resulting fragments were separated electrophoretically in an agarose gel. DNA transfer from the gel onto nitrocellulose membranes was performed by capillary blotting as described by Sambrook et al. (1989). Hybridization was carried out with a radiolabeled, single-stranded RNA probe generated by *in vitro* transcription using PCR products generated with oligonucleotides containing a T7 promoter at their 5' ends. The following oligonucleotides were used as templates: 5'-GATAA-TACGACTCACTATAGGGCACACAATTTAAGTAGATGCG-3' and 5'-GAT-AATACGACTCACTATAGGGTAAATTAATCAAAGGTCCAA-3' for *petG* and 5'-GATCCAAAACCTTGAGATAATGG-3' and 5'-TTTGTAGCATTTGGC-GACA-3' for *petN*.

RNA Gel-Blot Analysis

RNA gel-blot analysis was performed as described (Lezhneva and Meurer, 2007). The *petL* probe was amplified by PCR using oligonucleotides 5'-GGA-TGGATAGATGTTACAGATGATG-3' and 5'-GTCATTGAGATCATGTCAATT-CGGATTA-3'.

Preparation of Thylakoid Membranes, SDS-PAGE, and Immunoblot Analysis

Membrane proteins were isolated essentially as described (Umate et al., 2007). Proteins separated by SDS-Tris-Gly-PAGE (15% acrylamide; Laemmli, 1970) were transferred to polyvinylidene difluoride membranes (GE Healthcare), incubated with monospecific polyclonal antisera (Lezhneva et al., 2004), and visualized by the enhanced chemiluminescence technique (GE Healthcare).

Suc Density Gradient Centrifugation

Isolated thylakoid membranes (final chlorophyll concentration 1 mg/mL) were partially solubilized with 0.2% α -DM in 20 mM BisTris, 5 mM NaCl, and 5 mM MgCl₂ for 45 min at 4°C. After centrifugation at 18,000g, 4°C for 12 min, the solubilized fraction was layered onto 5% to 30% Suc gradients containing 0.06% α -DM. Gradients were run for 18 h in a Beckman SW40Ti rotor at 200,000g (4°C) and fractionated from top to bottom into 38 aliquots of 300 μL each, using an ISCO 640 gradient fractionator. The separation pattern of partially solubilized protein complexes in the gradients was verified by serology.

BN-PAGE

BN-PAGE analysis was performed as described earlier (Schwenkert et al., 2006). Thylakoids were isolated and solubilized with 1% β -DM for 10 min or with 1.5% digitonin for detection of PSI-LHCII-P supercomplexes (Zhang and Scheller, 2004) for 1 h, followed by centrifugation at 20,000g for 1 h at 4°C. The solubilized proteins were separated on a 4% to 12% polyacrylamide gradient gel. Excised gel lanes were denatured and analyzed on a 15% polyacrylamide gel containing 4 M urea. The gels were subsequently silver stained (Blum et al., 1987) or used for immunoblotting. Protein spots were assigned as described previously (Granvogl et al., 2006). For *in vivo* labeling experiments, primary leaves of 2-week-old mutant and wild-type seedlings were incubated for 40 min in ³⁵S-Met at a final concentration of 0.7 $\mu\text{Ci } \mu\text{L}^{-1}$ (GE Healthcare) as described (Amann et al., 2004).

Analysis of Phosphorylated Thylakoid Membrane Proteins

For phosphorylation experiments, all buffers were supplemented with 10 mM NaF. Wild-type and mutant plants were treated with light at 650 (PSII light) or 728 (PSI light) nm. To activate the protein kinase in isolated thylakoids in darkness, reduced duroquinol (1 mM) was added and the assays were incubated for 20 min at room temperature (Allen et al., 1989). The extent

of phosphorylation was detected with phospho-Thr antibodies (New England Biolabs).

Chlorophyll *a* Fluorescence Induction Kinetics

Chlorophyll *a* fluorescence induction kinetics of wild-type and mutant leaves was measured using a pulse-modulated fluorimeter (PAM101; Walz). Leaves, dark adapted for at least 15 min, were used to analyze minimal (F_0) and maximal (F_m) fluorescence yields, the latter being determined by application of a saturating light pulse (1-s duration, 4,500 $\mu\text{mol photons m}^{-2} \text{s}^{-1}$). The potential maximum quantum yield of PSII was measured as $(F_m - F_0)/F_m = F_v/F_m$ (Schreiber et al., 1998).

PSI Activity

PSI yield was measured on leaves as absorption changes at 820 nm induced by saturating pulses and far-red light (12 W m^{-2} as measured with a YSI Kettering model 65 A radiometer) in the absence or presence of actinic light (650 nm, 20 and 250 $\mu\text{mol m}^{-2} \text{s}^{-1}$) using the PSI attachment of PAM101 (Walz; Klughammer and Schreiber, 1994).

In Vitro Assay of PSI Cyclic Electron Transport Activity

Chloroplast isolation and assay of Fd-dependent PQ reduction in ruptured chloroplasts were performed as described (Munekage et al., 2002).

ACKNOWLEDGMENTS

We would like to thank Martina Reymers and Gisela Nagy for excellent technical assistance. We are grateful to Vera Bonardi for helpful suggestions. Further, we would like to express our gratitude to Dario Leister for critical reading of the manuscript and providing the *petC* mutant. Jean-David Rochaix is acknowledged for supplying PetL antibodies.

Received March 23, 2007; accepted June 2, 2007; published June 7, 2007.

LITERATURE CITED

- Allen JF (1992) Protein phosphorylation in regulation of photosynthesis. *Biochim Biophys Acta* **1098**: 275–335
- Allen JF (2004) Cytochrome *b₆f*: structure for signalling and vectorial metabolism. *Trends Plant Sci* **3**: 130–137
- Allen JF, Harrison MA, Holmes NG (1989) Protein phosphorylation and control of excitation energy transfer in photosynthetic purple bacteria and cyanobacteria. *Biochimie* **71**: 1021–1028
- Amann K, Lezhneva L, Wanner G, Herrmann RG, Meurer J (2004) ACCUMULATION OF PHOTOSYSTEM ONE1, a member of a novel gene family, is required for accumulation of [4Fe-4S] cluster-containing chloroplast complexes and antenna proteins. *Plant Cell* **11**: 3084–3097
- Anderson JM, Dean Price G, Soon Chow W, Hope AB, Badger MR (1997) Reduced levels of cytochrome *bf* complex in transgenic tobacco leads to marked photochemical reduction of the plastoquinone pool, without significant change in acclimation to irradiance. *Photosynth Res* **53**: 215–227
- Aro EM, Ohad I (2003) Redox regulation of thylakoid protein phosphorylation. *Antioxid Redox Signal* **1**: 55–67
- Barkan A, Miles D, Taylor WC (1986) Chloroplast gene expression in nuclear, photosynthetic mutants of maize. *EMBO J* **5**: 1421–1427
- Bellafiore S, Barneche F, Peltier G, Rochaix JD (2005) State transitions and light adaptation require chloroplast thylakoid protein kinase STN7. *Nature* **433**: 892–895
- Berthold D, Schmidt C, Malkin R (1995) The deletion of *petG* in *Chlamydomonas reinhardtii* disrupts the cytochrome *b₆f* complex. *J Biol Chem* **270**: 29293–29298
- Blum H, Beier H, Gross HJ (1987) Improved silver staining of plant proteins, RNA and DNA in polyacrylamide gels. *Electrophoresis* **8**: 93–99
- Bonardi V, Pesaresi P, Becker T, Schleiff E, Wagner R, Pfannschmidt T, Jahns P, Leister D (2005) Photosystem II core phosphorylation and photosynthetic acclimation require two different protein kinases. *Nature* **437**: 1179–1182

- Boynton JE, Gillham NW, Harris EH, Hosler JP, Johnson AM, Jones AR, Randolph-Anderson BL, Robertson D, Klein TM, Shark KB (1988) Chloroplast transformation in *Chlamydomonas* with high velocity microprojectiles. *Science* **240**: 1534–1538
- Breyton C, Tribet C, Olive J, Dubacqi JP, Popot JL (1997) Dimer to monomer conversion of the cytochrome b_6f complex. *J Biol Chem* **272**: 21892–21900
- Bruce BD, Malkin R (1991) Biosynthesis of the chloroplast cytochrome b_6f complex: studies in a photosynthetic mutant of *Lemna*. *Plant Cell* **3**: 203–212
- Choquet Y, Wostrikoff K, Rimbault B, Zito F, Girard-Bascou J, Drapier D, Wollman FA (2001) Assembly-controlled regulation of chloroplast gene translation. *Biochem Soc Trans* **4**: 421–426
- Cramer WA, Yan J, Zhang H, Kurisu G, Smith JL (2005) Structure of the cytochrome b_6f complex: new prosthetic groups, Q-space, and the 'hors d'oeuvres hypothesis' for assembly of the complex. *Photosynth Res* **85**: 133–143
- Cramer WA, Zhang H (2006) Consequences of the structure of the cytochrome b_6f complex for its charge transfer pathways. *Biochim Biophys Acta* **1757**: 339–345
- Dal Bosco C, Lezhneva L, Biehl B, Leister D, Strotmann H, Wanner G, Meurer J (2004) Inactivation of the chloroplast ATP synthase γ subunit results in high non-photochemical fluorescence quenching and altered nuclear gene expression in *Arabidopsis thaliana*. *J Biol Chem* **279**: 1060–1069
- de Vitry C, Breyton C, Pierre Y, Popot JL (1996) The 4-kDa nuclear-encoded PetM polypeptide of the chloroplast cytochrome b_6f complex. *J Biol Chem* **271**: 10667–10671
- de Vitry C, Finazzi G, Baymann F, Kallas T (1999) Analysis of the nucleus-encoded and chloroplast-targeted Rieske protein by classic and site-directed mutagenesis of *Chlamydomonas*. *Plant Cell* **11**: 2031–2044
- Fiebig A, Stengemann S, Schöttler R (2004) Rapid evolution of RNA editing sites in a small non essential plastid gene. *Nucleic Acids Res* **32**: 3615–3622
- Granvogel B, Reisinger V, Eichacker LA (2006) Mapping the proteome of thylakoid membranes by de novo sequencing of intermembrane peptide domains. *Proteomics* **12**: 3681–3695
- Hager M, Biehler K, Illerhaus J, Ruf S, Bock R (1999) Targeted inactivation of the smallest plastid genome-encoded open reading frame reveals a novel and essential subunit of the cytochrome b_6f complex. *EMBO J* **18**: 5834–5842
- Hamel P, Olive J, Pierre Y, Wollman FA, de Vitry C (2000) A new subunit of cytochrome b_6f complex undergoes reversible phosphorylation upon state transition. *J Biol Chem* **275**: 17072–17079
- Herrmann RG, Westhoff P, Alt J, Tittgen J, Nelson N (1985) Thylakoid membrane proteins and their genes. In L Vloten-Doting, G Groot, T Hall, Molecular Form and Function of the Plant Genome. Plenum Publishing, New York, pp 233–256
- Jahns P, Graf M, Munekage Y, Shikanai T (2002) Single point mutation in the Rieske iron-sulfur subunit of cytochrome b_6f leads to an altered pH dependence of plastoquinol oxidation in *Arabidopsis*. *FEBS Lett* **519**: 99–102
- Klughammer C, Schreiber U (1994) An improved method, using saturating light pulses, for the determination of photosystem I quantum yield via $P700^+$ -absorbance changes at 830 nm. *Planta* **192**: 261–268
- Koop HU, Steinmüller K, Wagner H, Rossler C, Eibl C, Sacher L (1996) Integration of foreign sequences into the tobacco plastome via polyethylene glycol-mediated protoplast transformation. *Planta* **199**: 193–201
- Kuras R, Wollman FA (1994) The assembly of cytochrome b_6f complexes: an approach using genetic transformation of the green alga *Chlamydomonas reinhardtii*. *EMBO J* **13**: 1019–1027
- Kurisu G, Zhang H, Smith J, Cramer W (2003) Structure of the b_6f complex of oxygenic photosynthesis: tuning the cavity. *Science* **302**: 1009–1014
- Laemmli UK (1970) Cleavage of structural proteins during the assembly of the head of bacteriophage T4. *Nature* **227**: 680–685
- Lezhneva L, Amann K, Meurer J (2004) The universally conserved HCF101 protein is involved in assembly of [4Fe-4S]-cluster containing complexes in *Arabidopsis thaliana* chloroplasts. *Plant J* **37**: 174–185
- Lezhneva L, Meurer J (2004) The nuclear factor HCF145 affects chloroplast *psaA-psaB-rps14* transcript abundance in *Arabidopsis thaliana*. *Plant J* **38**: 740–753
- Maiwald D, Dietzmann A, Jahns P, Pesaresi P, Joliet P, Joliet A, Levin JZ, Salamini F, Leister D (2003) Knock-out of the genes coding for the Rieske protein and the ATP-synthase δ -subunit of *Arabidopsis*. Effects on photosynthesis, thylakoid protein composition, and nuclear chloroplast gene expression. *Plant Physiol* **133**: 191–202
- Miles D (1982) The use of mutations to probe photosynthesis in higher plants. In M Edelman, RB Hallick, N-H Chua, eds, *Methods in Chloroplast Molecular Biology*. Elsevier Biomedical Press, Amsterdam, pp 75–107
- Minagawa J, Takahashi Y (2004) Structure, function and assembly of photosystem II and its light-harvesting proteins. *Photosynth Res* **82**: 241–263
- Monde RA, Zito F, Olive J, Wollman FA, Stern DB (2000) Post-transcriptional defects in tobacco chloroplast mutants lacking the cytochrome b_6f complex. *Plant J* **21**: 61–72
- Munekage Y, Hashimoto M, Miyake C, Tomizawa K, Endo T, Tasaka M, Shikanai T (2004) Cyclic electron flow around photosystem I is essential for photosynthesis. *Nature* **429**: 579–582
- Munekage Y, Hojo M, Meurer J, Endo T, Tasaka M, Shikanai T (2002) *PGR5* is involved in cyclic electron flow around photosystem I and is essential for photoprotection in *Arabidopsis*. *Cell* **110**: 361–371
- Munekage Y, Takeda S, Endo T, Jahns P, Hashimoto T, Shikanai T (2001) Cytochrome b_6f mutation specifically affects thermal dissipation of absorbed light energy in *Arabidopsis*. *Plant J* **28**: 351–359
- Ohad I, Dal Bosco C, Herrmann RG, Meurer J (2004) Photosystem II proteins PsbL and PsbJ regulate electron flow to the plastoquinone pool. *Biochemistry* **43**: 2297–2308
- Okegawa Y, Tsuyama M, Kobayashi Y, Shikanai T (2005) The *pgr1* mutation in the Rieske subunit of the cytochrome b_6f complex does not affect *PGR5*-dependent cyclic electron transport around photosystem I. *J Biol Chem* **280**: 28332–28336
- Rochaix JD (2007) Role of thylakoid protein kinases in photosynthetic acclimation. *FEBS Lett* **581**: 2768–2775
- Sambrook J, Fritsch EF, Maniatis T (1989) *Molecular Cloning: A Laboratory Manual*, Ed 2. Cold Spring Harbor Laboratory Press, Cold Spring Harbor, NY
- Schneider D, Berry S, Rich P, Seidler A, Rögner M (2001) A regulatory role of the PetM subunit in a cyanobacterial cytochrome b_6f complex. *J Biol Chem* **276**: 16780–16785
- Schneider D, Volkmer T, Rögner M (2007) PetG and PetN, but not PetL, are essential subunits of the cytochrome b_6f complex from *Synechocystis* PCC 6803. *Res Microbiol* **158**: 45–50
- Schöttler MA, Flügel C, Thiele W, Bock R (2007) Knock-out of the plastid-encoded PetL subunit results in reduced stability and accelerated leaf age-dependent loss of the cytochrome b_6f complex. *J Biol Chem* **282**: 976–985
- Schreiber U, Bilger W, Hormann H, Neubauer C (1998) Chlorophyll fluorescence, a diagnostic tool: basics and some aspects of practical relevance. In AS Raghavendra, ed, *Photosynthesis: A Comprehensive Treatise*. Cambridge University Press, Cambridge, UK, pp 320–336
- Schwenkert S, Umate P, Dal Bosco C, Volz S, Mlčochová L, Zoryan M, Eichacker LA, Ohad I, Herrmann RG, Meurer J (2006) PsbI affects the stability, function, and phosphorylation patterns of photosystem II assemblies in tobacco. *J Biol Chem* **281**: 34227–34238
- Shi LX, Schröder WP (2004) The low molecular mass subunits of the photosynthetic supracomplex, photosystem II. *Biochim Biophys Acta* **1608**: 75–96
- Shikanai T (2007) Cyclic electron transport around photosystem I: genetic approaches. *Annu Rev Plant Biol* **58**: 199–217
- Shinozaki K, Ohme M, Tanaka M, Wakasugi T, Hayashida N, Matsubayashi T, Zaita N, Chunwongse J, Obokata J, Yamaguchi-Shinozaki K, et al (1986) The complete nucleotide sequence of the tobacco chloroplast genome: its gene organization and expression. *EMBO J* **9**: 2043–2049
- Stroebel D, Choquet Y, Popot JL, Picot D (2003) An atypical haem in the cytochrome b_6f complex. *Nature* **426**: 413–418
- Stubbe W, Herrmann RG (1982) Selection and maintenance of plastome mutants and interspecific genome/plastome hybrids in *Oenothera*. In M Edelman, RB Hallick, N-H Chua, eds, *Methods in Chloroplast Molecular Biology*. Elsevier Biomedical Press, Amsterdam, pp 149–165
- Svab Z, Hajdukiewicz P, Maliga P (1990) Stable transformation of plastids in higher plants. *Proc Natl Acad Sci USA* **87**: 8526–8530
- Svab Z, Maliga P (1993) High-frequency plastid transformation in tobacco by selection for a chimeric *aadA* gene. *Genetics* **90**: 913–917
- Swiatek M, Kuras R, Sokolenko A, Higgs D, Olive J, Cinque G, Muller B, Eichacker LA, Stern DB, Bassi R, et al (2001) The chloroplast gene *ycf9* encodes a photosystem II (PSII) core subunit, PsbZ, that participates in PSII supramolecular architecture. *Plant Cell* **13**: 1347–1367

- Swiatek M, Regel R, Meurer J, Wanner G, Pakrasi HB, Ohad I, Herrmann RG** (2003) Effects of selective inactivation of individual genes for low-molecular-mass subunits on the assembly of photosystem II, as revealed by chloroplast transformation: the *psbEFLJ* operon in *Nicotiana tabacum*. *Mol Genet Genomics* **268**: 699–710
- Takahashi Y, Rahire M, Breyton C, Popot JL, Joliot P, Rochaix JD** (1996) The chloroplast *ycf7* (*petL*) open reading frame of *Chlamydomonas reinhardtii* encodes a small functionally important subunit of the cytochrome *b₆f* complex. *EMBO J* **15**: 3498–3506
- Umate P, Schwenkert S, Karbat I, Dal Bosco C, Mlcochova L, Volz S, Zer H, Herrmann RG, Ohad I, Meurer J** (2007) Deletion of PsbM in tobacco alters the QB site properties and the electron flow within photosystem II. *J Biol Chem* **282**: 9758–9767
- Vainonen JP, Hansson M, Vener AV** (2005) STN8 protein kinase in *Arabidopsis thaliana* is specific in phosphorylation of photosystem II core proteins. *J Biol Chem* **280**: 33679–33686
- Vener AV, Ohad I, Andersson B** (1998) Protein phosphorylation and redox sensing in chloroplast thylakoids. *Curr Opin Plant Biol* **3**: 217–223
- Vener AV, Van Kan P, Rich P, Ohad I, Andersson B** (1997) Plastoquinol at the quinol oxidation site of reduced cytochrome *b₆f* mediates signal transduction between light and protein phosphorylation: thylakoid protein kinase deactivation by a single-turnover flash. *Proc Natl Acad Sci USA* **94**: 1585–1590
- Wollman FA** (2001) State transitions reveal the dynamics and flexibility of the photosynthetic apparatus. *EMBO J* **20**: 3623–3630
- Yamazaki H, Tasaka M, Shikanai T** (2004) PPR motifs of the nucleus-encoded factor, PGR3, function in the selective and distinct steps of chloroplast gene expression in *Arabidopsis*. *Plant J* **38**: 152–163
- Zhang S, Scheller HV** (2004) Light-harvesting complex II binds to several small subunits of photosystem I. *J Biol Chem* **30**: 3180–3187
- Zito F, Finazzi G, Delosme R, Nitschke P, Picot D, Wollman FA** (1999) The Q_o site of cytochrome *b₆f* complexes controls the activation of the LHClI kinase. *EMBO J* **18**: 2961–2969
- Zito F, Vinh J, Popot JL, Finazzi G** (2002) Chimeric fusions of subunit IV and *petL* in the *b₆f* complex of *Chlamydomonas reinhardtii*. *J Biol Chem* **277**: 12446–12455

Deletion of PsbM in Tobacco Alters the Q_B Site Properties and the Electron Flow within Photosystem II^{*[5]}

Received for publication, August 23, 2006, and in revised form, January 17, 2007. Published, JBC Papers in Press, January 29, 2007, DOI 10.1074/jbc.M608117200

Pavan Umate^{†1,2}, Serena Schwenkert^{†1}, Izhar Karbat[§], Cristina Dal Bosco[‡], Lada Mlčochová[‡], Stefanie Volz[‡], Hagit Zer[¶], Reinhold G. Herrmann[‡], Itzhak Ohad^{||3}, and Jörg Meurer^{†4}

From the [†]Department of Biology I, Botany, Ludwig-Maximilians-University, Menzingerstrasse 67, 80638 Munich, Germany, the [§]Department of Plant Sciences, George S. Wise Faculty of Life Sciences, Tel-Aviv University, 69978 Ramat-Aviv, Tel-Aviv, Israel, [¶]Minerva Avron, Even-Ari Center of Photosynthesis Research, The Hebrew University of Jerusalem, 91904 Jerusalem, Israel, and the ^{||}Department of Biological Chemistry, Silberman Institute of Life Sciences, The Hebrew University of Jerusalem, 91904 Jerusalem, Israel

Photosystem II, the oxygen-evolving complex of photosynthetic organisms, includes an intriguingly large number of low molecular weight polypeptides, including PsbM. Here we describe the first knock-out of *psbM* using a transplastomic, reverse genetics approach in a higher plant. Homoplastomic $\Delta psbM$ plants exhibit photoautotrophic growth. Biochemical, biophysical, and immunological analyses demonstrate that PsbM is not required for biogenesis of higher order photosystem II complexes. However, photosystem II is highly light-sensitive, and its activity is significantly decreased in $\Delta psbM$, whereas kinetics of plastid protein synthesis, reassembly of photosystem II, and recovery of its activity are comparable with the wild type. Unlike wild type, phosphorylation of the reaction center proteins D1 and D2 is severely reduced, whereas the redox-controlled phosphorylation of photosystem II light-harvesting complex is reversely regulated in $\Delta psbM$ plants because of accumulation of reduced plastoquinone in the dark and a limited photosystem II-mediated electron transport in the light. Charge recombination in $\Delta psbM$ measured by thermoluminescence oscillations significantly differs from the 2/6 patterns in the wild type. A simulation program of thermoluminescence oscillations indicates a higher Q_B/Q_B^- ratio in dark-adapted mutant thylakoids relative to the wild type. The interaction of the Q_A/Q_B sites estimated by shifts in the maximal thermoluminescence emission temperature of the Q band, induced by binding of different herbicides to the Q_B site, is changed indicating alteration of the activation energy for back electron flow. We conclude that PsbM is primarily involved in the interaction of the redox components important for the electron flow within, outward, and backward to photosystem II.

Photosystem II (PSII),⁵ a supramolecular pigment-protein complex of photosynthetic organisms, utilizes absorbed light energy to oxidize water, releasing dioxygen and electrons that serve as the major source of reducing power in photosynthetic activity. The mechanisms of this process have been studied extensively. Based on biochemical (reviewed in Ref. 1), biophysical (2, 3), and structural analysis, including electron microscopy (4, 5) and x-ray diffraction (6–9), comprehensive knowledge of the basic steps of the water oxidation mechanism, electron transfer reactions, and organization of the individual components involved in these processes has been delineated. Information is also available on the structure of LHCII and the energy transfer to the inner antenna and the photochemical reaction center (10, 11), as well as on the components involved in the biogenesis of PSII (12–14). Most if not all genes encoding PSII subunits have been identified in cyanobacteria and higher plants, and their function, expression, and regulation have been studied extensively (15–17).

PSII is the most intricate assembly of thylakoid membrane systems consisting of more than 30 subunits. It assembles as a dimer together with the minor light-harvesting antenna CP24, CP26, and CP29 for each monomer and is further surrounded by trimeric LHCII protein complexes (5). Based on the similarity of subunit sequences, composition, and activity of PSII, it is generally accepted that the structure of the PSII core in eukaryotes is basically similar to that of cyanobacteria, for which x-ray diffraction structures between 3.8 and 3.0 Å resolution have been obtained (8, 9). However, despite sustained attempts to obtain a higher structural resolution for the PSII of higher plants (10), the heterogeneity of the photochemical center of PSII caused by light-induced changes has so far prevented the formation of crystals allowing a higher resolution of the complex.

One of the most intriguing features of the PSII core is the presence of 16 bitopic, intrinsic, or peripheral low molecular weight proteins. Knowledge about their roles in the overall pho-

* This work was supported in part by Deutsche Forschungsgemeinschaft Grant SFB-TR1 (to J. M. and R. G. H.). The costs of publication of this article were defrayed in part by the payment of page charges. This article must therefore be hereby marked "advertisement" in accordance with 18 U.S.C. Section 1734 solely to indicate this fact.

[5] The on-line version of this article (available at <http://www.jbc.org>) contains supplemental data S1–S5.

¹ Both authors contributed equally to this work.

² Recipient of a fellowship from the Deutsche Akademische Austauschdienst. Present address: Dept. Scientifico e Tecnologico, Università di Verona, Strada Le Grazie 15, 37134 Verona, Italy.

³ Supported by the Minerva Avron, Even-Ari Center for Photosynthesis Research, The Hebrew University, Jerusalem, Israel.

⁴ To whom correspondence should be addressed. Tel.: 49-89-17861288; Fax: 49-89-1782274; E-mail: joerg.meurer@lrz.uni-muenchen.de.

⁵ The abbreviations used are: PSI and PSII, photosystem I and II, respectively; BN, blue native; CP, chlorophyll-protein; DCMU, 3-(3,4-dichlorophenyl)-1,1-dimethylurea; LHC, light-harvesting complex of photosystem II; LMWs, low molecular weight subunits; PQ, plastoquinone; PQH₂, plastoquinol; TL, thermoluminescence; WT, wild type; bis-Tris, 2-[bis(2-hydroxyethyl)amino]-2-(hydroxymethyl)propane-1,3-diol; NPOQ, nonphotochemical quenching; qP, photochemical quenching; E, einstein.

tosynthetic process is still fragmentary. In eukaryotic PSII, 11 of them are encoded by plastid chromosomes, notably PsbE, -F, -H, -I, -J, -K, -L, -M, -N, -Tc, and -Z (reviewed in Refs. 5 and 16–19). The fact that most low molecular weight subunits (LMWs) of PSII have been highly conserved throughout the evolution implies that they perform essential functions, as indeed this has been established for PsbI, PsbT, the α and β subunits of the two-chain cytochrome b_{559} , PsbE and PsbF, respectively, as well as for PsbL and PsbJ, which fulfill crucial structural and functional roles (20–28). However, only limited information is available on the function and exact position of the other LMWs within the PSII complex. Moreover, studies on distinct LMWs from various organisms have indicated different roles (reviewed in Refs. 16, 17) or control of the same function, albeit to a different degree, as is the case for PsbJ in *Synechocystis* sp. PCC 6803 and tobacco (23). Apparently, the management of PSII electron flow in terms of energy dissipation and avoiding generation of oxygen radicals has to cope with different requirements in various organisms. Such differences may depend on the eco-physiological conditions under which different organisms thrive and the divergence of the outer antenna. It is therefore conceivable that the properties of the LMWs of PSII vary in different organisms.

The study of all chloroplast-encoded LMWs in one organism offers a better chance to understand the roles for each one of them in the same assembly. Therefore, we have inactivated plastid genes encoding LMWs of PSII using a transplastomic approach in tobacco, and we reported on the roles of six of them, including PsbE, PsbF, PsbL, PsbJ, PsbI, and PsbZ (23–28).

The PsbM polypeptide has been detected in PSII complexes isolated from *Chlamydomonas reinhardtii* (29), *Synechocystis* sp. PCC 6803 (30), and *Synechococcus vulcanus* (31), and its presence in *Synechocystis* sp. PCC 6803 (32) and pea (33) has been confirmed recently using proteomics approaches. However, mutation studies of PsbM have not yet been reported from any organism. Moreover, the exact position of PsbM within the PSII assembly as well as its function remains to be established (8, 17).

The analyses of the first PsbM knock-out presented here demonstrate that the biogenesis of PSII is not significantly altered in the absence of PsbM. However, properties of the Q_B site and its interaction with Q_A and charge recombination within PSII are specifically impaired in $\Delta psbM$ resulting in a shift of thermoluminescence (TL) B band oscillations, a decreased rate of oxygen evolution and forward electron flow, and thus an increased light-induced photoinactivation as well as dephosphorylation of LHCII. Because of a high plastoquinol (PQH_2) content in dark-adapted mutant plants, levels of LHCII phosphorylation are significantly elevated as compared with the wild type. Phosphorylation of the reaction center proteins D1/D2 is faintly detectable presumably because of conformational changes induced by loss of PsbM proteins.

EXPERIMENTAL PROCEDURES

Clone Construction to Inactivate the *psbM* Gene in Tobacco Chloroplasts—The recombinant plasmid B20 (tobacco plasmid clone bank) (34) containing a 17,235-bp insertion (nucleotide positions 26,191–43,426 in the plastid chromosome,

accession number Z00044) in the vector pBR322 was digested with BamHI, and the resulting 2,096-bp fragment containing *psbM* was subcloned into the singular BamHI restriction site of pBluescript II KS⁻ (Stratagene Inc., La Jolla, CA). Inactivation of the *psbM* gene (nucleotide position 30,861 (N) to 30,757 (C) bp, accession number Z00044) was achieved by insertion of the *aadA* cassette, including a terminator signal (35) at a unique BsgI restriction site in the N-terminal part of the gene (nucleotide position 30,844). Transformation of *Nicotiana tabacum* cv. Petit Havana, the selection procedure, and *in vitro* propagation of transformants were carried out essentially as described (25). Isolation of plastid chromosomes by orthogonal pulse-field gel electrophoresis was carried out as described (36). Tobacco lines carrying the *aadA* cassette in a neutral insertion site and referred to as RV plants were used as wild type (WT) control plants (25).

Preparation and Handling of Thylakoid Membranes—Thylakoid membranes isolated from 4-week-old plants grown under greenhouse conditions were chosen for immunoblot analysis, phosphorylation experiments, and analysis of their composition by the blue native gel (BN) method as described (25). For separation of photosynthetic chlorophyll-protein complexes by sucrose gradient centrifugation, 4-week-old *in vitro* grown ($10\text{--}20\ \mu\text{E m}^{-2}\ \text{s}^{-1}$ light intensity; 12-h photoperiod) plants were used.

Isolated thylakoid membranes (final chlorophyll concentration 1 mg/ml) were partially lysed during an incubation of 45 min on ice in darkness in bis-Tris/*n*-dodecyl- β -D-maltoside buffer (final concentrations of 20 mM bis-Tris/HCl, pH 6.5, 5 mM NaCl, 5 mM MgCl₂, and 1.0% *n*-dodecyl- β -D-maltoside). After centrifugation at $18,000 \times g$ and 4 °C for 12 min, the solubilized fraction was layered onto a linear (0.1–1.0 M) sucrose gradient in bis-Tris/*n*-dodecyl- β -D-maltoside buffer. The gradient was run at 4 °C for 18 h in a Beckman SW40Ti rotor at $200,000 \times g$.

Blue native-PAGE (BN-PAGE) was performed as described earlier with modifications (25). The appearing spots were sequenced by mass spectrometry and assigned accordingly (37).

For TL measurements, thylakoids were prepared by grinding a few leaves in a buffer containing 20 mM Tris-HCl, pH 7.4, 5 mM MgCl₂, 20 mM NaCl, and 100 mM sorbitol. The material homogenized at 0 °C was filtered through nylon micromeshes and used immediately for measurements.

Chlorophyll *a* Fluorescence Induction Kinetics—Chlorophyll *a* fluorescence induction kinetics was measured using a pulse amplitude-modulated fluorimeter (PAM-101, Waltz, Effeltrich, Germany) (38). Prior to measurements, leaves were dark-adapted for 5 min. The potential maximum quantum yield of PSII was measured as $(F_m - F_o)/F_m = F_v/F_m$. Red actinic light (650 nm, 20 and 250 $\mu\text{E m}^{-2}\ \text{s}^{-1}$) was used for measurements of fluorescence quenching. Photochemical (qP) and nonphotochemical (NPQ) quenching were determined by repetitive saturation pulses. The quenching coefficients, NPQ and qP, were calculated as $(F_m - F_m')/F_m'$ and $(F_m' - F)/(F_m' - F_o)$, respectively (38).

State Transition and Thylakoid Protein Phosphorylation—State transition in intact leaves was calculated using the PAM-101 fluorimeter as $(F_m' - F_m'')/F_m'$ (39). Protein phosphoryla-

Effect of *PsbM* Deletion on PSII Functions

tion was carried out using isolated thylakoids as described (25, 40). All buffers used during thylakoid preparation contained 10 mM NaF. Detection of the phosphorylation level of thylakoid membrane proteins was carried out by immunoblotting using anti-phosphothreonine antibodies (New England Biolabs) as described earlier (25).

Low Temperature Fluorescence Measurements—Thylakoid suspensions (20 μg of chlorophyll/ml) of WT and mutant leaves were frozen by immersing a liquid nitrogen-cooled glass rod (4 mm diameter) into the thylakoid suspension and rapidly returning it to the Dewar vessel of the sample holder of the fluorimeter filled with liquid nitrogen (Fluoromax-3, Horiba Jobin-Yvon, France). Fluorescence emission spectra were recorded using 430 nm excitation and 1.5 nm slits for both excitation and emission monochromators.

Photosystem I (PSI) Redox State—The redox state of PSI was measured on leaves using the PSI attachment of PAM101 (Walz, Effeltrich, Germany). The oxidation status of PSI at the light intensities indicated was expressed as the ratio $\Delta A/\Delta A_{\text{max}}$ (41).

Thermoluminescence Measurements—TL of thylakoid suspensions was measured using a home-built apparatus as described (42). Samples (400 μl) of 40 μg of chlorophyll/ml were placed on the TL stage, dark-adapted at 20 $^{\circ}\text{C}$ for 3 min, and rapidly frozen to -20°C by a stream of liquid nitrogen. The sample was then excited by saturating flashes delivered by a xenon arc discharge lamp (0.05 microfarad capacitor, charged at 1000 V, 3 μs at 70% light emission; EG and G), then heated at a rate of 0.6 $^{\circ}\text{C s}^{-1}$, and photons were counted. For measurements of the intensity of the B band emission oscillations ($Q_{\text{B}}^{-}/S_2, S_3$ charge recombination) as a function of the numbers of single turnover excitations, a train of flashes (1–6 flashes, about 300-ms interval between flashes) was given at 0 $^{\circ}\text{C}$ followed by rapid freezing.

For detecting the TL signal resulting from Q_{A}^{-}/S_2 recombination (Q band), the herbicides DCMU or ioxynil (Serva, Heidelberg, Germany), both binding to the Q_{B} site and thus preventing Q_{A}^{-} oxidation, were added at concentrations as indicated before dark adaptation. Concentrations of ioxynil higher than 20 μM were avoided because of the high fluorescence quenching induced by this herbicide. Glycerol (25% v/v) was added to the samples to avoid distortion of the linear heating rate during the ice-melting stage. The kinetics of the Q_{B}^{-} decay in darkness was measured following excitation of the dark-adapted sample by a single flash at 20 $^{\circ}\text{C}$, followed by further incubation in darkness for the indicated periods, and followed by rapid freezing to -20°C and starting the heating of the sample and photon-counting process.

A computer-based simulation program allowing the prediction of the S-states ratio and the occupancy ratio $Q_{\text{B}}/Q_{\text{B}}^{-}$ was employed (supplemental S1). The program simulates predicted oscillation profiles and checks for the correlation between simulated and measured values. The free parameters in the simulation are as follows: 1) the S-states and $Q_{\text{B}}/Q_{\text{B}}^{-}$ occupancy levels in the dark adapted state, which can vary between 0 and 1 in 0.1 steps; 2) the misses, *i.e.* the fraction of reaction centers that is not excited by a flash, which may vary between 0 and 0.5; and 3) the double hits, *i.e.* the fraction of reaction centers that

are excited twice by a single flash, which may vary between 0 and 0.5. The value $\sum_{1-6} |\text{intensity}_{\text{measured}} - \text{intensity}_{\text{simulated}}|$, where 1–6 represents the number of flashes, was used to estimate the correlation between measured and simulated results. The program used is given in the supplemental S1. Minimization of the cost function was performed by a simulated annealing algorithm (43).

Oxygen Evolution Measurements—Photosynthetic electron flow was determined using thylakoids isolated as described for TL measurements. The PSII specific electron acceptor *p*-benzoquinone was used under saturating light conditions using a Clark-type oxygen electrode for measuring oxygen evolution.

Measurements of Photoinhibition and Recovery Process—The sensitivity of PSII to oxidative stress has been determined with leaf disks (10 mm diameter, 5 disks per sample) of WT and ΔpsbM plants exposed to 500 $\mu\text{E m}^{-2} \text{s}^{-1}$ heterochromatic light. The photoinactivation of PSII was measured as changes in the F_v/F_m parameter as a function of exposure time. To estimate the contribution of the PSII recovery process during treatment with high light, leaf disks were infiltrated with a solution of D-threo-chloramphenicol (200 $\mu\text{g ml}^{-1}$) in darkness for 30 min prior to the exposure to high light. As a control, leaf disks were incubated in water. To assess the inhibition kinetics and the capacity to recover PSII activity, leaf disks were exposed to 1,500 $\mu\text{E m}^{-2} \text{s}^{-1}$ until an F_v/F_m of 0.17 was reached in both WT and ΔpsbM . The recovery was followed in low light (3 $\mu\text{E m}^{-2} \text{s}^{-1}$) for up to 6 h measuring the F_v/F_m level every 1 h.

RESULTS

Inactivation of *psbM*—Nine independent transformants with an identical phenotype were initially obtained, and three lines were used for further studies. Their homoplasmic status was confirmed by sequencing of the insertion site and by PCR analysis using isolated plastid chromosomes as template (Fig. 1A). Northern analysis with a strand-specific probe containing the coding region of the *psbM* gene demonstrated that not even traces of *psbM* transcripts were detectable confirming the homoplasmic state of the mutant (Fig. 1B).

Levels and Compositions of Thylakoid Membrane Complexes in ΔpsbM Resemble Those of the WT—Inactivation of *psbM* in tobacco caused a quite distinct phenotype. Different from several other LMWs mutants of the chloroplast, such as ΔpsbE , ΔpsbF , ΔpsbL , and ΔpsbJ , ΔpsbM plants are capable of photoautotrophic growth on soil. However, mutant leaves appeared bleached if the light intensity exceeded $\sim 200 \mu\text{E m}^{-2} \text{s}^{-1}$, thus indicating increased light sensitivity of the photosynthetic apparatus. To elucidate the function of *PsbM*, homoplasmic ΔpsbM mutants in tobacco were analyzed by biochemical and biophysical approaches.

The relative amounts and sizes of pigment-containing thylakoid membrane complexes in sucrose gradients of ΔpsbM did not differ significantly from those of the WT (Fig. 2A). Only PSII-LHCII supercomplexes were faintly diminished, and consequently trimeric LHCII antennae complexes showed a slight increase in ΔpsbM . Moreover, a significant increase in the LHCII-CP24-CP29 complex was observed in the mutant compared with WT. These results demonstrate that PSII can be assembled in the absence of *PsbM* and that its deletion does not

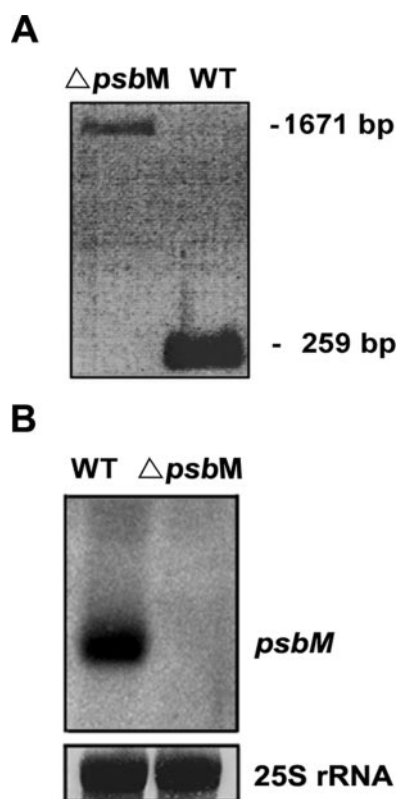


FIGURE 1. Inactivation of *psbM* by introduction of the *aadA* cassette in nucleotide position 30844 of the tobacco plastid chromosome. A, PCR analysis was performed using plastome-specific primers (5' GCGACTGAA-AATCCACATTTG3' and 5' GTTAATAATTAATCGTTTTGACT3') flanking the insertion site. The PCR only amplified an expected product of 1,671 bp in the mutant and a 259-bp product in the WT (24) indicating homoplasmy of the *aadA* insertion. B, RNA gel blot analysis using a strand-specific probe of the *psbM* gene demonstrates that insertion of the *aadA* cassette prevents expression of *psbM*. The amounts of 25S rRNA show equal loading.

alter significantly the assembly of thylakoid membrane complexes *in vivo*, or during the solubilization process. This finding was substantiated in two ways, by BN-PAGE and sucrose gradient centrifugation (Fig. 2, A and B) followed by denaturing SDS-PAGE (supplemental S2). In the first electrophoretic dimension, the separation profile of the native thylakoid membrane complexes in $\Delta psbM$ was close to that of WT, but again a very slight decrease in the amounts of PSII-LHCII supercomplexes was noticed (Fig. 2B). Comparably, immunoblot analyses showed no difference in the presence of the relative amounts of the intrinsic PSII subunits D1, D2, CP43, CP47, PsbE, PsbI, and PsbW, the extrinsic proteins PsbO, PsbP, PsbQ, and PsbR, involved in water oxidation, as well as the antenna proteins CP29, CP26, CP24, and LHCII (supplemental S3).

Levels of PSII relative to PSI were estimated by quantitative immunoblot analysis using D1 and PsdD antibodies and the AIDA software. We repeatedly used dilution series of WT and mutant thylakoids based on chlorophyll amounts to precisely quantify levels of D1 and PsdD (Fig. 2C). Based on this analysis, we calculated that D1 accumulates to $103.4 \pm 3.6\%$ and PsdD to $100.7 \pm 5.5\%$ in the mutant relative to the WT. Therefore, PSII and PSI levels are comparable in mutant and WT.

Levels of other thylakoid complexes, *i.e.* PSI, cytochrome b_6/f complex, ATP synthase, and antenna proteins remained unal-

tered as well in the mutant (supplemental S3). Because the water splitting complex could have been affected by the loss of *PsbM*, salt treatment of thylakoid membranes was performed with increasing Na_2CO_3 concentrations up to 200 mM demonstrating that PsbO, PsbP, PsbQ, and PsbR remain stably associated to the complex in $\Delta psbM$ comparable with WT (data not shown).

Inactivation of *PsbM* Affects Photosystem II Function—The measurement of chlorophyll fluorescence kinetics of photoautotrophically grown mutants showed a reduced quantum yield (F_v/F_m) of PSII (0.78 ± 0.012 versus 0.81 ± 0.003 in WT). Fluorescence quenching analysis uncovered at low light intensity ($20 \mu\text{E m}^{-2} \text{s}^{-1}$) that the mutant exhibits qP values comparable with those of WT (0.93 ± 0.009 versus 0.96 ± 0.006 in WT), but at higher light intensities ($250 \mu\text{E m}^{-2} \text{s}^{-1}$) this value remained much lower (0.34 ± 0.041 versus 0.54 ± 0.052 in WT), which could be due to a lower rate of PSII-dependent electron transport causing an increase in the ratio Q_A^-/Q_A in the mutant as compared with the WT. Lower NPQ values were also detected in the mutant at both light intensities indicating that mutant PSII is more susceptible to thermal dissipation (Table 1). Taken together, these results indicated that although PSII levels are comparable in mutant and WT, the quantum yield of PSII is significantly lower in $\Delta psbM$. The results above are also supported by our findings that PSII activity measured as O_2 evolution under saturating light was lowered to about 52% in $\Delta psbM$ as compared with WT thylakoids (Table 1).

Energy Transfer to PSII—The 77 K fluorescence emission of $\Delta psbM$ samples exhibited the same peaks as the WT at 685, 695, and 735 nm attributed to the major pigment-protein core complexes of PSII, CP43, CP47, and the PSI-LHCI complex, respectively (Fig. 3). However, a slight lowering of the PSII-related fluorescence emission bands compared with that of PSI was noted in $\Delta psbM$. This indicated an exiguous disconnection of the outer antenna of PSII and is consistent with the above finding that only levels of PSII supercomplexes are slightly decreased in the mutant.

The Oxidation State of PSI Is Increased in Light-exposed $\Delta psbM$ Plants—Absorption measurements showed a significantly higher oxidation state of PSI in $\Delta psbM$ as compared with WT at both 20 and $250 \mu\text{E m}^{-2} \text{s}^{-1}$ actinic light intensities (Table 1). These results indicate a lower rate of electron flow from PSII to the PQ pool, relative to that of PQH_2 oxidation via PSI activity, and support the conclusion that PSII activity is significantly lower in the mutant as compared with the WT. This conclusion was also supported by measurements of steady state fluorescence levels (F_s') elicited by 650 nm actinic light at an intensity of $34 \mu\text{E m}^{-2} \text{s}^{-1}$ on background of far-red light (12 watts m^{-2}). The ratio $F_s' \Delta psbM / F_s' \text{ WT}$ was 0.59 ± 0.06 , demonstrating that the electron flow to PQ is much lower than that from the reduced quinol to the electron sink via PSI.

State Transition and Phosphorylation of LHCII and D1/D2 Are Affected in $\Delta psbM$ —Phosphorylation/dephosphorylation of LHCII resulting in transition to state 2 or state 1 was induced by exposing leaves to PSII or PSI light for 15 min, respectively (39). The percentage of state transition was 8.4 for WT and 4.6 for $\Delta psbM$, corresponding to 55% of the WT activity in $\Delta psbM$.

Effect of *PsbM* Deletion on PSII Functions

It has been demonstrated that activation of the protein kinase phosphorylating LHCII is related to the process of plastoquinol oxidation by the cytochrome *b₆f* complex (44). Thus,

both light-dependent reduction of the PQ pool or addition of duroquinol in darkness induce phosphorylation of LHCII in the WT (Fig. 4A) (40). However, unlike WT, LHCII in $\Delta psbM$ was

unexpectedly highly phosphorylated in darkness even in absence of duroquinol. LHCII phosphorylation decreases significantly in light-exposed mutant samples in the absence or presence of DCMU but still increases upon incubation with duroquinol in darkness (Fig. 4A).

A phosphorylation pattern identical to that of isolated thylakoids was obtained when measuring LHCII phosphorylation *in vivo*. As in isolated thylakoids, LHCII was significantly phosphorylated in dark-adapted mutant leaves. Exposure of such leaves to red light and far-red light of low intensity preferentially exciting PSI caused dephosphorylation of LHCII indicating that the PQ pool in the mutant is reduced in darkness (Fig. 4B). Interestingly, different from WT the phosphorylation level of D1/D2 was strongly reduced under all experimental conditions, whereas that of CP43 was unchanged in the mutant (Fig. 4).

Thermoluminescence Emission Reveal an Increased Ratio for Q_B/Q_B^- in Dark-adapted Mutant Plants—Although PSII complexes in $\Delta psbM$ accumulate at levels comparable with the WT, the data presented so far indicated a significant impairment of PSII activity. To check disturbances of the forward/back electron flow within the PSII complex, thermoluminescence emission was recorded (45). Excitation by a single turnover flash of dark-adapted thylakoids advances the S-state cycle by one step, and the quinone or semiquinones bound to the Q_B site are fur-

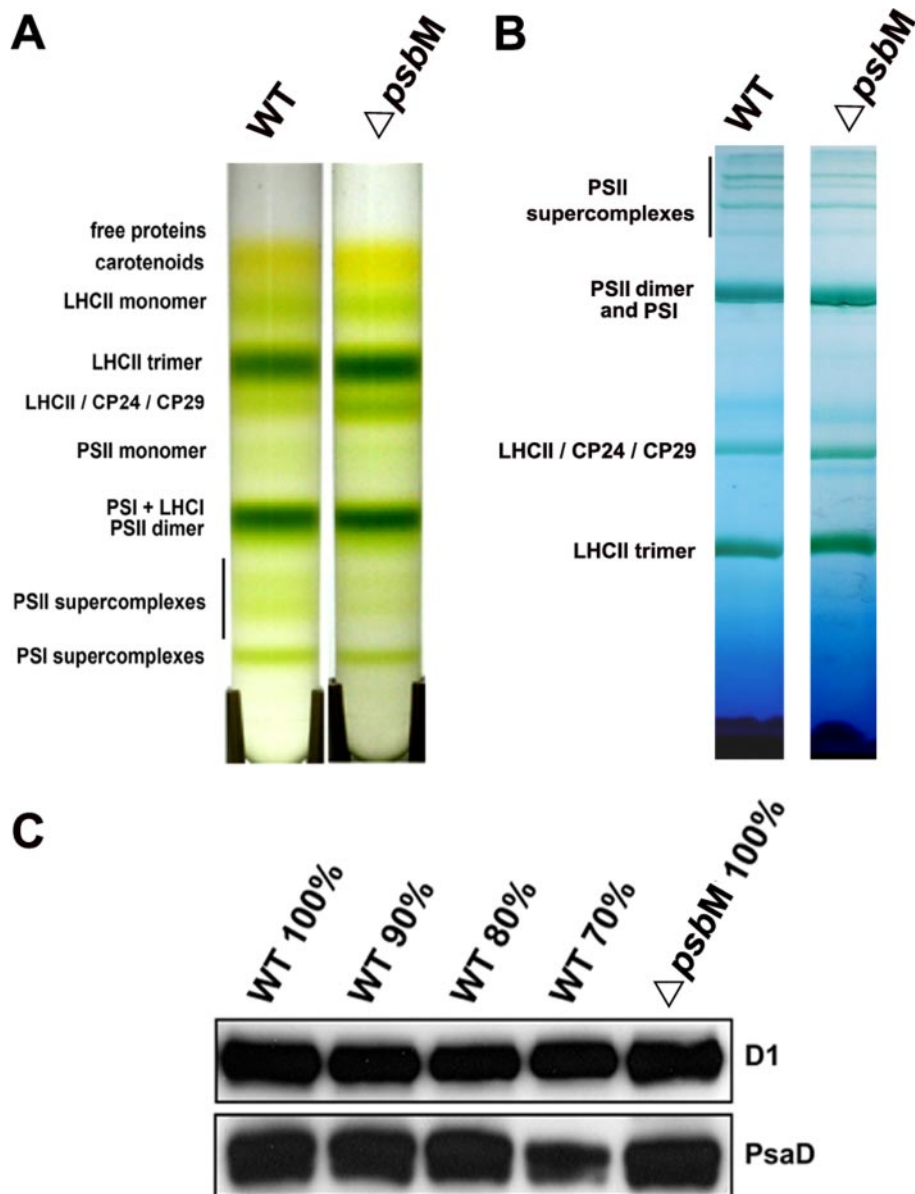


FIGURE 2. Separation of thylakoid protein complexes of WT and $\Delta psbM$ by sucrose gradient centrifugation, BN-PAGE, and quantification of PSII amounts by immunoblot analysis. *A*, thylakoid membrane complexes were separated on a continuous sucrose gradient (0.1–1 M) and labeled accordingly (25). *B*, complexes are labeled according to their identification by mass spectrometry (37). Note slightly reduced levels of PSII supercomplexes in $\Delta psbM$ and the higher accumulation of LHCII-containing complexes. *C*, representative immunoblot analysis of $\Delta psbM$ and of a dilution series of WT thylakoids for precise quantification of D1 and PsaD proteins. 100% corresponds to 8 μg of chlorophyll.

TABLE 1
Spectroscopic and fluorimetric data, and oxygen evolution rates for WT and $\Delta psbM$

	qP ^a		NPQ ^b		Oxidation state of photosystem I		Oxygen evolution ^c
	20 $\mu\text{E}/\text{m}^2 \text{ s}$	250 $\mu\text{E}/\text{m}^2 \text{ s}$	20 $\mu\text{E}/\text{m}^2 \text{ s}$	250 $\mu\text{E}/\text{m}^2 \text{ s}$	20 $\mu\text{E}/\text{m}^2 \text{ s}$	250 $\mu\text{E}/\text{m}^2 \text{ s}$	$\mu\text{mol O}_2 \text{ mg chl}^d \text{ h}$
WT	0.96 ± 0.006	0.54 ± 0.052	0.08 ± 0.001	1.38 ± 0.142	1%	28%	241 ± 27
$\Delta psbM$	0.93 ± 0.009	0.34 ± 0.041	0.09 ± 0.012	0.99 ± 0.146	4%	54%	125 ± 18

^a qP indicates quenching according to photochemistry.

^b NPQ indicates quenching according to heat dissipation (ΔpH), state transition, and/or photoinhibition.

^c Oxygen evolution was measured at 1,200 $\mu\text{E m}^{-2} \text{ s}^{-1}$ light intensity.

^d chl indicates chlorophyll.

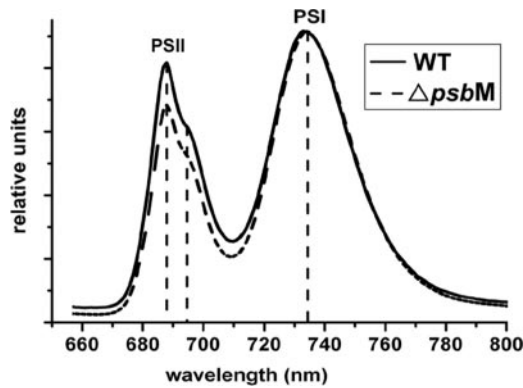


FIGURE 3. Fluorescence emission spectra of WT (solid line) and $\Delta psbM$ thylakoids (dashed line) at 77 K. Excitation of the samples was carried out at 430 nm. Note the slight decrease of the PSII-related emission at 685 and 695 nm relative to the 735 nm emission of PSI. Signals were normalized to the PSI emission intensity.

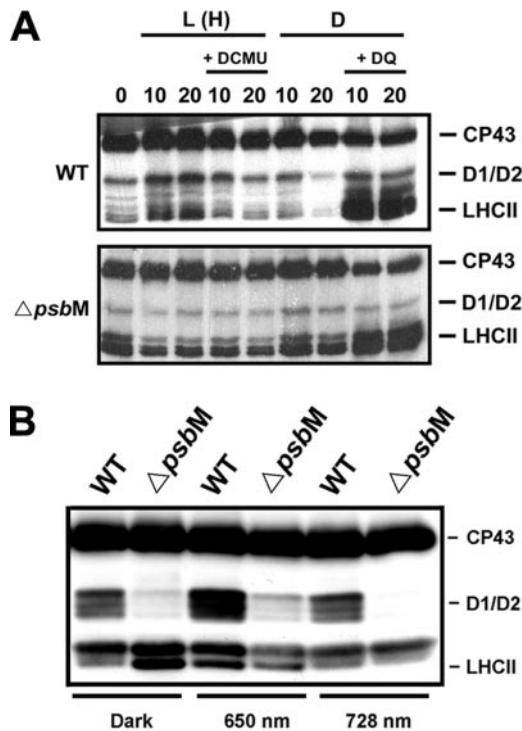


FIGURE 4. Analysis of the redox-controlled phosphorylation of LHCII as well as PSII core proteins CP43 and D1/D2 using phosphothreonine antibodies. *A*, thylakoid membranes were incubated for 10 or 20 min in light (L) ($60 \mu\text{E m}^{-2} \text{s}^{-1}$, H, heterochromatic light) or darkness (D) in the absence or presence of DCMU ($10 \mu\text{M}$) or reduced duroquinol (DQ) (1 mM), respectively. Note that unlike in WT, phosphorylation of LHCII in darkness was higher than that in illuminated samples in the absence of DCMU in $\Delta psbM$. Duroquinol induced phosphorylation in both WT and $\Delta psbM$ thylakoids. *B*, *in vivo* phosphorylation of PSII proteins in mutant and WT. Leaves were first dark-adapted and subsequently kept either under state 2 conditions induced by red light illumination (650 nm, $50 \mu\text{E m}^{-2} \text{s}^{-1}$ for 15 min) or under state 1 conditions induced by PSI-specific far-red illumination (728 nm, 6 watts m^{-2} for 15 min). Note the similarity of the phosphorylation pattern *in vivo* to that in isolated thylakoids (*A*). The phosphorylation level of the PSII core CP43 protein was identical in both WT and mutant material under all experimental conditions. However, phosphorylation of the D1/D2 proteins was significantly lowered in the $\Delta psbM$ mutant thylakoids.

ther reduced (46). The luminescence is emitted because of charge recombination between Q_B^- and the S_2^- or S_3^- states of the water splitting complex. The temperature at which this luminescence is maximal is related to the redox potential of the

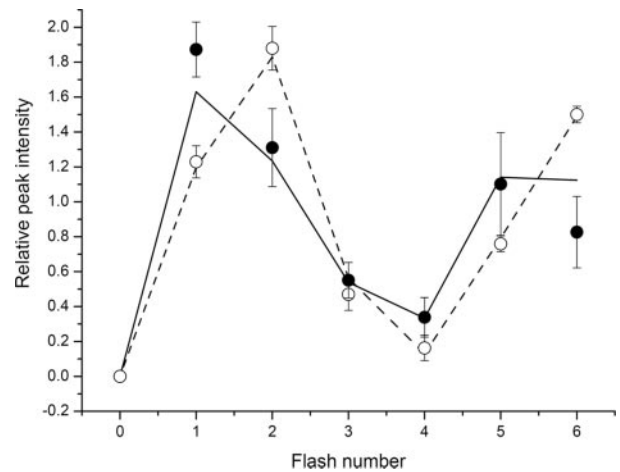


FIGURE 5. Oscillations of thermoluminescence emission of WT and $\Delta psbM$ thylakoids as a function of the number of exciting flashes. *A*, open (WT) and filled circles ($\Delta psbM$) represent relative TL peak heights as a function of the number of exciting flashes. Bars show the standard deviation values based in three repeats. Lines represent the results of fitting with the simulation program provided as supplemental S2. Solid line, WT (2/6 pattern); dotted line, representative $\Delta psbM$ mutant samples (1/5 pattern). Detailed results of the fitting procedure are shown in supplemental S1 and S4 and additional data showing less frequent different oscillation patterns of the mutant are given in supplemental S5.

$Q_B:Q_B^-$ and the S-state charge recombining pair and is designated as the B TL emission band. In tobacco, this band occurs at $\sim 35^\circ\text{C}$, as in vascular plants in general (24, 47, 48).

Because the emission temperature of the B band at 35°C was found to be the same in both mutant and WT, the activation energy for back electron flow and recombination process is not changed in $\Delta psbM$. The fraction of recombining pairs, $Q_B^-/S_2, S_3$ and the B band emission intensities oscillate with a period of four flashes showing a maximum emission at the 2nd and 6th flash in the WT (24). However, $\Delta psbM$ showed various oscillation patterns. In each case the first flash resulted in a higher B band emission than that induced by the second flash. A 1/5 oscillation pattern predominantly appeared in young and fast-expanding leaf material (Fig. 5), whereas binary and zigzag oscillations were rarely and almost exclusively observed in mature and slow growing mutant leaves (supplemental S4). These data clearly reflect a change in the recombination process within PSII in $\Delta psbM$.

The difference between the patterns of the TL signal oscillation intensity as a function of the number of exciting flashes could be due to deviation from the predicted S_0/S_1 ratio in the dark adapted state (1/3) and their respective Q_B/Q_B^- occupancies (1/1) (45). To test this possibility, a simulation program allowing the prediction of the occupancy of the S-states by semiquinone or oxidized quinone, respectively, was employed using the oscillation pattern measured as a function of the number of exciting flashes (supplemental S1).

The results indicate that the quinone occupancy of the Q_B site in $\Delta psbM$ significantly differs from that of the WT, showing an average of 2.5 higher ratios for Q_B/Q_B^- in the various mutant oscillation patterns. No coherent behavior of the S_0/S_1 ratio in the best fits reported by the simulation program could be observed (supplemental S4). The data presented so far indicate that the back electron flow from Q_B^- to the S-states of the

Effect of *PsbM* Deletion on PSII Functions

oxygen evolving complex in darkness can vary significantly in $\Delta psbM$.

When electron flow from Q_A to Q_B is inhibited by ligands binding to the Q_B site, such as urea or phenolic type herbicides (DCMU and ioxylin, respectively), light excitation results only in the reduction of the Q_A quinone. In this case, the related TL band temperature is downshifted, compatible with a lower energy required for back electron transfer to the manganese cluster. The resulting emission band is referred to as Q band (49–51). Binding of the herbicides to the Q_B pocket may slightly modify its structure, which in turn affects the redox potential gap between the Q_A and Q_B electron acceptors. This was shown to be the case for binding of DCMU that alters the $Q_A:Q_A^-/Q_B^-:Q_B$ potential (52, 53). The emission temperature of the Q band in $\Delta psbM$ was significantly downshifted in the presence of both DCMU (10 °C versus 15 °C in the WT) and ioxylin (–6 to 0 °C versus 3 °C in the WT) (Fig. 6, A and B). Furthermore, the intensity of the Q band emission increases with increasing ioxylin concentrations (5, 10 and 20 μM , respectively), whereas the B band emission persisted in the presence of low ioxylin concentrations and decreased significantly at 20 μM (Fig. 6A). These results indicate the presence of functionally distinct populations of PSII centers with altered Q_B sites in mutant thylakoids.

The variable and different B band oscillation patterns and the increased Q_B/Q_B^- ratio in the dark-adapted state of $\Delta psbM$ could be due to a slower back electron flow during the dark adaptation process. This could be caused by an insufficient dark adaptation time of the sample at 20 °C prior to light excitation and thus residual Q_B^-/S_1 , Q_B^-/S_2 , or even Q_B^-/S_3 populations may still be present. This in turn could affect the final ratio of the S_1/S_0 states and their occupancy by semiquinol or oxidized quinone. To check this possibility, the time course of the B band decay was measured at 20 °C in darkness. The results demonstrate a complete decay of the B band emission after 3 min of dark adaptation (Fig. 6C). The dark adaptation in all experiments was carried out at 20 °C for 3 min prior to application of single turnover flashes and thus was sufficient to allow complete decay of the $S_{2,3}$ -states. Therefore, loss of Q_B^-/S_2 or Q_B^-/S_3 recombination after dark adaptation cannot account for the observed departure from the normal TL oscillation pattern in thylakoids of $\Delta psbM$.

Photoinhibition and PSII Recovery—The alteration of PSII electron flow and activation energy of recombining pairs within PSII could increase the light sensitivity in $\Delta psbM$ because of singlet oxygen formation accompanied by a loss of variable fluorescence and degradation of the D1 protein (reviewed in Refs. 54 and 55). Therefore, repair of PSII activity requires *de novo* D1 protein synthesis. To compare the photosensitivity, WT and $\Delta psbM$ leaves were exposed to 500 $\mu\text{E m}^{-2} \text{s}^{-1}$ after treatment with chloramphenicol, an inhibitor of chloroplast translation activity. After 180 min of illumination, ~84% of PSII quantum yield was lost in $\Delta psbM$ as compared with only 55% in WT leaves. However, exposure to the same light intensity in the absence of chloramphenicol resulted in 70% loss of PSII activity in the mutant as compared with only 27% in WT (Fig. 7A).

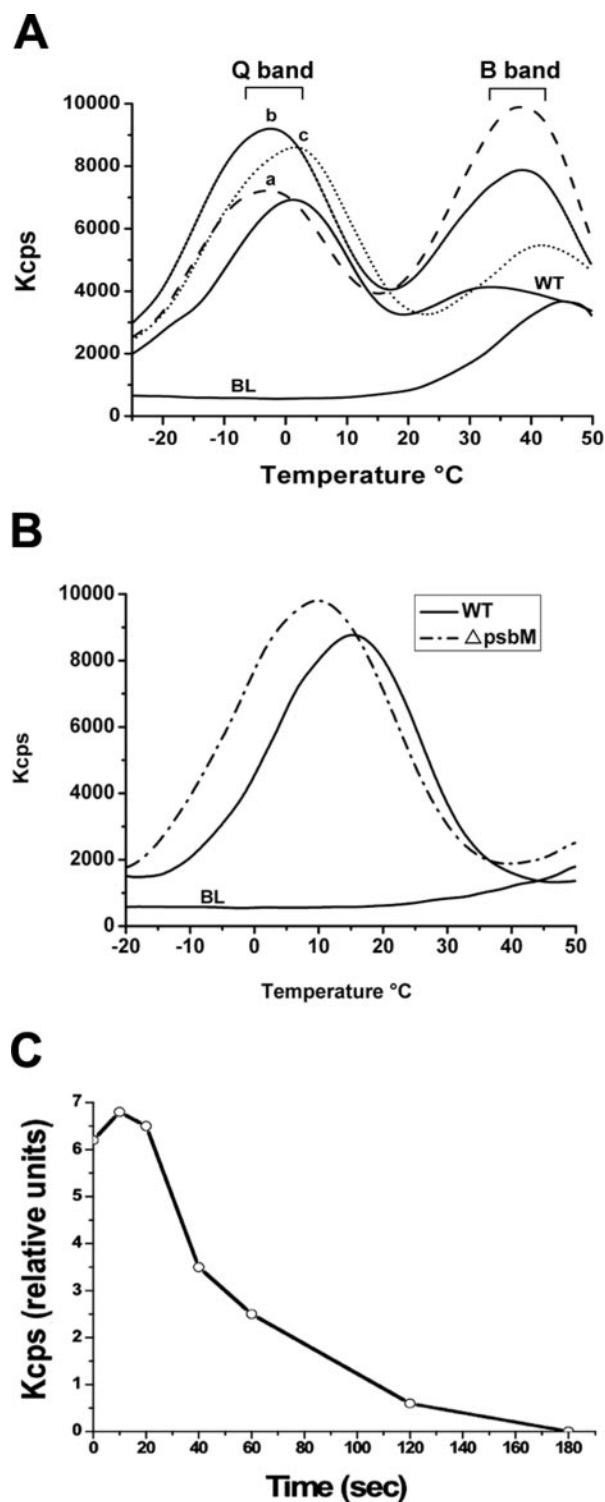


FIGURE 6. Thermoluminescence emission of thylakoids treated with herbicides. A, thermoluminescence emission because of Q_A^-/S_2 state recombination (Q band) generated by the addition of ioxylin (5 μM) for the wild type (WT; solid line) and curves a–c for $\Delta psbM$ thylakoids dark-adapted in the presence of 5, 10, and 20 μM ioxylin, respectively. Note the presence and changes in the residual emission of the mutant B band ($Q_B^-/S_2/S_3$) at 35 to 37 °C glow temperature persistent in the presence of ioxylin (traces a–c). B, the curves show representative Q band emissions of wild type and mutant samples in the presence of 10 μM DCMU. BL, base line of dark-adapted, unexcited mutant sample showing an after-glow band at 45 °C (46). C, time course of the B band decay in $\Delta psbM$ thylakoids in darkness. Excitation was given at 25 °C, and the sample temperature was maintained for times as indicated prior to fast cooling (10 s) to –20 °C before starting the measurements.

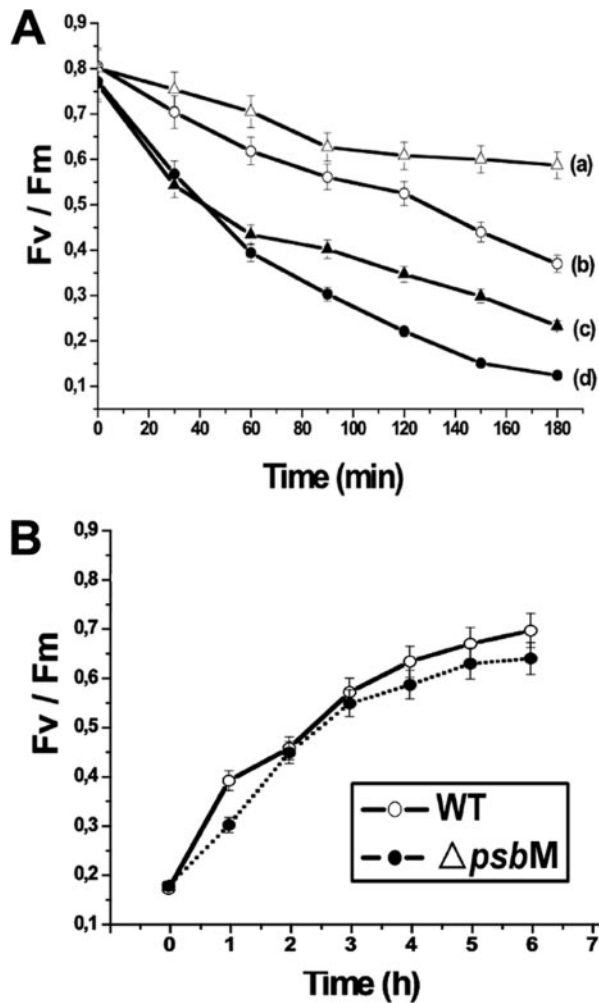


FIGURE 7. Photoinhibition of PSII and recovery kinetics in WT and mutant leaves. A, time course of photoinhibition at $500 \mu\text{E m}^{-2} \text{s}^{-1}$ for WT without (a) and with addition of chloramphenicol (b); $\Delta psbM$ leaves in the absence (c) or presence of chloramphenicol (d). B, recovery of WT (open circles) and mutant (closed circles) leaf samples after photoinhibition at $1,500 \mu\text{E m}^{-2} \text{s}^{-1}$ until a ratio F_v/F_m of 0.17 was reached. The temperature was maintained at 25°C , and recovery was initiated by lowering the light intensity to $3 \mu\text{E m}^{-2} \text{s}^{-1}$.

The PSII quantum yield measured in high light-exposed leaves is the result of a balance between the rate of PSII protein degradation (56) and the rate of *de novo* protein synthesis, reassembly, and photoactivation of the complex. To estimate the ability of the mutant to repair photoactivated PSII, WT and $\Delta psbM$ plants were irradiated with light of higher intensity ($1,500 \mu\text{E m}^{-2} \text{s}^{-1}$) to induce significant photoinhibition followed by incubation of the leaves at low light intensity to allow recovery of PSII activity. Before the photoinhibitory treatment, values of F_v/F_m were typical for WT and mutant leaves used in this experiment. Light exposure was continued until PSII was inactivated to a similar degree ($F_v/F_m = 0.17$). PSII activity recovered with the same kinetics and reached almost the initial value of F_v/F_m within 6 h in both mutant and WT (Fig. 7B), indicating that the capacity of *de novo* synthesis of the degraded protein(s), reassembly of the complex, and its photoactivation are not notably impaired by the mutation.

DISCUSSION

PsbM Is Not Required to Maintain the Assembly or Recovery of PSII—*PsbM* is a conserved hydrophobic LMW subunit of the PSII assembly. The sequence of higher plants *PsbM* shares $\sim 54\%$ identity with that of *Synechocystis* sp. PCC 6803 (16). The interface between the PSII core monomers forming the dimer that houses *PsbM* in the cyanobacterial PSII structure as resolved by x-ray diffraction at 3.5 (8) and 3.0 \AA (9) also contains the helix *PsbTc*, and both are close to helix *PsbL*. *PsbM*, *PsbTc*, and *PsbL* form a protein domain of six helices at the interface of the two PSII monomers. As such, inactivation of *psbM* results in the loss of two transmembrane helices in the dimeric axis of PSII. Based on the above, two prominent functions could be ascribed to *PsbM* as follows: (i) involvement in the interaction/binding of the two monomers, and (ii) a possible role in the controlled association/dissociation of the PSII dimer during the biogenesis and/or the photoinhibition/repair process. If so, loss of *PsbM* could weaken the dimer interconnection and possibly impair PSII repair during photoinhibitory illumination. However, deletion of *PsbM* does not prevent formation of dimers as well as assembly of active PSII supercomplexes and photoautotrophic growth under appropriate greenhouse conditions. This implies that *PsbM* is dispensable for the biogenesis of PSII. The results presented here clearly demonstrate that none of the proposed functions according to the localization within the complex can be assigned to *PsbM* in tobacco.

LHCII Dark Phosphorylation in $\Delta psbM$ —Our data indicate that loss of *PsbM* does not affect the accessibility of the corresponding kinase to LHCII nor its redox-regulated phosphorylation in the mutant. Normally, the PQ pool is relatively reduced under state 2 conditions (57). The unexpectedly high level of LHCII phosphorylation in dark-adapted mutant leaves could be due to persistence of a reduced PQ pool in the dark. This might have resulted from chlororespiration and/or NAD(P)H dehydrogenase activity (58, 59). On the other hand, an impaired PSII-mediated re-oxidation of PQH_2 in dark-adapted mutant plants could be responsible for the elevated PQ reduction level and consequently phosphorylation of LHCII (see below).

Because application of a weak far-red light was already sufficient to induce dephosphorylation of LHCII, the accessibility of the phosphatase seems to be unaltered. Alternatively, the presence of increased LHCII trimer levels in the mutant may cause aggregation of the trimers during illumination and, as a result, hinder the accessibility of the phosphorylation sites to the protein kinase (40, 60).

*Loss of *PsbM* Impairs Electron Transport Within, Outward, and Backward to PSII*—Inactivation of the intrinsic *PsbM* protein caused a reduced PSII activity increasing P700 oxidation and thus maintaining mutant plants in state 1 as revealed by fluorometric analysis and the phosphorylation status of LHCII in the light. This effect could be due to an increase in the redox potential gap between the Q_A and Q_B quinones. Furthermore, $\Delta psbM$ exhibits a departure from the 2/6 oscillation pattern of the TL B band emission (25).

Unlike WT, mutant plants display quite different patterns of TL oscillations with the number of exciting flashes (supplemental S4). The computational simulation of the dark-adapted PSII

states leading to these oscillation patterns indicates that the three different types observed in mutant plants can be generated by a higher Q_B/Q_B^- ratio in dark-adapted thylakoids (Fig. 5 and see supplemental S4 and S5).

A residual B band emission persisted even in the presence of 20 μM ioxynil in mutant thylakoids, whereas the emission of that band was already abolished by 5 μM ioxynil in the WT. Moreover, the emission temperature of the Q band induced by DCMU was downshifted by 5 $^\circ\text{C}$ in ΔpsbM as compared with the WT, implying a structural change in the Q_B site upon binding of DCMU inducing an effect on the activation energy of the recombination process from Q_A^- .

These results indicate the presence of a residual PSII population in which the Q_B sites after ioxynil treatment and dark adaptation are still occupied by PQ that can be reduced following light excitation to form a Q_B^- . Possibly, the Q_B site properties are progressively altered with the development of mutant leaves. This process varied among mutant leaves as indicated by the TL oscillations and the alteration of the Q_B/Q_B^- ratio as compared with the WT. Ioxynil binding at the Q_B site in ΔpsbM also suggests conformational changes in the structure of the Q_B binding pocket and its interaction with the Q_A site. This was shown by changes because of DCMU binding at the Q_B site and possible alteration of the activation energy for the back electron flow from Q_B semiquinone (52, 53). Thus, we propose that the Q_B site may also have variability in interacting or exchanging bound semiquinone with PQH_2 from the plastoquinol pool. The back electron flow during dark adaptation via deactivation of $S_{2/3}$ in the $S_{2/3}Q_B$ centers may need reduction of the Q_B quinone in darkness by a reduced plastoquinol to reach the predicted 1/3 ratio of S_0/S_1 and 1/1 ratio of Q_B/Q_B^- (45, 49). Thus it is possible that the alteration of the Q_B site interferes with this process resulting in more oxidized Q_B sites than semiquinone sites in the dark-adapted PSII populations of the mutant. This again would cause a shift to the 1/5 B band oscillations observed in the mutant. The elevated PQ reduction level and phosphorylation of LHCII in dark-adapted mutant plants may be a consequence of the impaired PSII-mediated reoxidation of PQH_2 involving the Q_B pocket. A similar function has also been proposed for the LMW subunit PsbI (25). Unlike ΔpsbI , dimeric PSII supercomplexes accumulate in ΔpsbM . Therefore, loss of PSII dimerization in ΔpsbI does not necessarily account for the observed effect on the 1/5 oscillation pattern and phosphorylation of LHCII in darkness.

To validate the ability of the simulation program to detect changes in the back electron flow, we have simulated the oscillation pattern of the ΔpsbI mutant as well. The oscillation patterns with the number of exciting flashes also fit with the measured values as reported for this mutant (25) when using the parameters in the simulation program as used in this work (supplemental S4). To obtain a good fit of the measured and simulated data, it is necessary to assume the presence of a residual amount of S_2 following dark adaptation. However, an increase in the ratio Q_B/Q_B^- of the dark-adapted thylakoids is suggested also for the ΔpsbI mutant, in which the Q_B/Q_A sites interaction is altered as well. Considering the binding properties at the Q_B site, these results reflect the most striking functional differences between ΔpsbM and WT.

The results of this work are in agreement with observations that the structure of the PSII core complex exhibits a certain degree of flexibility of the Q_B site conformation. This is indicated by the different effect of herbicide binding at this site on the midpoint potential of Q_A (53). Furthermore, alteration of the D-de loop of the D2 protein affects the properties of the Q_B -binding site of the D1 protein (61). It is thus conceivable that the structures of the quinone-binding sites harbored by the D1/D2 heterodimer and their interactions with surrounding protein helices are not rigid and are subject to fluctuations required for optimizing electron flow outward and within the PSII. Hence, removal of the PsbM helix pair from the interface region could cause a local conformational change that may affect the adjacent regions of the quinone-binding site(s) as well as D1/D2 phosphorylation. The phosphorylation level of CP43 is comparable in mutant and WT implying that its confirmation is unaltered in ΔpsbM allowing access of the corresponding kinase. The LMWs of PSII may play an important role in stabilizing the plasticity of these quinone-binding sites. In their absence, changes may occur in the PSII core that may be detrimental to its activity and light sensitivity.

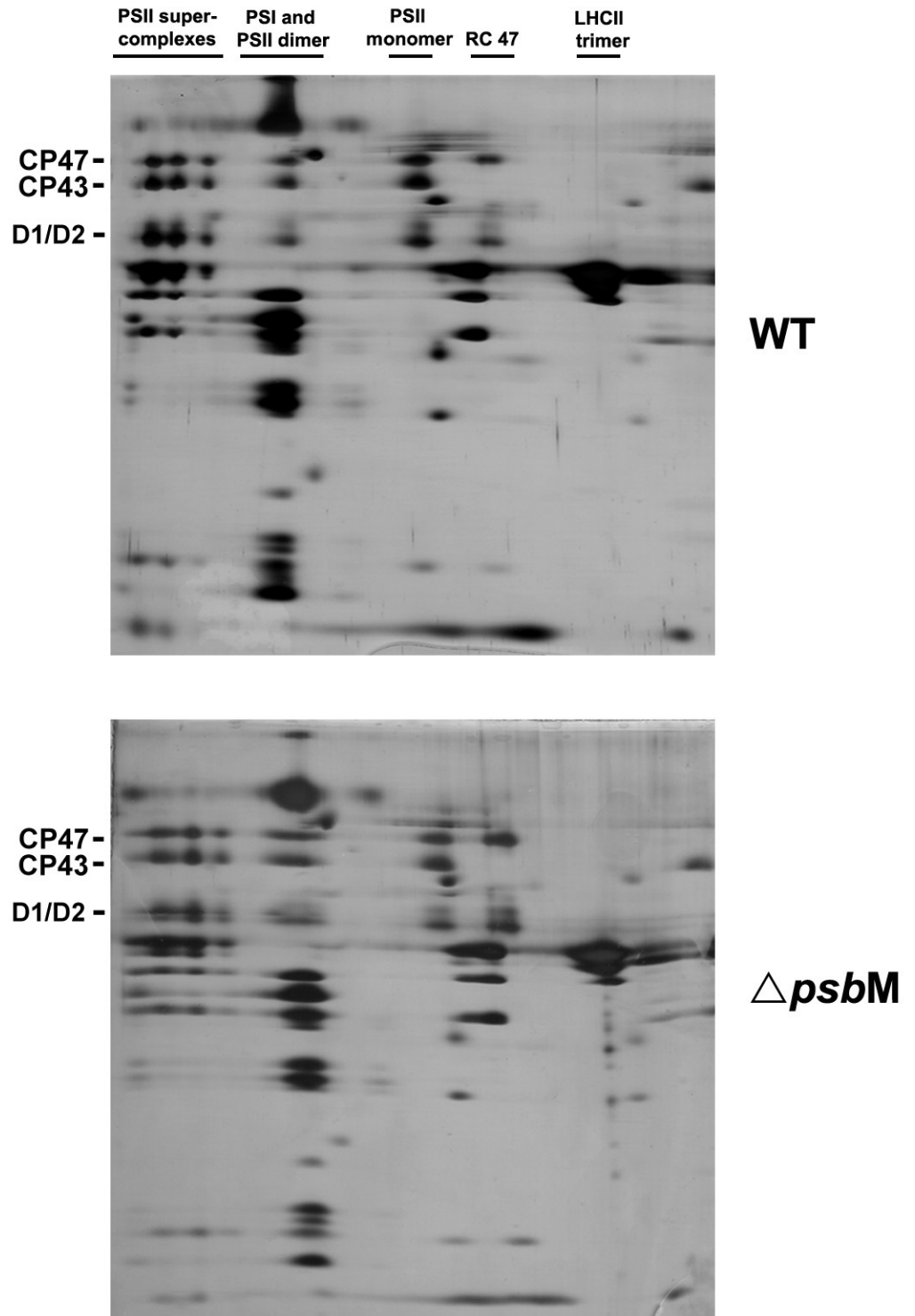
We conclude that the lower oxygen evolution rate, the reduced photosynthetic quantum yield, the increased light sensitivity, the shift of the Q_A midpoint potential, an alteration of the Q_B -binding site, and the modified oscillation pattern of the TL signals are related to the loss of PsbM. Our data suggest that the PsbM protein in tobacco plays an important role in ensuring an efficient and functional PSII-mediated electron transport rather than in maintaining the assembly, structure, and stability of the PSII complex.

Acknowledgments—The skilled technical assistance of Martina Reymers is gratefully acknowledged. Nir Keren is acknowledged for helpful suggestions and discussions.

REFERENCES

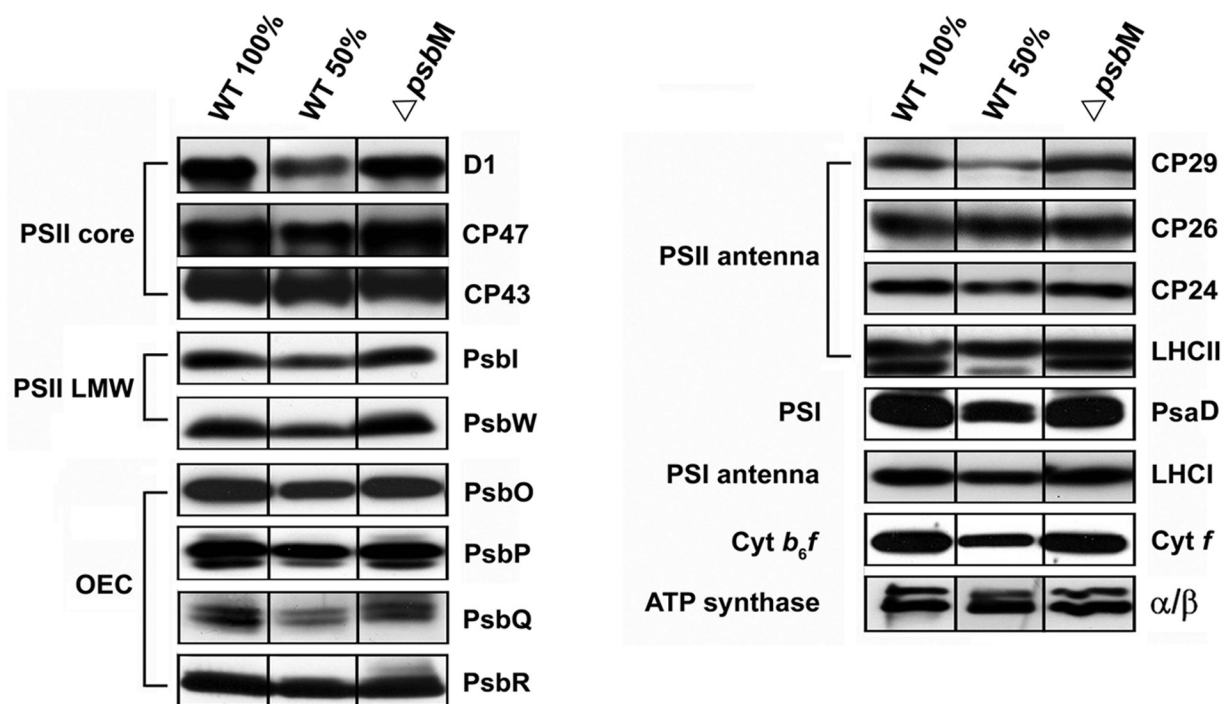
- Nelson, N., and Yocum, C. F. (2006) *Annu. Rev. Plant Biol.* **57**, 521–565
- Vrettos, J. S., and Brudvig, G. W. (2002) *Philos. Trans. R. Soc. Lond. B Biol. Sci.* **357**, 1395–1404
- Clausen, J., Debus, R. J., and Junge, W. (2004) *Biochim. Biophys. Acta* **1655**, 184–194
- Hankamer, B., Morris, E., Nield, J., Gerle, C., and Barber, J. (2001) *J. Struct. Biol.* **135**, 262–269
- Dekker, J. P., and Boekema, E. J. (2005) *Biochim. Biophys. Acta* **1706**, 12–39
- Kamiya, N., and Shen, J. R. (2003) *Proc. Natl. Acad. Sci. U. S. A.* **100**, 98–103
- Biesiadka, J., Loll, B., Kern, J., Irrgang, K. D., and Zouni, A. (2004) *Phys. Chem. Chem. Phys.* **20**, 4733–4736
- Ferreira, K. N., Iverson, T. M., Maghlaoui, K., Barber, J., and Iwata, S. (2004) *Science* **303**, 1831–1837
- Loll, B., Kern, J., Saenger, W., Zouni, A., and Biesiadka, J. (2005) *Nature* **438**, 1040–1044
- Liu, Z., Yan, H., Wang, K., Kuang, T., Zhang, J., Gui, L., An, X., and Chang, W. (2004) *Nature* **428**, 287–292
- Ruban, A. V., Solovieva, S., Lee, P. J., Illoia, C., Wentworth, M., Ganeteg, U., Klimmek, F., Chow, W. S., Anderson, J. M., Jansson, S., and Horton, P. (2006) *J. Biol. Chem.* **281**, 14981–14990
- Meurer, J., Plücker, H., Kowallik, K. V., and Westhoff, P. (1998) *EMBO J.* **17**, 5286–5297
- Ossenbühl, F., Inaba-Sulpice, M., Meurer, J., Soll, J., and Eichacker, L. A.

- (2004) *Plant Cell* **18**, 2236–2246
14. Peng, L., Ma, J., Chi, W., Guo, J., Zhu, S., Lu, Q., Lu, C., and Zhang, L. (2006) *Plant Cell* **18**, 955–969
 15. Rochaix, J. D. (2001) *Plant Physiol.* **125**, 142–144
 16. Shi, L.-X., and Schröder, W. P. (2004) *Biochim. Biophys. Acta* **1608**, 75–96
 17. Thornton, L. E., Roose, J. L., Pakrasi, H. B., and Ikeuchi, M. (2005) in *Photosystem II: The Water/Plastoquinone Oxidoreductase in Photosynthesis* (Wydrzynski, T., and Satoh, K., eds) pp. 121–138, Kluwer Academic Publishers Group, Dordrecht, The Netherlands
 18. Nelson, N., and Ben-Shem, A. (2004) *Nat. Rev. Mol. Cell Biol.* **12**, 971–982
 19. Minagawa, J., and Takahashi, Y. (2004) *Photosynth. Res.* **82**, 241–263
 20. Whitmarsh, J., and Pakrasi, H. B. (1996) in *Oxygenic Photosynthesis: The Light Reactions* (Ort, D. R., and Yocum, C. F., eds) pp. 249–264, Kluwer Academic Publishers Group, Dordrecht, The Netherlands
 21. Stewart, D. H., and Brudvig, G. W. (1998) *Biochim. Biophys. Acta* **1367**, 63–87
 22. Bondarava, N., De Pascalis, L., Al-Babili, S., Goussias, C., Golecki, J. R., Beyer, P., Bock, R., and Krieger-Liszkay, A. (2003) *J. Biol. Chem.* **278**, 13554–13560
 23. Regel, R. E., Ivleva, N. B., Zer, H., Meurer, J., Shestakov, S. V., Herrmann, R. G., Pakarasi, H. B., and Ohad, I. (2001) *J. Biol. Chem.* **276**, 41473–41478
 24. Ohad, I., Dal Bosco, C., Herrmann, R. G., and Meurer, J. (2004) *Biochemistry* **43**, 2297–2308
 25. Schwenkert, S., Umate, P., Dal Bosco, C., Volz, S., Mlèochová, L., Zoryan, M., Eichacker, L. A., Ohad, I., Herrmann, R. G., and Meurer, J. (2006) *J. Biol. Chem.* **281**, 34227–34238
 26. Swiatek, M., Kuras, R., Sokolenko, A., Higgs, D., Olive, J., Cinque, G., Müller, B., Eichacker, L. A., Stern, D. B., Bassi, R., Herrmann, R. G., and Wollmann, F. A. (2001) *Plant Cell* **13**, 1347–1367
 27. Ohnishi, N., Kashino, Y., Satoh, K., Ozawa, S. I., and Takahashi, Y. (2007) *J. Biol. Chem.* **282**, 10.1074/jbc.M606763200
 28. Swiatek, M., Regel, R. E., Meurer, J., Wanner, G., Pakarasi, H. B., Ohad, I., and Herrmann, R. G. (2003) *Mol. Genet. Genomics* **268**, 699–710
 29. de Vitry, C., Diner, B. A., and Popo, J. L. (1991) *J. Biol. Chem.* **266**, 16614–16621
 30. Ikeuchi, M., Inoue, Y., and Vermaas, W. (1995) in *Photosynthesis: From Light to Biosphere* (Mathis, P., ed) pp. 297–300, Kluwer Academic Publishers Group, Dordrecht, The Netherlands
 31. Ikeuchi, M., Koike, H., and Inoue, Y. (1989) *FEBS Lett.* **253**, 178–182
 32. Kashino, Y., Lauber, W. M., Carroll, J. A., Wang, Q., Whitmarsh, J., Satoh, K., and Pakarasi, H. B. (2002) *Biochemistry* **41**, 8004–8012
 33. Gomez, S. M., Nishio, J. N., Faull, K. F., and Whitelegge, J. P. (2002) *Mol. Cell. Proteomics* **1**, 46–59
 34. Sugiura, M., Shinozaki, K., Zaita, N., Kusuda, M., and Kumano, M. (1986) *Plant Sci.* **44**, 211–216
 35. Koop, H. U., Steinmüller, K., Wagner, H., Rossler, C., Eibl, C., and Sacher, L. (1996) *Planta* **199**, 193–201
 36. Swiatek, M., Greiner, S., Kemp, S., Drescher, A., Koop, H. U., Herrmann, R. G., and Maier, R. M. (2003) *Curr. Genet.* **43**, 45–53
 37. Granvogl, B., Reisinger, V., and Eichacker, L. A. (2006) *Proteomics* **6**, 3681–3695
 38. Schreiber, U., Bilger, W., Hormann, H., and Neubauer, C. (1998) in *Photosynthesis: A Comprehensive Treatise* (Raghavendra, A. S., ed) pp. 320–336, Cambridge University Press, Cambridge, UK
 39. Lunde, C., Jensen, P. E., Haldrup, A., Knoetzel, J., and Scheller, H. V. (2000) *Nature* **30**, 613–615
 40. Zer, H., Vink, M., Shochat, S., Herrmann, R. G., Andersson, B., and Ohad, I. (2003) *Biochemistry* **42**, 728–738
 41. Klughammer, C., and Schreiber, U. (1994) *Planta* **192**, 261–268
 42. Zer, H., Prasil, O., and Ohad, I. (1994) *J. Biol. Chem.* **269**, 17670–17676
 43. Corana, A., Marchesi, M., Martini, C., and Ridella, S. (1987) *ACM Transactions on Mathematical Software* **13**, 262–280
 44. Vener, A. V., van Kann, P. J., Rich, P. R., Ohad, I., and Andersson, B. (1997) *Proc. Natl. Acad. Sci. U. S. A.* **94**, 1585–1590
 45. Rutherford, A. W., Govindjee, and Inoue, Y. (1984) *Proc. Natl. Acad. Sci. U. S. A.* **81**, 1107–1111
 46. Haumann, M., Liebisch, P., Müller, C., Barra, M., Grabolle, M., and Dau, H. (2005) *Science* **310**, 1019–1021
 47. Vass, I. (2003) *Photosynth. Res.* **76**, 303–318
 48. Ducruet, J. M. (2003) *J. Exp. Bot.* **54**, 2419–2430
 49. Rutherford, A. W., Crofts, A. R., and Inoue, Y. (1982) *Biochim. Biophys. Acta* **682**, 457–465
 50. DeVault, D., Govindjee, and Arnold, W. (1983) *Proc. Natl. Acad. Sci. U. S. A.* **80**, 983–987
 51. Demeter, S., and Vass, I. (1984) *Biochim. Biophys. Acta* **764**, 24–32
 52. Krieger-Liszkay, A., and Rutherford, A. W. (1998) *Biochemistry* **37**, 17339–17344
 53. Rutherford, A. W., and Krieger-Liszkay, A. (2001) *Trends Biochem. Sci.* **26**, 648–653
 54. Adir, N., Zer, H., Shochat, S., and Ohad, I. (2003) *Photosynth. Res.* **76**, 343–370
 55. Szilard, A., Sass, L., Hideg, E., and Vass, I. (2005) *Photosynth. Res.* **84**, 15–20
 56. Schuster, G., Timberg, R., and Ohad, I. (1988) *Eur. J. Biochem.* **177**, 411–416
 57. Allen, J. F. (2005) *Curr. Biol.* **15**, 929–932
 58. Feild, T. S., Nedbal, L., and Ort, D. R. (1998) *Plant Physiol.* **116**, 1209–1218
 59. Munekage, Y., Hojo, M., Meurer, J., Endo, T., Tasaka, M., and Shikanai, T. (2002) *Cell* **110**, 361–371
 60. Zer, H., Vink, M., Keren, N., Dilly-Hartwig, H. G., Paulsen, H., Herrmann, R. G., Andersson, B., and Ohad, I. (1999) *Proc. Natl. Acad. Sci. U. S. A.* **96**, 8277–8282
 61. Kless, H., Oren-Shamir, M., Ohad, I., Edelman, M., and Vermaas, W. (1993) *Z. Naturforsch.* **48**, 185–190



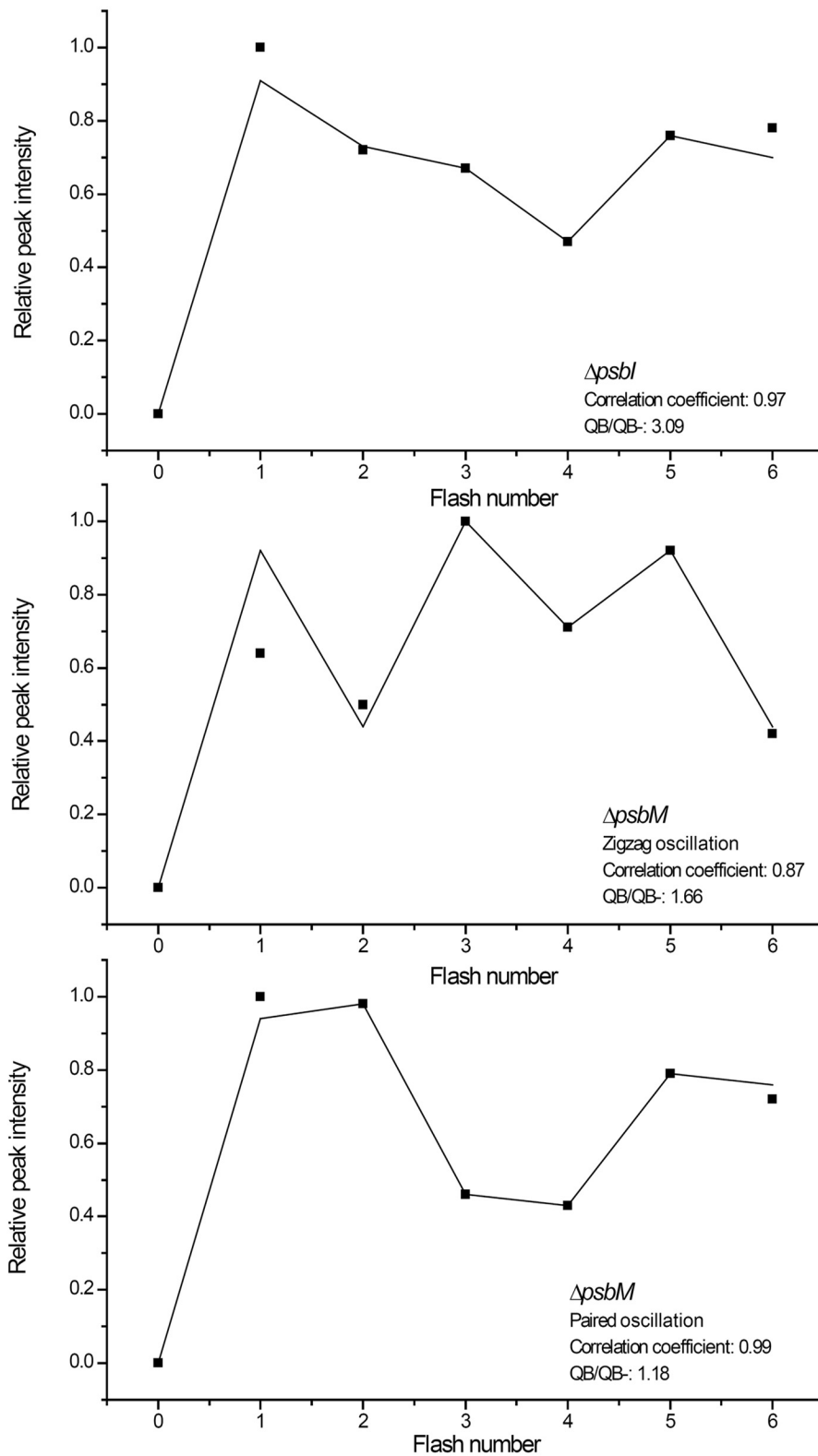
Supplemental Figure 2
Umate et al. 2007

BN/SDS-PAGE gel electrophoresis of thylakoid membrane complexes. WT and mutant thylakoids were solubilized with 1% n-dodecyl- β -D-maltoside and electrophoresis was performed in the first (BN-PAGE) and second (SDS-PAGE) dimension. Individual protein spots were silver-stained. The WT control was used as described (25).



Supplemental Figure 3
Umate et al. 2007

Immunological analysis of representative proteins of the thylakoid membrane protein complexes PSII, PSI, cytochrome b_6f (*cyt b₆f*) and ATP synthase.



Supplemental Figure 4 Umate et al. 2007

Simulations of dark oscillation patterns in mature $\Delta psbM$ and $\Delta psbI$ leaves.

TL oscillation as a function of the number of exciting flashes as presented by squares. The fit by the simulation program is presented as a full line. The free parameters in the fit were the S_0 , S_1 , QB , QB^- occupancy levels and misses and double hits. In the case of the zigzag oscillation pattern the S_2 state had to be included to achieve a good fit.

TL raw data

Δ PsbM 1/ Flash no.	expt. 1	expt. 2	expt. 3	average	error		
0.00	0.00	0.00	0.00	0.00	0.00		
1.00	5.00	5.00	4.30	4.76	0.40	1.87	0.16
2.00	2.70	3.50	3.80	3.33	0.57	1.31	0.22
3.00	1.30	1.70	1.20	1.40	0.26	0.55	0.10
4.00	0.70	0.70	1.20	0.86	0.29	0.34	0.11
5.00	3.60	2.70	2.10	2.80	0.75	1.10	0.30
6.00	2.70	1.70	1.90	2.10	0.52	0.83	0.20

WT 2/6 pa Flash no.	expt. 1	expt. 2	expt. 3	average	error		
0.00	0.00	0.00	0.00	0.00	0.00		
1.00	0.71	0.71	0.62	0.68	0.05	1.23	0.09
2.00	1.00	1.00	1.12	1.04	0.07	1.88	0.12
3.00	0.28	0.31	0.21	0.26	0.05	0.47	0.09
4.00	0.14	0.06	0.09	0.09	0.04	0.16	0.07
5.00	0.42	0.45	0.40	0.42	0.03	0.76	0.05
6.00	0.85	0.84	0.80	0.83	0.03	1.50	0.05

(values indicate signal intensities of glow emission)

Simulation results

Δ PsbM	expt. 1				expt. 2				expt. 3				QB/QB-	
	0	S1	S2	S3	S0	S1	S2	S3	S0	S1	S2	S3		
QB	0.23	1.00	0.00	0.00	QB	0.18	1.00	0.00	QB	0.00	1.00	0.00	0.00	1.01
QB-	0.27	0.24	0.00	0.00	QB-	0.59	0.05	0.00	QB-	0.53	0.46	0.00	0.00	
	Misses = 0.09				Misses = 0.14				Misses = 0.21					
	Double Hits = 0.03				Double Hits = 0.01				Double Hits = 0.09					
WT	S0	S1	S2	S3	S0	S1	S2	S3	S0	S1	S2	S3	QB/QB-	
QB	0.00	0.79	0.00	0.00	QB	0.03	0.79	0.00	QB	0.00	0.63	0.00	0.00	0.56
QB-	0.81	0.25	0.00	0.00	QB-	0.94	0.12	0.00	QB-	0.50	0.62	0.00	0.00	
	Misses = 0.10				Misses = 0.10				Misses = 0.12					
	Double Hits = 0.00				Double Hits = 0.00				Double Hits = 0.00					

Statistical analysis

	Average QB/QB-	SD
Δ PsbM	1.76	0.72
WT	0.69	0.11

Using a two sample t-test the mean of the mutant QB/QB- ratio is greater than the mean of the WT ratio at a significance level of 0.05

Impact of PsbTc on Forward and Back Electron Flow, Assembly, and Phosphorylation Patterns of Photosystem II in Tobacco

Pavan Umate^{1,2†}, Christine Fellerer^{1†}, Serena Schwenkert¹, Mikael Zoryan¹, Lutz A. Eichacker¹, Abbagani Sadanandam³, Itzhak Ohad⁴, Reinhold G. Herrmann¹, and Jörg Meurer^{1,*}

Department Biology I, Botany, Ludwig-Maximilians-University Munich,
Menzingerstr. 67, 80638 Munich, Germany.

Footnotes:

This work was supported by the Deutsche Forschungsgemeinschaft (DFG, SFB-TR1) to JM and RGH, the Deutsche Akademische Austauschdienst (DAAD) to PU, and the Minerva Avron, Even-Ari Center for Photosynthesis Research, The Hebrew University, Jerusalem, Israel to IO.

¹Department Biology I, Botany, Ludwig-Maximilians-University Munich, Menzingerstr. 67, 80638 Munich, Germany.

²Present address - Plant Molecular Biology, International Centre for Genetic Engineering and Biotechnology (ICGEB), Aruna Asaf Ali Marg, New Delhi 110 067, India.

³Department of Botany, Kakatiya University, Warangal, 506 009, India

⁴Department of Biological Chemistry and the Minerva Center of Photosynthesis Research, The Hebrew University of Jerusalem, Jerusalem 91904, Israel.

*Address correspondence to: Jörg Meurer, Department Biology I, Botany, Ludwig-Maximilians-University Munich, Menzingerstr. 67, 80638 Munich, Germany; Tel. +49 (0)89-17861288; Fax. +49(0)89-1782274; E-mail: joerg.meurer@lrz.uni-muenchen.de

†Both authors contributed equally to this work.

Abbreviations:

aadA, amino glycoside 3' adenylyl transferase; BN, blue native; CP, chlorophyll protein; DCMU, Diuron, 3-(3,4-Dichlorophenyl)-1,1-dimethylurea; DM, dodecylmaltoside; LHC, light harvesting complex; LMW, low molecular weight; PS, Photosystem; PQ, plastoquinone; RC, reaction center; TL, Thermoluminescence; WT, wild type.

ABSTRACT

Photosystem II (PSII) of oxygen evolving cyanobacteria, algae and land plants mediates electron transfer from the Mn_4Ca cluster to the plastoquinone pool. It is a dimeric supramolecular complex comprising more than 30 subunits per monomer of which 16 are bitopic or peripheral, low-molecular-weight (LMW) components. Directed inactivation of the plastid gene encoding the LMW peptide PsbTc in tobacco does not prevent photoautotrophic growth. Mutant plants appear normal green and levels of PSII proteins are not affected. Yet, PSII dependent electron transport, stability of PSII dimers and assembly of PSII-light harvesting complexes (LHCII) are significantly impaired. PSII light sensitivity is moderately increased and recovery from photoinhibition is delayed leading to faster D1 degradation in $\Delta psbTc$ under high light. Thermoluminescence emission measurements revealed alterations of mid-point potentials of Q_A/Q_B interaction. Only traces of CP43 and no D1/D2 proteins are phosphorylated presumably due to structural changes of PSII in $\Delta psbTc$. In striking contrast to WT, LHCII in the mutant is phosphorylated in darkness consistent with its association with PSI indicating an increased pool of reduced plastoquinone (PQ) in the dark. Finally, we provide evidence that *in vivo* the Q_B site, the properties of which are altered in $\Delta psbTc$, is required for oxidation of reduced plastoquinone in darkness in an oxygen dependent manner. These data present novel aspects of plastoquinone redox regulation, chlororespiration, and control of LHCII phosphorylation.

INTRODUCTION

Photosystem II, the oxygen evolving pigment-protein complex of the thylakoid membrane system, is present in photosynthetic organisms from cyanobacteria to vascular plants. The proteins of the photochemically active reaction center (RC), the heterodimeric polypeptides PsbA (D1) and PsbD (D2) and the LMW subunits PsbE and PsbF, the α and β chains of cytochrome b_{559} , coordinate the redox cofactors necessary for primary PSII photochemistry. Electron flow following charge separation occurs via several electron carriers of the reaction center including pheophytin a , as well as the primary and secondary quinones, Q_A and Q_B . The striking similarities between cyanobacterial and land plant PSII core components including the intrinsic light harvesting antennae, the chlorophyll-binding proteins CP43 and CP47, as well as their interactions during photosynthetic charge separation, suggest a high degree of structural and functional conservation. Thus, much of the information obtained from crystallisation of a cyanobacterial PSII can be applied to that of higher plants (Zouni *et al.*, 2001; Kamiya and Shen, 2003; Ferreira *et al.*, 2004; Loll *et al.*, 2005; Nield and Barber, 2006).

Besides the RC, the PSII core contains a remarkably high number (16) of intrinsic or peripheral LMWs. Five of them are encoded in eukaryotes by nuclear (*psbR*, Tn, W, X, Y1/Y2) and 11 by plastid genes (*psbE*, *psbF*, *psbL*, *psbJ*, *psbK*, *psbM*, *psbI*, *psbTc*, *psbN*, *psbH*, and *psbZ*) of which most are parts of conserved operons (reviewed in Minagawa and Takahashi, 2004; Shi and Schroeder, 2004; Thornton *et al.*, 2005; Müh *et al.* 2008). PSII cores of higher plants and cyanobacteria form a functional dimer. In chlorophyll a/b -lineages, the additional chlorophyll proteins LHCII, forming trimers, CP24, CP26, and CP29 are associated with dimeric PSII complexes and, except CP24, partially with PSI depending on the energy balance between the two photosystems (Dekker and Boekema, 2005; Takahashi *et al.*, 2006). This process is regulated by reversible phosphorylation of these chlorophyll-binding proteins. Excess light excitation of PSII relative to the accessibility of the electron sink induces back electron flow and charge recombination that generates singlet oxygen species, generally considered as the major cause of photoinactivation and related light-dependent degradation of the D1

protein (Vass *et al.*, 2007) as well as of a genetically programmed stress response (Wagner *et al.*, 2004).

The conservation of PSII LMWs throughout the evolution from cyanobacteria to plastids suggests that these proteins that are not harboring any of the electron carrier components play distinct roles in the structural organization, dynamics, and regulation of PSII electron flow and its protein turnover. Possible roles for the LMWs in these processes have been discussed for cyanobacteria, algae, and land plants (Minagawa and Takahashi, 2004; Shi and Schroeder, 2004; Thornton *et al.*, 2005; Müh *et al.* 2008). In this context it is relevant to mention that inactivation of some of these genes often resulted in different phenotypes in distantly related organisms (Regel *et al.*, 2001; Ohad *et al.*, 2004; Schwenkert *et al.*, 2006). Detailed analyses of knockout mutants of PSII LMWs in tobacco have revealed specific roles for PsbE, PsbF, PsbL, and PsbJ (Regel *et al.*, 2001; Swiatek *et al.*, 2003a; Ohad *et al.*, 2004) as well as for PsbZ (Swiatek *et al.*, 2001), PsbI (Schwenkert *et al.*, 2006), and PsbM (Umate *et al.*, 2007).

Two different LMWs associated with PSII have been originally designated PsbT. PsbTc of 4 kDa originates from a chloroplast gene and the unrelated protein PsbTn of 11 kDa from a nuclear gene (reviewed in Shi and Schroeder, 2004; Müh *et al.* 2008). PsbTc is an intrinsic, bitopic LMW protein harbouring a single transmembrane helix and, different from most LMWs, exposes its N-terminal tail into the luminal phase of the thylakoid membrane (Shi and Schroeder, 2004). The *psbTc* gene is located in a highly conserved operon, together with the PSII genes *psbB* and *psbH*, the cytochrome *b₆f* complex genes *petB* and *petD*, encoding cytochrome *b₆* and subunit IV, and *psbN* on the opposite strand. The operon is transcribed into a primary product of 5.7 kb that is processed in a complex way (Barkan, 1988; Kohchi *et al.*, 1988; Westhoff and Herrmann, 1988).

As part of an ongoing project, individual thylakoid LMWs were systematically disrupted in tobacco to elucidate the effect of each in the same organism. Here, the first study of the effect of *psbTc* inactivation on PSII function in a higher plant is presented. Our data show that Q_A and Q_B site properties, forward and back electron flow, phosphorylation, assembly, and stability of PSII proteins are affected in the mutant. In addition,

experiments performed with the WT reveal that *in vivo* the Q_B site of PSII is responsible for oxidation of reduced plastoquinone and reduction of O₂ in the dark, presumably to keep the acceptor side of PSII oxidized. This sheds new light on the nature of a terminal oxidase working during chlororespiration.

RESULTS

Inactivation of *psbTc*

To selectively inactivate *psbTc*, we inserted a terminator-less amino glycoside 3' adenylyl transferase (*aadA*) cassette into a newly introduced restriction site in the 5' region of the gene to avoid expression of a functional or truncated protein (Fig. 1A). Homoplastomy of transformed lines was confirmed by PCR analysis of isolated chloroplast chromosomes (Fig. 1B). Primers used for PCR did not amplify the 1,021 bp product obtained for the WT but exclusively the *aadA*-containing product of 1,952 bp in $\Delta psbTc$. Insertion of the selection cassette into a pentacistronic operon could affect expression, processing, and/or stability of transcripts originating from the same operon or, in the present case, from the oppositely transcribed *psbN*. Therefore, integrity and levels of well known processed RNA species (Westhoff and Herrmann, 1988) were estimated by Northern blot analyses using strand specific probes for *psbTc*, *psbH*, and *psbN* as well as random primed labeled probes for *psbB* and *petB* (Fig. 1C). The data confirmed the homoplastomic state of mutant plants since spliced and unspliced pentacistronic transcripts, detected with *psbB*, *psbT*, *psbH*, and *petB* probes, as well as dicistronic *psbB-psbT* transcripts are expectedly up-shifted by the size of the *aadA* cassette. Although no monocistronic *psbTc* transcripts could be detected in WT, the *psbB-psbTc* intergenic region was processed in the mutant resulting in the accumulation of a *psbTc-aadA* transcript of about 1.3 kbp. The analysis further demonstrated that processing and expression levels of *psbH*, *psbN* and *petB* containing transcripts located downstream of *psbTc* are not notably affected by the *aadA* insertion (Fig. 1C). Mutant plants grew photoautotrophically under greenhouse conditions on soil and appear green, comparable to WT. In contrast to WT, *PsbTc* could

not be detected in mutant thylakoid membranes by mass spectrometry using a novel approach, which will be published elsewhere (data not shown). To ensure that the phenotype was not caused by random nuclear background mutations and inherited solely via chloroplasts we performed backcrosses with the WT using three independently generated homoplasmic $\Delta psbTc$ mutants as female parents. This resulted in a 100% offspring of the mutant phenotype with respect to photosynthetic parameters such as reduction of the potential maximum quantum yield of PSII, F_v/F_m , to about 0.68 ± 0.03 as compared to 0.82 ± 0.01 in the WT using at least 20 individuals from each cross. This unequivocally indicates that exclusively loss of *PsbTc* accounts for the phenotype. Three chosen mutant lines, $\Delta psbTc$ -1-3, were used for detailed studies.

Composition of thylakoid membrane proteins in $\Delta psbTc$ -1

The protein composition of thylakoids isolated from $\Delta psbTc$ and WT plants was estimated by immunoblot analysis using antisera raised against individual thylakoid proteins (Schwenkert *et al.*, 2006). Levels of PSII proteins D1, D2, CP47, *PsbI*, and the extrinsic polypeptide *PsbO* of the oxygen-evolving complex in $\Delta psbTc$ -1 were comparable to WT (Fig. 2A). Also, no notable differences were found for the major LHCII (*Lhcb1*), LHCI (*Lhca1*), and minor antenna apoproteins CP29, CP26, and CP24, nor for components of PSI, cytochrome *b₆f* complex, and ATP synthase (Fig. 2A and data not shown). This corroborates that translation and accumulation of *petB* and *petD* transcripts downstream of *psbTc*-1 are not affected by the *aadA* insertion.

Assembly of PSII-LHCII supercomplexes and stability of PSII dimers is affected in $\Delta psbTc$ -1-3

To gain information on the assembly and stability of PSII in $\Delta psbTc$ plants, controlled partial lysates of isolated thylakoids solubilized with 1% β -DM were resolved by blue native (BN)-PAGE and subsequent SDS-PAGE. The protein patterns uncovered that PSII-LHCII supercomplexes were almost missing and levels of dimeric PSII complexes were reduced, whereas trimeric LHCII complexes, as well as monomeric PSII reaction center

complexes lacking CP43, called RC47, were increased in $\Delta psbTc$ -1-3 thylakoids as compared to WT (Fig. 2B and Supplemental Fig. 1A). Levels and sizes of all other detectable thylakoid membrane complexes were not significantly affected. To estimate a possible loss of unstable PSII-supercomplexes in the mutant during sample preparation, milder separation of thylakoid lysates by sucrose density gradient centrifugation and BN-PAGE using 1.5% digitonin (Schwenkert *et al.* 2007) was applied. Separation profiles confirmed reduced levels of PSII-LHCII supercomplexes in the mutant (Supplemental Figs. 2A and B). Levels of monomeric RC47 complexes and trimeric LHCII complexes were increased in $\Delta psbTc$ -1 (Supplemental Figs. 2A and B), suggesting that assembly and/or stability of higher order PSII complexes is affected or that they could not be readily isolated in $\Delta psbTc$ thylakoids. Therefore, a third approach was chosen to discern whether formation or stability of PSII-LHCII supercomplexes and dimeric complexes is affected in $\Delta psbTc$ -1. Leaves were labeled with ^{35}S -methionine and isolated thylakoids were analyzed by 2D BN-SDS-PAGE (Fig. 2C). This approach showed that the mutant is capable of assembling RC47, PSII monomers, and dimers efficiently but not PSII-LHCII supercomplexes as compared to the WT. Since steady state levels of dimers are severely reduced we conclude that stability of dimeric PSII complexes is affected by the mutation presumably due to conformational changes induced by the absence of PsbTc. The relative amount of assembled PSII-LHCII complexes even after a short five min pulse resembles the pattern after a pulse of 40 min (Fig. 2C) indicating that the supercomplexes are not lost because of severe instability during the labeling period in $\Delta psbTc$ -1. Improper assembly of LHCII may result secondarily from conformational changes of the PSII dimer (Fig. 2C).

Light sensitivity: photoinactivation and recovery of PSII activity

Upon excessive illumination D1 protein is damaged and degraded resulting in impaired PSII activity. The extent of PSII light sensitivity and its ability to recover from photoinactivation was therefore studied by measuring Fv/Fm as an estimation of the

potential PSII quantum yield in WT and mutant plants. In order to distinguish between PSII damage and repair (*de novo* D1 synthesis) processes, the effect of the chloroplast protein synthesis inhibitor D-threo-chloramphenicol (CAP) was examined. For this, WT and $\Delta psbTc-1-3$ leaf discs were illuminated at $1,200 \mu E m^{-2} s^{-1}$ after pre-treatment with CAP. In the absence of CAP (control conditions) Fv/Fm is reduced to about 50% of the initial value in all three mutant lines as compared to only $66\% \pm 1.2$ in the WT after 4 h of illumination (Fig. 3A; Supplemental Fig. 1B). Addition of CAP induced a more pronounced PSII inactivation in both WT and $\Delta psbTc-1-3$ plants to $33\% \pm 1.3$ and 20 - 23% of their initial value, respectively (Fig. 3A, Supplemental Fig. 1B). This shows that in the mutants recovery principally takes place and that PSII is more sensitive to high light exposure. To further analyze the efficiency of the recovery process, WT and $\Delta psbTc-1$ leaf disc samples were exposed to $1,200 \mu E m^{-2} s^{-1}$ until the PSII quantum yield reached 0.17 in all samples and then allowed to recover PSII activity under very low light intensity ($3 \mu E m^{-2} s^{-1}$) (Fig. 3B). After two hours recovery was about two times faster in the WT as compared to $\Delta psbTc-1$. Mutant leaf samples finally recovered $70.4 \pm 8\%$ of their initial PSII activity, as compared to $84.2 \pm 7\%$ in WT within six hours, indicating a delayed recovery of PSII activity from inhibition in $\Delta psbTc-1$. To further analyze photosensitivity on the protein level immunological analysis of two h high light treated WT and mutant plants was performed in the absence and presence of CAP (Fig. 3C). The data confirmed that the photoinhibitory effect in $\Delta psbTc-1$ was indeed due to D1 degradation and that CAP induced a more pronounced degradation of D1 in the mutant as compared to the WT again indicating an increased light sensitivity of PSII in $\Delta psbTc-1$ (Fig 3C).

Activities of PSII and PSI

The maximum quantum yield of PSII, Fv/Fm, was decreased in all independently selected and backcrossed mutant lines ($\Delta psbTc-1-3$) and ranged from 0.65 to 0.71 vs. 0.82 ± 0.01 in WT which was due to an increased Fo and/or a decreased Fv again indicating dissociation of the outer PSII antenna and/or malfunction of PSII electron

transport activity. Further photosynthetic parameters have been measured in the three lines (Figs. 4A - D). The photochemical quenching parameter (qP) as well as the effective PSII yield (Φ_{PSII}) were decreased at 5 and 45 $\mu\text{E m}^{-2} \text{s}^{-1}$ red actinic light in $\Delta\text{psbTc-1-3}$ mutant plants (Fig. 4A and C), indicating a partial loss of PSII function. Nonphotochemical quenching (NPQ) was also significantly lower at both light intensities amounting to only about 50% in the mutants as compared to the WT at red light intensity of 45 $\mu\text{E m}^{-2} \text{s}^{-1}$ indicating a decreased transmembrane proton gradient due to lower PSII activity (Fig. 4B). The PSI oxidation state at 5 and 45 $\mu\text{E m}^{-2} \text{s}^{-1}$ red light intensities was about sevenfold and fourfold higher, respectively, in $\Delta\text{psbTc-1-3}$ as compared to WT (Fig. 4D). Since NPQ is significantly decreased at both light intensities the increased oxidation level of P700 can be solely attributed to a lower capacity of electron transfer from PSII to the PQ pool in the mutants. This inference is supported by steady-state fluorescence measurements (F_s') elicited by 650 nm actinic light at an intensity of 34 $\mu\text{E m}^{-2} \text{s}^{-1}$ on far-red background light (12 W m^{-2}). The ratio $F_s' \Delta\text{psbTc-1}/F_s' \text{WT}$ was 0.77, illustrating that the rate of electron flow towards plastoquinone is lower than that from plastoquinol to the electron sink *via* PSI in the mutant. The results above are also supported by a lowered PSII activity ranging from 65 to 76% in three mutant plants as compared with WT thylakoids measured as O_2 evolution under saturating light conditions in the presence of uncouplers.

Electron flow within PSII as measured by thermoluminescence

Thermoluminescence (TL) measurements were performed to further investigate the effect of *psbTc* inactivation on electron flow within PSII. Activation energy required for back electron flow from Q_B^- to the $\text{S}_{2,3}$ states of the Mn_4Ca donor side of PSII via P_{680}^+ charge recombination is supplied by temperature rise and accompanied by light emission. The temperature at which recombination and light emission are maximal is related to the redox potential difference between the recombining charge separated pairs and thus to the energy input required to drive the back electron flow (Krieger-Liszkay and Rutherford, 1998; Rutherford and Krieger-Liszkay, 2001). Charge

recombination between Q_B^- and oxidised states of S_2 or S_3 occurs at about 35°C. The luminescence emission appearing at this temperature is designated as B band (Schwenkert *et al.*, 2006; Ducruet *et al.*, 2007). Blocking electron flow to the Q_B site results in back electron flow from Q_A^- and charge recombination with the $S_{2/3}$ state resulting in the Q band emission. Due to the lower energy gap between these recombining pairs, the Q band temperature occurs at about 3 - 5°C. This is the case when phenolic type herbicides, such as loxynil, bind at the Q_B site (Krieger-Liszkay and Rutherford, 1998; Cser and Vass, 2007; Umate *et al.*, 2007). However, binding of urea-type herbicides such as 3-(3,4-dichlorophenyl)-1,1-dimethylurea (DCMU) affects the Q_B site conformation, and thus alters its interaction with the Q_A site resulting in a decrease of the $Q_A:Q_A^-/Q_B^-:Q_B$ redox potential gap and thus an up-shift of the required energy input to drive back electron flow that occurs at 12 - 15°C (Krieger-Liszkay and Rutherford, 1998; Rutherford and Krieger-Liszkay, 2001; Ohad *et al.*, 2004).

The B band emission temperature was up-shifted to about 38 - 42°C (Fig. 5A) while the Q band temperature emitted in the presence of DCMU was strongly down-shifted to about 3°C in mutant thylakoids (Fig. 5A). The TL emission temperature in the presence of loxynil also shows a severe downshift of the Q band emission temperature to -10°C in $\Delta psbTc-1$ and $\Delta psbTc-2$ (Fig. 5B). Strikingly, the concentration of loxynil (5 μ M) that is sufficient to saturate the Q_B site in WT thylakoids, resulting only in emission of the Q band at 3°C, does not completely abolish the B band emission in the mutant, which shows an increase in Q band and a decrease of the B band emission intensity with increasing loxynil concentration up to 20 μ M (Fig. 5B). These results demonstrate that the absence of PsbTc induces significant conformational changes with respect to the Q_A and Q_B site properties.

The oxidation/reduction of the Mn_4Ca cluster usually occurs with a period of four stable steps (S_0 - S_3) during oxygen evolution (Haumann *et al.*, 2005) while that of the Q_B site occurs in two steps, Q_B and Q_B^- . Following transition from light to darkness, back electron flow from the reduced electron carriers of PSII (pheophytin $^-$, Q_A^- and Q_B^-) occurs resulting in accumulation of about 25% S_0 and 75% S_1 states and a 1/1 ratio of Q_B^-/Q_B (Rutherford *et al.*, 1982 and 1984; Krieger-Liszkay and Rutherford, 1998; Umate

et al., 2007). The intensity of TL B band emission of dark-adapted tobacco thylakoids, following single turnover excitations (1 to 6 flashes), is proportional to the number of recombining $Q_B^-/S_{2,3}$ pairs and oscillates with the number of exciting single turnover flashes with maximal emission at flashes 2 and 6 in WT (Umate *et al.*, 2007). Since deletion of PsbTc shows drastic effects on the Q_A/Q_B site interactions and charge recombination, one would expect changes also in the oscillation pattern of the B band emission with the number of excitation flashes. Results of experiments addressing this question indeed showed an alteration of the TL B band oscillation patterns for $\Delta psbTc-1$ and $\Delta psbTc-2$ exhibiting emission maxima at flash 1 and 5 (Fig. 5C). Using a simulation program for oscillation patterns (Umate *et al.*, 2007), the ratio Q_B/Q_B^- present in dark-adapted thylakoids prior to the flash excitations was significantly increased in $\Delta psbTc-1$ (1.68 vs. 0.90 in the WT) (Supplemental Table 1). These results support the conclusion that the back electron flow within PSII is altered in the mutant presumably because of alterations of the Q_B binding site properties.

Effect of the mutation on redox-controlled phosphorylation of LHCII and PSII core proteins

Plants have developed several mechanisms to efficiently adjust their energy conversion to different light qualities and quantities. Shifting their antenna from one photosystem to the other (state transition) allows optimal adaptation to changing light conditions. Thus, phosphorylation and dephosphorylation of a mobile pool of CP29, CP26, and LHCII are induced under light, which preferentially excites PSII (state II) and PSI (state I), respectively (Rochaix, 2007). Regulation of phosphorylation of the D1, D2, and CP43 proteins is less understood. Therefore, phosphorylation and antenna association experiments have been performed (Fig. 6A and B). Strikingly, in the absence of PsbTc, the PSII core proteins D1/D2 were not phosphorylated and CP43 was only marginally phosphorylated under both state I and state II conditions in all three mutant lines (Fig. 6A and Supplemental Fig. 1C). On the other hand, in contrast to WT, LHCII was already highly phosphorylated in darkness and dephosphorylated under

state II light conditions in $\Delta psbTc$ -1-3. To check whether phosphorylation in the mutants results from a reduced plastoquinone pool in darkness, state I conditions were adjusted with far red light. This light treatment abolished LHCII phosphorylation in both WT and mutant plants (Fig. 6A). Mild solubilization of thylakoids with digitonin and separation of lysates by BN-PAGE allows the detection of LHCII-PSI supercomplexes under state II light conditions in WT (Schwenkert *et al.*, 2007). In contrast, in the mutant LHCII-PSI supercomplexes were formed only in darkness, consistent with the phosphorylation pattern and the reduced state of the plastoquinone pool (Fig. 6B, upper panel). The composition of the bands representing the LHCII-PSI supercomplex was also demonstrated by immunoblot analysis of the native gel using antibodies raised against LHCII and PsaA/B (Fig. 6B, lower panels). These data indicate a role of the PSII protein PsbTc in oxidation of reduced plastoquinone in the dark.

The Q_B binding site is required for oxidation of PQH₂ in the dark

Reduction of plastoquinone takes place via several non-photochemical pathways and re-oxidation often depends on oxygen (reviewed in Rumeau *et al.*, 2007). A prominent functional effect of the mutation seems to be an alteration in the role of the Q_B binding site important for efficient forward electron flow in the light and presumably re-oxidation of the plastoquinone pool, that is reduced by non-photochemical reduction in darkness. Were this true, inhibition of the Q_B site with DCMU or Ioxynil in the WT should prevent plastoquinol oxidation even in the presence of O₂ in the dark. In order to check this assumption, WT leaves were first treated with far red light for one hour to allow complete oxidation of plastoquinol and dephosphorylation of LHCII (Fig. 6C). Subsequently leaves were incubated in the dark over night under aerobic and anaerobic conditions. In the presence of O₂ LHCII remained in a dephosphorylated state, indicating that PQ remains oxidized. In contrast, in the absence of O₂ phosphorylation of both LHCII and CP29 was increased, indicative of a reduced PQ pool. DCMU or Ioxynil was added one hour after far red light treatment and leaves were maintained in strict darkness. Indeed, using both inhibitors LHCII and CP29 were highly

phosphorylated after 12 hours dark incubation even under aerobic conditions (Fig. 6C). Since binding of loxynil does not change the Q_B site conformation it is unlikely that phosphorylation of antenna proteins under aerobic conditions is due to structural changes within PSII allowing easier access of the corresponding kinase(s) to the target. Therefore, we conclude that the Q_B binding site is directly involved in the oxidation of PQH₂ in an oxygen dependent manner. Accordingly, our data indicates that presence of PsbTc is directly or indirectly required to keep the Q_B site in proper conformation for the re-oxidation of PQH₂.

DISCUSSION

Effect of PsbTc deletion on assembly, stability, and structure of PSII

Studies on PsbTc deletion mutants were reported from *Synechocystis* 6803 (Iwai *et al.*, 2004) and two *Thermosynechococcus* species (Henmi *et al.*, 2008) representing eubacterial organisms, and from *Chlamydomonas reinhardtii* (Monod *et al.*, 1994; Ohnishi and Takahashi, 2001; Ohnishi *et al.*, 2007). Data obtained with *Thermosynechococcus* suggested that PsbTc is involved in the assembly of dimeric PSII complexes. However, since deletion of *psbTc* in the *Chlamydomonas* mutant resulted only in a weakly impaired PSII, it was concluded that this protein is not essential for the organization and function of PSII. Solubilization studies of proteins labeled *in vivo* indicate that PsbTc in tobacco is not required for the assembly but rather for the stability of the dimeric PSII core (Fig. 2B and C).

The absence of PSII-LHCII assemblies in $\Delta psbTc$ -1-3 is intriguing since PsbTc has been placed to the region interconnecting PSII monomers next to the central two-fold axis (Ferreira *et al.*, 2004; Loll *et al.*, 2005). From its outlined function and position, PsbTc could be involved in the attachment of the outer antenna, possibly through interaction with adjacent proteins, like CP47, and therefore, exerts a long distance effect.

The proposed positions of PsbTc, PsbL, and PsbM close to the central axes of the PSII dimer previously suggested that these LMWs are involved in dimerisation (Ferreira *et al.*, 2004; Nield and Barber, 2006). However, PsbI has been shown to represent a component required for formation of the dimer presumably by forming a 'bracket' (Schwenkert *et al.*, 2006), whereas apparently neither PsbTc nor PsbM are essential for PSII dimer assembly. Loss of PsbTc may affect the function and/or conformation of other adjacent proteins, like PsbL. However, $\Delta psbL$ knockouts are clearly distinct from $\Delta psbTc$ plants with respect to photoautotrophic growth, assembly of PSII dimers, photosynthetic performances, and levels of PSII proteins indicating that neither function nor localization of PsbL are impaired in $\Delta psbTc$ knock out plants (Ohad *et al.*, 2004). We cannot rule out that loss of PsbTc causes removal of PsbM, since the corresponding mutant also shows a 1/5 B band oscillation type and increased LHCII phosphorylation in the dark (Umate *et al.*, 2007). However, phosphorylation of CP43 and recovery of PSII from photoinhibition is not affected in $\Delta psbM$ indicating that major deficiencies are due to $\Delta psbTc$ inactivation. It is intriguing that specific deletions of the predictably closely located proteins PsbTc, PsbL, and PsbM result in quite diverse phenotypes in higher plants (Ohad *et al.*, 2004; Umate *et al.*, 2007).

Lack of PsbTc results in increased D1 degradation

Increased rates of PSII-mediated plastoquinone reduction exceeding plastoquinol oxidation results in an increased back electron flow and charge recombination causing damage to PSII core proteins (Keren *et al.*, 1997; Zer and Ohad, 2003; Vass *et al.*, 2007). Only under strong illumination PSII activity and D1 levels were reduced in the *Chlamydomonas* mutant. In contrast to the data obtained with tobacco mutants photosensitivity and D1 degradation in presence of CAP was apparently not changed in the *Chlamydomonas* mutant suggesting that PsbTc may not be relevant for photoprotection but required for an efficient recovery of photodamaged PSII in the algae (Ohnishi and Takahashi, 2001). Furthermore, PsbTc appeared to be involved in the activation of forward Q_A electron flow during repair of PSII from photoinhibition in

C. reinhardtii (Ohinishi *et al.*, 2007). Photosensitivity is more striking with translation inhibitors in $\Delta psbTc$ tobacco plants than without. The net difference of photoinhibition with and without inhibitors as indicator of recovery is the same in WT and mutant plants. This indicates that mutant plants are capable to repair from photoinhibition although delayed when compared to the WT suggesting a similar function of PsbTc in Q_A activation during the repair process in tobacco.

Although the function of PsbTc in different organisms is similar some species-specific features may reflect adaptations to their ecophysiological niches. Yet, it is conceivable that light sensitivity in tobacco might represent a secondary effect of the mutation since facilitated back electron flow results in increased rates of charge recombination and related oxidative damage in $\Delta psbTc$.

Effect of PsbTc deletion on Q_A and Q_B Site properties and PSII electron flow

The conformational changes in the organization of PSII induced by the loss of PsbTc affect Q_A and Q_B site properties and/or interaction resulting in an increased ratio Q_B/Q_B^- and alterations in the PSII charge recombination as judged from TL measurements. This indicates that there are more oxidized Q_B sites than semiquinones in the mutant causing an impaired back electron flow and reduction of the PQ pool in dark-adapted PSII populations. However, it still remains controversial which plastoquinone-binding site is largely or directly affected by the absence of PsbTc, because both peaks of Q and B bands in transformants plants were shifted compared with those of WT plants. Due to the closer vicinity of PsbTc to Q_A it is conceivable that conformational changes at the Q_A site may affect its interaction with the Q_B site. Therefore, the effect on the Q_B site could well represent a secondary effect of the mutation as has also been implicated for the long distance effect on the assembly of PSII-LHCII supercomplexes and stability of PSII dimers in $\Delta psbTc$.

The increase in the B band emission temperature and down-shift of the Q band also implies an increase in the redox potential gap between the Q_A/Q_B sites and a decrease of the pheophytin/ Q_A redox potential gap, thus lowering the forward electron flow and

promoting charge recombination by back electron flow from Q_A . This is supported by a decreased photosystem II dependent electron transport capability, measured as O_2 evolution rate, in $\Delta psbTc$ to about 72% of WT levels.

PsbTc deletion alters the redox-state of the PQ Pool and phosphorylation of PSII proteins

It is well established that association of LHCII, CP26, and CP29 with PSII and partially with PSI (state I and state II, respectively) is regulated *via* reversible phosphorylation of the chlorophyll a/b binding apoproteins (Kargul and Barber, 2008). Activation of the respective kinase(s) is regulated by interaction of reduced plastoquinone with the oxidation site of the cytochrome b_6f complex (Vener *et al.*, 1997). The orthologous protein kinases, STT7 and STN7 in *Chlamydomonas* and *Arabidopsis*, respectively, are involved in the regulation of phosphorylation of LHCII, CP26, and CP29 although the primary targets of the kinases still remains unknown (Rochaix, 2007).

In this study it could be shown that accumulation of reduced PQ leads to phosphorylation of LHCII in darkness in $\Delta psbTc$ mutant plants. Moreover, BN-PAGE analysis revealed that LHCII is not only phosphorylated but also attached to PSI in dark-adapted mutant plants. Apparently no light-induced signals cause migration of the LHCII antenna to PSI in the mutant. Therefore, the data uncover a new level of control of LHCII phosphorylation in darkness.

Although the related protein kinase, STN8, triggers phosphorylation of all three PSII core proteins, D1, D2 and CP43 (reviewed in Vener, 2006), phosphorylation of D1/D2 proteins is considerably more responsive than that of CP43 to redox regulation in tobacco WT plants (Fig. 6A; Umate *et al.*, 2007) indicating that additional kinases could be involved in PSII core proteins phosphorylation. Phosphorylation of outer antenna proteins and presumably of PSII core proteins is affected not only by activation/deactivation of respective protein kinase(s) but also by the exposure of segments of substrates containing phosphorylation sites at thylakoid membrane surfaces, and thus on their accessibility to the active site of the respective protein

kinase(s) (Vink *et al.*, 2000; Zer *et al.*, 1999 and 2003). Phosphorylation of the core proteins CP43, D1, and D1 is almost completely abolished in $\Delta psbTc$ under all light conditions. The same has been described for $\Delta psbI$ in tobacco (Schwenkert *et al.*, 2006). As both mutants lack stable PSII-LHCII supercomplexes it is likely that accessibility for the kinase(s) that phosphorylate PSII core proteins is blocked by structural changes of the PSII dimer in the mutants. In contrast, alterations of phosphorylation patterns of PSII antenna proteins are likely due to physiological consequences rather than structural changes. The effect of PsbTc knockouts on phosphorylation of PSII core and antenna proteins is unknown from other organisms and it would be challenging to check whether lack of PsbTc in *Chlamydomonas* induces similar effects.

Non-photochemical reduction and re-oxidation of plastoquinone takes place via several pathways (reviewed in Rumeau *et al.*, 2007). The plastid terminal plastoquinone oxidase (PTOX) has been suggested to be involved in re-oxidation of reduced plastoquinone. Alternatively, re-oxidation of the PQH₂ pool may be mediated by charge recombination with Q_B and probably subsequently with cytochrome *b*₅₅₉ (Bondarava *et al.*, 2003). Impaired re-oxidation of plastoquinol could account for LHCII phosphorylation in darkness in $\Delta psbTc$ plants. Finally, we provide evidence that PsbTc stabilizes the Q_B binding site *in vivo* that is essential for oxidation of reduced plastoquinone in darkness in an oxygen dependent manner, possibly to keep the PSII acceptor side oxidized. Our data suggest that predominantly the PSII dependent oxidation of PQH₂ in darkness controls the redox state of the plastoquinone pool. Therefore, this effect is prevalent when compared with other activities known to oxidize plastoquinol, like the PTOX localized in stroma lamellae (Rumeau *et al.*, 2007), or with a non-enzymatic PQH₂ oxidation. We postulate that PSII could represent the hitherto unidentified major terminal oxidase involved in chlororespiration in leaves (Nixon, 2000, Bennoun, 2002). A protective role of PSII mediated O₂ reduction and plastoquinol oxidation in the light driven electron transport to avoid over-reduction of plastoquinone and harmful charge recombination leading to damage of PSII remains to be shown.

MATERIALS AND METHODS

Vector construction and plant transformation

The plastid *psbTc* gene was inactivated by targeted disruption with a selectable terminator-less chimeric *aadA* cassette conferring spectinomycin resistance (Koop *et al.*, 1996). The cassette was inserted in the orientation of the operon (Fig. 1). Using a PCR-based site-directed mutagenesis approach, a diagnostic *HpaI* restriction site was generated at the 5' region of *psbTc* with the oligonucleotides *psbTcmut2* for 5'-atc tat gga agc att ggt taa cac att cct ctt agt ctc gac-3' and *psbTcmut1rev* 5'-gtc gag act aag agg aat gtg tta acc aat gct cca tag at-3'. The DNA fragment amplified using the oligonucleotides *psbTc* for 5'-ttc tac ggc ggt gaa ctc aac g-3' and *psbTcrev* 5'-tcctaccgcagttcgtcttgga-3' was inserted into a pDrive cloning vector (QIAGEN, Hilden, Germany) to produce plasmid p Δ Tc (Fig. 1A). The chimeric *aadA* gene cassette was excised as a 916 bp *SmaI-HindIII* fragment, blunted and ligated into the *HpaI* site of p Δ Tc. *Nicotiana tabacum* cv. Petit Havana plastids were transformed essentially as described (Svab *et al.*, 1990). Selection, culture conditions of the transformed material and assessment of the homoplasmic state of transformed lines was carried out as described (Swiatek *et al.*, 2003b), using the oligonucleotides 5'-tactttgaaatccgatggtg-3' and 5'-ctc caa aat aat aga tag aaa tac c-3' (Fig. 1B). All seven independent transformants obtained showed the same phenotype with respect to the Fv/Fm ratio ranging between 0.65 and 0.71. Three lines, Δ *psbTc*-1-3, were selected for further studies on photosynthetic performances, assembly, photosensitivity, and phosphorylation patterns of PSII proteins (Figs. 2 - 6; Supplemental Fig. 1).

Northern blot analysis

Northern analysis was performed as described (Lezhneva and Meurer, 2004) using either radio-labeled DNA probes or end labeling of specific oligonucleotides with T4 polynucleotide kinase (Biolabs New England, USA). Strand specific end labeling was performed for *psbT*, *psbH* and *psbN* with the oligonucleotides 5'-ggc ggt tct cga aaa aag ata gcg aa aaa aat tat ccc tag agt cga gac taa gag gaa tgt ata aac caa tgc ttc cat-3', 5' ttc

aat ggt ttt aat aaa tct cct acc gca gtt cgt ctt gga cca gat cta gaa ctg ttt tca aca gtt tgt gta gcc at-3' and 5'-cta gtc tcc atg ttc ctc gaa tgg atc tct tag ttg ttg aga agg ttg ccc aaa agc ggt ata taa gg cgt acc cag taa-3', respectively. The *petB* and *psbB* probes were amplified with the oligonucleotides 5'-gca ttg tat att tcc gga ata tga gta aag-3', 5'-cgt tct tcg aac caa tca taa act tta ctc-3', and 5'-ttg ttc cgg gag gaa tag cct-3', 5'-gcc agt cca gca cta act ctt cg-3', respectively (Fig. 1C).

Preparation of thylakoid membranes, SDS-PAGE and immunoblot analysis

Thylakoid membrane proteins were isolated, separated by SDS-PAGE and subjected to immunoblot analysis as described (Umate *et al.*, 2007).

Sucrose density gradients

Thylakoid membrane complexes were separated by sucrose gradient centrifugation using four-week-old *in vitro*-grown plants (10 - 20 $\mu\text{E m}^{-2} \text{s}^{-1}$ light intensity; 12 h photoperiod) as described (Schwenkert *et al.*, 2006).

Blue native polyacrylamide gel electrophoresis

BN-PAGE was performed as described earlier (Schwenkert *et al.*, 2007). Thylakoid fractions were solubilized either with 1% β -DM or 1.5% digitonin. Lysates were separated on a 4 - 12% polyacrylamide gel. Proteins were either transferred onto PVDF membranes or gel lanes were excised and run on a second dimension using 15% SDS-PAGE. *In vivo* labeling was performed using ^{35}S -methionine (Schwenkert *et al.*, 2006).

Thylakoid protein phosphorylation assay

State I conditions were adjusted by either keeping plants in darkness for 24 h or treatment with light at 728 nm (PSI light) of 20 $\mu\text{E m}^{-2} \text{s}^{-1}$ for 30 min. For state II conditions leaves were illuminated with light at 650 nm (PSII light) of 45 $\mu\text{E m}^{-2} \text{s}^{-1}$ for

30 min. All buffers used for thylakoid preparations contained 10 mM NaF. Phosphorylated proteins were detected using anti-phosphothreonine antisera (Biolabs New England, USA). Anaerobic conditions were generated by placing leaves in a humid screw-cap vial flushed for 10 min with pure Argon at room temperature.

PSII quantum yield and fluorescence quenching analysis

A Pulse Amplitude Modulated Fluorimeter (PAM-101, Waltz, Effeltrich, Germany) was used to study chlorophyll *a* fluorescence kinetics. Leaves dark-adapted for not less than 5 min were used for measurements. Red actinic light (650 nm, 5 and 45 $\mu\text{E m}^{-2} \text{s}^{-1}$) was used for measurements of fluorescence parameters. The maximum quantum yield of PSII was determined as $(F_m - F_o)/F_m = F_v/F_m$ and the effective quantum yield of PSII, Φ_{PSII} , was expressed as $F_m' - F_s'/F_m'$ (Genty *et al.*, 1989). Photochemical (qP) and non-photochemical (NPQ) quenching were determined by repetitive saturation pulses. The quenching coefficients, NPQ and qP were calculated as $(F_m - F_m')/F_m'$ and $(F_m' - F)/(F_m' - F_o)$, respectively (van Kooten and Snel, 1990).

Photosystem I activity

Photosystem I activity was investigated on leaves as absorption changes of PSI at 830 nm induced by far red light (ΔA_{max}) and actinic light (ΔA) using the PSI attachment of PAM101 (Walz, Effeltrich, Germany). The redox condition of PSI at indicated light intensities was expressed as the ratio $\Delta A/A_{\text{max}}$ (Klughammer and Schreiber, 1994).

Oxygen evolution measurements

Photosystem II electron transport activity was determined using a Clark-type oxygen electrode as described (Umate *et al.*, 2007). In order to measure exclusively PSII dependent electron transport, the PSII specific electron acceptor *p*-benzoquinone as well as the uncouplers NH_4Cl (5 mM) and gramicidin (3 μM) were used under saturating light conditions.

Thermoluminescence measurements

Thermoluminescence measurements of thylakoids were measured using a home-built apparatus as described (Schwenkert *et al.*, 2006). The Q band emission resulting from Q_A^-/S_2 charge recombination was measured by blocking electron flow to Q_B with the addition of DCMU (10 μM) or loxynil (5, 10 and 20 μM) during dark adaptation. Concentrations of loxynil higher than 20 μM were avoided due to high fluorescence quenching induced by this herbicide.

A computer-based simulation program allowing the prediction of S-states ratio and the occupancy ratio Q_B/Q_B^- was employed. The program simulates predicted oscillation profiles and checks for the correlation between simulated and measured values (Umate *et al.*, 2007).

PSII photoinactivation and recovery kinetics

The sensitivity of PSII to oxidative stress was determined using leaf discs of WT and $\Delta psbTc$ plants exposed to 1,200 $\mu\text{E m}^{-2} \text{s}^{-1}$ heterochromatic light. Photoinactivation of PSII was measured as changes in the Fv/Fm parameter as a function of exposure time. To estimate the contribution of the PSII recovery process during treatment with high light, leaf discs were infiltrated with a solution of CAP (200 $\mu\text{g ml}^{-1}$) in darkness for 30 min prior to exposure to high light. To assess photoinhibition kinetics and capacity to recover PSII activity, leaf discs were exposed in absence of CAP pre-treatment to high light (1,200 $\mu\text{E m}^{-2} \text{s}^{-1}$) until an Fv/Fm of 0.17 was reached in WT and $\Delta psbTc$ and then allowed to recover PSII activity by lowering the light intensity to 3 $\mu\text{E m}^{-2} \text{s}^{-1}$ for up to 6 h, measuring the Fv/Fm level every 1 h.

ACKNOWLEDGEMENTS

We wish to acknowledge Noam Adir, Technion Institute, Haifa, Israel, for helpful discussions and Dario Leister for kindly reading the manuscript.

LITERATURE CITED

1. Barkan A (1988) Proteins encoded by a complex chloroplast transcription unit are each translated from both monocistronic and polycistronic mRNAs. *EMBO J* 7: 2637–2644
2. Bondarava N, De Pascalis L, Al-Babili S, Goussias C, Golecki JR, Beyer P, Bock R, Krieger-Liszkay A (2003) Evidence that cytochrome *b₅₅₉* mediates the oxidation of reduced plastoquinone in the dark. *J Biol Chem* 278: 13554–13560
3. Cser K, Vass I (2007) Radiative and non-radiative charge recombination pathways in Photosystem II studied by thermoluminescence and chlorophyll fluorescence in the cyanobacterium *Synechocystis* 6803. *Biochim Biophys Acta* 1767: 233–243
4. Dekker JP, Boekema EJ (2005) Supramolecular organization of thylakoid membrane proteins in green plants. *Biochim Biophys Acta* 1706: 12–39
5. Ducruet JM, Peeva V, Havaux M (2007) Chlorophyll thermofluorescence and thermoluminescence as complementary tools for the study of temperature stress in plants. *Photosynth Res* 93: 159–171
6. Ferreira KN, Iverson TM, Maghlaoui K, Barber J, Iwata S (2004) Architecture of the photosynthetic oxygen-evolving center. *Science* 303: 1831–1837
7. Genty B, Briantais JM, Baker NR (1989) The relationship between the quantum yield of photosynthetic electron transport and quenching of chlorophyll fluorescence. *Biochim Biophys Acta* 990: 87–92
8. Haumann M, Liebisch P, Muller C, Barra M, Grabolle M, Dau H (2005) Photosynthetic O₂ formation tracked by time-resolved x-ray experiments. *Science* 310: 1019–1021
9. Henmi T, Iwai M, Ikeuchi M, Kawakami K, Shen JR, Kamiya N (2008) X-ray crystallographic and biochemical characterizations of a mutant photosystem II complex from *Thermosynechococcus vulcanus* with the *psbTc* gene inactivated by an insertion mutation. *J Synchrotron Radiat* 15:304-307
10. Iwai M., Katoh H, Katayama M, Ikeuchi M (2004) PSII-Tc protein plays an important role in dimerization of photosystem II. *Plant Cell Physiol* 45: 1809–1816.
11. Kargul J, Barber J. (2008) Photosynthetic acclimation: structural reorganisation of light harvesting antenna--role of redox-dependent phosphorylation of major and minor chlorophyll a/b binding proteins. *FEBS J* 275: 1056-1068
12. Kamiya N, Shen JR (2003) Crystal structure of oxygen evolving photosystem II from *Thermosynechococcus vulcanus* at 3.7-Å resolution. *Proc Natl Acad Sci USA* 100: 98–103

13. Keren N, Berg A, van Kan PJ, Levanon H, Ohad I (1997) Mechanism of photosystem II photoinactivation and D1 protein degradation at low light: The role of back electron flow. *Proc Natl Acad Sci USA* 94: 1579–1584
14. Klughammer C, Schreiber U (1994) An improved method, using saturating light pulses, for the determination of photosystem I quantum yield via P700⁺-absorbance changes at 830 nm. *Planta* 192: 261–268
15. Kohchi T, Yoshida T, Komano T, Ohyama K (1988) Divergent mRNA transcription in the chloroplast *psbB* operon. *EMBO J* 7: 885–891
16. Koop HU, Steinmüller K, Wagner H, Rossler C, Eibl C, Sacher L (1996) Integration of foreign sequences into the tobacco plastome via polyethylene glycol-mediated protoplast transformation. *Planta* 199: 193–201
17. Krieger-Liszkay A, Rutherford AW (1998) Influence of herbicide binding on the redox potential of the Quinone acceptor in photosystem II: Relevance to photodamage and phytotoxicity. *Biochemistry* 37: 17339–17344
18. Lezhneva L, Meurer J (2004) The nuclear factor HCF145 affects chloroplast *psaA-psaB-rps14* transcript abundance in *Arabidopsis thaliana*. *Plant J* 38: 740–753
19. Loll B, Kern J, Saenger W, Zouni A, Biesiadka J (2005) Towards complete cofactor arrangement in the 3.0 Å resolution structure of photosystem II. *Nature* 438: 1040–1044
20. Minagawa J, Takahashi Y (2004) Structure, function and assembly of Photosystem II and its light-harvesting proteins. *Photosynth Res* 82: 241–263
21. Monod C, Takahashi Y, Goldschmidt-Clermont M, Rochaix JD (1994) The chloroplast *ycf8* open reading frame encodes a photosystem II polypeptide which maintains photosynthetic activity under adverse growth conditions. *EMBO J* 13: 2747–2754
22. Müh F, Renger T, Zouni A (2008) Crystal structure of cyanobacterial photosystem II at 3.0 Å resolution: A closer look at the antenna system and the small membrane-intrinsic subunits. *Plant Physiol Biochem* 46:238-264
23. Nield J, Barber J (2006) Refinement of the structural model for the Photosystem II supercomplex of higher plants. *Biochim Biophys Acta* 1757: 353–361
24. Ohad I, Dal Bosco C, Herrmann RG, Meurer J (2004) Photosystem II proteins PsbL and PsbJ regulate electron flow to the plastoquinone pool. *Biochemistry* 43: 2297–2308
25. Ohnishi N, Takahashi Y (2001) PsbT polypeptide is required for efficient repair of photodamaged photosystem II reaction center. *J Biol Chem* 276: 33798–33804

26. Ohnishi N, Kashino Y, Satoh K, Ozawa S, Takahashi Y (2007) Chloroplast-encoded polypeptide PsbT is involved in the repair of primary electron acceptor Q_A of photosystem II during photoinhibition in *Chlamydomonas reinhardtii*. *J Biol Chem* 282: 7107–7115
27. Regel RE, Ivleva NB, Zer H, Meurer J, Shestakov SV, Herrmann RG, Pakarasi HB, Ohad I (2001) Deregulation of electron flow within photosystem II in the absence of PsbJ protein. *J Biol Chem* 276: 41473–41478
28. Rochaix JD (2007) Role of thylakoid protein kinases in photosynthetic acclimation. *FEBS Lett* 58: 2768–2775
29. Rumeau D, Peltier G, Cournac L (2007) Chlororespiration and cyclic electron flow around PSI during photosynthesis and plant stress response. *Plant Cell Environ* 30: 1041–1051
30. Rutherford AW, Krieger-Liszkay A (2001) Herbicide-induced oxidative stress in photosystem II. *Trends Biochem Sci* 26: 648–653
31. Rutherford AW, Crofts AR, Inoue Y (1982) Thermoluminescence as a probe of photosystem II photochemistry; the origin of the flash-induced glow peaks. *Biochim Biophys Acta* 682: 457–465
32. Rutherford AW, Govindjee, Inoue Y (1984) Charge accumulation and photochemistry in leaves studied by thermoluminescence and delayed light emission. *Proc Natl Acad Sci USA* 81: 1107–1111
33. Schwenkert S, Legen J, Takami T, Shikanai T, Herrmann RG, Meurer J (2007) Role of the low-molecular-weight subunits PetL, PetG, and PetN in assembly, stability, and dimerization of the cytochrome *b₆f* complex in tobacco. *Plant Physiol* 144: 1924–1935
34. Schwenkert S, Umate P, Dal Bosco C, Volz S, Mlčochová L, Zoryan M, Eichacker LA, Ohad I, Herrmann RG, Meurer J (2006) PsbI affects the stability, function and phosphorylation patterns of photosystem II assemblies in tobacco. *J Biol Chem* 281: 34227–34238
35. Shi L-X, Schröder WP (2004) The low molecular mass subunits of the photosynthetic supracomplex, photosystem II. *Biochim Biophys Acta* 1608: 75–96
36. Svab Z, Hajdukiewicz P, Maliga P (1990) Stable transformation of plastids in higher plants. *Proc Natl Acad Sci USA* 87: 8526–8530
37. Swiatek M, Kuras R, Sokolenko A, Higgs D, Olive J, Cinque G, Müller B, Eichacker LA, Stern DB, Bassi R, Herrmann RG, Wollmann FA (2001) The chloroplast gene *ycf9*

- encodes a Photosystem II (PSII) core subunit, PsbZ, that participates in PSII supramolecular architecture. *Plant Cell* 13: 1347–1367
38. Swiatek M, Regel RE, Meurer J, Wanner G, Pakarasi HB, Ohad I, Herrmann RG (2003a) Effects of selective inactivation of individual genes for low-molecular-mass subunits on the assembly of photosystem II, as revealed by chloroplast transformation: the *psbEFLJ*-operon in *Nicotiana tabacum*. *Mol Genet Genomics* 268: 699–710
 39. Swiatek M, Greiner S, Kemp S, Drescher A, Koop HU, Herrmann RG, Maier R M (2003b) PCR analysis of pulsed-field gel electrophoresis-purified plastid DNA, a sensitive tool to judge the hetero-/homoplastomic status of plastid transformants. *Curr Genet* 43: 45–53
 40. Takahashi H, Iwai M, Takahashi Y, Minagawa J (2006) Identification of the mobile light-harvesting complex II polypeptides for state transitions in *Chlamydomonas reinhardtii*. *Proc Natl Acad Sci USA* 103: 477–482
 41. Thornton LE, Roose JL, Pakrasi HB, Ikeuchi M (2005) The low molecular weight proteins of photosystem II. In: Wydrzynski TJ, Satoh K, eds, *Photosystem II: The Light-Driven Water: Plastoquinone Oxidoreductase*. *Advances in Photosynthesis and Respiration*, Ed 1 Vol 22. Springer, Dordrecht, pp 121-138.
 42. Umate P, Schwenkert S, Karbat I, Dal Bosco C, Mlcòchová L, Volz S, Zer H, Herrmann RG, Ohad I, Meurer J (2007) Deletion of PsbM in tobacco alters the Q_B site properties and the electron flow within photosystem II. *J Biol Chem* 282: 9758–9767
 43. van Kooten O, Snel JFH (1990) The use of chlorophyll fluorescence nomenclature in plant stress physiology. *Photosyn Res* 25: 147-150
 44. Vass I, Cser K, Cheregi O (2007) Molecular mechanisms of light stress of photosynthesis. *Ann N Y Acad Sci* 1113: 114–122
 45. Vener AV (2006) Environmentally modulated phosphorylation and dynamics of proteins in photosynthetic membranes. *Biochim Biophys Acta* 1767: 449–457
 46. Vener AV, van Kan PJ, Rich PR, Ohad I, Andersson B (1997) Plastoquinol at the Q_o-site of reduced cytochrome *bf* mediates signal transduction between light and protein phosphorylation: Thylakoid protein kinase deactivation by a single turnover flash. *Proc Natl Acad Sci USA* 94: 1585–1590
 47. Vink M, Zer H, Herrmann RG, Andersson B, Ohad I (2000) Regulation of Photosystem II core protein phosphorylation at the substrate level: light induces exposure of the CP43 chlorophyll *a* protein complex to the protein kinase(s) *Photosynth Res* 64: 209–221

48. Wagner D, Przybyla D, Op den Camp R, Kim C, Landgraf F, Lee KP, Würsch M, Laloi, C, Nater M, Hideg E, Apel K (2004) The genetic basis of singlet oxygen-induced stress responses of *Arabidopsis thaliana*. *Science* 306: 1183–1185
49. Westhoff P, Herrmann RG (1988) Complex RNA maturation in chloroplasts. The *psbB* operon from spinach. *Eur J Biochem* 171: 51–64
50. Zer H, Ohad I (2003) Light, redox state, thylakoid-protein phosphorylation and signaling gene expression. *Trends Biochem Sci* 28: 467–470
51. Zer H, Vink M, Keren N, Dilly-Hartwig HG, Paulsen H, Herrmann RG, Andersson B, Ohad I (1999) Regulation of thylakoid protein phosphorylation at the substrate level: Reversible light-induced conformational changes exposes the phosphorylation site of the light harvesting complex II (LHCII). *Proc Natl Acad Sci USA* 96: 8277–8282
52. Zer H, Vink M, Shochat S, Herrmann RG, Andersson B, Ohad I (2003) Light affects the accessibility of the thylakoid light harvesting complex II (LHCII) phosphorylation site to the protein kinase(s). *Biochemistry* 42: 728–738
53. Zouni A, Witt HT, Kern J, Fromme P, Krauss N, Saenger W, Orth P (2001) Crystal structure of photosystem II from *Synechococcus elongatus* at 3.8 Å resolution. *Nature* 409:739–743

FIGURES

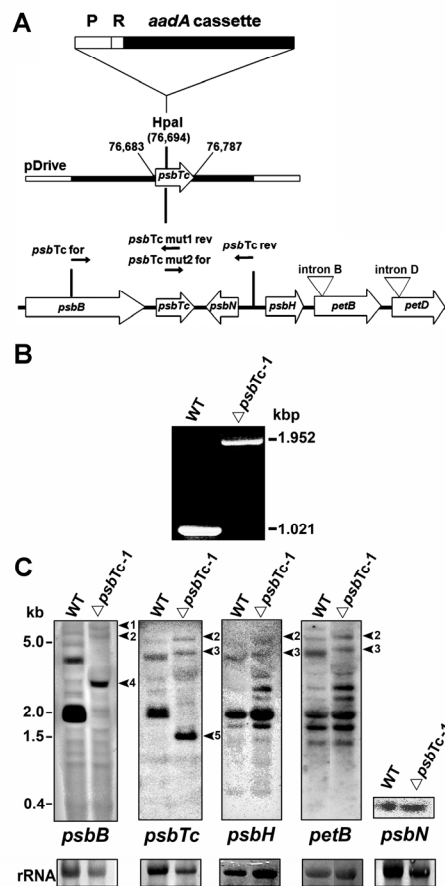


Figure 1: A, Strategy for inactivation of the chloroplast *psbTc* gene. The organization of the *psbB* operon with the genes *psbB*, *psbTc*, *psbH*, *petB*, *petD* and *psbN* on the opposite strand is indicated. Arrows designate the direction of their transcription. The *aadA* selection cassette without termination signal and its 16S rDNA promoter (P) and ribosome-binding site (R) was inserted into the introduced *HpaI* restriction site (plastome position 76,694 bp) of the *psbTc* coding frame (plastome position 76,683 - 76,787 bp). B, PCR products of the *psbTc* region in WT and mutant indicate the homoplasmic state of the insertion. C, Northern analysis of WT and $\Delta psbTc-1$ using double-strand (*petB* and *psbB*) and single-strand probes (*psbTc*, *psbH* and *psbN*). Arrows indicate shifted *psbTc*-containing transcripts confirming the homoplasmic state of the *aadA* insertion. Arrows 1 - 3 correspond to the up-shifted *aadA* containing primary spliced and unspliced transcripts in $\Delta psbTc-1$. Arrows 4 and 5 indicate the up-shifted *psbB-psbTc-aadA* and the appearing *psbTc-aadA* transcript in the mutant, respectively. Ribosomal RNA (rRNA) was stained with methylene blue as a loading control.

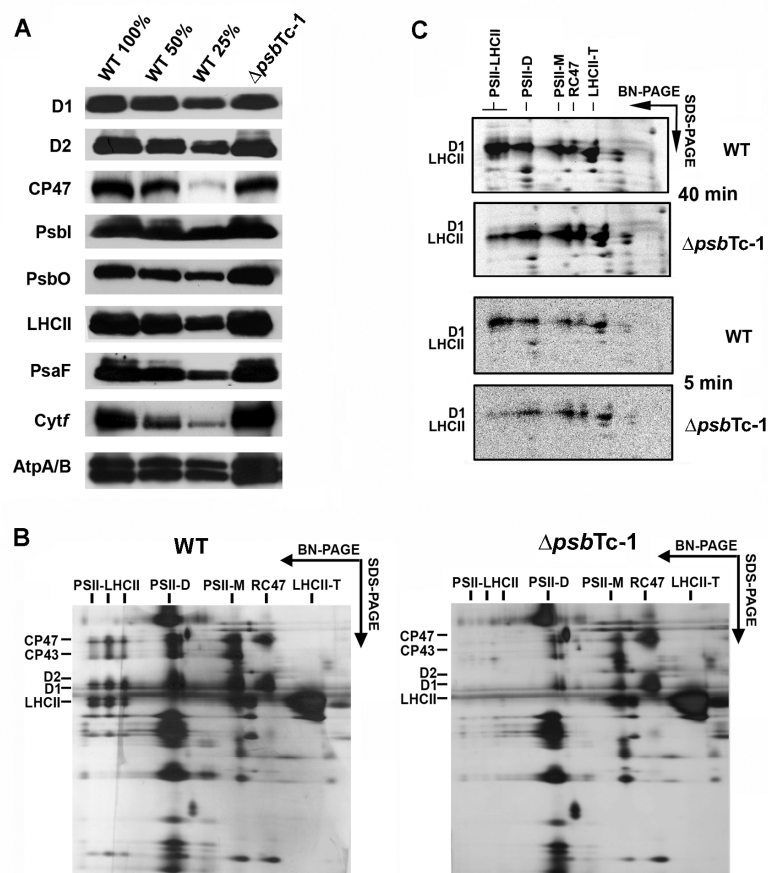


Figure 2: A, Western analysis of WT and $\Delta psbTc-1$ thylakoid proteins. 100% corresponds to 5 μ g chlorophyll. B, Separation of WT and $\Delta psbTc-1$ thylakoid protein complexes by BN-SDS-PAGE. Complexes and silver-stained proteins are labeled according to their identification by mass spectrometry. Comparable results have been obtained from two further independently generated mutant plants (see Supplemental Fig. 1A). D, dimer; M, monomer; T, trimers; RC47, reaction center 47. Note that PSII-LHCII supercomplexes are lacking and levels of PSII dimers are reduced. C, Autoradiograph of *in vivo* radiolabeled thylakoid membrane protein complexes separated of by BN- and SDS-PAGE. Intact leaves labeled for 40 and 5 min showed impaired assembly of PSII-LHCII supercomplexes whereas dimer assembly is not affected in $\Delta psbTc-1$.

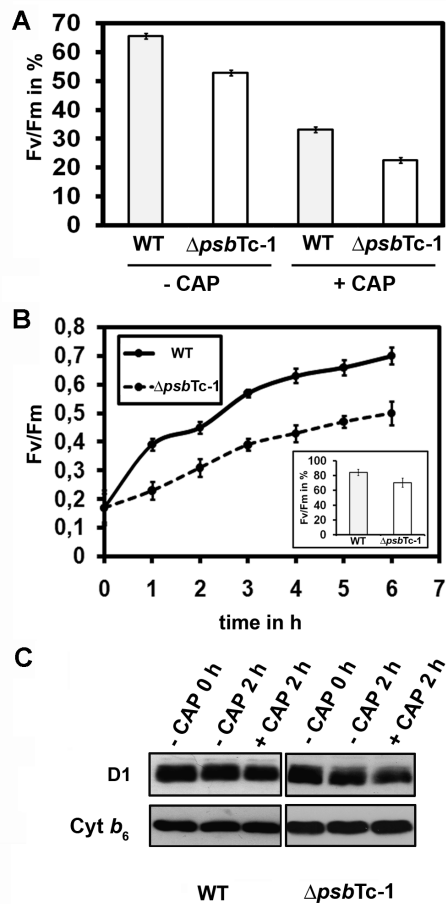


Figure 3: Photoinhibition of PSII and recovery kinetics of high light-treated WT and mutant leaves. A, Loss of quantum yield (Fv/Fm) with and without CAP after exposition to $1,200 \mu\text{E m}^{-2} \text{s}^{-1}$ for 4 h. Fv/Fm ratios are expressed relative to the initial values before starting the experiment in WT (Fv/Fm ~ 0.82) and mutants (Fv/Fm ~ 0.68), respectively (see data of independent transformants in Supplemental Fig. 1B). B, PSII recovery from photoinhibition of WT and $\Delta psbTc-1$ mutant leaves exposed to photoinhibition at $1,200 \mu\text{E m}^{-2} \text{s}^{-1}$ until a ratio Fv/Fm of 0.17 was reached by each sample. PSII recovery was followed by further incubation of the samples at $3 \mu\text{E m}^{-2} \text{s}^{-1}$ for times as indicated. The total recovery after 6 h is depicted as a ratio of Fv/Fm in percentage of the original Fv/Fm in WT and mutant. Error bars in panels (A) and (B) represent SD of at least three independent experiments. C, Immunoblot analysis of WT and $\Delta psbTc-1$ with D1-specific antibodies before (0 h) and after (2 h) photoinhibition at $1,200 \mu\text{E m}^{-2} \text{s}^{-1}$, with and without CAP. Five μg of chlorophyll and equal loading was checked by immunoblot analysis with antibodies raised against cytochrome b_6 .

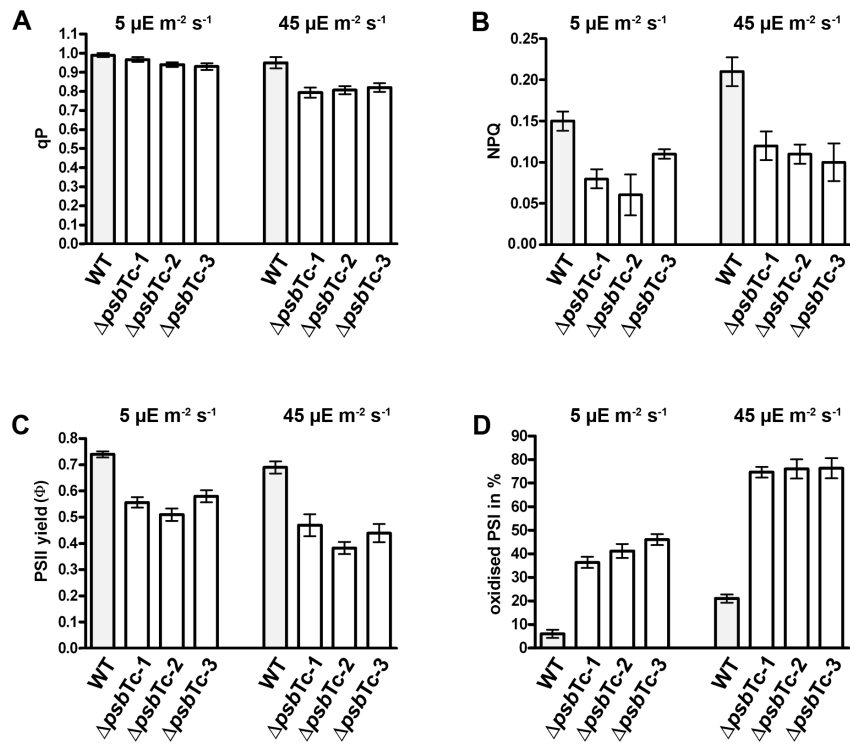


Figure 4: Photosynthetic performances in WT and the three mutant lines $\Delta psbTc-1-3$. Photosynthetic parameters as indicated by A, qP, B, NPQ, C, Φ_{PSII} values, and D, P700 oxidation ratio measured as $\Delta A/\Delta A_{max}$ were calculated from WT and mutant plants kept in the steady state at $5 \mu E m^{-2} s^{-1}$ and $45 \mu E m^{-2} s^{-1}$ red light intensities. Error bars represent SD of at least three independent experiments.

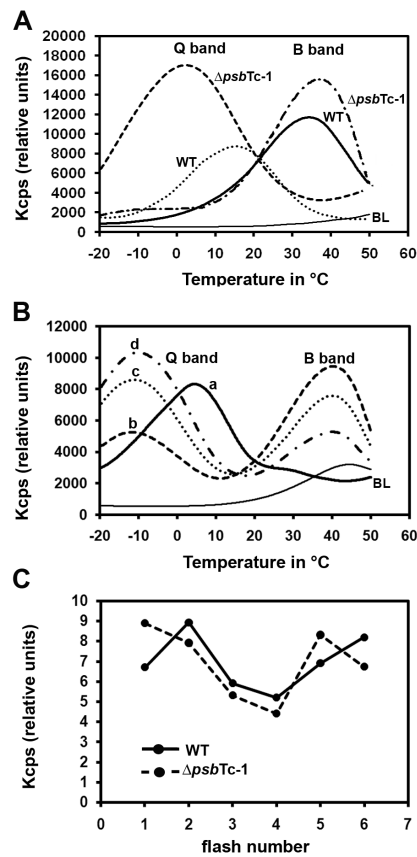


Figure 5: Thermoluminescence measurements of WT and $\Delta psbTc-1$ thylakoids. A, The B band occurring at 35°C in the WT is slightly up-shifted to 38°C in the mutant. The Q band emission in the presence of DCMU (10 μM) occurs at 15°C in WT and at 3°C in $\Delta psbTc$. BL indicates the baseline signal generated from dark-adapted, unexcited samples. B, Q band emission of WT (a = 5 μM loxynil) and $\Delta psbTc-1$ (b = 5 μM , c = 10 μM and d = 20 μM loxynil) thylakoid samples. The Q band emission temperature is downshifted to -10°C at all loxynil concentrations as compared to 3 - 5°C in WT. Note, curves b, c and d depict a persistent B band emission in the presence of loxynil. BL, base line. C, The B band oscillation pattern shows a 1/5 oscillation type in $\Delta psbTc-1$ as compared to the typical 2/6 type for WT. All SDs are below 0.5%. Comparable results were obtained with $\Delta psbTc-2$ plants.

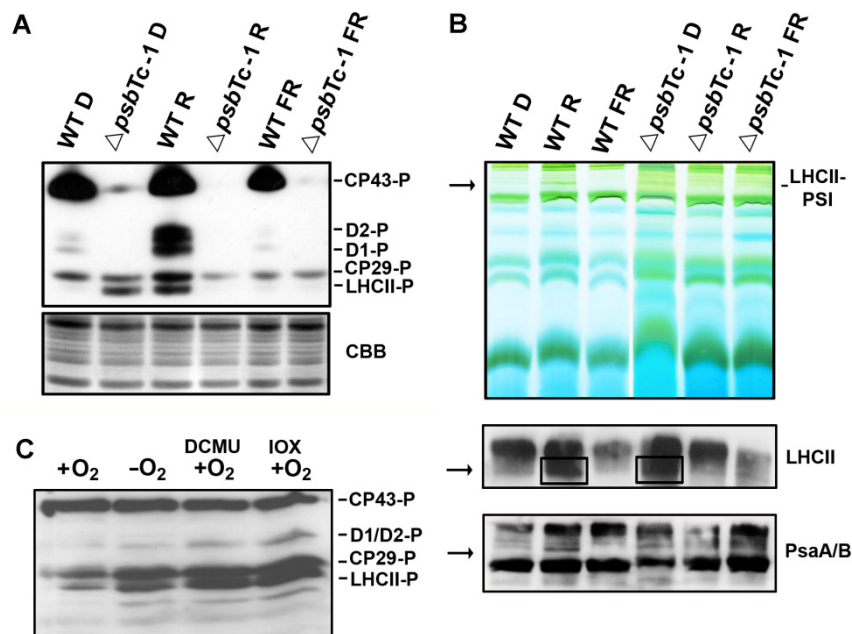
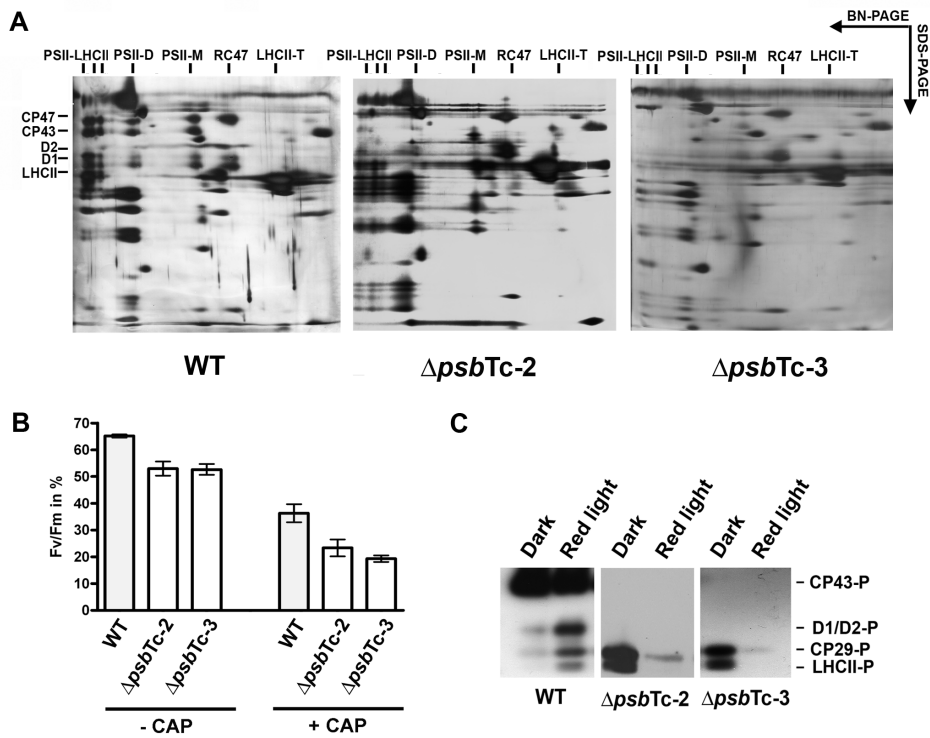
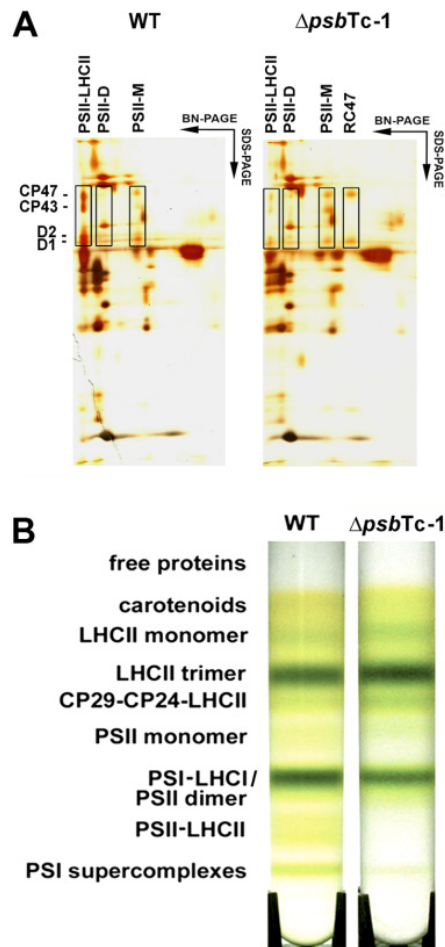


Figure 6: Phosphorylation patterns of PSII proteins and PSI-LHCII association in WT and $\Delta psbTc-1$. A, Phosphorylation analysis of D1/D2, CP43 and LHCII proteins after 24 h dark adaptation (D), after 20 min red light illumination (R) and after treatment with far-red light (FR). Phosphorylation was detected with phosphothreonine antibodies. Coomassie Brilliant Blue (CBB) staining is shown as a loading control (lower panel). The two independent lines $\Delta psbTc-2$ and $\Delta psbTc-3$ show the same light dependent phosphorylation pattern (Supplemental Fig, 1C). B, Analysis of protein complexes separated by BN-PAGE in the first dimension (upper panel). Immunoblot analysis of protein complexes separated by BN-PAGE using LHCb1 and PsaA/B antibodies demonstrates the presence of LHCII-PSI supercomplexes (indicated by arrows and boxes) in WT under state II conditions and in the mutant after dark adaptation (lower two panels). C, LHCII phosphorylation after dark incubation of WT leaves under aerobic (+O₂) and anaerobic (-O₂) conditions in the presence and absence of DCMU and IOX.

SUPPLEMENTAL MATERIAL



Supplemental Figure 1: Studies on assembly, photoinhibition, and phosphorylation patterns of the independent transformants $\Delta psbTc-2$ and $\Delta psbTc-3$. A, Separation of thylakoid protein complexes by BN-SDS-PAGE. Complexes and silver-stained proteins are labeled according to their identification by mass spectrometry. D, dimer; M, monomer; T, trimers; RC47, reaction center 47. B, Photoinhibition of PSII of high light-treated WT and mutant leaves. Loss of quantum yield (Fv/Fm) with and without CAP after exposition to $1,200 \mu E m^{-2} s^{-1}$ for 4 h. Fv/Fm ratios are expressed relative to the initial values before starting the experiment in WT (Fv/Fm ~ 0.82) and mutants (Fv/Fm ~ 0.68), respectively. Error bars in panels represent SD of at least three independent experiments. C, Phosphorylation analysis of D1/D2, CP43 and LHCII proteins after 24 h dark adaptation, after 20 min red light illumination. Phosphorylation was detected with phosphothreonine antibodies.



Supplemental Figure 2: A, Separation of WT and $\Delta psbTc-1$ thylakoids by BN-SDS-PAGE using 1.5% digitonin. Complexes and individual proteins are silver-stained. D, dimer; M, monomer; T, trimers; RC47, reaction center 47. B, Sucrose density gradient (0.1 to 1.0 M) profiles illustrating separation of chlorophyll containing thylakoid complexes for WT and $\Delta psbTc-1$ and absence of PSII-LHCII in the mutant.

Supplemental Table 1: Computer-based simulation for the prediction of the S-states ratios and the occupancy ratio Q_B/Q_B^- .

Supplemental Table 1: Computer-based simulation for the prediction of the S-states ratios and the occupancy ratio Q_B/Q_B^-

No. of flashes	WT				$\Delta psbTc$			
	Data	S1	S2	S3	Data	S1	S2	S3
1.	6.7	6.7	6.7	6.7	8.9	8.82	8.9	8.9
2.	8.9	8.9	8.95	8.95	7.9	7.92	7.9	7.9
3.	5.9	5.9	5.9	5.9	5.3	5.3	5.3	5.3
4.	5.2	5.2	5.2	5.2	4.4	4.4	4.4	4.4
5.	6.9	6.9	6.9	6.9	8.3	8.3	8.3	8.3
6.	8.1	6.85	8.9	8.9	6.8	6.51	6.8	6.8
Correlation coefficients		0.927936	0.84254	1		0.997765	0.997765	1
Q_B/Q_B^- ratio		1.35	0.9	0.9		2.07	1.68	1.68

Chloroplast HCF101 is a Scaffold Protein for [4Fe-4S] Cluster Assembly

**Serena Schwenkert¹, Jeverson Frazzon², Jeferson Gross¹, Eckhard Bill³, Daili J. A. Netz⁴,
Antonio J. Pierik⁴, Roland Lill⁴, and Jörg Meurer^{1,5}**

Biozentrum der LMU München, Botanik, Großhaderner Str. 2-4, 82152 Planegg-Martinsried,
Germany

¹ Biozentrum der LMU München, Botanik, Großhaderner Str. 2-4, 82152 Planegg-Martinsried, Germany

²Department of Food Sciences, ICTA, Federal University of Rio Grande do Sul, Porto Alegre, RS, 91051-970, Brazil

³Max-Planck-Institut für Bioanorganische Chemie, Stiftstrasse 34-36, 45470 Mülheim/Ruhr, Germany

⁴Institut für Zytobiologie und Zytopathologie, Phillips University Marburg, Marburg, D35033 Germany

*Address correspondence to: Jörg Meurer, Biozentrum der LMU München, Botanik, Großhaderner Str. 2-4, 82152 Planegg-Martinsried, Germany; Tel. +49 (0)89-218074556; Fax. +49(0)89-218074599; E-mail: joerg.meurer@lrz.uni-muenchen.de

ABSTRACT

Oxygen evolving chloroplasts contain their own iron-sulfur cluster assembly machinery thus requiring specialized proteins. HCF101 has been shown to be essential for the accumulation of the membrane complex photosystem I and the soluble ferredoxin-thioredoxin reductase, both containing [4Fe-4S] clusters. The protein belongs to the FSC superfamily of P-loop ATPases, several members of which play a crucial role in [Fe-S] cluster biosynthesis. Using Mössbauer and EPR spectra we provide evidence that HCF101 binds a [4Fe-4S] cluster, although none of the cysteine motifs for [Fe-S] cluster binding within the FSC family are conserved in chloroplast HCF101 homologues. *In vitro* approaches using site-directed mutagenesis identified three HCF101-specific cysteine ligands required for cluster binding. We could further demonstrate that the reconstituted cluster is transiently bound and transferred from HCF101 onto target Fe-S proteins. HCF101 appeared to be part of a 140 kDa complex in *Arabidopsis* chloroplasts. Our findings unveil that HCF101 is the first chloroplast scaffold protein that assembles and transfers [4Fe-4S] clusters indicating that it directly supplies the cofactor to chloroplast membrane and soluble protein complexes.

INTRODUCTION

Iron-sulfur ([Fe-S]) clusters are ancient co-factors of proteins required for various essential processes. Being able to transfer electrons they are important players in photosynthesis and respiration, nitrogen and sulfur metabolism, redox regulation and sensing as well as gene expression, as they are indispensable prosthetic groups of many enzymes (Beinert, 2000; Frazzon and Dean, 2003; Johnson *et al.*, 2005). The biogenesis of such clusters from elemental iron and sulfur is an enzymatic process and requires a set of specialized proteins. As a first step sulfur is mobilized from sulfidril groups of cysteines catalyzed by a cysteine desulfurase (Zheng *et al.*, 1993), while elemental iron is relocated from cellular stores. Several scaffold proteins form a transient clusters from these resources, which is subsequently transferred to apo-proteins. The components responsible for this maturation step have been mostly characterized in eubacteria where three different systems for Fe-S cluster biogenesis are known, the encoding genes of which are organized in operons. The ISC (iron-sulfur-cluster) assembly machinery, responsible for general [Fe-S] cluster assembly (Zheng *et al.*, 1998), the independent SUF (sulfur-mobilization) system (Takahashi and Tokumoto 2002) and the NIF (nitrogen-fixation) machinery, which catalyses the assembly of nitrogenase in nitrogen fixating bacteria (Jacobsen *et al.*, 1998). In eukaryotes the existence of diverse cellular environments requires compartmentalized iron-sulfur biogenetic machineries. A ISC homologous system has been demonstrated to be operational in yeast mitochondria. This ISC machinery not only supports the organellar demand for the cofactor but also assemble Fe-S clusters that are essential for maturation of cytosolic, extra-organellar apo-proteins. Nonetheless, additionally cytosolic scaffold proteins for Fe-S cluster formation have been discovered (reviewed in Lill and Mühlenhoff, 2005 and 2008).

Although several [Fe-S] cluster containing proteins are indispensable for photosynthesis and redox processes in plants, relatively little is known about the factors involved. As the plant organelles originate from endosymbiotic bacteria they are likely to possess their own assembly machinery. Chloroplasts contain numerous iron-sulfur proteins, such as the Photosystem I subunits, which contain three attached [4Fe-4S] prosthetic groups. They are especially in need of their own set of proteins for [Fe-S] cluster synthesis as those are often quite sensitive to oxygen, which is produced in large amounts within the organelle. In recent years some of the participating proteins have been identified (Balk and Lobreaux, 2005,

Kessler and Papenbrock 2005; Pilon *et al.*, 2006). A candidate for sulfur mobilization in chloroplasts, CpNifS, has been shown to act as a cysteine desulfurase *in vitro* and *in vivo* (Ye *et al.*, 2005; van Hoewyk *et al.*, 2007). This process seems to be stimulated by CpSufE (Ye *et al.*, 2006). Not surprisingly homologue genes of both proteins are found in bacteria serving similar functions and they are related to the bacterial SUF system, which is known to be active under oxidative stress conditions in bacteria (Kessler and Papenbrock 2005). For the second step in [Fe-S] cluster assembly the plastid scaffold protein NFU2 has been shown to carry a [2Fe-2S] cluster, which can be transferred to ferredoxin. As PSI is decreased in mutant plants, NFU2 is proposed to be also involved in the accumulation of [4Fe-4S] proteins (Yabe *et al.*, 2004; Touraine *et al.*, 2004), although the exact mechanism remains unclear. Two further plastid scaffold proteins carrying a transient [2Fe-2S] cluster have been identified recently, CplscA (Abdel-Gahny *et al.*, 2005) and two glutathione reductases, GrxS14 and Grx16 (Bandyopadhyay *et al.*, 2008), all of which were demonstrated to assemble and transfer [2Fe-2S] clusters *in vitro*. An IscA homologue in *Synechocystis*, has been shown to assemble a [2Fe-2S] cluster and to reactivate apo-adenylyl sulfate reductase, which requires a [4Fe-4S] cluster for activity (Wollenberg *et al.*, 2003). However, up to date plastid candidates, which directly transfer [4Fe-4S] clusters have not been described.

Apart from PSI, which contains three [4Fe-4S] clusters, a number of other chloroplast enzymes depend upon this cofactor, such as the heterodimeric ferredoxin-thioredoxin reductase (FTR) complex, the plastid nitrite and sulfite reductases, and presumably the NAD(P)H dehydrogenase (NDH) (Amann *et al.*, 2004). Two plastid proteins, HCF101 and APO1, have been described as essential and specific factors for assembly of [4Fe-4S] cluster containing proteins. Whereas APO1 interferes with translation of photosystem I transcripts *psaA* and *psaB*, HCF101 exerts its function on a posttranslational step. In addition to the lack of PSI, both mutants accumulate less heterodimeric FTR complex, whereas levels of [2Fe-2S] cluster containing proteins are not affected (Lezhneva *et al.*, 2004; Amann *et al.*, 2004). APO1 is only conserved among higher plants, whereas HCF101 belongs to an ancient and ubiquitously distributed protein family of soluble P-loop ATPases. According to the proposed function of HCF101 and its relatives in iron-sulfur metabolism the FSC ([4Fe-4S]-cluster) superfamily consisting of five classes has been defined, members of which share a highly conserved protein signature and represent bacterial, plastid, mitochondrial, and cytoplasmic proteins (Lezhneva *et al.*, 2004). Plastid homologues possessing an N-terminal extension of

unknown function (DUF59, pfam PF01883) and eubacterial forms belong to class 1. The eubacterial representatives could further be divided into subclasses, depending on the presence of the DUF59 domain and the positions of the cysteines. Of the eubacterial FSC proteins, the function of ApcC in *Salmonella* has been studied and the protein apparently plays a role in the maturation of [Fe-S] clusters (Skovran and Downs 2003; Boyd *et al.*, 2008). Class 2 members are found only in eukaryotes and are targeted to the mitochondria. Members of classes 3 and 4, like Nbp35 and Cfd1 in yeast, have been shown to form a stable complex and to act in [4Fe-4S] cluster assembly in the cytosol (Roy *et al.*, 2003; Hausmann *et al.*, 2005; Netz *et al.*, 2008). Archaeal proteins are also found in the latter two classes according to their function as a host in the first endosymbiotic event.

In this study we present a detailed biochemical and spectroscopic characterization of HCF101. It is part of a larger complex in the plastid stroma presumably involving additional interaction partners. Combined biochemical, spectroscopic, and site directed mutagenic analysis demonstrate that HCF101 carries a transient [4Fe-4S] cluster, ligated by three specific cysteines only conserved among the plastid members of the class 1 subgroup of the FSC family. Our results are consistent with a proposed function for HCF101 as a scaffold protein that assembles a [4Fe-4S] cluster and transfers the cofactor to client apo-proteins, putatively the PSI and FTR complexes.

RESULTS

Expression and purification of HCF101

To investigate the function of HCF101 the mature sized protein without the predicted transit peptide was cloned into a pET23a⁺ vector and overexpressed without a tag in the *E. coli* strain BL21(DE3)/pLysS. Five hours after induction of overexpression with isopropylthio- β -galactoside (IPTG) the total amount of HCF101 protein, which accumulated at an apparent molecular mass of about 53 kDa (calculated mass 50.507 kDa), reached approx. 20% of the total soluble *E. coli* protein extract. After purification with anion exchange chromatography the protein was found to be 90% pure (Figure 1A). The protein had a brownish colour, already indicating the presence of iron-sulfur clusters, even if purification was performed

under aerobic conditions. Further, UV-visible absorption spectra of the purified protein showed a peak at 330 nm and a characteristic shoulder at 420 nm likewise indicating the presence of [4Fe-4S] clusters (Figure 1B).

HCF101 binds a [4Fe-4S] cluster

For better investigation of the cluster type, the cofactor was chemically reconstituted by anaerobic incubation of the purified HCF101 protein with a five fold molar excess of iron and sulfur over the HCF101 protein concentration of iron and sulfur. UV-visible absorption spectra of the sample showed that the intensity of the characteristic shoulder at 420 nm was increased up to three fold as compared to the purified protein (Figure 1B). Determination of the iron and sulfur content of the purified and reconstituted sample confirmed this observation. Upon protein purification under aerobic conditions approximately 75% of the proteins lost their cluster, depending on the preparation, whereas in the fully reconstituted sample about 4 iron and 4 sulfur ions could be quantified per monomer, again indicating that HCF101 binds a single [4Fe-4S] clusters per monomer (Fig 1C). The reconstituted cluster proved to be somewhat oxygen sensitive, as the 420 nm shoulder slowly decreased after treatment with oxygen and the reconstituted cluster was completely lost after 4 h (Supplemental Figure 1).

The zero-field Mössbauer spectrum recorded of whole cells after overexpression of HCF101 wild type (WT) in ^{57}Fe enriched media at 80 K showed a superposition of two quadrupole doublets with intensity ratio 89:11 (Figure 2A, upper panel). The moderately low isomer shift, $\delta = 0.50 \text{ mms}^{-1}$ and quadrupole splitting, $\Delta E_Q = 1.04 \text{ mms}^{-1}$ of the major species are typical of [4Fe-4S] clusters in the diamagnetic (2+) state. The iron sites, which formally are two Fe^{2+} and two Fe^{3+} ions, are indistinguishable because of complete valence delocalization. The 11% minority subspectrum, in contrast, has a very large isomer shift, $\delta = 1.26 \text{ mms}^{-1}$ and large quadrupole splitting, $\Delta E_Q = 3.23 \text{ mms}^{-1}$, which are typical of high-spin Fe(II) with six hard ligands. We assign the component to adventitiously bound iron, which is probably even in different cell compartments.

The Mössbauer spectrum of the C128S control sample shows also two quadrupole doublets (Figure 2A, lower panel), which both appear to originate from non-specifically bound iron, but not from an [Fe-S] cluster. The major species (61%) has lower isomer shift and

quadrupole splitting than expected for cubane [Fe-S] clusters, $\delta = 0.39 \text{ mms}^{-1}$ and $\Delta E_Q = 0.89 \text{ mms}^{-1}$. The values are close to what is known for γ -FeOOH or similar hydroxides (isomer shift $\delta = 0.37 \text{ mm/s}$, $\Delta E_Q = 0.57 \text{ mm/s}$) (Greenwood and Gibbs, 1971) from iron precipitations. Oxidized 3Fe clusters, which might be considered as possible alternative explanation, although the isomer shift would be untypically high, can be excluded because of the absence of the sizable EPR signals from such clusters (see below). The second component in the Mössbauer spectrum again represents non-specifically bound Fe(II): $\delta = 1.36 \text{ mms}^{-1}$ and $\Delta E_Q = 2.86 \text{ mms}^{-1}$. Thus, signals from iron sulfur clusters can not be detected in the Mössbauer spectrum of the mutated protein C128S.

Reconstituted HCF101 showed a weak EPR signal at $g = 2.02$ from a $[3\text{Fe-4S}]^{1+}$ cluster (Figure 2B, top trace). The integrated intensity amounted to no more than 1% of the HCF101 molecules. Such a species could be derived from breakdown of a minor proportion of the $[4\text{Fe-4S}]^{2+}$ cluster, which could not be detected in the Mössbauer spectrum. Upon reduction with dithionite a broad rhombic EPR signal with g -values of 2.024 and 1.928 was observed (Figure 2B, bottom trace), which was accompanied by a sharp isotropic $g = 2.003$ radical signal, derived from dithionite breakdown products. The rhombic EPR signal had an integrated intensity of 0.05 spin/HCF101 in two different preparations. Since Mössbauer spectroscopy (Figure 2A), iron and sulfide analysis and the extent of reduction as judged from visible spectroscopy (Figure 1B) indicated the presence of a stoichiometric amount of $[4\text{Fe-4S}]^{1+/2+}$ in HCF101 we were puzzled by the low intensity. Inspection of the low field region revealed a broad signal at $g = 5$ from a $S = 3/2$ form of the $[4\text{Fe-4S}]^{1+}$ cluster (Figure 2C, bottom trace). This signal appeared upon reduction and was thus not from adventitiously bound high spin ferric ions, like the sharp $g = 4.3$ signal in the top trace of Figure 2C which disappeared upon reduction. It is likely that the $g = 5$ signal encompasses the majority of the $[4\text{Fe-4S}]^{1+}$ clusters in HCF101, since upon double integration such weak signals represent more spins than sharp $S = 1/2$ signals. Such broad anisotropic $S = 3/2$ signals have been observed for the $[4\text{Fe-4S}]^{1+}$ cluster of the nitrogenase Fe-protein (Hagen *et al.*, 1985), the activator of 2-hydroxyglutaryl-CoA dehydratase (Hans *et al.*, 2000), the Fx cluster in the photosynthetic reaction centre (Heinrich *et al.*, 2006) and the Cfd1/Nbp35 complex (Netz, Pierik and Lill, unpublished). Since to our knowledge $S = 3/2$ signals do not occur in natural $[2\text{Fe-2S}]^{1+}$ clusters, the presence of the $g = 5$ signal in dithionite reduced HCF101

corroborates the presence of a $[4\text{Fe-4S}]^{1+/2+}$ cluster in HCF101 as shown by Fe/S analysis, UV-visible and Mössbauer spectroscopy.

Sequence alignment analysis with HCF101 homologues

The mature HCF101 protein without the predicted transit peptide contains eight cysteine residues. All cysteines are rather conserved among higher plants (Supplemental Figure 2). Two of them are located in the N-terminal DUF59 domain. Especially C128 is highly conserved in DUF domains and HCF101, as it is also present in eubacteria, possibly indicating an important role as a [Fe-S] cluster ligand (Supplemental Figure 2). Conservation of the cysteine in bacterial proteins only consisting of the DUF59 domain proposed to be part of ring hydroxylating complexes in phenylacetic acid catabolic reactions indicates that this pathway requires [Fe-S] clusters.

Homologues members of the FSC family in *Arabidopsis*, yeast, and prokaryotes share several conserved cysteine residues (Figure 3 and Supplemental Figure 2) but strikingly, not even one of those required for [4Fe-4S] cluster binding (Roy *et al.*, 2003; Hausmann *et al.*, 2005; Netz *et al.*, 2007; Bych *et al.*, 2008; Boyd *et al.*, 2008) is present in the same position in HCF101. The *Arabidopsis* homologue HCF101-L1, predicted to be localized in mitochondria, shares conserved N-terminal and C-terminal cysteines with the cytoplasmic homologue yeast proteins Nbp35 and Cfd1, respectively. Those two proteins are part of the cytosolic Fe-S assembly machinery (CIA) in *Saccharomyces cerevisiae* and form a complex. They both bind a transient [4Fe-4S] cluster at the C-terminus and Nbp35 binds an additional [4Fe-4S] cluster at the N-terminus (Netz *et al.*, 2008). The bacterial homologue ApbC also shares the C-terminal cysteines and has likewise been shown to be involved in [Fe-S] cluster biosynthesis (Skovran and Downs 2003; Boyd *et al.*, 2008). Furthermore, characteristic motives known to be likely ligands for [Fe-S] clusters, such as CXXC are present in the N- and/or C-termini of the eukaryotic proteins and in eubacteria, like the *Salmonella* homologue ApbC, but are lacking in the plastid HCF101 form (Figure 3 and Supplemental Figure 2). The mitochondrial targeted homologue Ind1 (HCF101-L1) has lately been shown to act as a scaffold protein for Fe-S biogenesis in mitochondria of the yeast *Yarrowia lipolytica*, where it is essential for the formation of the mitochondrial complex I (Bych *et al.*, 2008).

Cysteine residues of HCF101 involved in ligation of the [4Fe-4S] cluster

As the motives of the cysteine residues in HCF101 differ so much from those of the members of the FSC family and often of other cluster binding Fe-S proteins, it was particularly challenging to investigate the cysteines involved in binding the iron-sulfur cluster. As a first approach the ability to bind a cluster was analyzed *in vitro*. For this purpose we mutated all eight cysteines to serines by site directed mutagenesis. The recombinant proteins were expressed, purified and compared to the WT protein. After the purification process the typical brownish color was lost in three of the mutant forms C128S, C347S and C319S. UV-visible spectra analysis confirmed that the characteristic shoulder at 420 nm was completely absent in the mutants (Figure 4). All other recombinant proteins showed similar absorption spectra to the WT, although slightly lesser amounts of iron-sulfur clusters were bound in all mutants (data not shown). The involvement of at least three cysteines is in agreement with the finding that one [4Fe-4S] cluster is bound per monomer.

HCF101 is part of a complex in *Arabidopsis* chloroplasts

The antibodies specifically raised against the purified HCF101 protein recognized the protein at an expected size of approximately 53 kDa in WT protein extracts from *Arabidopsis*. The *Arabidopsis* mutant *hcf101* lacked the protein completely, as expected. HCF101 was mainly found as a soluble protein in the chloroplast stroma, although a slight band could be detected in the membrane fraction (Figure 5A), as has been reported previously (Stöckel *et al.*, 2004). However, HCF101 does not contain any hydrophobic domain and the protein is only loosely attached to the membrane and it is easily removed from the lipid environment after treatment with low salt concentrations (data not shown). The oligomeric state of the *E. coli* purified protein was investigated by size-exclusion chromatography and SDS page, both under reducing and non-reducing conditions. In both experiments the protein was found as a monomer, indicating that, at least when expressed in *E. coli*, the protein had no ability to form an oligomer (data not shown). To analyze the situation *in vivo* in *Arabidopsis*, size-exclusion chromatography was performed with stromal WT proteins. HCF101 was detected by SDS-PAGE and immunoblotting of the fractions (Figure 5B). The protein was detected in fractions corresponding to an approximate molecular weight of 145 kDa. The experiment was performed under reducing and non-reducing conditions to test whether proteins within

the detected complex were connected through disulfide bonds *in vivo*. However, the size of the oligomer was not changed, indicating that HCF101 is part of a stable complex *in vivo*.

Apo-Leu1 activation by [Fe-S] cluster transfer from HCF101

Our previous data had suggested a specific scaffold function of HCF101 in [Fe-S] cluster biogenesis of PSI and presumably the FTR complex (Lezhneva *et al.*, 2004). A common feature of scaffold proteins is their capability to transfer the bound labile [Fe-S] cluster to the apoform of acceptor proteins (for reviews see Johnson *et al.*, 2005; Lill 2006 and 2008). We tested the putative scaffold function of HCF101 *in vitro*. It is not feasible to transfer the [Fe-S] cluster to apo-PSI complexes, as this is not stable in *in vitro* studies. Therefore we chose yeast apo-Leu1 as a model acceptor protein. The isopropylmalate isomerase activity of the target protein acquired upon [Fe-S] cluster binding was measured (Netz *et al.*, 2008). Apo-HCF101 was chemically reconstituted to its holoform (typically containing 3.6 ± 1.2 Fe and 3.0 ± 0.8 S per monomer) and mixed with apo-Leu1. Isopropylmalate isomerase enzyme activity developed fast (within 2 min) and efficiently (more than 90% conversion of apo-Leu1; Figure 5C). In contrast, upon chemical reconstitution of apo-Leu1 with iron and sulphide instead of a transferable [Fe-S] cluster, a rather slow and inefficient generation of the Leu1 activity was observed. Even after 30 min only about one third of the activity was detected as compared to that using HCF101 as a donor after 2 min. Taken together, these data clearly indicate that HCF101 fulfils a critical requirement for a scaffold function, i.e. the capacity to transfer a labile [Fe-S] cluster to a target protein under conditions when chemical reconstitution fails.

DISCUSSION

HCF101 is part of the chloroplast [Fe-S] cluster assembly machinery

In the present study we investigated the molecular function of the plastid representative HCF101 of the FSC superfamily of P-loop ATPases. The protein was previously shown to be localised in the chloroplast and to function as an essential assembly factor for PSI. Levels of PSI and FTR complexes harbouring three and one [4Fe-4S] clusters, respectively, were

significantly reduced in the *hcf101* mutant (Lezhneva *et al.*, 2004). Bacterial, cytosolic, and mitochondrial members of the FSC family have been described to bind [4Fe-4S] clusters underlining their role in [Fe-S] cluster biogenesis presumably in all organelles and organisms (Hausmann *et al.*, 2005; Netz *et al.*, 2008; Boyd *et al.*, 2008; Stehling *et al.*, 2008). However, despite the overall striking conservation of the protein signatures, surprisingly none of the typical and conserved cluster binding motives are present in HCF101 (Lezhneva *et al.*, 2004). Therefore it was controversial whether HCF101 has the ability to bind a [Fe-S] cluster or possibly acquired other functions in the course of evolution. Members of the FSC family display a diverse phenotype regarding their cluster binding abilities. Some agrobacteria for example lost all cysteine residues, indicating that they do not assemble [Fe-S] clusters. Other members such as HCF101 or IndI (Bych *et al.*, 2008) bind one [4Fe-4S] cluster, whereas Nbp35 proteins even bind two [4Fe-4S] clusters, but it remains to be investigated whether they are both transferable (Netz *et al.*, 2008).

Nevertheless, HCF101 contains eight cysteines that may provide possible ligands for Fe-S clusters. These are strictly conserved among higher plants, however only partially preserved among eubacteria (i.e. the class 1). Like mitochondria plastids contain their own [Fe-S] cluster assembly machinery, which is mainly of eubacterial origin. So far nothing is known about the formation [4Fe-4S] clusters in plastids and their insertion into PSI and other chloroplast complexes. In this study we could unequivocally demonstrate by UV-visible, Mössbauer and EPR analysis that HCF101 does bind a [4Fe-4S] cluster, despite the lack of characteristic binding motives. Therefore, HCF101 may represent a divergent type of [Fe-S] cluster binding proteins, which presumably evolved as an adaptation to oxygen evolution in the chloroplast. This is further corroborated by the presence only in HCF101 homologues in plastids of a domain of unknown function DUF971 (COG3536) at the C-terminal part of the protein. *In vitro* analyses using site directed mutagenesis identified three cysteines required to bind the cluster. As expected the most conserved cysteine C128 is involved in cluster binding. The context of the other two cysteines involved in cluster binding, C347 and C419, both represent the second cysteine of a CX₇C and a CX₄C motif, respectively, closely resemble metal binding sites. The other two cysteines of these motives are also likely to be involved in cluster binding and/or stabilization as the cluster of the respective purified mutant forms were more unstable as compared to the WT protein (data not shown). In contrast to all other organisms a cysteine is present in the highly conserved P-loop domain

of the chloroplast HCF101 (CKGGVGKS). This might indicate a change of function of this domain during evolutionary development, although the newly evolved cysteine in the P-loop does also not seem to be involved in cluster binding. HCF101 does not seem to function as a homodimer as is the case for the related NifH, the Fe protein of the nitrogenase (Georgiandis *et al.*, 1992), or other chloroplast [2Fe-2S] cluster scaffold proteins NFU2 or IscA (Yabe *et al.*, 2004; Touraine *et al.*, 2004; Abdel-Gahny *et al.*, 2005). Two cluster binding cysteines (C97 and C131) have been identified in the homodimeric protochlorophyllid oxidoreductase subunit BchL, a NifH-like protein sharing sequence homologies with HCF101. One of those cysteines (C131) is conserved in HCF101, corresponding to C303, yet it might have lost its function as a cluster ligand (Bröcker *et al.*, 2008).

The data obtained further demonstrate a scaffold function for HCF101. Since it is not feasible to establish an *in vitro* assay for the transfer of [4Fe-4S] clusters on the apo-PSI complex we used the yeast apo-Leu1 protein as an unspecific target. HCF101 efficiently transferred its cluster to apo-Leu1 demonstrating that it binds a transient cluster that could potentially be transferred onto other chloroplast Fe-S proteins. The ability of HCF101 to assemble and transfer [4Fe-4S] clusters lead to a model for two possible functions for HCF101 in [Fe-S] cluster assembly in plastids, which are summarized in Figure 6. As scaffold proteins such as NFU2 for [2Fe-2S] have been described in chloroplasts it is likely to assume that these assembled clusters can be transferred onto HCF101 forming transient [4Fe-4S] clusters. This seems especially likely as *Arabidopsis nfu2* mutants have a milder phenotype than *hcf101* regarding PSI accumulation, although the NFU2 protein does not bind [4Fe-4S] clusters (Yabe *et al.*, 2004; Touraine *et al.*, 2004). Moreover HCF101 is part of a larger protein complex in the chloroplast stroma, allowing speculations for interactions with other scaffold or target proteins. Yet, a possible transfer of the cluster or interaction between these two proteins remains to be shown. The fact that HCF101 is found attached to the membrane fraction of chloroplasts favours the idea that a direct interaction with PSI is possible.

Alternatively or additionally HCF101 may have the ability to directly form [4Fe-4S] clusters as reconstitution *in vitro* from abnormal high amounts of elemental iron and sulfur is possible. So far not much is known about the maturation of [4Fe-4S] clusters. In bacteria a scaffold function has been described for IscU, which apparently forms a homodimer that assembles two [2Fe-2S] clusters on each monomer. These units are further combined to a [4Fe-4S] cluster by reductive coupling (Chandramuli *et al.*, 2007). In the chloroplast a factor with such

a function has not been identified and HCF101 might act in a similar fashion. Although HCF101 has a transient [Fe-S] cluster it remains a challenge to identify the exact mechanism of transfer to the final target proteins, especially PSI.

MATERIAL AND METHODS

Protein overexpression and purification

The complete cDNA was obtained from a cDNA library (Meurer *et al.*, 1998). To express HCF101 without the predicted transit peptide the cDNA fragment corresponding to amino acid residues 64 to 533, including the stop codon, was cloned into the *NdeI* and *BamHI* restriction sites of pET23a⁺ (Novagen). Plasmids were transformed into *E.coli* strain BL21 (DE3)/pLysS (Novagen) and initially grown at 37°C in LB medium. Overexpression was induced at OD₆₀₀ of 0.6 by the addition of 1 mM IPTG and cells were harvested after 5 h growth at 30°C. Cells were broken in a French press (Microfluidics, Lampertheim, Germany) in a buffer containing 25 mM Tris-HCl, pH 8.1, 4 mM MgCl₂, 10% glycerol and 1 mM DTT, if not otherwise indicated. After removal of the membranes by centrifugation at 22000 g for 30 min, DNA was precipitated with 1% streptomycin sulfate and centrifuged as above. The supernatant was applied to a HiPrep 16/10 DEAE Sepharose Fast Flow IEX column (GE Healthcare, Braunschweig, Germany) and eluted with a 0 - 0.5 M NaCl gradient in the same buffer as above. Fractions containing the purified protein were concentrated with amicon ultra centrifuge units (Millipore, Billerica, USA) and protein concentration was determined with Bradford reagent (Bradford, 1976). Proteins were visualized by 15% Tris-Glycine-SDS-PAGE and coomassie staining as described (Laemmli, 1970).

For Mössbauer analysis of whole cells BL21(DE3)/pLysS cells containing the respective plasmids were grown on M9 minimal medium. ⁵⁷Fe (Chemotrade, Leipzig, Germany) was prepared as described (Shima *et al.*, 2005) and added in a final concentration of 50 μM ⁵⁷FeCl₂ 1 h before induction of overexpression. Cells were harvested 7 h after induction and frozen rapidly in liquid nitrogen.

Site directed mutagenesis of all cysteine residues of HCF101

All cysteine residues were exchanged by serine residues in the expression vector using site directed mutagenesis as described (Kunkel *et al.*, 1987). The oligonucleotides used to insert the point mutations are listed in supplemental Table 1. The presence of the mutated bases was confirmed by DNA sequencing.

Spectroscopic methods

UV-visible absorption spectra were recorded with a Jasco V-550 spectrometer in a 1 ml quartz cuvette sealed with a rubber bung containing 0.5-1 mg/ml of HCF101 protein in buffer A.

Mössbauer data were recorded on a spectrometer with alternating constant acceleration. The minimum experimental line width was 0.24 mms^{-1} (full width at half-height). The sample temperature was maintained constant in an Oxford Instruments Variox cryostat and the $^{57}\text{Co/Rh}$ source (1.8 GBq) was at room temperature. Isomer shifts are quoted relative to iron metal at 300K. The zero-field spectra have been simulated by using Lorentzian doublets.

For EPR analysis purified HCF101 was transferred to EPR tubes (4.7 outer diameter, 0.45 mm wall thickness, Ilmasil-PN high purity quartz, Quarzschmelze Ilmenau, Langewiesen, Germany) directly after reconstitution and desalting. For reduction of the [Fe-S] cluster of HCF-101 a freshly prepared solution of sodium dithionite in buffer A was added to a final concentration of 2 mM. After mixing the sample was capped with rubber tubing stoppered with a perspex rod and shock-frozen in liquid nitrogen. EPR spectra were recorded with a Bruker E500 ELEXSYS continuous-wave X-band spectrometer with a standard ER4102ST cavity and an ESR910 Oxford Instruments helium-flow cryostat. The magnetic field was calibrated with an ER035M Bruker NMR probe and the microwave frequency was measured with a HP5352B Hewlett–Packard frequency counter.

Chemical reconstitution of [Fe-S] clusters and cluster transfer to apo-Leu1

Purified recombinant apo-HCF101 used for chemical reconstitution contained only approximately 0.2 moles Fe and S per monomer. Before chemical reconstitution of the [Fe-S] clusters in an anaerobic chamber (Coy Laboratory Products, Ann Arbor, MI) apo-HCF101 (60

μM) was reduced with 10 mM DTT in 25 mM Tris-HCl pH 8.0, 150 mM NaCl (buffer A) for one hour. A five molar excess over the HCF101 protein concentration of ferric ammonium citrate and lithium sulphide per HCF101 monomer was added, and the sample was incubated for 30 min at 23°C. Non-bound iron and sulphide was removed by desalting on a 10 ml Sephadex G-25 column (GE Healthcare, Braunschweig, Germany) equilibrated in buffer A. Protein concentration was determined with the Microbiuret method at 545 nm (Bensadoun, A. and Weinstein, D. 1976). Iron was determined colorimetrically after treatment with 1% (w/v) HCl at 80°C for 10 min and addition of ferene as iron chelator (Pierik *et al.*, 1992). Acid-labile sulfur was determined using methylene-blue method (Pierik *et al.*, 1992). For [Fe-S] cluster transfer holo-HCF101 was mixed with recombinant, reduced apo-Leu1 (Netz *et al.*, 2008). Aliquots were analysed at various time points for Leu1 activity.

Plant material and growth conditions

Wild-type and mutant strains were grown on sucrose-supplemented medium as described and the *hcf101* mutant strain was selected as described (Lezhneva *et al.*, 2004). Screen for segregation was facilitated using a chlorophyll fluorescence imaging system (FluorCam690M; Photon System Instruments, Brno, Czech Republic).

Chloroplast protein isolation, SDS-PAGE, immunoblotting and antibody production

Soluble and membrane proteins from *Arabidopsis* were isolated, separated on 15% SDS-PAGE and transferred onto PVDF membrane as described (Lezhneva *et al.*, 2004). For the production of HCF101 specific antibodies three rabbits were immunized with the purified protein without transit peptide. The IgG fraction of the obtained antisera were affinity purified by Protein A chromatography (Pineda, Berlin, Germany).

Size-exclusion chromatography

Three weeks old *Arabidopsis* leaves were homogenized in a buffer containing 50 mM HEPES/KOH, 330 mM Sorbitol, 2mM EDTA, 1 mM MgCl_2 , and 1 mM MnCl_2 . The homogenate was filtrated and centrifuged at 1500 g for 8 min. Chloroplasts were lysed in a buffer containing 25 mM Tricine pH 7.9 and 50 mM KCl. 0.6 mg of protein were loaded onto a

Superdex 200 column (GE Healthcare, Braunschweig, Germany) and eluted with the same buffer. The column was calibrated with a HMW calibration kit (GE Healthcare, Braunschweig, Germany). For analysis of the *E.coli* purified protein 200 µg of protein were loaded onto a Superdex 200 column and elution was monitored at 280 nm.

ACKNOWLEDGEMENTS

We wish to acknowledge the DFG (ME 1794/4 and SFB TR1) to J. M. for financial support. We are especially grateful to Lutz A. Eichacker for the supply of his FPLC.

LITERATURE CITED

1. Abdel-Ghany SE, Ye H, Garifullina GF, Zhang L, Pilon-Smits EA, Pilon M. (2005) Iron-sulfur cluster biogenesis in chloroplasts. Involvement of the scaffold protein CplscA. *Plant Physiol* **138**: 161-172
2. Amann K, Lezhneva L, Wanner G, Herrmann RG, Meurer J. (2004) Accumulation of Photosystem one 1, a member of a novel gene family, is required for accumulation of [4Fe-4S] cluster-containing chloroplast complexes and antenna proteins. *Plant Cell* **16**: 3084-3097
3. Balk J, Lobréaux S (2005) Biogenesis of iron-sulfur proteins in plants. *Trends Plant Sci* **7**: 324-331
4. Bandyopadhyay S, Gama F, Molina-Navarro MM, Gualberto JM, Claxton R, Naik SG, Huynh BH, Herrero E, Jacquot JP, Johnson MK, Rouhier N (2008) Chloroplast monothiol glutaredoxins as scaffold proteins for the assembly and delivery of [2Fe-2S] clusters. *EMBO J* **27**: 1122-1133
5. Beinert H (2000) Iron-sulfur proteins: ancient structures, still full of surprises. *J Biol Inorg Chem* **5**: 2-15
6. Bensadoun A, Weinstein D (1976) Assay of proteins in the presence of interfering materials. *Anal Biochem* **70**: 241-250
7. Boyd JM, Pierik AJ, Netz DJ, Lill R, Downs DM. (2008) Bacterial ApbC Can Bind and Effectively Transfer Iron-Sulfur Clusters. *Biochemistry In press*
8. Bradford, MM (1976) A rapid and sensitive for the quantitation of microgram quantities of protein utilizing the principle of protein-dye binding. *Analytical Biochemistry* **72**: 248-254
9. Bröcker MJ, Virus S, Ganskow S, Heathcote P, Heinz DW, Schubert WD, Jahn D, Moser J (2008) ATP-driven reduction by dark-operative protochlorophyllide oxidoreductase from *chlorobium tepidum* mechanistically resembles nitrogenase catalysis. *J Biol Chem* **283**: 10559-10567
10. Bych K, Kerscher S, Netz DJ, Pierik AJ, Zwicker K, Huynen MA, Lill R, Brandt U, Balk J (2008) The iron-sulphur protein Ind1 is required for effective complex I assembly. *EMBO J* **27**: 1736-1746
11. Frazzon J, Dean DR (2003) Formation of iron-sulfur clusters in bacteria: an emerging field in bioinorganic chemistry. *Curr Opin Chem Biol* **2**: 166-173
12. Georgiadis MM, Komiya H, Chakrabarti P, Woo D, Kornuc JJ, Rees DC (1992) Crystallographic structure of the nitrogenase iron protein from *Azotobacter vinelandii*. *Science* **257**: 1653-1659
13. Greenwood N, Gibb TC (1971) *Mössbauer Spectroscopy*. Chapman and Hall Ltd: London

14. Hagen WR, Eady RR, Dunham WR, Haaker H (1985) A novel $S = 3/2$ EPR signal associated with native Fe-proteins of nitrogenase. *FEBS Lett* **189**: 250-254
15. Hans M, Buckel W, Bill E. (2000) The iron-sulfur clusters in 2-hydroxyglutaryl-CoA dehydratase from *Acidaminococcus fermentans*. Biochemical and spectroscopic investigations. *Eur J Biochem* **267**: 7082-7093
16. Hausmann A, Aguilar Netz DJ, Balk J, Pierik AJ, Mühlenhoff U, Lill R. (2005) The eukaryotic P loop NTPase Nbp35: an essential component of the cytosolic and nuclear iron-sulfur protein assembly machinery. *Proc Natl Acad Sci U S A.* 102, 3266-71.
17. Heinnickel M, Agalarov R, Svensen N, Krebs C, Golbeck JH (2006) Identification of FX in the heliobacterial reaction center as a [4Fe-4S] cluster with an $S = 3/2$ ground spin state. *Biochemistry* **45**: 6756-6764
18. Jacobson MR, Brigle KE, Bennett LT, Setterquist RA, Wilson MS, Cash VL, Beynon J, Newton WE, Dean DR (1989) Physical and genetic map of the major nif gene cluster from *Azotobacter vinelandii*. *J Bacteriol* **171**: 1017-1027
19. Johnson DC, Dean DR, Smith AD, Johnson MK. (2005) Structure, function, and formation of biological iron-sulfur clusters. *Annu Rev Biochem* **74**: 247-281
20. Kessler D, Papenbrock J (2005) Iron-sulfur cluster biosynthesis in photosynthetic organisms. *Photosynth Res.* **86**: 391-407
21. Kunkel TA, Roberts JD, Zakour RA (1987) Rapid and efficient site-specific mutagenesis without phenotypic selection. *Methods Enzymol* **154**: 367-382
22. Laemmli UK (1970) Cleavage of structural proteins during the assembly of the head of bacteriophage T4. *Nature* **227**: 680-685
23. Lezhneva L, Amann K, Meurer J (2004) The universally conserved HCF101 protein is involved in assembly of [4Fe-4S]-cluster-containing complexes in *Arabidopsis thaliana* chloroplasts. *Plant J* **37**: 174-185
24. Lill R, Mühlenhoff U (2005) Iron-sulfur-protein biogenesis in eukaryotes. *Trends Biochem Sci* **3**: 133-141
25. Lill R, Mühlenhoff U (2006) Iron-sulfur protein biogenesis in eukaryotes: components and mechanisms. *Annu Rev Cell Dev Biol* **22**: 457-486
26. Lill R, Mühlenhoff U (2008) Maturation of Iron-Sulfur Proteins in Eukaryotes Mechanisms, Connected Processes, and Diseases. *Annu Rev Biochem* **77**: 669-700
27. Meurer J, Plücken H, Kowallik KV, Westhoff P (1998) A nuclear-encoded protein of prokaryotic origin is essential for the stability of photosystem II in *Arabidopsis thaliana*. *EMBO J* **17**: 5286-5297

28. Netz DJ, Pierik AJ, Stümpfig M, Mühlenhoff U, Lill R (2008) The Cfd1-Nbp35 complex acts as a scaffold for iron-sulfur protein assembly in the yeast cytosol. *Nat Chem Biol* **3**: 278-286
29. Pierik J, Wolbert R, Mutsaers P, Hagen W, Veeger C (1992) Purification and biochemical characterization of a putative [6Fe-6S] prismatic-cluster-containing protein from *Desulfovibrio vulgaris* (Hildenborough) *Eur J Biochem* **206**: 697-704
30. Pilon M, Abdel-Ghany SE, Van Hoewyk D, Ye H, Pilon-Smits EA (2006) Biogenesis of iron-sulfur cluster proteins in plastids. *Genet Eng (N Y)* **27**: 101-117
31. Reiss B, Klemm M, Kosak H, Schell J. (1996) RecA protein stimulates homologous recombination in plants. *Proc Natl Acad Sci U S A* **93**: 3094-3098.
32. Roy A, Solodovnikova N, Nicholson T, Antholine W, Walden WE (2003) A novel eukaryotic factor for cytosolic [Fe-S] cluster assembly. *EMBO J* **22**: 4826-4835
33. Shima S, Lyon EJ, Thauer RK, Mienert B, Bill E. (2005) Mössbauer studies of the iron-sulfur cluster-free hydrogenase: the electronic state of the mononuclear Fe active site. *J Am Chem Soc* **127**: 10430-10435
34. Skovran E, Downs DM (2003) Lack of the ApbC or ApbE protein results in a defect in [Fe-S] cluster metabolism in *Salmonella enterica* serovar Typhimurium. *J Bacteriol* **185**: 98-106
35. Stehling O, Netz DJ, Niggemeyer B, Rösser R, Eisenstein RS, Puccio H, Pierik AJ, Lill R. (2008) The human CIA component huNbp35 is essential for both cytosolic iron-sulfur protein assembly and iron homeostasis. *Mol Cell Biol In press*
36. Stöckel J, Oelmüller R (2004) A novel protein for photosystem I biogenesis. *J Biol Chem* **279**: 10243-10251
37. Takahashi Y, Tokumoto U (2002) A third bacterial system for the assembly of iron-sulfur clusters with homologs in archaea and plastids. *J Biol Chem* **277**: 28380-28383
38. Touraine B, Boutin JP, Marion-Poll A, Briat JF, Peltier G, Lobréaux S (2004) Nfu2: a scaffold protein required for [4Fe-4S] and ferredoxin iron-sulphur cluster assembly in *Arabidopsis chloroplasts*. *Plant J* **40**: 101-111
39. Van Hoewyk D, Abdel-Ghany SE, Cohe CM, Herbert SK, Kugrens P, Pilon M, Pilon-Smits EA (2007) Chloroplast iron-sulfur cluster protein maturation requires the essential cysteine desulfurase CpNifS. *Proc Natl Acad Sci U S A* **104**: 5686-5691
40. Wollenberg M, Berndt C, Bill E, Schwenn JD, Seidler A (2003) A dimer of the FeS cluster biosynthesis protein IscA from cyanobacteria binds a [2Fe2S] cluster between two protomers and transfers it to [2Fe2S] and [4Fe4S] apo proteins. *Eur J Biochem* **270**: 1662-1671
41. Yabe T, Morimoto K, Kikuchi S, Nishio K, Terashima I, Nakai M. (2004) The *Arabidopsis* chloroplastic NifU-like protein CnfU, which can act as an iron-sulfur cluster scaffold protein, is required for biogenesis of ferredoxin and photosystem I. *Plant Cell* **16**: 993-1007

42. Ye H, Abdel-Ghany SE, Anderson TD, Pilon-Smits EA, Pilon M (2006) CpSufE activates the cysteine desulfurase CpNifS for chloroplastic [Fe-S] cluster formation. *J Biol Chem* **281**: 8958-8969
43. Ye H, Garifullina GF, Abdel-Ghany SE, Zhang L, Pilon-Smits EA, Pilon M. (2005) The chloroplast NifS-like protein of *Arabidopsis thaliana* is required for iron-sulfur cluster formation in ferredoxin. *Planta* **220**: 602-608
44. Zheng L, White RH, Cash VL, Jack RF, Dean DR (1993) Cysteine desulfurase activity indicates a role for NIFS in metallocluster biosynthesis. *Proc Natl Acad Sci U S A* **90**: 2754-2758

FIGURES

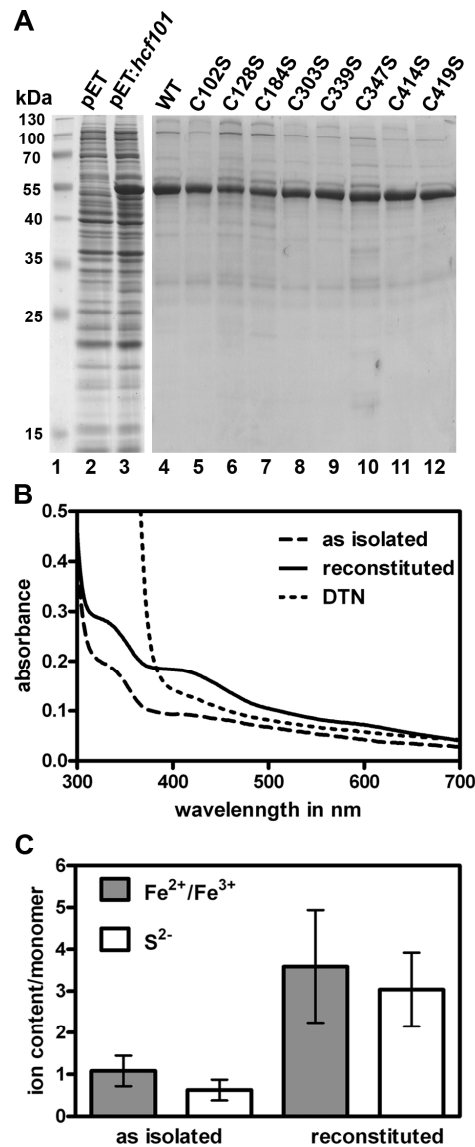


Figure 1: Purified HCF101 binds one [4Fe-4S] cluster per monomer *in vitro*. **A**, Separation by SDS PAGE and coomassie staining of overexpressed HCF101 *E.coli* extract 5 h after induction and the empty pET23a⁺ vector as control (lanes 3 and 2). Lanes 4-12 show the purified WT and the eight recombinant mutant proteins after anion exchange chromatography. **B**, UV-visible absorption spectra of showing a distinct shoulder at 420 nm in the aerobically isolated WT sample and after the chemical reconstitution under anaerobic conditions. The peak disappeared after reduction with 1 mM sodium dithionite. **C**, Determination of the Fe-S content of the purified protein before and after reconstitution was performed of six independent preparations. The iron content of 1.1 ± 0.3 (as isolated) and 3.6 ± 1.2 (reconstituted) and the sulfur content of 0.6 ± 0.2 (as isolated) and 3.0 ± 0.8 (reconstituted) indicate binding of one [4Fe-4S] cluster per monomer after reconstitution.

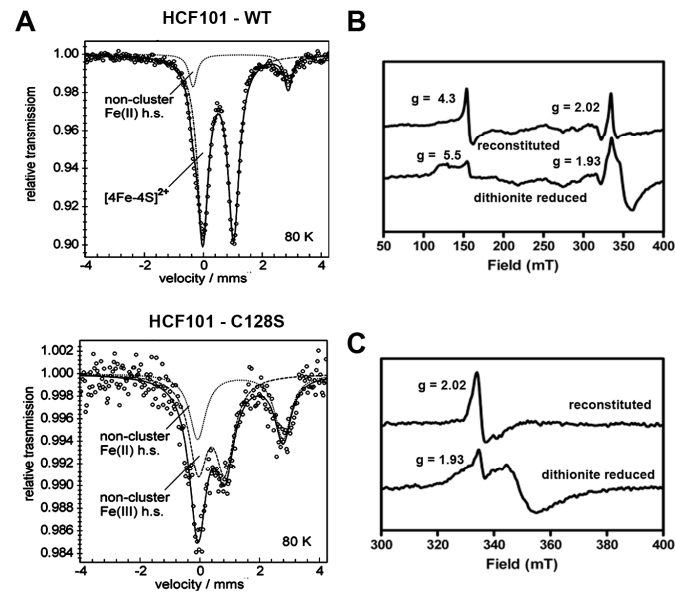


Figure 2: Spectroscopic analysis of HCF101. A, Mössbauer spectra of whole cells after overexpression of HCF101 WT (upper panel) and HCF101 C128S (lower panel) in ^{57}Fe enriched media. B, EPR spectra of reconstituted HCF101 before (top trace) and after reduction (bottom trace) with 2 mM sodium dithionite. EPR conditions: temperature 10 K; microwave frequency, 9420 ± 1 MHz; modulation amplitude, 1.25 mT; modulation frequency, 100 kHz; microwave power 1.26 mW. C, As in (B), but at 20 mW microwave power.

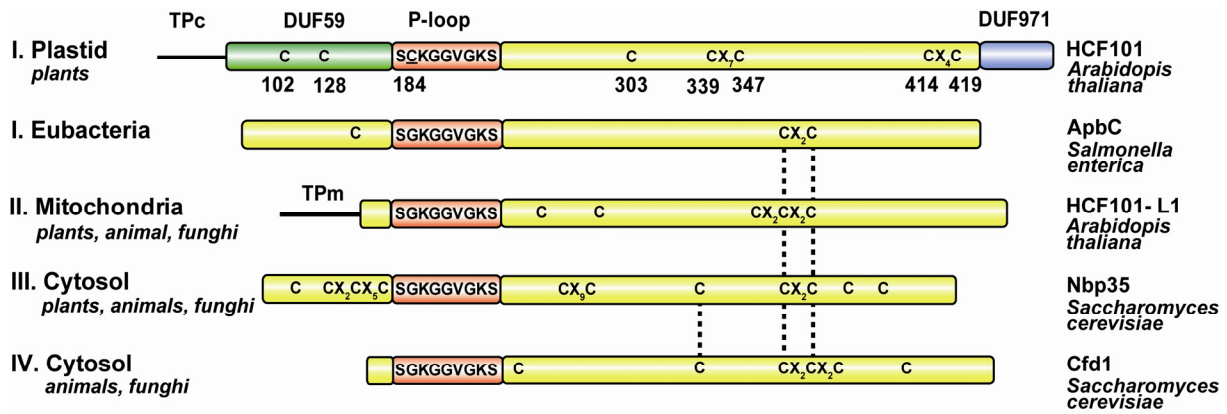


Figure 3: Conserved cysteine residues in members of the FSC superfamily in *Arabidopsis*, yeast and Eubacteria. The schematic sequence alignment shows homologues P-loop ATPases in eukaryots and eubacteria. Represented are the plastid and mitochondrial forms found in *Arabidopsis*, as well as the cytosolic class 3 and 4 homologues (Nbp35 and Cfd1) and the eubacterial homologue ApbC. Conserved cysteines among the FSC classes are indicated with dotted lines. All indicated cysteines are highly conserved within the four classes, but none of those cysteines are conserved in the chloroplast HCF101 of higher plants. TPm and TPc indicate mitochondrial and chloroplast target sequences respectively.

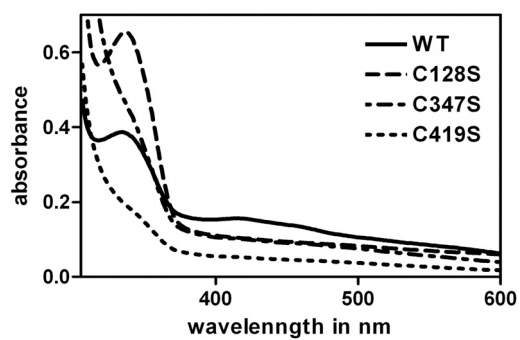


Figure 4: Cysteines of HCF101 required for [Fe-S] cluster binding *in vitro*. UV-visible absorption spectra of purified WT and mutated proteins HCF101 protein (C128S, C347S, C419S), lacking the shoulder at 420 nm.

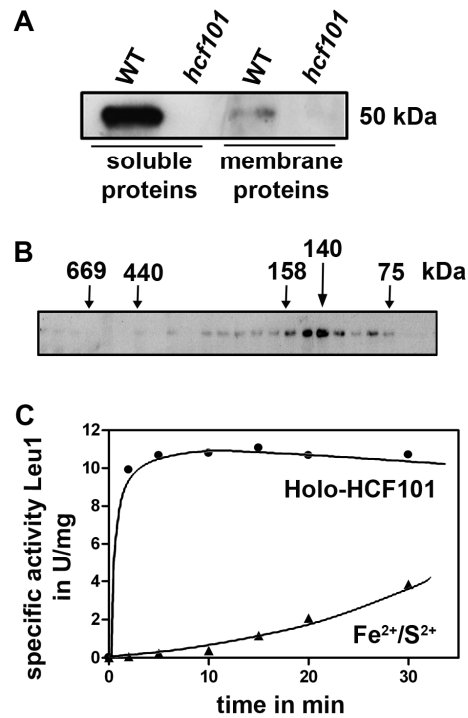


Figure 5: HCF101 is part of a complex in *Arabidopsis* and the labile Fe/S cluster can be efficiently transferred to Leu1. A, Immunoblot analysis of soluble and membrane proteins of WT and *hcf101* using specific HCF101 antibodies. B, Gel filtration analysis of stromal chloroplast proteins. Elution of the HCF101 protein was monitored by SDS-PAGE and immunoblot analysis with HCF101 antibodies. HCF101 eluted with a peak in fraction 23 corresponding to 145 kDa (fraction 1 corresponds to the void volume). C, Reconstituted and desalted holo-HCF101 (3.85 μ M) was mixed with reduced apo-Leu1 (2.45 μ M) at 23°C in buffer A. Isopropylmalate isomerase activity was measured at the indicated time points (circles). In a subsequent control experiment, activation of 2.45 μ M apo-Leu1 with ferric ammonium citrate and Li₂S at concentrations identical to those present in HCF101 (15.4 μ M each) was assayed (squares).

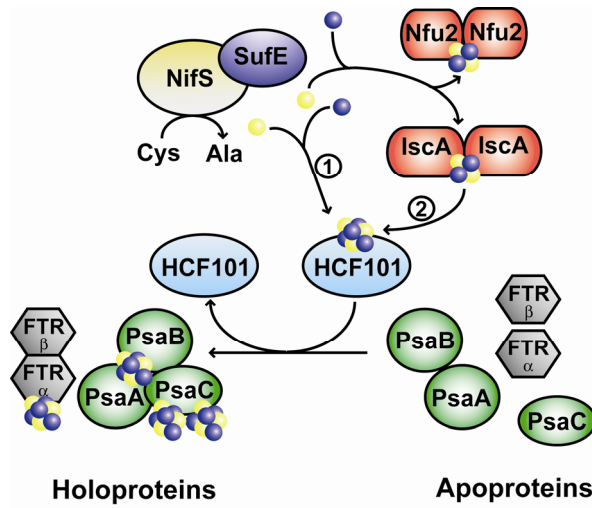
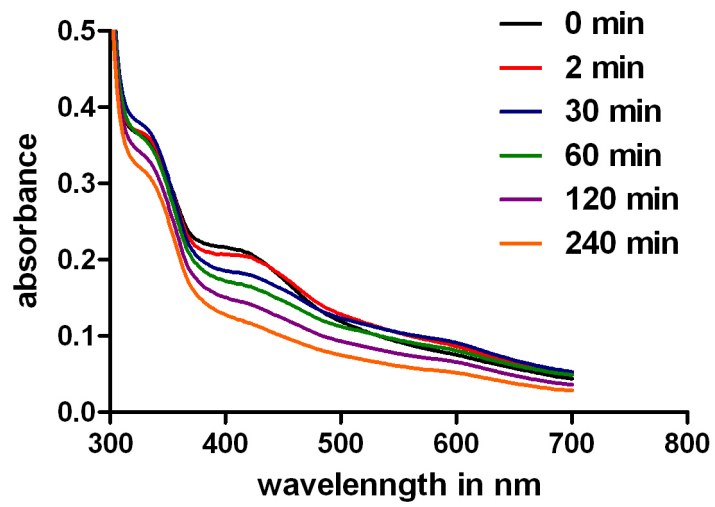


Figure 6: HCF101 acts as a scaffold protein for [4Fe-4S] clusters in the chloroplast – a working model. Two possible pathways for the assembly of [4Fe-4S] on HCF101 are presented. In either case the cysteine desulfurases CpNifS and SufE activate sulfur from cysteine. Either the ions are directly assembled to an [4Fe-4S] cluster on HCF101 ①, or previously assembled [2Fe-2S] clusters are transferred from scaffold proteins such as NFU or IscA to HCF101 ②. Finally the apo-target protein complexes, such as PSI or FTR, are provided with [4Fe-4S] clusters from HCF101.

SUPPLEMENTAL MATERIAL

Supplemental Table 1: Oligonucleotides used for site directed mutagenesis as indicated in material and methods.

C102S-for	5'-GGAGCTGACAACACCCGCATcTCCAGTCAAAGAC-3'
C102S-rev	5'-GAAACAATATCTGTCCCAAATCAGGATC-3'
C128S-for	5'-CATCATCGCTGTTTCTAGTTctAAGGGTGGTG-3'
C128S-rev	5'-GTGTTGTCAGCTCCAAACGGAACGAAACCTC-3'
C184S-for	5'-GATATACAACCTGACCTTATctCAGGTTGCGC-3'
C184S-rev	5'-CTAGAAACAGCGATGATGTTGAAATTC-3'
C303S-for	5'-CTCAAACTTAAGGTGCCTTctGTTGCTGTTGTG-3'
C303S-rev	5'-TAAGGTCAGTTGTATATCACCAGTTCAG-3'
C339S-for	5'-CTCAAACTTAAGGTGCCTTctGTTGCTGTTGTG-3'
C339S-rev	5'-GCACCTTAAGTTTTGAGAACATCCTTACAC-3'
C347S-for	5'-GCTGTTGTGGAGAATATGTctCACTTTGACGC-3'
C347S-rev	5'-CATATTCTCCACAACAGCAACGCAAGGC-3'
C414S-for	5'-CGTTCAGGATCTTGGTGTATcTGTAGTGCAAC-3'
C414S-rev	5'-CACCAAGATCCTGGAACGTTCTGGCAACG-3'
C419S-for	5'-GTGTATGTGTAGTGCAACAA TctGCCAAGATAC-3'
C419S-rev	5'-TGTTGCACTACACATACACCAAGATCCTGGA-3'



Supplemental Figure 1: Oxygen sensitivity of reconstituted HCF101 protein. Purified HCF101 protein was reconstituted as described above. Decay of the shoulder at 420 nm in the presence of O₂ was monitored with UV-visible spectra.

102 128

```

Arabidopsis HCF101 : EKDVLKALSQIIDPDFGTDIVSCGFVKDI---GINEALGEVSFRLELTPACEVVKDMFENKANEVVAAPWVKVNVMTSA
Oryza sativa      : KKDVLVALSQQIIDPDFGTDIVSCGFVKDI---EISEALEEVSFRLELTPACEIKDMFEEKANEVVAAPWVKVNVMTSA
Populus          : ESDVLKALSQIIDPDFGTDIVSCGFVKDI---NIDEAQGEVSFRLELTPACEVVKDMFEQKANEVVAAPWVKVNVMTSA
Vitis vinifera   : EADVLKALSQIIDPDFGTDIVSCGFVKDI---QINEALGEVSFRLELTPACEIKDMFEQKANEVVAMPWVKVNVMTSA
Physcomytrella  : KKDVLGALSQIIDPDFGTDIVTCGFVKEL---TVDESTGEVSFQLELTPACEVVKDMFEQQAQEKVSAAPWVKVNVKMTA
Selaginella     : GHDVLVALSTIIDPDFGADIVTCGFVKDI---QADKSSGEVAFRLELTPACEVVKDMFEQQAQEKVVAAPWVTNVKVTMSA
Volvox          : EEQVLAKLNRVIDPDFGEDIVACGFVRQI---EVDASVGFVSELTTPACEVVKEMFQRQSTQFVKELPWVRDVSIKLTA
Ostreococcus tauri : ESEVLSKLRVIDPDFGEDIVNCGFVKAL---VIDESAGSLEFALTELTTPACEVKAEEFERQAKAFVEEDWVKRVSVMTA
Micromonas      : EADVLNLRVIDPDFGEDIVNCGFVKDI---RVSDAGDVTFLELTPACEVKEEFDRLSKQYVTALEWAKSCNVNMTA
Galdieria maxima : QKQVLELLKNIEDPDLKQNVIELGFVQNLERVAKEDGKYDVRFTLQLTTPACEIKEKFNQDAKEWVSSLLWVRNVEDLRA
Cyanidioschyzon : TEQLLSALKAVVDPDLGQDIVTLGFVQNI---QFGDEHYGTVSFDELTPACEIKERFREECTRLEASPPFVTRANVRLTA
Phaeodactylum : QGEVLSLTKSVIDPDLGSDIVTLGFVQNI---KLDGRDVSEFDELTPACEVKEQFQLDCQQLVQDLPWTNNIQVTMTA
Thalassiosira   : QSQILAAALSVINDPDLNADIVSLGFVQNI---KIDESSNIVSLDELTPACEVVKDLFVQOCQDIINGLAWTRGADVTLTS
Chloroflexus    : EDQILAAALRQVQEPBELGGDIVSRQMKHI---AICDGIVRTIELTTPACEIKDKQIRSEAAEAVLAVPGVREVHDEFTA
Cytophaga       : QEQVLEALKTVPEPDLKLDLVTLNMRDI---AIDQNISETVVLTPACELKLIRNSCTEAIHKVPSGTAVVVNMT
Nostoc punctiforme : SRSILELRPVDEBELRKSIVLNMIRNV---KIDGGKVSFTLVLTTPACELREFIVEDCQKAVKELPGVTVDSIEVTA
Synechococcus   : AAAILEALRPVQPELRRSLVELNMRDI---RVEPGRVAFTLVLTTPACELREFIVEECKAARQAPIEAIDVTVTA
Magnetococcus   : EPQVRDALRMVVDPEVAGRDIVSAGYVSGI---EIHAGEVAEQLFRRPESADYKQLQEQCAQVILGATPGVERVTVNMSS
Salmonella      : RAMVAGTIANFQHPETLKHNLITLKAHHV---AWMDDTLHVELVMPFVWNSAFEVLKEQC SADLLRTGAKAIDWKLISY
Arabidopsis-L1  : -----MATVALRSIRRRELHAAHTISA
Chlamydomonas-L1 : -----MGWRQGAEEWLLSNAASGWRGAASAALAGGASGTARAGAPAGASRGA
Homo sapiens    : -----VCGRQLSGAGSETLK
Yarrowia lipolytica : -----MRGFR IAPTQRSIAIISRLQPIITANFHSSPALRSHENPLGPKSLP
Arabidopsis-L2  : -----MENGDIPEDANEHCPSGQSESAKSDSCAGCPNQEACAT
Chlamydomonas-L2 : -----MASSASAAPTGEVDPDANQHCPTASDQAGKSAAACAGCPNQSICAT
Homo sapiens    : -----MEEVTHDCPGADSAQAGRGASCCGCPNQLCAS
Saccharomyces Nbp35 : -----MTEILPHVNDVLPAAEYELNQPETHCPGPESDMAGKSDACGGCANKEICES
Drosophila     : -----
Homo sapiens    : -----
Danio rerio     : -----
Saccharomyces Cfb1 : -----

```

184

```

Arabidopsis HCF101 : QPAKPIFAGQLPFG---SRISNIIAVSSCKGGVGKSTVAVNLAYTLAQMCAK---VGLFDADVFGPSLPTMVNPE SRIEMN
Oryza sativa      : QPARPAYAGELPEG---IQKISNIIAVSSCKGGVGKSTVAVNLAYTLAQMCAK---VGLFDADVFGPSLPTMVSPE NRRLVMN
Populus          : QPARPVYAGQLPQG---IQTISNIIAVSSCKGGVGKSTVAVNLAYTLAQMCAK---VGLFDADVFGPSLPTMVSPE NRRLEMN
Vitis vinifera   : QPARPVFAGQLPAG---IQTISNIIAVSSCKGGVGKSTVAVNLAYTLAQMCAK---VGLFDADVFGPSLPTMVSPE NRRLEMN
Physcomytrella  : QPAKPLIADDVPAG---IPKVSNIIVAVSSCKGGVGKSTVAVNLAAYSLSAQMCAK---VGLFDADIVGPSLPTMVSPE VKVQMN
Selaginella     : QPAKALAAEGLPRS---IQNVSNIIAVSSCKGGVGKSTVAVNLAAYSLSAQMCAK---VGLFDADVFGPSLPTMVSPE LRVQMV
Volvox          : QPPKPLLPEGRPGG---IPKVRHIIIVAVSSCKGGVGKSTVAVNLAYTLAQMCAK---VGLFDADVFGPSLPTMVNPE IKVEMD
Ostreococcus tauri : QPARNDAPE-IVEG---IPRRVSHIIIVAVSSCKGGVGKSTVAVNLAYTLAQMCAK---VGLFDADVFGPSLPTMISPDPVPEMD
Micromonas      : QPVTNDMPD-AVEG---IPKVRHIIIVAVSSCKGGVGKSTVAVNLAYTLAQMCAK---VGLFDADVFGPSLPTMISPPE QAVQMD
Galdieria maxima : NEINRAQAGDRP---IPNKVKHIIIVAVSSCKGGVGKSTVAVNLAFTLTKLGGK---VGLFDADIVGPSLPTMVSPE NKI QYK
Cyanidioschyzon : QTPSAAAEAGGSRDPISQVSNIVLVTSAKGGVAKSTTAVNLA FVLA RLCAK---VGLFDADIVGPSLPTMVNPE HNEKRIR
Phaeodactylum : QPSVQET---ATLG---MSQVGAIIIVAVSSCKGGVGKSTVAVNLA FSL QRLGAT---VGLFDADVFGPSLPTMIPDDT R FV
Thalassiosira   : QPTAAPS---DAPLG---MSQIGAVIIIVAVSSCKGGVGKSTVAVNLA FALS LCAK---VGLFDADVFGPSLPTMVTPE DDN R FV
Chloroflexus    : NVRRPAGIPEQSA---IPGVANVIAVAAGKGGVGKSTVAVNLA VALA QMCAQ---VGLFDADVFGPSLPTMIGVRRQPVAVS
Cytophaga       : ADVTTGRFNSGPV---IPHVKNIIIVAVSSCKGGVGKSTITANLA VALA SKS CAK---VGLFDADIVGPSLPTMFDVE DVRPNVI
Nostoc punctiforme : ETPQQKSLPDRTG---IPSGVKNIIIVAVSSCKGGVGKSTVAVNVA VALA QTC AK---VGLFDADIVGPNDFPMI GLADAQ VVR
Synechococcus   : ETPRSPSLPNRQS---IPGVRNIIIVAVSSCKGGVGKSTVAVNVA VALA QSC AR---VGLFDADIVGPNVPELMLGLDRS VVQ
Magnetococcus   : NEQQQAEPL-----IPGVKVIIVAVSSCKGGVGKSTITMNLALALQQLGAK---VGLFDADIVGPSLPRMVGHGIPRMEA
Salmonella      : NIATLKRKVNQPG---IPNGVKNIIIVAVSSCKGGVGKSTTAVNLA LALA AEC AK---VGLFDADIVGPSLPTMIGA DQRPTSP
Arabidopsis-L1  : YKFSSASAGGRTELRLPHGVKDIIVAVSSCKGGVGKSTTAVNLA VALA NKCELK---IGLFDADVFGPSLPTMNNINQKPVQVQ
Chlamydomonas-L1 : AASRGAAAAGPQKKLGPDKVQHIVAVSSCKGGVGKSTTAVNVA VAMA TRLGLR---VGLFDADVFGPSLPTMNLNRGKPELDK
Homo sapiens    : QRRTQIMSRGLPKQKPEHGKQVIVAVSSCKGGVGKSTTAVNLA LALA ANDSSKAI GLD VDVV GPSVPEKMMNLKGNPELSQ
Yarrowia lipolytica : ASAPRIPRKTTRRPEPIAGVKKTIIVAVSSAKGGVGKSTVAVNLA LSLA KRCLR---VGLFDVDIVGPSLPTMFGLSGEP R MTH
Arabidopsis-L2  : -APKGPDPDLVAIAERMSTVKKHKLIVLSSCKGGVGKSTFSAQLS FALA GMDHQ---VGLFDIDICGPSIPKMLGLGQE THQS
Chlamydomonas-L2 : -APKGPDPDLAAIAARM SRVKKHKLIVLSSCKGGVGKSTFSAHLA HGLA EDENTQ---IALFDIDICGPSIPKIMGLGQE THSS
Homo sapiens    : GAGATPDTAIEEIKEMKTVKKHKLIVLSSCKGGVGKSTFSAHLA HGLA EDENTQ---IALFDIDICGPSIPKIMGLGQE THQS
Saccharomyces Nbp35 : L-PKGPDPDIPLITDNLSCIEHKHKLIVLSSCKGGVGKSTFSAAM SWAL SADEDLQ---VGLFDLDICGPSLPHMLGCIKETVHES
Drosophila     : -----mldkvknviviivlsgkggvgkstvtstqlslalrknqfkl---vglldidlcgpsvpyllglgrdfqk
Homo sapiens    : -----meaaaepgnlagvrhailvls gkggvgkstiitelalalrhagkk---vglldvdlcgpsiprmlgaggrahqk
Danio rerio     : -----MDGSGKGNPDQVKEHVLVLSGKGGVGKSTITTELALAFRHACKK---VGLIDVDLCGPSIPRMLSVGKPEVHC
Saccharomyces Cfb1 : -----MEEQEIIVPAASLAGIKHILVLSGKGGVGKSSVTTQTALTLCSMFKK---VGLIDIDLIGPSLPRMFLGLENESVYQG

```


Arabidopsis HCF101 : PEKKT---IIPTEYM--GVKLVSFGEAG---QGRALMRGPMVSGVINOLLTTTEWGEILDYLVDMPPPGTGDIQLTLCOVAP
 Oryza sativa : PESRS---IIPTEYL--GVKLVSFGEAG---QGRALMRGPMVSGVINOLLTTTDWGEILDYLVDMPPPGTGDIHLTLCOVAP
 Populus : PEKRT---IIPTEYL--GVKLVSFGEAG---QGRALMRGPMVSGVIDOLLTTTEWGEILDYLVDMPPPGTGDIQLTLCOVVP
 Vitis vinifera : PEKRS---IIPTEYL--GVKLVSFGEAG---QGRALMRGPMVSGVINOLLTTTEWGEILDYLVDMPPPGTGDIQLTLCOVVP
 Physcomytrella : PETRA---IIPTEYL--GVKLVSFGEAG---QGSALMRGPMVSGVINOLFLTTTDWGEILDYLVDMPPPGTGDIQLTLCOVVP
 Selaginella : EDTKQ---IIPTEYL--GVKLVSFGEAG---QGTALMRGPMVSGVINOLLTTTDWGEILDYLVDMPPPGTGDIQLTLCOVVP
 Volvox : PATKA---IIPTEYE--GVKLVSFGEAG---QGSALMRGPMVSGLIQOMLTTAAWGEILDYLVDFPPPGTGDIQLTLCOIVS
 Ostreococcus tauri : KETGT---IKPVEYE--GVKLVSFGEAG---QGSALMRGPMVSGLINOLLTTTDWGEILDYLVDMPPPGTGDIQLTLCOVVP
 Micromonas : KETGS---IIPTEYE--GVKLVSFGEAG---QGSALMRGPMVSGLINOLMLTTTAWGEILDYLVDMPPPGTGDIQLTLCOVLP
 Galdieria maxima : DGR----IIPTEYE--NVKLVSGFYIN--PESALMRGPMIANNMOLLTTTDWGSILDYLVDMPPPGTGDIQLTLCOIVS
 Cyanidioschyzon : LTPDGL--MVPLTRA--GVKLVSGFYIN--SDPAMLRGPMVSSLLTOLIQQTDWGSILDYLVDMPPPGTGDIQLTLCOVLP
 Phaeodactylum : GRQ----VAPLORN--CVRVLSFGYVY--DGSALMRGPMVTOQLDOLFSVTHWGEILDYLVDMPPPGTGDIQLTLCOVLP
 Thalassiosira : DANGQPM--MLPLSNH--GIKLVSMGFLLID-ESQPVVWRGPMVSQLRQFLYQVAVAPILDYLVDMPPPGTGDIQLTLCOVLP
 Chloroflexus : ENENGKPTIIPTEQY--GVKLVSIGFTSP-AESAVVWRGPMVASSAIRCFISDCDWGEILDYLVDMPPPGTGDIQLTLCOVLP
 Cytophaga : STETGDI-LEPAFNH--GVKLVSMGFLLID-RDQPVVWRGPMVNGVTRCFLYQVQVGEILDYLVDMPPPGTGDIQLTLCOVLP
 Nostoc punctiforme : KREDGGEDIFLENY--GVKLVSMGFLLVQ-RDQPVVWRGPMVNGVTRCFLYQVQVGEILDYLVDMPPPGTGDIQLTLCOVLP
 Synechococcus : EKGQK---VTPMEKY--GVKLVSMGFLLVQ-RDQPVVWRGPMVNGVTRCFLYQVQVGEILDYLVDMPPPGTGDIQLTLCOVLP
 Magnetococcus : DMK----MIPVENY--GVKLVSMGFLLVQ-RDQPVVWRGPMVMSALAKMTKGVDEWDLILVDMPPPGTGDIQLTLCOVLP
 Salmonella : SGTGAL--MLPKENY--RVKLVSMGFLLVQ-RDQPVVWRGPMVNNAFDKMLFGTEWGEILDYLVDMPPPGTGDIQLTLCOVLP
 Arabidopsis-L1 : SNL----MRPLLNH--GIKLVSMGFLLVQ-RDQPVVWRGPMVMSALAKMTKGVDEWDLILVDMPPPGTGDIQLTLCOVLP
 Chlamydomonas-L1 : EGK----LIPMSKF--GIQVSMGFLLVQ-RDQPVVWRGPMVMSALAKMTKGVDEWDLILVDMPPPGTGDIQLTLCOVLP
 Yarrowia lipolytica : NLGWS--PVYVEDN--LGVMSIGFLLPNSDEAVIWRGPMVNGVTRCFLYQVQVGEILDYLVDMPPPGTGDIQLTLCOVLP
 Arabidopsis-L2 : GAGWS--PVYVEDN--LAVMSIGFLLPNSDEAVIWRGPMVNGVTRCFLYQVQVGEILDYLVDMPPPGTGDIQLTLCOVLP
 Chlamydomonas-L2 : GSGWS--PVYVEDN--LGVMSIGFLLPNSDEAVIWRGPMVNGVTRCFLYQVQVGEILDYLVDMPPPGTGDIQLTLCOVLP
 Homo sapiens : NSGWT--PVYVTDN--LATMSIQVYLPEDDSAILWRGSKNLLIKKELKDVWDKEDYLVDMPPPGTGDIQLTLCOVLP
 Saccharomyces Nbp35 : ddgww--pvytde-qtlavmsigfllknredpvvrgpkkmmirgfltdvrwdddyliadtppgtsdehltvmecklk
 Drosophila : drgwa--pvfldre-qsislmsvgfllkpkdeavvrgpkknalikgfvsvdvwageldylyvdtppgtsdehltvmecklk
 Homo sapiens : DSGWV--PVYADPQQQLALMSIAFLLEDSDAVIWRGPKKTKALIGQFVSDVAVWGEILDYLVDMPPPGTGDIQLTLCOVLP
 Danio rerio : PEGWQPV-KVETNST-GSLVVISLGLFLLGDRGNSVWRGPKKTKSMIKQFISDVAVWGEILDYLVDMPPPGTGDIQLTLCOVLP
 Saccharomyces Cfb1 :

339 347

Arabidopsis HCF101 : LTA----AVIVTTPQKLAFLDVAKGVRMES--KLRVPCVAVVENMCFE---DAD---GKRYYPFCGCSGSEVVKQFGIP
 Oryza sativa : LTA----AVIVTTPQKLAFLDVAKGVRMES--KLRVPCVAVVENMCFE---DAD---GKRYYPFCGCSGSAVQQQFGIP
 Populus : LTA----AVIVTTPQKLAFLDVAKGVRMES--KLRVPCVAVVENMCFE---DAD---GKRYYPFCGCSGSAVQQQFGIP
 Vitis vinifera : LTA----AVIVTTPQKLAFLDVAKGVRMES--KLRVPCVAVVENMCFE---DAD---GKRYYPFCGCSGSAVQQQFGIP
 Physcomytrella : LTA----AVIVTTPQKLAFLDVAKGVRMES--KLRVPCVAVVENMCFE---EGD---DKRYYPFCGCSGSAVVEQFGIP
 Selaginella : LTA----AVIVTTPQKLAFLDVAKGVRMES--KLRVPCVAVVENMCFE---DAD---GKRYYPFCGCSGSAVQQQFGIP
 Volvox : FSA----AVIVTTPQKLAFLDVAKGVRMES--KLRVPCVAVVENMCFE---EAD---GKRYYPFCGCSGSAVQQQFGIP
 Ostreococcus tauri : ITA----AVIVTTPQKLAFLDVAKGVRMES--KLRVPCVAVVENMCFE---EVD---GVKHKPFCECSGAKICEQYVVP
 Micromonas : ITA----AVIVTTPQKLAFLDVAKGVRMES--KLRVPCVAVVENMCFE---DGD---GKRYYPFCGCSGSAVQQQFGIP
 Galdieria maxima : IDA----AVIVTTPQKLAFLDVAKGVRMES--KLRVPCVAVVENMCFE---KRD---GKRYYPFCGCSGSAVQQQFGIP
 Cyanidioschyzon : ATA----AVIVTTPQKLAFLDVAKGVRMES--KLRVPCVAVVENMCFE---KRD---GKRYYPFCGCSGSAVQQQFGIP
 Phaeodactylum : ITA----AVIVTTPQKLAFLDVAKGVRMES--KLRVPCVAVVENMCFE---EAD---GKRYYPFCGCSGSAVQQQFGIP
 Thalassiosira : ITA----AVIVTTPQKLAFLDVAKGVRMES--KLRVPCVAVVENMCFE---EAD---GKRYYPFCGCSGSAVQQQFGIP
 Chloroflexus : ITG----ALIVTTPQKLAFLDVAKGVRMES--KLRVPCVAVVENMCFE---KRD---GKRYYPFCGCSGSAVQQQFGIP
 Cytophaga : VTG----AVIVTTPQKLAFLDVAKGVRMES--KLRVPCVAVVENMCFE---KRD---GKRYYPFCGCSGSAVQQQFGIP
 Nostoc punctiforme : MAG----AVIVTTPQKLAFLDVAKGVRMES--KLRVPCVAVVENMCFE---KRD---GKRYYPFCGCSGSAVQQQFGIP
 Synechococcus : LAG----AVIVTTPQKLAFLDVAKGVRMES--KLRVPCVAVVENMCFE---KRD---GKRYYPFCGCSGSAVQQQFGIP
 Magnetococcus : LSG----AVIVTTPQKLAFLDVAKGVRMES--KLRVPCVAVVENMCFE---KRD---GKRYYPFCGCSGSAVQQQFGIP
 Salmonella : VTG----AVIVTTPQKLAFLDVAKGVRMES--KLRVPCVAVVENMCFE---KRD---GKRYYPFCGCSGSAVQQQFGIP
 Arabidopsis-L1 : LSG----AVIVTTPQKLAFLDVAKGVRMES--KLRVPCVAVVENMCFE---KRD---GKRYYPFCGCSGSAVQQQFGIP
 Chlamydomonas-L1 : LSG----AVIVTTPQKLAFLDVAKGVRMES--KLRVPCVAVVENMCFE---KRD---GKRYYPFCGCSGSAVQQQFGIP
 Homo sapiens : ITG----AVIVTTPQKLAFLDVAKGVRMES--KLRVPCVAVVENMCFE---KRD---GKRYYPFCGCSGSAVQQQFGIP
 Yarrowia lipolytica : IDG----AVIVTTPQKLAFLDVAKGVRMES--KLRVPCVAVVENMCFE---KRD---GKRYYPFCGCSGSAVQQQFGIP
 Arabidopsis-L2 : PIGIDG--AVIVTTPQKLAFLDVAKGVRMES--KLRVPCVAVVENMCFE---KRD---GKRYYPFCGCSGSAVQQQFGIP
 Chlamydomonas-L2 : VGGGGA--AVIVTTPQKLAFLDVAKGVRMES--KLRVPCVAVVENMCFE---KRD---GKRYYPFCGCSGSAVQQQFGIP
 Homo sapiens : TAHIDG--AVIVTTPQKLAFLDVAKGVRMES--KLRVPCVAVVENMCFE---KRD---GKRYYPFCGCSGSAVQQQFGIP
 Saccharomyces Nbp35 : ESGIDG--AVIVTTPQKLAFLDVAKGVRMES--KLRVPCVAVVENMCFE---KRD---GKRYYPFCGCSGSAVQQQFGIP
 Drosophila : evgchg--avivttppqkllaflldvdkgvrnfcr--kvgvplvgvvenmsglsqplldlvacsevfdsgeaercremvevp
 Homo sapiens : pyqplg--avivttppqkllaflldvdkgvrnfcr--kvgvplvgvvenmsglsqplldlvacsevfdsgeaercremvevp
 Danio rerio : KHRVDG--AVIVTTPQKLAFLDVAKGVRMES--KLRVPCVAVVENMCFE---KRD---GKRYYPFCGCSGSAVQQQFGIP
 Saccharomyces Cfb1 : YSKPDG--AVIVTTPQKLAFLDVAKGVRMES--KLRVPCVAVVENMCFE---KRD---GKRYYPFCGCSGSAVQQQFGIP

Arabidopsis HCF101 : HFDLPIRP-----TTSASGDSGTBEVVSDLSDVARTEQDLGVCVVQQCAKIRO---QVSTAVTYDKYLKAIRVKVP
 Oryza sativa : HFDLPIRP-----TTSASGDTGTEVVVADEQGDVAKTRQNLGVCVVQQCAKIRO---QVSTAVSYDRSIRAIRVKVP
 Populus : HFDLPIRP-----TTSASGDTGMEVVAADQGEVAKIEQNLGICIVQQCAKIRO---QVSTAVTYDKSIIKAIRVKVP
 Vitis vinifera : HFDLPIRP-----TTSASGDSGMEVVADELGEIQTQNLGVCVVQQCAKIRO---QVSTAVTYDKFIKAIRVKVP
 Physcomytrella : HFDLPIRP-----ETSAAGDTGNBEVVVDEQGOVANIESDVGVCVVQQCAKLRQ---AVSTAVMYDKAINAIRVKVP
 Selaginella : NFFELPIRPEARLYKAISAAGDSGTBEVVHDEQGDVARSSELGVCVVQQCAKIRO---QVSTAVTYDDAMRAIKVKVP
 Volvox : NIVREPIVP-----DTSAGDGGQPLVVADETSATAAEMDLGAAVREVAKMAGR---PARQAVYDPPQKDVISVQLP
 Ostreococcus tauri : NLLQMPIVP-----DTSAGDTGRPIVLRDETCETSSRQEVAAATVREVAKLNNG---KKPRVDIDPGYDGAFRVEIP
 Micromonas : NLFQMPIVP-----DTSAGDTGRPIVLRDEA-GDVSTINGAVAAKVVEVAKL---QAGPKGSLALDTEGVAGVDGA
 Galdieria maxima : FVESFPIDE-----DTCRWSNNGIPAVLALSESKISQLQSLASAVVQIAKNAFGN-GKRIPQVFFSDSKCIIVISCN
 Cyanidioschyzon : STFQPIWP-----ETNAAGDTGTPEVLLTLETSEIFQCRREIAENLVQECARVRF--AVPIQARWDADHREIVVQLQ
 Phaeodactylum : HSFSPIPLN-----KTAANGDNGTPEVLEFD-SPPKIKIQELASAVVSEVAKTKFA--KSMRPSVQYDAESHLLQVSN
 Thalassiosira : HTYSVPIMG-----QTAQNGDSGTPEILLDNK-SPODINRQAKSVSEVAKIKFCTGKGRPSVSYDVEKSIILRVDDG
 Chloroflexus : VLGQPIPGM-----SVREGGDNQPAVISDAP-DAYDIERELARQVAARISVLQYAMV-----
 Cytophaga : LFGQPIVQ-----GREGSDMCKEAVIN-LD-KITQAARKETAAQVVAIRNASLAETRKVEIKV-----
 Nostoc punctiforme : LFGCVPEI-----STRVGGDSGVPVIVGDE-SASAKALTAALTAGKVSVAALT-----
 Synechococcus : LFGRIPEI-----ATRQGGACQPIVISQEE-SASQALRQAKTAGRVSMALGAG-----
 Magnetococcus : FLGHIPISE-----DIRKDSACKPIVVARDE-SPOQQLLEARNVSKLQDGAG--APKMPKIVIE-----
 Salmonella : LFGQPIHI-----SIREDLRGTPEVVSRESEFTAIRREIADRVAQLYWQGEVIPGETAFRAV-----
 Arabidopsis-L1 : LIGEPIEM-----SIREGSDGCVVVVSSG-SIVSKAQDPAQNVKGLKELREN-PDNEIQMKNLVPHSSHSS-----
 Chlamydomonas-L1 : VLGQPIHV-----DQTRSDACTPEVVAEEG-GALGAVGTAERTHAKLLAL-----
 Homo sapiens : VLGDIPIHL-----NIREASDTGQPIVFSQEE-SDEKAMLRVAEVVRRLLPSPSE-----
 Yarrowia lipolytica : VLGNVPIDE-----QCSQSDMCKEVAVSGGVQAKYDKIAEGVAEQIGV-----
 Arabidopsis-L2 : FLGKVPMDP-----QCKAAEQCKSCFEDNKC-LISAPALKSTIQKVPSTVMTE-----
 Chlamydomonas-L2 : LFGRIPIDE-----GGAADACRSVPEAAG-AAGDAVKGGLGEGAP-----
 Homo sapiens : LFGRIPIDE-----LFGKNCCKQCSFFIDA-D-SPATLARSTIQRIQEFNLHQSKENLISS-----
 Saccharomyces Nbp35 : FLGSVPIDP-----RFGKSCDMCESEFDNYED-SPASSAVLNVEATRDVAVG---DV-----
 Drosophila : hlgtpidp-----rvgilagttsvldelldsttevlthvekktmlvs-----
 Homo sapiens : flgsvpldp-----almrtleeghdfiqefqg-spafaaltsiaqkildatpaclp-----
 Danio rerio : FLGSVPIDP-----LUTESLEECRDFIQAFEE-SSTFTAISHANTLNLSLNA-----
 Saccharomyces Cfb1 : YLGNVPIDE--KFVEMTENQVSSKKTIVEMYRE-SSLCPIEELMKKARKQDITTPVVDKHEQPQIESPK-----

Arabidopsis HCF101 : NS-----DEEFLHPATVRRNDRSAQS-VDEWTGEQKVLVY--GDVAEDIEPEDIRPMGNYAVSITWPDGFSQIAPYDQL
 Oryza sativa : DS-----DEEFLHPATVRRNDRSAQS-VDEWTGEQKVQY--GDIPEDIEPEEIRPMGNYAVSITWPDGFSQIAPYDQL
 Populus : DS-----EEEFLHPATVRRNDRSAQS-VDEWTGEQKLQY--ADVPEDIEPEEIRPMGNYAVQITWPDGFSQIAPYDQL
 Vitis vinifera : DS-----EEEFLHPATVRRNDRSAQS-VDEWTGEQKLQY--ADVPEDIEPEEIRPMGNYAVSITWPDGFSQIAPYDQL
 Physcomytrella : GT-----TEEFLHPATVRRNDRSAKS-IDEWSGEQKLRY--TDVAEDLAPESIRPMGNYAAAINWPDGFSQIAPYDQL
 Selaginella : GT-----EEFFYLHPATVRRNDRSAKS-IDEWTGEQKLRY--GDVREDIEPEAIQPLGNYAVMISWPDGFSQIAPYDQL
 Volvox : G-----ETEFLPPVVVRENDTSAQS-IDEWTGQRK-R---DEVPQDARPAAINPLGNYAVQISWSDGFSQIAPYDQL
 Ostreococcus tauri : GENN----DKAFWITAKNVRLSDESARVKGSDSPDRLLNG--APIPDDIAPVEMSVIGNYAMISITWPDGFSQIAPYDQL
 Micromonas : LRVQLADEGGMPFYVRGCDVRRSDKSAATA-DGESKKADFLMDGVTPVDDIAPVEAHVVGNYAVQISWPDGFSQIAPYDQL
 Galdieria maxima : DQOGIAWNNENKVEVSPWELRNACSCASC-VDEFTGKRHWK----SVDNRVQLQIQTAGNYAFSVIWSGDGHSQIAPYDQL
 Cyanidioschyzon : D-----HMEERIQPAALRRACRCAAC-VDECTGKQLLDP--NSVDDNIYPMQMMNVGNYALAVNWSGDGHSQIAPYDQL
 Phaeodactylum : GVGSTDEE--HVATLPPAALRRACRCAAC-VEELTGRQILVP--SSVSDKIAPRNMVPTGNYALSVDWSDGHSQIAPYDQL
 Thalassiosira : DIQN-----ATISPAELRRACRCAAC-VEELTGRQILNP--ASISESVKPLNMSPTGNYALSVDWSDGHSQIAPYDQL
 Chloroflexus : -----
 Cytophaga : -----
 Nostoc punctiforme : -----
 Synechococcus : -----
 Magnetococcus : -----
 Salmonella : -----
 Arabidopsis-L1 : -----
 Chlamydomonas-L1 : -----
 Homo sapiens : -----
 Yarrowia lipolytica : -----
 Arabidopsis-L2 : -----
 Chlamydomonas-L2 : -----
 Homo sapiens : -----
 Saccharomyces Nbp35 : -----
 Drosophila : -----
 Homo sapiens : -----
 Danio rerio : -----
 Saccharomyces Cfb1 : -----

Supplemental Figure 2: Multiple Sequence Alignment of the FSC family. Representative protein sequences of different organisms are shown subdivided according to the proposed four FSC Classes (Lezhneva *et al.*, 2004). Organism names are coloured according to the class affiliation. Green background represents plants and algae taxa belonging to the class 1. Yellow background represents eubacterial class 1 proteins. Gray background corresponds to class 2 members. Blue and magenta congregated taxa belonging to the class 3 and class 4, respectively. Note that algae and plants class 1 proteins have a C-terminal extension corresponding to the DUF971 (COG3536). Not conserved N-terminal and C-terminal regions are not shown in the alignment. Amino acids coloured with black background are 100% conserved. Amino acids coloured with gray background and written with white characters are 60% conserved. Amino acids coloured with gray background and written with black characters are 40% conserved. Cysteines conserved in at least two sequences are depicted in blue background. Numbers above the conserved cysteines in plants and algae correspond to the position of the residue in the sequence of the *Arabidopsis* HCF101 protein. Accession numbers of the sequences are available under request to Jörg Meurer.

EHRENWÖRTLICHE VERSICHERUNG

Ich versichere hiermit ehrenwörtlich, dass die vorgelegte Dissertation von mir selbstständig und ohne unerlaubte Hilfe angefertigt wurde. Ich habe weder anderweitig versucht, eine Dissertation einzureichen oder eine Doktorprüfung durchzuführen, noch habe ich diese Dissertation oder Teile derselben einer anderen Prüfungskommission vorgelegt.

München, den _____

Serena Schwenkert

ACKNOWLEDGEMENTS

I would like to express my thanks to ...



... *PD Dr. Jörg Meurer* for teaching me how to be a good scientist with his contagious enthusiasm and hopeless optimism



... *Prof. Dr. Jürgen Soll* for reviewing this work



... *Prof. Dr. Dario Leister* for his helpful support and the opportunity to perform my studies in his lab



... *Prof. Dr. Reinhold G. Herrmann* for his continuing commitment to our projects and his numerous inspirations



... *Prof. Dr. Itzhak Ohad* for many fruitful discussions and his never-ending energy



... my collaboration partners:

Prof. Dr. Jeverson Frazzon for introducing me to the secrets of iron, sulfur columns and many Biergarten excursions

Prof. Dr. Roland Lill, Daili Netz and Antonio Pierik for their very friendly welcome in Marburg and their helpful input

Dr. Eckhard Bill for performing Mössbauer spectra measurements



... *Prof. Dr. Lutz Eichacker* for many collaborations and his very generous supply of the FPLC



... all my colleagues for the great time we had every day. *Tine and Kristina* for the perfect execution of my instructions without complaint, *Pavan* for collaboration on the PSII project and especially *Rhea* for standing behind me at all times and knowing when to soothe me with chocolate



... *Gerhard* for believing in me



... *my family* for supporting me from the very first day.

Curriculum Vitae

PERSONAL DATA

Family name: Schwenkert
First name: Serena
Place of birth: Munich, Germany
Date of birth: April 28th, 1980
Citizenship: German

ACADEMIC EDUCATION

1/2006-9/2008 Post-graduate studies
University: Ludwig-Maximilians-Universität München,
Department Biology I, Botany, Munich, Germany
PhD thesis: *Factors for Stability, Assembly and Function of
Photosynthetic Complexes*
Supervisor: PD Dr. Jörg Meurer

10/2000-11/2005 Course of studies: Biology
University: Ludwig-Maximilians-Universität München,
Department Biology I, Botany, Munich, Germany
Diploma thesis: *The Role of Low Molecular Mass Subunits in
Stability, Assembly, and Function of Photosynthetic Complexes:
A Reverse Genetics Approach*
Supervisor: Prof. Dr. Reinhold G. Herrmann
Final grade: 1.3

SCHOOL EDUCATION

1/1993-7/2000 Allgemeine Hochschulreife (Advanced Education)
Katharinen-Gymnasium, Ingolstadt, Germany
Final grade: 1.8

1/1991-1993 Primary School
Sunridge Park, Port Elizabeth, South Africa

ORAL PRESENTATIONS

9/2007 Botany Congress (Botanikertagung)
Hamburg, Germany

POSTER PRESENTATIONS

8/2006 3rd summer school in proteomics basics

2/2007 Plant molecular biology (Molekularbiologie der Pflanzen)
Dabringhausen, Germany

PUBLICATIONS

Schwenkert S, Umate P, Dal Bosco C, Volz S, Mlčochová L, Zoryan M, Eichacker LA, Ohad I, Herrmann RG, Meurer J. (2006) PsbI affects the stability, function, and phosphorylation patterns of photosystem II assemblies in tobacco. *J Biol Chem.* 281, 34227-34238.

Schwenkert S, Legen J, Takami T, Shikanai T, Herrmann RG, Meurer J. (2007) Role of the low-molecular-weight subunits PetL, PetG, and PetN in assembly, stability, and dimerization of the cytochrome *b_f* complex in tobacco. *Plant Physiol.* 144, 1924-1935.

Philippar K, Geis T, Ilkavets I, Oster U, Schwenkert S, Meurer J, Soll J. (2007) Chloroplast biogenesis: the use of mutants to study the etioplast-chloroplast transition. *Proc Natl Acad Sci U S A.* 104, 678-683.

Umate P, Schwenkert S, Karbat I, Dal Bosco C, Mlčochová L, Volz S, Zer H, Herrmann RG, Ohad I, Meurer J. (2007) Deletion of PsbM in tobacco alters the Q_B site properties and the electron flow within photosystem II. *J Biol Chem.* 282, 9758-9767.

Umate P, Fellerer C, Schwenkert S, Zoryan M, Eichacker LA, Sadanandam A, Ohad I, Herrmann RG, Meurer J. (2008) Impact of PsbTc on forward and back electron flow, assembly, and phosphorylation patterns of photosystem II in tobacco. *Plant Physiol.* in press